EVALUATION OF ANTIMICROBIAL, ANTIDERMATOPHYTIC, ANTIPROLIFERATIVE AND CYTOTOXIC ACTIVITY OF SECONDARY METABOLITES ISOLATED FROM *Calpurnia aurea* subsp. *aurea* (Aiton) Benth (L'HERIT) AND ASSOCIATED FUNGAL ENDOPHYTES

WANGA LUCY AKETCH

A Thesis Submitted to the Graduate School in Partial Fulfillment of the Requirements of the award of Doctor of Philosophy Degree in Biochemistry of Egerton University

EGERTON UNIVERSITY

OCTOBER, 2025

DECLARATION AND RECOMMENDATION

Declaration

This thesis is my original work and has not been submitted or presented for examination in any other institution.

Signature…… …… Date……27.10.2025……...

Wanga Lucy Aketch

SD14/22028/18

Recommendation

This thesis has been submitted to the graduate school for examination with our approval as University supervisors.

Signature…… ……Date……27.10.2025……

Prof. J. C. Matasyoh

Department of Chemistry

Egerton University

Signature…… ……..Date……27.10.2025……

Dr. Indieka S. Abwao

Department of Biochemistry and Molecular Biology

Egerton University

Signature…… ...……Date…27.10.2025……

Prof. Dr. Michael Spiteller

Department of Chemistry

Technical university of Dortmund, Germany

DEDICATION

To my parents, Mr. Gabriel Lukas Wanga and Mrs. Roseline Adhiambo Wanga. Thank you for your guidance, Motivation and prayers.

ACKNOWLEDGEMENTS

I would like to express my heartfelt gratitude to the almighty God for His guidance, blessings, and for granting me the ability and good health to successfully complete my PhD research and studies. I would like to express my heartfelt appreciation to my supervisors and mentors, Professor Josphat C. Matasyoh, Dr. Stephen Indieka, and Prof. Dr. Michael Spitteller, for their invaluable guidance and support during this research. I would like to express my gratitude to the German Academic Exchange Service (DAAD) and the German Ministry of Education and Research (BMBF) for partially funding this research work under the "Partnership for Sustainable Solutions in Sub-Saharan Africa" grant number SSA2015-33-074. I would like to express my sincere gratitude to the EU-HORIZON 2020 MYCOBIOMICS grant number 101008129, as well as the Alexander von Humboldt Foundation and its projects, for their support in funding my research stay in Germany and the Czech Republic, which enabled me to achieve the results presented in this study. I would like to express my gratitude to Egerton University for providing me with the opportunity to pursue my Ph.D. studies, and to the Department of Biochemistry and Molecular Biology for their invaluable assistance and guidance throughout this journey. I would like to express my gratitude to the Helmholtz Centre for Infection Research, particularly to Prof. Dr. Marc Stadler, head of the department of microbial drugs, and to Dr. Miroslav Kolarik from the Institute of Microbiology at the Czech Academy of Sciences, for their support during my research visits and for hosting me throughout this part of my research. I express my gratitude to the late Prof. S. T. Kariuki from the Department of Biological Sciences at Egerton University for his exceptional expertise in taxonomy, identification, and authentication of the plant specimens utilized in this research. I express my gratitude to Wera Collisi for performing the antimicrobial, cytotoxic, and antiproliferative bioassay, as well as to C. Kakoschke and C. Schwager for documenting the HPLC-MS and NMR data, respectively, at the Helmholtz Institute of Infectious Diseases in Braunschweig, Germany. I express my gratitude to the Institute of Microbiology, Czech Academy of Sciences, Prague, Czech Republic, for the research visit during which antidermatophytic assays were conducted. I am deeply thankful to my colleagues and friends, Dr. Caroline Kosgei and Dr. Divina Nyamboki for their invaluable support throughout this research. I extend my heartfelt gratitude to my parents, Mr. and Mrs. Wanga, as well as the entire Wanga family, for your unwavering moral support throughout my studies. Lastly, I want to sincerely thank my husband Dr. Oscar Donde for his constant support in every aspect of my studies and research work.

ABSTRACT

Antimicrobial resistance has been recognized as a significant threat to healthcare systems globally, affecting both developing and developed countries, resulting in increased rates of skin infections caused by bacterial and dermatophytic pathogens. Cancer cases have increased over the years, and existing management options often entail undesirable side effects. Medicinal plants and endophytic fungi provide alternative solutions to these challenges. This research focused on the isolation of antimicrobial, antidermatophytic, antiproliferative, and cytotoxic secondary metabolites from *Calpurnia aurea* subsp. *aurea* and its associated endophytic fungi. The leaves and stem bark of this medicinal plant were used for the isolation of endophytic fungi, while the remaining portions were used for secondary metabolite extraction using methanol. Isolated fungal endophytes were identified through molecular techniques and fermented on rice media for the extraction of secondary metabolites. All extracts from leaves, stem bark, and endophytic fungi were purified using High Performance Liquid Chromatography (HPLC) to isolate pure compounds. The structures of the isolated compounds were elucidated using 1D and 2D NMR spectroscopy, as well as Liquid Chromatography Mass Spectrometry techniques. The bioactivities (antimicrobial, antidermatophytic, antiproliferative, and cytotoxicity) of the isolated compounds were also analyzed. Nineteen endophytes were isolated, classified into the classes *Eurotiomycetes*, *Sordariomycetes*, *Coleomycetes*, and *Agariomycetes*. Together with other known compounds, five (5) previously undescribed compounds were reported, namely; quinolizidine alkaloids (**46-49**) and a tirucallane triterpenoid (**67**), additionally ten (10) phenolic compounds were reported for the first time in this study. The phenolic and quinolizidine alkaloids demonstrated antidermatophytic activity, with minimum inhibitory concentration (MIC) values ranging from 6.6 µg/mL to 300 µg/mL against *Trichophyton rubrum*, *Trichophyton interdigitalle*, *Trichophyton benhamiae*, *Microsporum canis*, and *Nannizia gypsea*. The cinnamic acid (**65**) demonstrated antimicrobial activity against *Bacillus subtilis* (MIC of 16.6 µg/mL), comparable to oxytetracycline (MIC 16.6 µg/mL). The phenolic compounds also exhibited antiproliferative and cytotoxic effects on KB3.1 and L929 cell lines, with compound **65** demonstrating an IC_{50} value of 18 µg/mL. The results of this study demonstrate the significance of *C. aurea* subsp. *aurea* and endophytic fungi as sources of antimicrobial, antidermatophytic, antiproliferative, and cytotoxic secondary metabolites, which may serve as lead compounds in drug development. Additionally, this study scientifically validates the use of *C. aurea* subsp. *aurea* in alternative medicine.

TABLE OF CONTENTS

LIST OF TABLES

LIST OF FIGURES

LIST OF PLATES

LIST OF ABBREVIATIONS AND ACRONYMS

ACN	Acetonitrile
AMR	Antimicrobial Resistance
BLAST	Basic Local Alignment Search Tool
Ca	*Calpurnia aurea* subsp. *aurea*
CFU	Colony Forming Units
CLSI	Clinical and Laboratory Standards Institute
COSY	Correlated Spectroscopy
CRPA	Carbapenem Resistant *Pseudomonous aeroginosa*
DAD	Diode Array Detector
DEPT	Distortionless Enhancement by Polarization Transfer
ESI- TOF	Electron Spray Ionization- Time of Flight
ETD	Electron Transfer Dissociation
FBS	Fetal Bovine Serum
FGF2	Fibroblast Growth Factor 2
HMBC	Heteronuclear Multiple Bond Correlation
HPLC	High Performance Liquid Chromatography
HR-ESIMS	High Resolution Electron Spray Ionization Spectrometry
HSQC	Heteronuclear Single Quantum Correlation
IC	Inhibitory Concentration
ITS	Internal Transcribed Spacer
LSU	Large Subunit
MALDI-MS	Matrix-Assisted Laser Desorption/Ionization Mass Spectrometry
MEA	Malt Extract Agar
MEGA	Molecular Evolutionary Genetics Analysis
MIC	Minimum Inhibitory Concentration
MMP	Matrix Metalloproteinase
MRSA	Multidrug Resistance *Staphylococcus aureus*
MUSCLE	Multiple Sequence Comparison by Log- Expectation
NMR	Nuclear Magnetic Resonance
NOESY	Nuclear Overhauster effect Spectroscopy
OTU	Operational Taxonomic Unit
PBS	Phosphate Buffered Saline
PDA	Potato Dextrose Agar

SSTI	Skin and Soft Tissue Infections
TAE	Tris Acetate EDTA
TBNC	Triple Negative Breast Cancer
TSA	Tryptic Soy Agar
UPLC	Ultra Performance Liquid Chromatography
VEGF	Vascular Endothelial Growth Factor
WHO	World Health Organization
YLL	Years of Life Lost

CHAPTER ONE
INTRODUCTION

1.1 Background Information

Antimicrobial resistance (AMR) is a condition that emerges when microorganisms such as fungi, bacteria, parasites and viruses are able to thrive in the presence of medications that once inhibited them (Prestinaci *et al.,* 2015; Sagar *et al.,* 2019). AMR has been reported to cause significant threat to the healthcare systems not just in the developing countries but all over the world (Prestinaci *et al.,* 2015). According to reports by WHO, there has been an alarming increase in resistance among prevalent bacterial pathogens (World Health Organization, 2022). It has become an undisputed fact that some infectious diseases cannot be managed or treated with the commercially available antibiotics, a fact that depicts an unknown future in the healthcare system (Chokshi *et al.,* 2019). Infections that results from these resistant strains leads to serious illnesses and prolonged hospital stay, increase in healthcare costs, higher costs in second line drugs and sometimes treatment failures (Chokshi *et al.,* 2019; ECDC, 2019; Prestinaci *et al.,* 2015). Additionally, infections by antimicrobial resistant strains compromises human system's capacity in fighting infectious diseases thereby contributing to other serious complications in vulnerable patients undergoing dialysis, surgery and chemotherapy (Shrestha *et al.,* 2018). Patients with underlying conditions such as diabetes, rheumatoid arthritis and asthma are more vulnerable and are heavily impacted by antibiotic resistance (Sagar *et al.,* 2019). Since the effectiveness of the available antibiotics have reduced due to antibiotics resistance, healthcare workers and physicians tend to use the last line of medications such as polymyxins and carbapenems which are not readily available especially in developing countries. Additionally, these drugs are expensive especially to low income earners in developing countries and they also have different negative side effects on patients (World Health Organization, 2015). Hence the need to develop novel antimicrobial especially from natural sources.

As part of some of the complications experienced from antimicrobial resistance, skin infections have also been on the rise worldwide. The skin is the most extensive organ of the body and is naturally inhabited by a vast range of microbiota (Burstein *et al.,* 2020). Naturally, the skin is adapted to provide a mechanical barrier against invasion by various microorganisms through the keratinous surface (Lipsky *et al.,* 2022). Apart from its major contribution to the body homeostasis, the skin also facilitates removal of microorganisms through shading off of the epidermal cells and keratin. There two are responsible for the production of acidic sebaceous secretions and assist in resolving the tissue damage

respectively (Monteiro-Riviere, 2010). Infections on the skin generally occurs due to puncture or cuts, animal and insect bites, breaks due to pricks and surgery (Abubakar, 2009). Other factors that contribute to skin infections are recurrent dermatophytosis due to frequent use of corticosteroids, HIV/AIDS, diabetes mellitus and atopy (Bishwabidyalay *et al.*, 2019; Burstein *et al.*, 2020). The spectrum of these infections may range from asymptomatic bacterial and fungal infections, worst case scenarios would result to death especially in cases of necrotizing fasciitis (Arif *et al.*, 2016; Esposito *et al.*, 2016). Some of the common microorganism associated skin infections results from inflammation of the subcutaneous connective tissues which results to conditions such as cellulitis, carbuncles, impetigo, ringworm, foot odor, furuncles and acne (Hollestein & Nijsten, 2014). Most of these conditions are frequently experienced by people in developing countries (Afsar, 2010), with the highest burden of infection occurring among immune-compromised individuals (Hay *et al.*, 2014). These infections are treated or managed by topical and/or oral antimicrobial formulations (Stevens *et al.*, 2014). However, negative treatment outcome due to the harmful effects associated with synthetic antimicrobial drugs such as nephrotoxicity and hepatotoxicity have been reported (Morales-Alvarez, 2020). Additionally, emergence of drug resistant skin pathogens such as *Staphylococcus aureus* resistant to methicillin, carbapenem-resistant *Pseudomonas aeruginosa* and other dermatophytes makes the treatment of such infections a great challenge in the medical field.There also reports of treatment failure in some of the reported cases (Amirthalingam *et al.*, 2015). This calls for the search for novel antimicrobial with different modes of action and origin from the ones currently in use.

Cancer patients are also at a higher risk of contracting infectious diseases caused by either bacteria or fungi (Zembower, 2014). In the past decade, cancer has become a major health problem becoming the second leading cause of global mortality (Gezici & Şekeroğlu, 2019). There are different modes of treatments in managing different cancer cases such as immune therapy, chemotherapy, hormone therapy, radiation, and targeted therapy. However, these modes of treatment have negative side effects as well as significant deficiencies (Beddok *et al.*, 2021). A number of medicinal plants have been reported to be used in alternative medicine for the prevention and treatment of cancer (Gezici & Şekeroğlu, 2019). These plants are considered due to their rich chemo-protective and anti-carcinogenic properties. Additionally, these plants are reported to be less toxic anticancer, anti-tumor and anti-proliferative agents than the modern therapeutic methods (Kaur *et al.*, 2018; Shukla & Mehta, 2015). Nevertheless, there are only a few number of natural anti-tumor products including podophyllotoxin, vincristine, vinblastine, camptothecin and paclitaxel (Taxol) in

the market (Carcache *et al.*, 2021; Zishan *et al.*, 2017). Hence it is postulated that natural products could be a great source of anti tumor agents that can be used in modern anticancer therapy. The novel anticancer secondary metabolites from natural products could also effectively be used to prevent, treat as well as manage the chemotherapy and radiotherapy related side effects.

Calpurnia aurea subsp. *aurea* (syn. *Calpurnia subdecadra* (L'Herit) belongs to the genus *Calpurnia* and family *Fabaceae*. It is a shrub like slender tree that grows up to 15 m tall on forest margins. Traditionally, the leaves and seeds are used to treat hypertension, malaria, rabies, diabetes and wounds (Umer *et al.*, 2013; Wasihun *et al.*, 2023). The plant tissues are a host of bacteria and fungi that inhabit these tissues without causing any apparent symptoms commonly known as endophytes (Mengistu, 2020; Rai *et al.*, 2021). Endophytic microorganisms are a great source of novel secondary metabolites with promising antimicrobial activities; some drugs commonly used in the market were sourced from endophytes for instance, Taxol produced from *Taxomyces andreanae* an endopyhtic fungi isolated from *Taxus brevifolia* (Vélëz *et al.*, 2022; Stierle *et al.*,1993). Development of this drug triggered intensive investigation on the diversity of fungal endophytes in most plants and their capacity to produce metabolites of commercial and medicinal value (Kaul *et al.*, 2012; Keshri *et al.*, 2021; Shubhpriya Gupta *et al.*, 2020). Research shows that, production of secondary metabolites from endophytes is more or less correlated to their ecological niche. Therefore, synthesis of biologically active secondary metabolites is highly favored by metabolite interaction of the endophyte with its host (Ludwig-Müller, 2015; Patil *et al.*, 2016). Currently, medicinal plants and their fungal endophytes are considered as an outstanding source of natural products since they occupy biological niche in unique environments such as tropical ecosystem which has contains adverse angiosperm population (Ludwig-Müller, 2015; Patil *et al.*, 2016). However endophytic fungi from C. aurea subsp. aurea have not been studied despite reports on beneficial endophytes from other plants. Hence In line with the aforementioned concept, this study focused on the isolation of secondary metabolites from endophytic fungi, leaves and bark of *C. aurea* subp *aurea*, and evaluation of their potential to manage selected bacterial and fungal pathogens as well as their cytotoxic and antiproliferative potential.

1.2 Statement of the Problem

Antimicrobial resistance (AMR) poses a growing threat globally, linking infectious diseases, cancer progression, and dermatological conditions. Dermatophytic, bacterial, and

fungal infections pose significant risks, particularly for immunocompromised individuals. Additionally, resistant fungal and bacterial pathogens complicate treatment of these common infections, leading to prolonged illness, chronic inflammation, and increased risk of cancer. Infections are typically managed using topical and oral antimicrobial formulations, including available antibiotics and anti-fungal agents, which are predominantly synthetic and often regarded as relatively costly, particularly the last-line antibiotics. The main issue is identifying methods to manage prevalent infections caused by both gram-positive and gram-negative bacteria, including *Staphylococcus aureus*, *Pseudomonas aeruginosa*, and *Escherichia coli*, which have acquired antimicrobial resistance. Furthermore, dermatophytes have been documented to exhibit diminished susceptibility to existing pharmacological treatments. The emergence of antimicrobial resistance presents significant clinical and financial implications, including patient non-responsiveness to therapy and reliance on costly last-line antimicrobial. Inaccessibility to these treatments exacerbates social costs and increases morbidity and mortality rates, adversely affecting families and the overall economy of a country due to an unnecessary burden of disease. The articulated rationale highlights the necessity for alternative strategies in the control and management of skin and other microbial infections. This is mainly through the utilization of natural products that are not associated with adverse side effects, in contrast to synthetic pharmaceuticals. Additionally, there is limited information regarding the antimicrobial activity of secondary metabolites derived from fungal endophytes associated with *C. aurea* subsp. *aurea* hence need for the study.

Antimicrobial resistance (AMR) is greatly recognized as a key threat in oncology. Cancer patients, especially those undergoing radiotherapy, chemotherapy, or surgical procedures, are immunocompromised and hence highly susceptible to infections. Radiotherapy and chemotherapy are recognized as the most effective and widely utilized methods for cancer management. Nevertheless, these two methods are linked to adverse effects, including gastrointestinal toxicity, oral mucositis, hepatotoxicity, injury to the hematopoietic system, nephrotoxicity, cardio-toxicity, and neurotoxicity, which may impede their clinical applications. The high cost of available drugs, coupled with their detrimental side effects, frequently diminishes the quality of life for cancer patients, potentially resulting in the discontinuation of therapy and ultimately increasing the risk of mortality. AMR creates a vicious cycle, where ineffective antimicrobial therapy increases infection rates, immune dysfunction and inflammation, ultimately linking microbial persistence with development of cancer and impaired systemic and skin health. Combating AMR is therefore necessary for infection control and cancer prevention. In order to achieve this, it is essential to develop

innovative and effective strategies for managing and controlling the side effects induced by chemotherapy and radiotherapy.

1.3 Objectives

1.3.1 General Objective

To evaluate the antimicrobial, antidermatophytic, antiproliferative and cytotoxic activities of secondary metabolites isolated from *C. aurea* subsp *aurea* (Aiton) Benth (L'Herit) and its associated fungal endophytes

1.3.2 Specific Objectives

i. To isolate and characterize endophytic fungi from the leaves, stem bark and roots of *C. aurea* subsp *aurea*.
ii. To isolate and characterize secondary metabolites from *C. aurea* subsp *aurea* leaves, bark and associated fungal endophytes.
iii. To determine antimicrobial, antidermatophytic and cytotoxic potential of the crude extracts and pure compound isolated from *C. aurea* subsp. *aurea* leaves, bark and axenic cultures of associated fungal endophytes.

1.4 Research Questions

i. Do the fungal endophytes composition in the leaves, stem bark and roots of *C. aurea* subsp. *aurea* have similar morphological and molecular characteristic?
ii. Do the secondary metabolites isolated from the leaves, stem bark and associated endophytic fungi have similar chemical characteristics?
iii. Do the crude extracts and isolated secondary metabolites have broad spectrum antibacterial, antidermatophytic, antiproliferative and cytotoxic activities?

1.5 Justification of the Study

Numerous significant leads or medicinal compounds, including antimicrobials, antifungals, anticarcinogens, immunosuppressants, and antioxidants, have been isolated from fungi and plants. Prospecting for novel and effective antimicrobials targeting dermatophytic, bacterial, and fungal infections, along with antiproliferative and cytotoxic secondary metabolites derived from ethnobotanically recognized medicinal plants and their associated endophytic fungi, represents a logical initial approach. *C. aurea* subsp. *aurea* has been traditionally utilized for managing various ailments. However, the understanding of the plant's chemical constituents is limited, indicating a need for further research to identify compounds

or lead compounds suitable for drug development. Furthermore, studies on endophytic fungi have demonstrated that they serve as promising sources of novel antimicrobial compounds. This study evaluated the antidermatophytic, antimicrobial, antiproliferative, and cytotoxic secondary metabolites derived from this medicinal plant and its associated endophytes. This study aligns with United Nations Sustainable Development Goal 3, which aims to enhance health and well-being.

CHAPTER TWO
LITERATURE REVIEW

2.1 Antimicrobial Resistance

The long term human battle with microbes especially bacteria has been experienced throughout history in different populations around globally (Tenover, 2006). Antimicrobial resistance (AMR) is the ability of bacteria and fungi as well as other microorganisms, to survive and become viable in the presence of antimicrobial agents. These antimicrobial agents include disinfectants, antibiotics, and food preservatives can inhibit their capacity to proliferate, multiply and even kill them. Antimicrobial agents may be from natural sources, semi-synthetic and synthetic and they have unique mechanisms capable of causing major changes on the metabolic and physiological level of the microorganisms. The mechanisms of action of these antimicrobial agents include cell wall synthesis modification, inhibition of protein synthesis, metabolic pathway inhibition and inhibition of DNA synthesis replication and translation (Tenover, 2006; Zhou *et al.*, 2015). Antimicrobial resistance is considered as of major concern within the healthcare systems all over the world. With the increasing usage of antibiotics around the world, the microorganism tend to develop more complicated resistance against these antibiotics. This results to the natural development of a modified bacterial strain that has reduced chances of treatment or elimination effectively from patients leading to profound consequences such as morbidity, mortality or worsened clinical complications (Khameneh *et al.*, 2016; Tenover, 2006; Zhou *et al.*, 2015). Extensive and prolonged use of antibiotics over time has been considered as the major cause of resistance within the bacterial population. In the 21st century, the levels of antimicrobial resistance has reached a high paradoxical level causing serious health challenges with potential global impact hence the call for early and serious interventions (Evolution & Health, 2014). In addition, there has been significant evidence proving that antibiotics misuse may eventually result to the development of resistance (Alam *et al.*, 2019). Moreover, insufficient availability of antibiotics reduces the risk of prevention and management of immuno-compromised health conditions like cancer, surgical procedures, diabetes, and HIV (WHO, 2018). Though antimicrobial resistance is considered as a natural processes, incomplete knowledge about the dangers of antibiotics resistance in accordance with the passive human activities like misuse of antibiotics by physicians and patients, inappropriate prescription methods, and improper diagnosis increased the rate of antimicrobial resistance (Bartlett *et al.*, 2013; Morgan *et al.*, 2011). Hence a continuation of this trend may lead to "post-antibiotics era" in which common infections and minor injuries become a major leading cause of mortality (Alam_*et al.*, 2019). To avoid this detrimental

outcome, there has to be alternative ways of coming up with lead compound that can be used in the development of novel antibiotic from medicinal plants and their endophytic fungi.

2.2 Skin Infections

Normally, the skin is known to provide a mechanical barrier against invasion by microorganisms in the body due to is interface with the environment. This is achieved through the keratin surface which allows the removal of microbes through shedding off the keratin layer and also through the acid sebaceous secretions (Baquero *et al.,* 2021; Gilaberte *et al.,* 2016). The skin is also adapted to functions such as protections from excessive water loss (Kolarsick *et al.,* 2011), sensation, temperature regulation, insulation, storage and synthesis of vitamin D (Lloyd & Patel, 2012). Cases like surgery, cuts and bites from animals or insects, pricks and burns results to a break in the skin which if not treated properly can lead to invasion, colonization and infection by pathogens such as bacteria, fungi and viruses (Abubakar, 2009; Ruchti & LeibundGut-Landmann, 2023). The spectrum of infection in such cases may range from asymptomatic colonization by the pathogens to bacteremia, fungemia and which may ultimately lead to death in adverse scenarios (Gnat *et al.,* 2021; Zhou *et al.,* 2021).

As noted by Afsar, (2010), skin infections are encountered by people all over the world, but the highest burden of infections occur in the developing countries. The highest magnitude of these infections have been reported in immune compromised individuals (Dropulic & Lederman, 2016), whereby these infections tend to occur as secondary infections. Treatment and management of these infections requires use of oral antimicrobial as well as topical formulations which have been used over the years (Dryden, 2014; Stevens *et al.,* 2014). There have been however negative reports of the treatment outcome due to the harmful effects associated with these synthetic antimicrobial that are available in the market. Some of these reports include nephrotoxicity and hepatotoxicity as a result of the continuous and sometimes inappropriate use of these drugs (Karimi *et al.,* 2015). More alarming is the continuous emergence of resistant pathogens such as *S. aureus* strain resistant to methicillin (MRSA), *P. aeruginosa* and other dermatophytes. This makes the treatment of such infections a challenge and are often not successful (Amirthalingam *et al.,* 2015).

2.2.1 Skin and Soft Tissue Bacterial Infections

The most frequently reported infections due to bacterial pathogens is the skin and soft tissue bacterial infections in human (Hatlen & Miller, 2021; Mussin *et al.,* 2021) with the reported incidences increasing marginally between the years 1990 and 2019 (Xue *et al.,* 2022). With the increasing number of critically ill patients or immuno-compromised individuals and

the ever increasing cases of multi-drug resistance among clinically important bacterial pathogens, there has been a worrying steady increase in the incidences of SSTIs globally (Alfouzan *et al.,* 2021). Clinically, skin and soft tissue infections present symptoms ranging from mild to very serious life-threatening infections and diseases irrespective of the age group or host. Depending on the patient's immune system status, history of antimicrobial treatment, geographical location, trauma, surgery and animal bites or exposure the etiology of these infections may differ (Miller *et al.,* 2015). Additionally, due to similarities on the clinical symptoms, there has been reported cases of misdiagnosis of these infections for instance in cases of dermatitis and honey bee sting (Breyre & Frazee, 2018). Pyoderma, which is refers to inflammatory diseases of the skin caused by *Streptococcus pyogenes* and *S. aureus*, is another commonly occurring infection of the skin (Brook *et al.,* 1997).

These inflammatory diseases include but are not limited to impetigo, folliculitis, cellulitis, furuncle, topical ulcers and carbuncles among others and are mainly characterized by pus production (Mahé *et al.,* 2005). Another common skin infection especially among adolescents is acne vulgaris caused by *Propionibacterium acnes* located in the sebaceous glands (Borelli *et al.,* 2006). If not managed this infection can lead to serious psychological and social disorders such as reduced self-esteem, anxiety and depression among the adolescents (Kelly *et al.,* 2021). Beta lactamase producing enterobacterium and carbapenem resistant *P. aeruginosa* are reported to cause approximately 11.1 and 11.9% of skin and soft tissue infections respectively (Ballus *et al.,* 2015) while strains such as *P. auroginosa* and *Stenotrophomonas maltophilia* may also lead to therapy induced cytotoxic granulocytopenia which is experienced in patients that have undergone transplant of the bone marrow (Bodey, 2000). Despite the high and ever increasing frequency of bacterial skin infections and major cause of morbidity, there is limited knowledge and information on the fluctuation incidences of common bacterial skin infections such as folliculitis, impetigo and erysipelas (Bernard, 2008). Additionally, the effects of skin and soft tissue infections in relation to serious permanent disability has not been well analyzed and evaluated hence there is need for further research in the sector (Poulakou *et al.,* 2019).

2.2.2 Fungal Skin Infections (Dermatophytosis)

Dermatophytosis is an infection caused by dermatophytes on the outer most layer of the skin (Al-Khikani, 2020). Dermatophytes depend on the keratin in the skin, nails and hair hence considered as parasitic. Depending on their reservoirs, dermatopyhtes can be classified as zoophilic, geophillic or anthropophillic (Hassanzadeh Rad *et al.,* 2018). The zoophilic

dermatophytes such as *Microsporum canis* are adapted to living on animals and can infect human. The geophillic species are specifically human pathogens but they can affect animals (Gnat *et al.,* 2020). On invasion into the skin, these dermatophytes break the keratin and are capable of invading other tissues leading to injuries. Dermatophytes can impact any external body surface; however, moist and warm environments may exacerbate and contribute to increased infection rates in specific areas, particularly those with high skin folds and perspiration (Brown *et al.,* 2012). The severity of these infections may depend on various factors such as the general health of the host, site of infection, co-infection rate in infecting dermatophyte species and the respective individual immune response (Cock & Van Vuuren, 2020). Approximately forty (40) pathogens have been identified as the causative agents in human dermatophytosis infections. However, almost all of the reported infections are caused by closely related dermatophytes or fungal pathogens that belong to three genera namely; *Microsporum, Trichophyton* and *Epidermatophyton* species.

The infections caused by dermatophytes present more or less similar symptoms in most patients, this is due to their similarity, hence fungal or dermatophytes infections are classified depending on the site of infection rather that the causative pathogens generally referred to as tinea infections (Cock & Van Vuuren, 2020). For instance, infection of the foot, generally known as athlete's foot or tinea pedis. This infection is reported to affect about 15% of the world's estimated total population at any given point in time (Brown *et al.,* 2012). Tinea pedis clinically presents symptoms such as itching, cracking, redness and feet inflammation. It may affect any part of the foot and may be worsened by moist and warm conditions around the soles of the feet between the toes. This infection is caused by a combination of *Microsporum, Epidermatophyton* and *Trichophyton* species which are found in infected bedding, soil, or clothing's, house-hold surfaces as well as skin to skin contacts with infected individuals (Cock & Van Vuuren, 2020; Julien *et al.,* 2021). Another common tinea infection is Jock itch (*Tinea cruris*) which occur as a co-infection with *Tinea pedis* mainly on male individuals. This infection is mainly caused by *Trichophyton rubrum* however other causative agents are *E. Floccosum* and *T. mentagrophytes* (Darade *et al.,* 2020). A *Candida albicans* co-infection may also contribute to the development of symptoms related to *Tinea cruris* infection. Despite not being classified as a dermatophyte, infections by *C. albicans* is also aided by humid and moist conditions and they also present symptoms that are identical to dermatophytosis hence regarded as one of the major channels of dermatophytosis infections (Ganaie & Wani, 2021). *Tinea corporis*, (body ringworm) is a common infection among the school going children. This infection presents as scaly, circular, itchy and red rash that occurs in the legs, arms and trunk

sections of the body. Ringworms are generally versatile and are caused by about 40 fungal species belonging to the genera *Microsporum*, *Trichophyton* and *Epidermatophyton*. Similar ring-shaped symptoms of dermatophytic infection may occur when these fungal pathogens affect other regions of the body such as the hands (*tinea manum*), face (*tinea faciel*), or scalp (*tinea capitis*). Nail infections is commonly known as *tinea unguium* or onchomycosis which is also caused by multiple fungal strains belonging to the previously mentioned three genera. Onchomycosis may also be caused by *Fusarium* species and *C. albicans* (Gnat *et al.,* 2020; Ramos-e-Silva *et al.,* 2010; Sobel, 2007).

2.2.3 Global Burden of Dermatophytosis and Skin and Soft Tissue Infections

The global report in 2010 shows that skin diseases are the fourth leading cause of non-fatal infections in human. This burden of skin conditions or infections is highly reported in both developed and developing countries (Hollestein & Nijsten, 2014). Notably, skin infections are a high threat to patients who are immune compromised and infected by HIV/AIDS since they present as opportunistic infections. Statistics show that approximately 92% of individuals affected by HIV suffer from mucosal and cutaneous complications (Shahabudin *et al.,* 2024). It is therefore proven that skin health is a great aspect in the Kenyan healthcare system particularly for HIV-AIDS patients. Approximately 7% of the Kenyan population are affected by a great number of fungal infections for example recurrent vaginitis and tinea capitis infections which account for approximately 82% of the infections at any given point in time (Boakye-Yiadom *et al.,* 2024). Tinea infections among the low income population with overcrowding, poor hygiene and sharing of the amenities has remained to be the greatest challenge in the public health sector among the Kenyan communities (Wamalwa, 2019). These infection rates are distributed all over the world, however, most cases have been reported in Africa, Asia, East and Southern Europe (Oguzkaya *et al.,* 2013). The rates of tinea infections range between 10-30% with Africa having the highest number of infections, this is mostly experienced among the school going children (Birhanu *et al.,* 2023). In Kenya, approximately 11.2% of the total population have been reported to be affected by tinea infection among the people living in low income settlement areas such as Kibera, Korogocho, Mukuru kwa Njenga and Mathare slums in Nairobi, Kenya (Moto *et al.,* 2015). The residents of these slums are faced with challenging living conditions such as poor health and housing which are reported to be a great factor contributing towards the high tinea infection rates (Mutisya & Yarime, 2011). Apart from low-income settlements, a high rate of tinea infection is also experienced in rural

populations. The people in these areas are always in close contact with livestock and animals which provides an extra avenue of zoonotic infection (Cock & Van Vuuren, 2020).

The data on the SSTIs' prevalence of in Kenya is not very conclusive, however, in a study which aimed at examining antibiotic prescription patterns among patients in Kenyan hospitals, it was reported that, skin and soft tissue infections formed around 68% of patients who received inappropriate treatment (Maina *et al.,* 2013; Maina *et al.,* 2020). In a retrospect study to map and model the burden of diseases in Kenya, it is reported that, specific ethnicity were associated with Years of Life Lost (YLL) (Frings *et al.,* 2018) due to a higher risk of skin diseases and other communicable diseases (Adler & Newman, 2017). Approximately 6% of the reported infections are due to infection on the surgical site which may be regarded as secondary infection leading to prolonged stay in the hospital (Kalagouda *et al.,* 2022). Due to increased levels of poverty, a great majority of the Kenyan population depend on traditional medicine and over-the-counter drugs in the management of SSTIs' hence further contributing to the inconclusive data on the prevalence in the country (Wanga & Nyamboki, 2023).

2.3 Cancer and their Global Burden

Research shows that cancer is the second most common causes of worldwide mortality after cardiovascular diseases (McGuire, 2016; Wang *et al.,* 2016). Reports by World Health Organization in 2020 indicate that approximately 19 million people were diagnosed with cancer and over 10 million died as a result. Latest predictions show that cancer related mortality will increase to more than 30 million by 2030 with approximately 75 % occurring in low- and middle-income countries such as Kenya. Radiotherapy and chemotherapy are considered the most extensive and effective approaches for cancer management. These methods have, however, been shown to have negative and adverse side effects such as gastrointestinal toxicity, oral mucositis, nephrotoxicity, hepatotoxicity, hematopoietic system injury, cardiotoxicity and neurotoxicity. These harmful side effects subsequently tend to reduce the quality of life in cancer patients, leading to discontinuation of therapy and even death. (Shapiro, 2016; Turcotte *et al.,* 2017). Therefore, there is need to develop effective strategies of controlling and managing radiotherapy and chemotherapy-induced side effects. Crude extracts, bio-active compounds enriched fractions and even pure compounds from various natural products and herbal formulations have been shown to prevent and even treat various types of cancers (Sanders *et al.,* 2016). Clinical trials and preclinical studies reveal that some products from nature such as plants can reduce the radiotherapy and chemotherapy induced conditions such

as gastrointestinal toxicity, oral mucositis, nephrotoxicity, hepatotoxicity, hematopoietic system injury and cardio-toxicity (Zhang *et al.*, 2018).

Research has shown that natural dietary supplements that contain extracts from Ginseng, Grape seeds and Curcumin tend to promote recovery from severe illness and relieve the above mentioned side effects of chemotherapy and radiotherapy (Currò, 2018). The gut microbiota significantly influences drug action and overall health. Consequently, extracts and secondary metabolites from natural sources, which exhibit lower toxicity, can enhance gut health. This improvement may alleviate severe symptoms associated with chemotherapy and radiotherapy and help prevent abnormal cell proliferation in humans (Peterson *et al.*, 2018). Hence the aim of this study of isolating anti-proliferative and cytotoxic secondary metabolites from *C. aurea* subsp. *aurea* and their associated endophytes. This study draws special attention to the recent findings about the efficacy of supplements from natural sources and the modulation of natural products on gut microbiota for the protection and management of toxicity induced by cancer therapy (Zhang *et al.*, 2018).

2.4 Medicinal Plants

Over the years, medicinal plants have been used in the management of human and animal diseases. This is attributed to the presence of phytochemical constituents which are naturally occurring in plants (Suroowan *et al.*, 2017). These phytochemicals includes terpenoids, alkaloids and various phenolic compounds (Kaushik *et al.*, 2021). It is well documented that several medicinal plants have been used and are still being used in the treatment of various health problems. This is because they are considered to be relatively safe, less toxic and economical, additionally, medicinal plants have been well documented as a reliable source for antimicrobial, antiviral, cytotoxic and antidermatophytic secondary metabolites and drugs (Jabborova *et al.*, 2019). Due to their capability in combating antimicrobial resistance of various microorganisms, medicinal plants have been increasingly used as a source of raw materials for the production of new antimicrobials (Chen *et al.*, 2021). There has been an interestingly increase in the demand for medicinal plants in both developing and developed countries proving that nature still has more to provide when it comes to combating various illnesses among human populations (Sharma *et al.*, 2017). The medicinal plant of interest in this study was *Calpurnia aurea* subsp *aurea* that was collected from Mount Elgon national park in Kenya.

2.4.1 Medicinal Plants in the Family *Fabaceae*

The *Fabaceae*, also known as *Leguminosae*, is often regarded as the bean, legume or

the pea family. It is the third largest plant family after the *Orchidaceae* and *Asteraceae* in terms of the number of plant species within each family (Christenhusz & Byng, 2016). The *Fabaceae* family consists of about 19,500 species and approximately 770 genera (Azani *et al.,* 2017; Christenhusz & Byng, 2016) that are recorded all through the years in all of the biomes in the world except the high Arctic and Antarctica (Maroyi, 2023). The dominating ability of these medicinal plants and shrubs within the family to grow in several hospitable and already disturbed habitats is attributed to their nitrogen fixation capability hence they can thrive in nutrient poor soils (Sprent, 2008; Sprent *et al.,* 2017; Van Wyk, 2019). Research has proven that from their morphological and molecular characteristics, the family *Fabaceae* has a common descendant in terms of evolutionary history hence regarded as monophyletic (Christenhusz & Byng, 2016). This family is divided into six sub-families namely; *Cercidoideae* (12 genera and 335 species), *Caesalpinioideae* (148 genera and 4400 species), *Detarioideae* (84 genera and 760 species), *Duparquetioideae* (monotypic genus), *Dialiodeae* (17 genera and 85 species) and *Faboideae* (or *Papilionoideae*) (503 genera and 14,000 species) (Christenhusz & Byng, 2016).

The members of the *Fabaceae* family include shrubs, trees, woody lianas, sub-shrubs, climbing annuals, aquatics and herbs (Maroyi, 2023). Morphologically, the flowers are asymmetrical, radially symmetric or bilateral symmetric and they are pollinated by insects, bats and birds (Maroyi, 2023). The majority of plants in this family have compound leaves, double compound or trifoliate leaves with sometimes swelling base, superior ovary with one locular, and their fruits are usually two-halved with dehiscent pod or indehiscent pod and occasional segmentation (Koekemoer *et al.,* 2013; Leistner, 2000). These plants are considered economically and traditionally important throughout the world hence they are used as a great source of traditional medicine, timber, food, garden ornamental, fibers, dyes, gums, insecticides and fuels (Semenya & Maroyi, 2018). The importance of these plants towards the general well-being of the ecosystem and the human race at large has been well documented in several countries of the world (Maroyi, 2017; Molares & Ladio, 2012). Phytochemical studies have shown that members of this family contain various bio-active chemical constituents such as flavonoids, lectins, phenolic acids, alkaloids, carotenoids and saponins (Usman *et al.,* 2022). Pharmacologically, some species within this family have potent antioxidant, anticancer, antimicrobial, analgesic, anti-inflammatory, anti-ulcer, anti-rheumatic, anti-diabetic, cytotoxic and anti-parasitic properties (Ahmad *et al.,* 2016; Obistioiu *et al.,* 2021; Usman *et al.,* 2022). Hence an extensive pharmacological and phytochemical evaluation of plants in this family may result to the discovery and development of new pharmaceutical products, great food ingredients

as well as cosmetic products. Despite the discovery of many secondary metabolites in the *Fabaceae*, there is unfortunately a disproportional small attention in terms of ethno-pharmacological research (Maroyi, 2017). Hence the interest in one of the medicinal plants that belong to this family for this study.

2.4.2 *Calpurnia aurea* subsp. *aurea*

Calpurnia aurea subsp. *aurea* (L'Herit), commonly known as wild laburnum belongs to the genus *Calpurnia* which comprises of flowering plants within the family *Fabaceae*. This genus comprises of small trees or shrubs that are found in or along forest margins. *Calpurnia aurea* subsp. *aurea* is considered native in Ethiopia and is widely distributed in Africa in countries such as Angola, Sudan, Democratic republic of Congo (DRC), Eritrea, Kenya, Uganda, Mozambique, Tanzania, Zimbabwe and Eastern South Africa (Beaumont *et al.*, 1999; Korir *et al.*, 2014). Naturally, this plant grows as a bush or small tree that grow up to 7m high. The leaves are ovate or oblong and slightly symmetrical at the base. These leaves are approximately 6 to 24 cm long with 5 to 15 pairs of leaflets which are approximately 2 to 4 cm in length and vary from rounded to notch at the apex (Plate 2.1). Its flowers are golden yellow while the pods are flattened approximately 5 -12 cm long with narrowly winged structure which may turn straw colored to brown when mature (Mulatu, 2020).

Plate 2.1*:* The Flowers (A), leaves (B) and Bark (C) of *Calpurnia aurea* subsp *aurea* (Photo courtesy of Prof. I. N. Wagara)

Calpurnia aurea subsp. *aurea* is one of the important medicinal plant used in the management of amoebic dysentery, eye diseases as well as a potent toxicant in the control of storage pests (Hiruy *et al.*, 2018; Yeshitila, 2018). Traditionally, various parts of this medicinal plants have been used in the management of different animal and human diseases since time immemorial as part of phytomedicine (Gemechu *et al.*, 2013). For instance, in the native country, Ethiopia, powdered roots and leaves is used in the treatment of malaria, rabies, syphilis, diabetes, lung tuberculosis (TB), diarrhea, hypertension, Leishmaniasis, *Taenia*

capitis, elephantiasis, trachoma, swellings, bowel and bladder disorders among other infections (Ejeta & Abdisa, 2018; Tadeg *et al.,* 2005). In the southwestern part of Ethiopia, the juice obtained from the leaves of this medical plant combined with other plant species parts are used to treat earaches in humans by applying through the auricular for two (2) days (Yineger & Yewhalaw, 2007). In this same region, this medicinal plant has been known to be used traditionally in the management of rheumatism (Yineger *et al.,* 2008). In other East Africa and Southern Africa countries, this medicinal plant has also been used in the management of various infections, for instance, in South Africa, its extracts have been used in the treatment of maggots infested wounds (Jansen, 1981; Zorloni *et al.,* 2010). In northern Kenya, the Borana people use the leaf extracts soaked in cold water to treat louse infestation in both human and calves (Nana, 2010). Pharmacological studies have shown that the methanol leaf extracts from this medicinal plants have antibacterial and antioxidant activity (Adedapo *et al.,* 2008) which validates the traditional use for the treatment of bacterial dermatitis and other microbial infections (Tadeg *et al.,* 2005). This plant is also used as a natural pesticide to improve grain storage as illustrated in a research done by Louis *et al.,* 2007, which showed that the water and methanol extracts exhibited insecticidal activity against rice weevils (*Sitophilus oryzae*).

2.4.3 Secondary Metabolites Isolated from *Calpurnia aurea* subsp *aurea*

Earlier phytochemical studies reported the isolation of a series of quinolizidine alkaloids which are considered as characteristic chemotaxonomic markers for the *Fabaceae* family (Korir *et al.,* 2014). Some of the isolated alkaloids include 13-hydroxylupanine (**1**), hydroxylupanine (**2**), calpurnine (**3**), virgiline (**4**) and pyrrocarboxylic acid esters isolated from the leaves and bark of Ethiopian species. From the pods, 10, 13- dihydroxylupanine (**5**) was isolated using CH_2Cl_2, Calpurmenine (**6**) (Figure 2.1) was isolated from the South African species (Adedapo *et al.,* 2008; Asres *et al.,* 1986; Kubo *et al.,* 1984).

Apart from the quinolizidine alkaloids, flavonoids have also been isolated from *Calpurnia aurea* subsp *aurea* making them the second largest class of secondary metabolites isolated in the family *Fabaceae* (De Nysschen *et al.,* 1998). In a study done by (Korir *et al.,* 2014), five isoflavones that are reported to show moderate activity against breast cancer and renal melanoma cell lines tested. These compounds were isolated from the stem bark and they included Genistein (**7**), 5', 7-dihydroxy-3'-methoxyisoflavone (**8**), 7-hydroxy4', 8-dimethoxyisoflavone (**9**), 7-acetoxy-4',8- dimethoxyisoflavone (**10**), 3',7-dihydroxy- 4',8-dimethoxyisoflavone (**11**) (fig. 2.1).

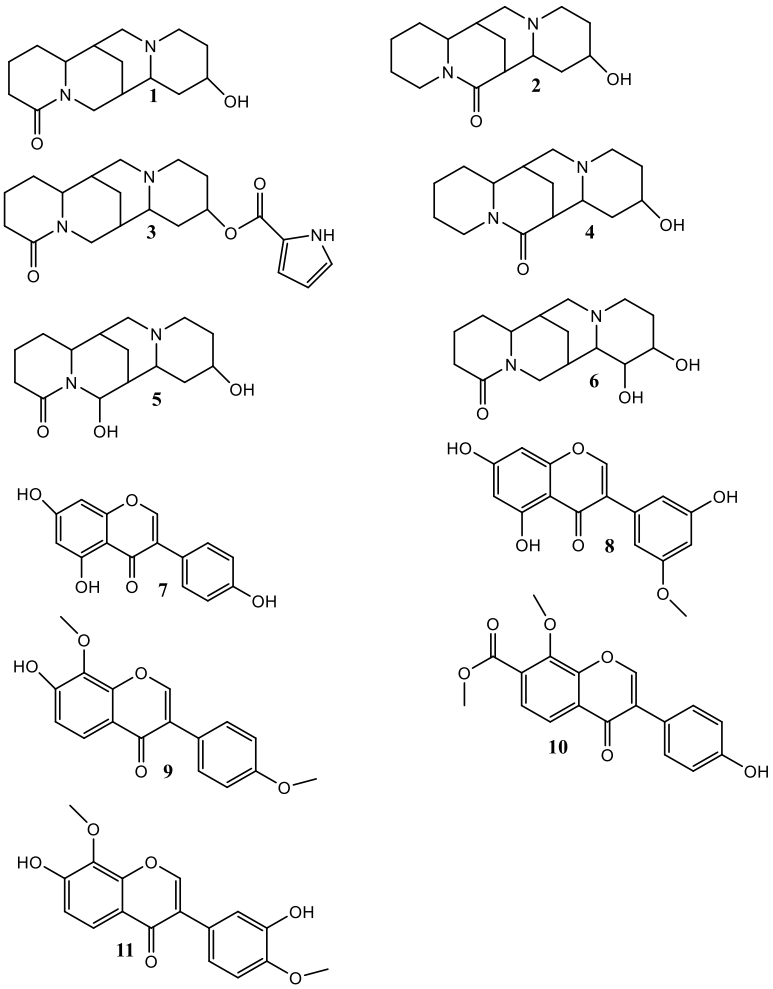

Figure 2.1: Quinolizidine alkaloids and Flavonoids isolated from *C. aurea* subsp *aurea*

2.5 Endophytes

Endophytes are endosymbionts either bacteria, fungi or unicellular organisms that are in association with plants either intracellularly or intercellularly which can be grown via specific growth medium (Rajivgandhi *et al.*, 2022). This colonization of the plant tissues by the endophytes have been demonstrated to be necessary for the health benefits and survival of the host plants (Potshangbam *et al.*, 2017). Some of the roles of microbial endophytes within the plant tissues include; secondary metabolites synthesis, alleviation of stress, nutrient absorption, plant disease resistance, enhancement of plant growth and promotion of resistance against disease causing pathogens (Hardoim *et al.*, 2015; Parthasarathi, 2012).

The mechanisms through which association of endophytes benefits the host plants include production of sidophores, fixation of nitrogen, phosphate solubilization and production of phytohormones (Yan *et al.*, 2018). Due to these factors, microbial endophytes have become a hot spot of research in areas of secondary metabolite production, plant

growth promoting factors and plant disease resistance. Despite their importance on plant health and growth, endophytic communities within a host plant are affected by parameters such as environmental conditions and host types (Santoyo *et al.,* 2016; Dudeja & Giri, 2014). Endopyhtes have been reported to be a great reservoir of metabolites that play an important role in growth of plants, development and act against disease causing pathogenic micro-flora. The production of these metabolites in their natural ecosystem specifically targets the pathogens of the host plants (Mousa & Raizada, 2013).

The most common metabolites that have been isolated from endophytic microorganisms are classified as alkaloids, steroids, quinones, polyketides, phenolic acids, aliphatic compounds, saponins, steroids, and terpenes (Mousa & Raizada, 2013). These secondary metabolites have been shown to have antimicrobial, cytotoxic, anti-insect and anti-pathogenic properties (Ghasemnezhad *et al.,* 2021). This study focused on the isolation and characterization of fungal endophytes for secondary metabolites isolation due to their previously reported benefits as source of novel and medicinal secondary metabolites.

2.5.1 Diversity of Fungal Endophytes in Plants

Endophytic fungal communities associated with host plants spend either entire life cycle or part of the life-cycle inside host tissues without causing any disease symptoms to the host plants. Unlike the mycorrhizal fungi which colonize the root tissues and extend beyond the rhizosphere, the true endopyhtes reside within the plant tissues for their entire life and when the plants die some of these endophytes become saprophytic (Puri *et al.,* 2016; Schulz & Boyle, 2007). The host plant of these fungal endophytes may contain obligate, competent, passenger type of microbial population or they may reside in a facultative association (Aamir *et al.,* 2020). The colonization of fungal endophytes in the host plants could occur inside leaf segments, root tissues, seeds, fruits, buds, over stems and or sometimes inflorescence of weed plants (Stępniewska & Kuåniar, 2013). Additionally, these fungal endopytes may colonize plant tissues through asexual and vertical transmission whereby the fungal endophytes colonize ovaries and florets of flowers and are later transmitted to the developing embryos (Liu *et al.,* 2017). The approximated number of fungal endophyte diversity in tropical plants is around 1.5 million to which other literature sources suggests that this number is underestimated (Arnold & Lutzoni, 2007; Shipunov *et al.,* 2008). Within the tropical ecosystem, the plant diversity includes non-vascular plants, vascular plants, grasses, ferns and allies, angiosperms and gymnosperms.

Two main groups of endophytic fungi tend to vary depending on taxonomic position,

eco-functioning and evolutionary relatedness. For instance the clavicipitaceous endophytes (C- endophytes) tend to infect the grasses while the non-clavipitaceous (NC-endophytes) are frequently charaterized from asymptomatic tissues of the plant species (Roy & Banerjee, 2018). The clavicipitaceous endophytes are Ascomycetes that belong the family *Clavipitaceae* and it comprises of species such as *Myriogenospora*, *Epichloë*/*Neotyphodium, Balansia*, *Claviceps* and *Cordyceps*. The non-clavicipataceous endophytes belong to the phylum Ascomycota and Basodiomycota and they are represented by the genera *Phoma*, *Aspergillus, Arthrobotrys, Paecilomyces, Colletotrichum, Cladosporium, Curvularia, Coprinellus, Fusarium, Phanerochaete, Penicillium* and *Alternaria* (Roy & Banerjee, 2018). Fungal endophytes are common in both photosynthetic and other plant tissues in biome that range from hot tropical deserts to rainforest and tundra (Arnold & Lutzoni, 2007). However, the extent of their diversity and patterns of host association are not well known and studied (Roy & Banerjee, 2018).

2.5.2 Pharmacological Potential of Fungal Endophytes

Fungal endophytes produce novel bio-active secondary metabolites in suitable media, under conditioned growth parameters and specific nutrient requirements which enhances their metabolism (Gakuubi *et al.,* 2022; Patil *et al.,* 2016). Hence some of the important pharmacological properties of major bio-active compounds synthesized from fungal endophytes include;

2.5.2.1 Antifungal

Isolation of novel antimicrobial secondary metabolites from fungal endophytes has provided an alternative means of tackling drug resistance by pathogens (Gill *et al.,* 2015). Examples of antimicrobial secondary metabolites isolated from fungal endophytes isolated from tissues of various medicinal plants include clavatol (**12**), guignardic acid (**13**), chaetomugilin D (**14**), viridicatol (**15**), enfumafungin (**16**), phomopsin A (**17**), fusarithioamide A (**18**), pestaloside (**19**), penijanthine A (**20**) (Gouda *et al.,* 2016) (Fig. 2.2).

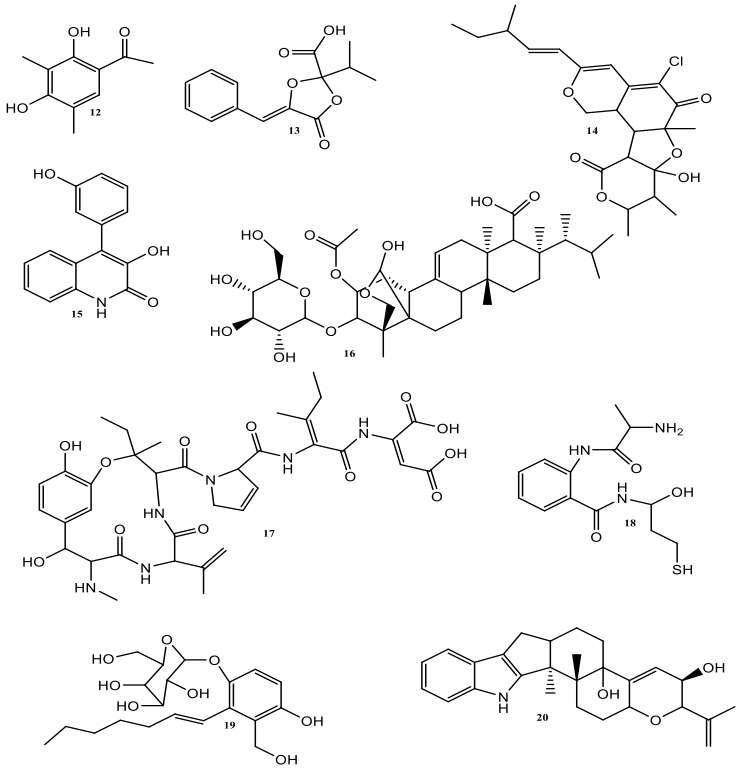

Figure 2.2: Antifungal secondary metabolites isolated from various fungal endophytes

2.5.2.2 Anticancer

Some of the anticancer secondary metabolites that have been isolated from various fungal endophytes include Taxol (**21**) isolated from *Taxomyces andreanae* which is associated with the bark of *Taxus brevifolia*. This drugs has been shown to prevent proliferation, growth and the spread of cancer cells which led to its approval by the Food and Drug Administration (FDA) and hence considered for treating cancer (Adhikari *et al.,* 2023). Furthermore, phenylpropanoid amides such as Brasiliamide A (**22**) produced from *Penicillium brasilianum* isolated from the root bark of *Melia azedarach* has been shown to have anticancer properties (Fill, 2010). Other sources of anticancer agents are podophyllotoxin (**23**) isolated from *Phialocephala fortini* associated with *Trametes hirsute* and *Juniperus communis* inhabiting the endosphere of *Podophyllum peltatum* and *Juniperus recurve* (Motyka *et al.,* 2023). The structures are shown in Figure 2.3.

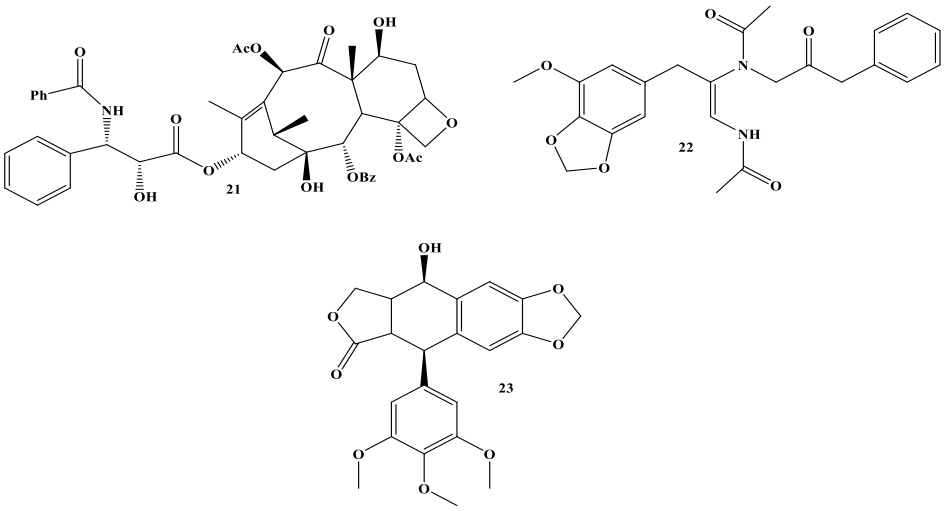

Figure 2.3: Anticancer secondary metabolites isolated from endophytic fungi

2.5.2.3 Antidiabetic

Diabetes, a disorder of individuals with high blood glucose, caused by due to lack of or insufficient insulin production or improper response of the cells within the body to insulin (Adeleke & Babalola, 2021). Due to concerning increase in diabetic cases worldwide, several research have been geared towards obtaining antidiabetic drugs from natural sources including microorganism. Fungal endophytes have been reported for antidiabetic and antilipidemic activities (Rathnayake *et al.,* 2019), for instance antidiabetic peptides isolated from endophytic fungi *Aspergillus awamori* isolated from *Acacia nilotica* (Singh & Kaur, 2016). Furthermore, certain antidiabetic secondary metabolites derived from endophytic fungi include N-acetylgalactosamine (**24**), produced by *Alternaria* sp., an endophytic fungus isolated from *Viscum album* (Melappa & Govindappa, 2015), and the nonpeptidal metabolite dimethyl asterriquinone B-1 (**25**), produced by *Pseudomassiria* spp. isolated from the African rainforest (Shubhpriya Gupta *et al.,* 2020). (S)-(+)-2-cis-4- trans-abscisic acid (**26**), 4-des-hydroxyl altersolanol A (**27**) and 7*0*-hydroxy-abscisic acid (**28**) isolated from *Nigrospora oryzae* associated with the leaves of *Combretum dolichopetalum* have been reported for their potential in reducing fasting blood sugar levels (Uzor *et al.,* 2017). 8-hydroxy-6,7-dimethoxy-3-methyl iso-coumarins (**29**) (Fig 2.4) produced by an endopyhtic fungi from *Xylariaceae* spp. form the stem of *Quercus gilva* Blume has been reported for its strong α-glucosidase inhibitory activity (Indrianingsih & Tachibana, 2017).

Additionally, extracts from *Phoma* spp and *Aspergillus* spp. isolated from *Salvadora oleoides* were reported to reduce blood sugar levels in winster albino rats when administered orally (Nonyelum *et al.,* 2015). The endophytic fungi from *Leucas ciliate* and *Rauwolfia densiflora* have also been reported for their prospects in treating diabetes has been reported

(Akshatha *et al.,* 2014). Compounds isolated from *Alternaria* spp., and *Fusarium* spp. have been reported as precursors to alpha glucosidase inhibitors have been reported in literature (Fadiji & Babalola, 2020). Hence, this together with the other mentioned reports establishes fungal endophytes a promising source of anti-diabetic secondary metabolites and a great source of pharmaceuticals.

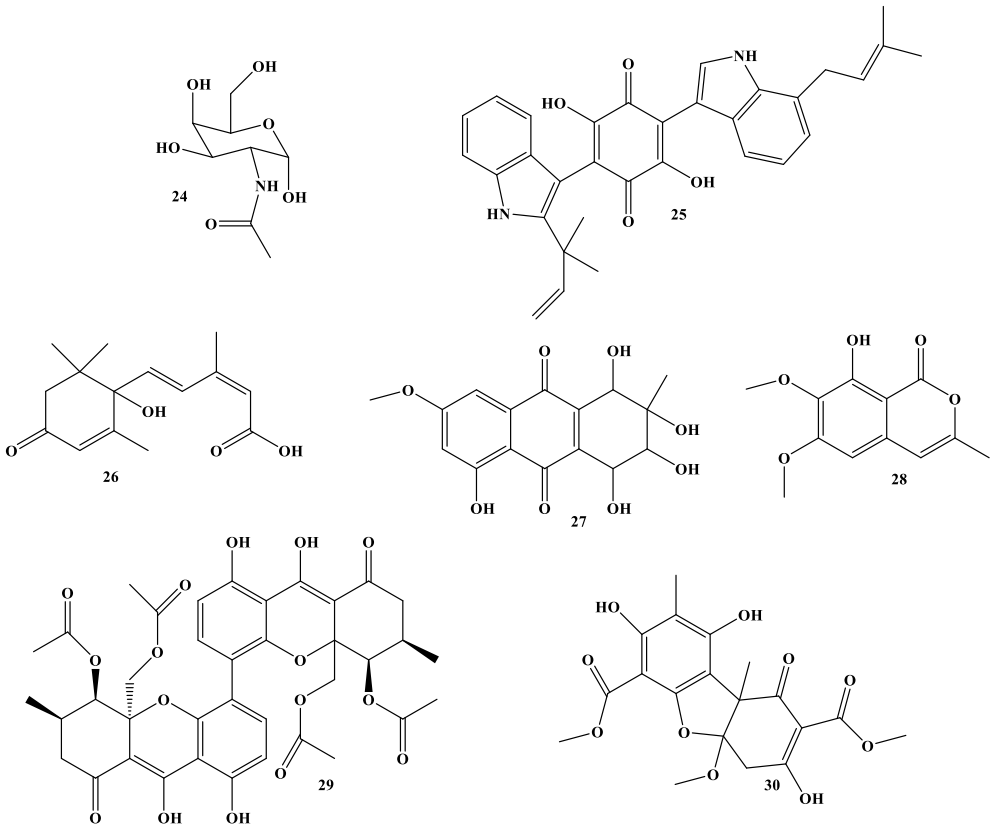

Figure 2.4: Antidiabetic secondary metabolites isolated from endophytic fungi

2.5.2.4 Antimalarial and Antiparasitic

Parasitism is a symbiotic association that occurs between organisms causing harm to one while the other benefits. A parasite therefore feeds on the hosts causing damage to the host cells (Adeleke & Babalola, 2021). The etiological agent of malarial parasite is *Plasmodium* species such as *Plasmodium malariae, P. vivax, P. falciparum*, and *P. ovale* causing more than 3.3 billion deaths upon infection (Ateba *et al.,* 2018). With the current rise in drug resistance by the malarial parasite there is need for urgent need for alternative and effective antimalarial drugs from natural sources and microorganisms. Fungal endophytes are of great potential in the synthesis of novel antimalarial drugs in the pharmaceutical industry. Cercosporin (**31**) produced by *Mycosphaerella* spp. isolated from *Psychotoria horizontalis* has been known to effectively control *Plasmodium falciparum, Trypanosoma cruzi* and

Leishmania donovani, hence considered as a great anti-parasitic agent (Wang *et al.,* 2017). Endopyhtic fungi, *Diaporthe miriciae* has been reported to produce bio-active antimalarial metabolite epoxy-cytochalasin H (**32**) (Fig. 2.5) which exhibited a great inhibition against *P. falciparum* resistant strain (Kumarihamy *et al.,* 2019).

In addition 19, 20- epoxycytochalasins C and D, 18-deoxy-19,20-epoxy-cytochalasin C and cytochalasins synthesized by *Nemania* spp. isolated from *Torreya taxifolia* exhibited phytotoxicity and antiplasmodial activity (Kumarihamy *et al.,* 2019). Similarly, antiplasmodial extracts were reported from an endopyhtic fungi isolated from *Symphonia globulifera*. Other endopyhtic strains such as *Aspergillus versicolor*, *Neocosmospora rubicola, Trichoderma afroharziamun, Penicillium citrillium* and *Fusarium* spp. have been reported as a potential source of antiplasmodial and antiparasitic secondary metabolites.

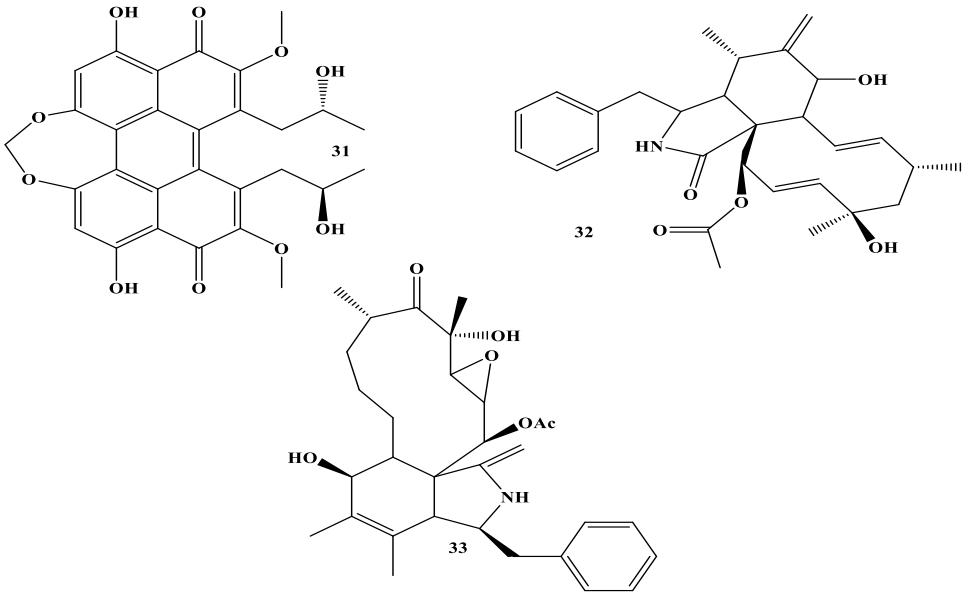

Figure 2.5: Antimalarial and antiparasitic secondary metabolites isolated from endophytic fungi

2.5.2.6 Antiviral

Endophytic fungi have been known to stand a chance as a great source of bio-active secondary metabolites in different pharmaceutical fields and that includes the antiviral properties hence making it a fascinating area of study. Although the bio prospecting of antiviral secondary metabolites is a promising field, there is little information documented in this area of exploration. Inappropriate or inefficient antiviral screening measures has been stated as a major constraint encountered in the discovery of antiviral drugs. Antiviral agents

such as cyclosporine U, podophyllotoxin (**23**) , sequoiatones C (**33**)-F, and cytonic acid A (**34**), and B, have been reported from different endophytic fungal species (Gupta *et al.*, 2020). Reports have also been made on antiviral secondary metabolites against human cytomegalovirus, Dengue virus (Raekiansyah *et al.*, 2017), influenza A virus (Liu *et al.*, 2019) and Human immunodeficiency virus (HIV) (Akash *et al.*, 2016). Cytonic acid A and B isolated from *Cytonaema* spp. have also been reported for their antiviral properties (Kumar *et al.*, 2017). Hinnuliquinone (**35**), a bioactive secondary metabolites produced by endophytic fungi colonizing the leaves of *Quercus coccifera* has been considered as an inhibitor against HIV-1 protease (Kumar *et al.*, 2017; Uzma *et al.*, 2018). Similarly, pullularins A (**36**)-D (Fig. 2.6) produced by *Pullularia* spp. is reported to exhibit antimalarial and antiviral activities against herpes simplex virus (HSV), additionally, Pestalotheo C produced by *Pestalotiopsis theae* isolated from an identified tree on jianfeng mountain, china has been reported to possess anti-HIV properties (Kumar *et al.*, 2017). *Alternaria tenuissima*, an endophytic fungi has been shown to synthesize Altertoxins which are effective against HIV-1 virus, several secondary metabolites produced by *Emericella* spp. such as dehydroaustin, emerimidine (A and B), austinol (**37)**, spernidine (**38**) (A, B), Austin (**39**), emeriphenolicins (A, D) and acetoxy dehydroaustin (**40**) (Fig. 2.6) have been reported to exhibit antiviral activities against influenza A virus (Raekiansyah *et al.*, 2017).

2.5.2.7 Immunosuppressive Effects

The search for immunosuppressive secondary metabolites as a source of immunomodulatory compounds which are important in the treatment of autoimmune disorders such as rheumatoid arthritis, insulin dependent diabetes and as precursors that are used to avert allograft declination in transplant patients (Kim & Moudgil, 2017). Research has proven that fungal endophytes have the capability of producing immunosuppressive secondary metabolites (Egbuta *et al.*, 2017), such as 13-*O*-acetylsydowinin B (**41**), sydoxanthone A (**42**) and B, dibenzofurane, methylpeniphenone, subglutinol A (**43**) and B, mycousnine (**44**) (Fig. 2.7) xanthone derivatives, benzophenone derivatives, lipopeptide, peniphenone, polyketide benzannulated spiroketal, (-) colutellin A, and polyketide benzannulated spiroketal (Leroy *et al.*, 2015).

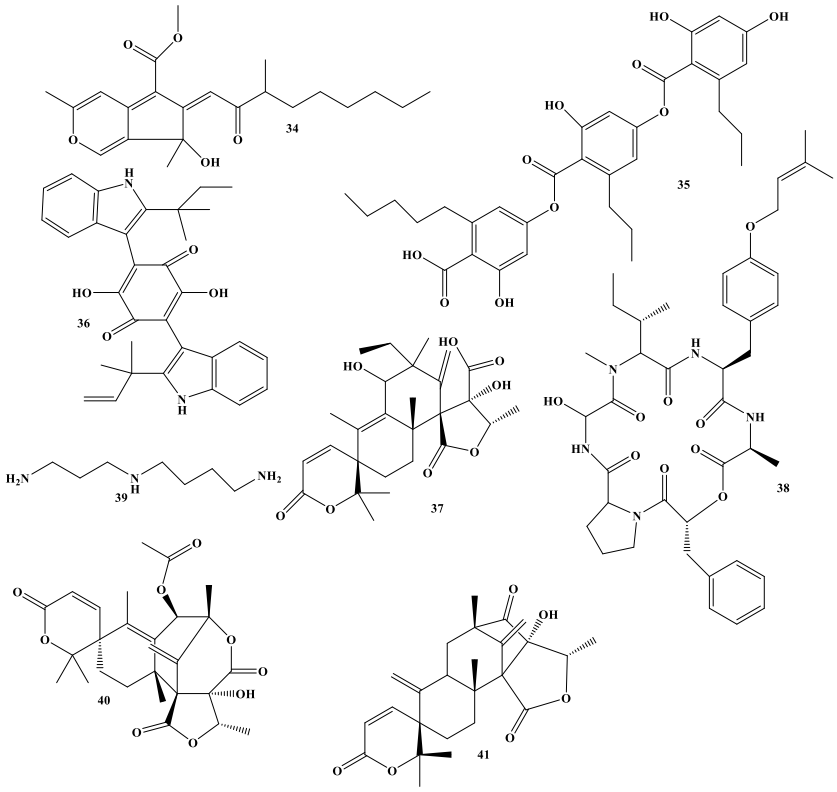

Figure 2.6: Antiviral secondary metabolites isolated from fungal endophytes

Additionally, Cyclosporin A synthesized by *Tolypocladium inflatum* and *Trichoderma polysporum* have been reported (El-Gowelli & El-Mas, 2015). *Fusarium subglutinam*, an endophytic fungi colonizing *Tripterygium wilfordii* has been reported to produce diterpene pyrenes and subglutinol A and B which exhibited a great immunosuppressive activity (Nalini & Prakash, 2017; Vasundhara *et al.,* 2016). A potent immunosuppressant Mycophenolic acid (**45**) (Fig. 2.8) used in medicine to the treatment of autoimmune diseases and in prevention of tissue rejection after transplant, is a secondary metabolites synthesized for endophytic fungi from the genera *Septoria*, *Bussochlamys*, *Aspergillus* and *Penicillium* has been reported in literature (Lin *et al.,* 2014; Song *et al.,* 2020). Subglutinol A and Colutellin A both produced from endophytic fungi can be used as an alternative drug for the treatment of immunosuppressive disorders, however, the actual molecular specificity and explicit mode of action of these drugs has not yet been identified (Lin *et al.,* 2014; Strobel, 2018).

In conclusion, these novel secondary metabolites from fungal endophytes can be used to accomplish the ever-increasing demand for novel and affordable immunosuppressive therapeutic drugs that can be used in the treatment of autoimmune diseases and post-transplantation care.

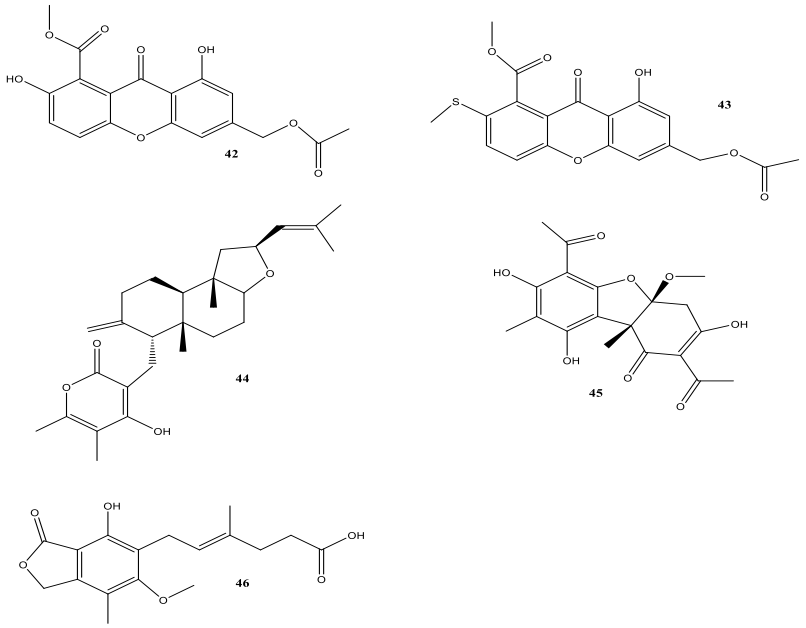

Figure 2.7: Immunosuppressive secondary metabolites isolated from fungal endophytes

CHAPTER THREE
ANTIDERMATOPHYTIC ACTIVITY OF FUNGAL ENDOPHYTES ASSOCIATED WITH *C. aurea* subsp. *aurea*

Abstract

Endophytes are microorganisms that live inside plant tissues without causing any harm to the host plant. They can be found in various plant parts, including leaves, roots, flowers, and stem bark. They also influence secondary metabolite formation in host plants. In this study, fungal endophytes were isolated from leaves, stem bark and roots of *C. aurea* subsp. *aurea* collected from Mt. Elgon National Forest. Prior to endophytes isolation, the explants were surface sterilized using 70% ethanol and 1% sodium hypochlorite and plated on PDA media amended with streptomycin (2 g/L). Pure isolates were obtained through subculturing, morphologically characterized, and identified using specific DNA bar-codes. Dual culture assays were conducted to evaluate antagonistic activities of the endophytes against *Trichophyton rubrum* (IDE 242), *T. interdigitalle* (LY34), *T. banhamiae* (IHEM 47010), *Microsporum canis* (D106) and *Nannzzia gypsea* (SK2458120) dermatophytes. A total of nineteen isolates were obtained from leaves, stem bark and roots. Morphological characterization, barcode identification and phylogenetic analysis, revealed that the isolates belonged to the phylum Ascomycota and Basidiomycota, representing 78.96 % and 21.04 % of the isolates, respectively. Furthermore, the endophytes belonged to the orders *Eurotiales*, *Diaportharales*, *Sphaeropsidales* and *Polyporales*. Dual culture assays generally showed that majority of the endophyte isolates possessed antagonistic activity against the dermatophytes tested. However, *Paraconiothyrium hawaiiense*, exhibited the greatest activity against *T. benhamiae, N. gypsea*, *T. interdigitalle* and *M. canis,* with a mean inhibition zone of 23 ± 0.5 mm. The results obtained suggests that the fungal endophytic composition of *C. aurea* subsp. *aurea* is diverse and possess antidermatophytic activities. The fungal endophytes that exhibited great antidermatophytic activities were considered for secondary metabolites isolation as described in chapter four. To the best of my knowledge, this is the first report on isolation of endophytic fungi from tissues of *C. aurea* subsp. *aurea* and thus paving way for screening endophytes capable of producing important secondary metabolites.

3.1 Introduction

For part or all their life cycles, endophytic fungi exist in healthy tissues of the stems, leaves, roots, flowers, and branches without causing any apparent symptoms to the host plant (Thi Hoa *et al.,* 2023). Generally, plant-microorganism associations are a product of years of

evolution, as evidenced by the presence of microorganisms in fossilized stem and leaf tissues (Taylor, 2000). Studies on fungal endophytes have expanded over the years, from cataloging the species to examining their interactions with host plants. Furthermore, isolates from medicinal plants have been of great interest in the race towards discovery of novel secondary metabolites and understanding their ecosystem benefits (Romina Gazis & Chaverri, 2010). Currently, endophytic fungi are an important source of biologically active secondary metabolites or lead compounds for the development of antifungals, antibacterial, antitumor, antidiabetic, antiviral, insecticidal, immunosuppressants, and phytohormones (Thi Hoa *et al.,* 2023). Additionally, endophytic fungi contribute towards plant growth as bio-fertilizers and protection of the host as bio-pesticides and thus could be useful in the agricultural sector (Murphy *et al.,* 2014).

Traditional methods of identifying endophytic fungi are direct observation of the fungal structures within the plant tissues under a light or electron microscope and cultivation-dependent techniques, whereby the endophyte is isolated from the tissues (Xiang Sun & Guo, 2012). However, the direct observation method only allows for the visualization of hyphal structures, limiting its use for definitive identification at different taxonomic levels. Additionally, endophytic isolates cannot be obtained for further downstream analysis or use (Deckert *et al.,* 2001). The cultivation-dependent technique efficiently retrieves a high number of endophytic fungal species from plant tissues. However, this method is influenced by factors such as sterilization techniques, incubation conditions, and the sporulating capabilities of the endophytic fungi, among others. Furthermore, a large number of fungi taxons cannot be identified based on their morphological characteristics due to their inability to sporulate (Xiang Sun & Guo, 2012).

Molecular techniques, like DNA bar-coding and sequencing, help overcome challenges in identifying fungal endophytes based on morphology. DNA bar-coding system entails the use of an effective, short and standardized gene region that is used to identify species (Hebert *et al.,* 2003). In DNA bar-coding, the inter-specific distance of the bar-code region should not exceed the intra-specific distance (Gaytán *et al.,* 2020). Additionally, the DNA sequence of choice should be specific, unique and constant to a single species (Letourneau *et al.,* 2010). Mycologists have assessed various DNA fragments for their suitability in fungal DNA bar-coding. For instance, the cytochrome C oxidase subunit 1 (*CO1* gene) evaluated first, however, introns with various lengths in fungi was discovered and hence found unsuitable as a fungal DNA bar-code (Vialle *et al.,* 2009; Zhao *et al.,* 2011). The internal transcribed spacer (ITS) region has been identified as a good candidate for fungal DNA bar-coding, with advantages

such as high successful amplification rates among all lineages of fungi using universal primers. It is of a suitable fragment length coupled with availability of large number of databases (Druzhinina *et al.,* 2005; Nilsson *et al.,* 2009). The main disadvantage of ITS bar-code is the presence of various inter- and intra-specific distances among different fungal groups making it difficult to unify the ITS divergence threshold for fungal species (Sun *et al.,* 2014; Zhao *et al.,* 2011). Additionally, a number of research has demonstrated that ITS is not sufficient for some species delimitation especially among the rapidly evolving species, diverse genera or even species complexes (Gazis *et al.,* 2011; Lacap *et al.,* 2003). Despite these disadvantages' mycologists agree that ITS is the most widely used DNA bar-code in molecular identification and has shown great potential in diversity and ecological studies (Sun *et al.,*2014). There are other DNA bar-codes that are used in addition to ITS bar-codes namely; large sub-unit (LSU), Translation elongation factors (TEF1α) and beta- tubulin proteins (J. Xu, 2016).

Dermatophytes are pathogenic fungi that are highly specialized to infect nails, hair, or the stratum corneum. Their virulence is mainly attributed to the secreted proteolytic activity of the endo- and exo-proteases (Monod, 2008). An increase in the number of dermatophytosis cases has been reported in recent years, with alarming cases of recurrent and recalcitrant cases reported in some parts of the world (Shankarnarayan *et al.,* 2020). These infections include those that were previously considered responsive to commercially available oral and topical antifungal agents. Some of the reasons for treatment failure with these antifungals include poor compliance with the treatment regime, misuse of strong topical corticosteroids or steroid combinations, variability in the quality of the antifungal drugs, including generic products, and host immune dysfunction (Sardana *et al.,*2021). These features partially explain the spread and transmission of dermatophytic infections within a population. However, resistance to antifungals by disease-causing dermatophytes is also increasingly reported globally, and it has been cited as a further reason behind the recent increase in recalcitrant or recurrent fungal skin disease (Sardana *et al.,* 2021). The rising cases of antifungal resistance by various dermatophytic strains necessitate the search for alternative ways of managing these conditions from natural sources such as medicinal plants, tropical fungi, and endophytic fungi (Khan *et al.,* 2022).

To date, several plant species have been studied for the presence of endophytic fungi, and results show that they are rich in endophytic fungal composition (Schneider *et al.,* 2008). However, there are no reports on the endophytic fungal composition of *C. aurea* subsp. *aurea* (*Ca*). This chapter therefore focused on the isolation, morphological, and molecular characterization of fungal endophytes from *Ca* using ITS as the primary barcode, followed by

LSU and *Tef*. Additionally, the antagonistic (antimicrobial) potential of these endophytes was determined against disease-causing dermatophytes via the dual culture method.

3.2 Material and Methods

3.2.1 Site and Sample Collection

Fresh leaves (3 leaves from the crown of each tree), roots (collected from three different tree rhizosphere sites), and stem bark (one meter above the ground and collected from three different sites) samples of *Ca* were randomly collected from Mt. Elgon National Park, a conserved region at an altitude of 2080 msl (N 01º 01.955′, E 034º 46.815′). This region was selected because of the great biodiversity and being an undisturbed area. Three sites were selected within the sampling area, which were approximately 1 km apart from each other. From each site, one tree was randomly chosen for sample collection. Three apparently healthy leaves were collected randomly from the crown of each tree. Similarly, three samples from the roots and the stem bark were cut out using a sterilized knife. For the stem bark samples, pieces of approximately 3×6 cm in size were collected from approximately one meter above the ground. The samples were packed in khaki bags and endophytes isolated within 24 hours. The identity of the tree was authenticated by a botanist from Egerton University Kenya (Prof. S. T. Kariuki) and the voucher specimen deposited at the University of Nairobi, Biological Sciences Department herbarium, under the voucher specimen number JCM_UON2020_001.

3.2.2 Isolation of Fungal Endophytes

In the lab, samples were washed under running tap water to remove soil particles and blot-dried using sterile paper towels. The samples were then surface sterilized following the procedure described by Arnold *et al.* (2001), by emersion in 70% ethanol for 2 minutes, followed by 1% sodium hypochlorite for 3 minutes, and rinsed in three changes of sterile distilled water to remove any traces of disinfectants. The surface sterilization of these tissues eliminated unwanted epiphytes and other surface contaminants. This method of surface sterilization has been widely used in various endophytic fungi isolation (Santamaría *et al.,* 2005); hence, the preprint control was not used to test for the growth of epiphytes. The sterile leaves, barks, and root tissues were aseptically cut into smaller portions of approximately 1 mm x 4 mm and inoculated into petri dishes containing potato dextrose agar (PDA) medium amended with streptomycin (2 g/liter) to eliminate the growth of endophytic bacteria. The plates were incubated at 25 ± 2 °C for 1-4 weeks with frequent monitoring to check for hyphal growth. Hyphal tips of the developing fungal colonies were transferred to freshly prepared PDA media for pure culture growth.

3.2.3 Morphological Characterization of Endophytes

The pure fungi isolates were first identified based on morphological characteristics of the colonies as observed on PDA media under ambient daylight conditions. They were identified to morphospecies level using the following parameters: colony appearance, mycelium color, type of anamorph, and base color, indicating the metabolites produced in the growth media. This formed the basis of further analysis using molecular tools.

3.2.4 Molecular Identification of the Endophytes

3.2.4.1 DNA Isolation

The isolated endophytes were identified using molecular techniques according to the procedures described by Kolařík *et al.* (2023). Pure cultures of the fungal endophytes were grown in PDA media at 28 °C for 7 days to allow fungal mycelia growth for DNA isolation. DNA was isolated using BIO BASIC EZ-10® Genomic DNA Kit following the manufacturer's instructions. Briefly, fungal hyphae (60 mg) obtained from 7-day-old axenic cultures were placed in 1.5 mL screw-caped microfuge tubes. Precellys® ceramic beads (6-10, 1.4 mm) and plant cell lysis (PCB) buffer (600 µl) were added and the mixture homogenized. After homogenization, β-mecaptoethanol (12 µl) was added (to aid in protein degradation), and the mixture was vortexed and incubated at 65 ^{o}C for 25 minutes in a metal block. Approximately 600 µl of chloroform was added (to aid in the solubilization of the polysaccharides and proteins from the DNA), and the mixture was centrifuged at 10,000 rpm for 2 minutes. The supernatant was later transferred into a clean tube, and the rest of the pellets were discarded. Binding buffer (BD buffer) was added to the supernatant (to allow for the binding of the DNA to the column) and the mixture vortexed (to allow for uniform mixing). After which, ethanol (200 µl) was added and the sample vortexed again. The mixture was transferred into the EZ-10 column placed in a 2 mL collection tube and then centrifuged for 1 minute at 12,000 rpm. The supernatant was discarded, and then PW buffer (500 µl) was added (to aid in the removal of the extra proteins and colored contaminants), and the mixture was centrifuged again at 12,000 rpm for 1 minute and the supernatant discarded. The isolated DNA was washed by centrifugation at 12,000 rpm for 1 minute using 500 µl of wash solution diluted with ethanol (to aid in the removal of extra salts). The supernatant was discarded and the column centrifuged once again in the same condition to remove the excess wash solution that might have remained. The empty column was then transferred into an empty 1.5 ml eppendorf tube, and 70 µl of warmed TE buffer was added to the center of the EZ membrane to increase elution efficiency.

The sample was then incubated for 2 minutes and then centrifuged at 12,000 rpm for 2 minutes to enable the DNA elution. The isolated DNA was stored at 4 °C for further analysis.

3.2.4.2 Polymerase Chain Reaction (PCR) Amplification

Three nuclear ribosomal regions, internal transcribed spacer (ITS), large subunit (LSU), and elongation factor 1 alpha (EF1α), were targeted for identification of fungal isolates. Firstly, a 560 base pair nuclear rDNA fragment containing the internal transcribed spacers (ITS1 and ITS2) and a 5.8S subunit was amplified using universal DNA barcode primers ITS1 and ITS4 (Table 3.1). Secondly, the EF1α gene was amplified using primer pairs EF-728F and EF-986R (Table 3.1). The LSU gene was amplified using forward primer NL-1 with reverse primer NL-4 or LR7 (Table 3.1). The PCR mixture (20 µl total reaction volume) contained 14.2 µl PCR water, 4 µl of 5× MyTaq PCR buffer (Bioline, London, UK), 0.2 µl MyTaq DNA polymerase (Bioline GmbH; 5 U μl^{-1}), 0.3 µl each primer (10 µM stock concentration) and 1 µl (50 ng ml^{-1}) genomic DNA. The PCR reaction conditions in a Master Cycler Gradient Thermocycler (Eppendorf, Hamburg, Germany) were as follows for all the amplified regions: initial denaturation at 93 °C for 2 min; 38 cycles of 93 °C for 30 s, 55 °C–60 °C for 30 s, 72 °C for 60 s; and final extension at 72 °C for 10 min. DNA template was substituted with PCR water for the control. For each PCR product, 1-µL aliquots were mixed with Midori green dye and subjected to electrophoresis using 0.8% agarose gel in 1× TAE buffer for 30 minutes at 100 volts. The gels were visualized using a UV transilluminator (Nippon Genetics Europe GMbH). The remainder of the amplified PCR products (19 µl) were purified with ExoSAP cleanup reagent (Thermo Fischer Scientific, Waltham, MA, USA) following the manufacturer's instructions.

3.2.4.3 Sequencing of PCR Fragments and Phylogenetic Analysis

The cleaned PCR products were sent to Macrogen, Europe (Amsterdam, Netherlands) in a 96 well plate after mixing together with the respective primers and sequenced through the paired-end Sanger technique using primers described in Table 1. The forward and reverse sequences were manually edited using Bio Edit® sequence alignment editor version 7.2.5 (Hall, 2013). The consensus sequences were then compared against respective sequences deposited at GenBank's database in the National Center for Biotechnology Information (NCBI) website (http://www.ncbi.nlm.nih.gov/) using the BLASTN program (Altschul *et al.*,1997). Molecular identification of the isolates using consensus sequences for all the DNA barcodes was based on query and subject sequences having identity scores of 100%, e-values of 0 and query coverage ≥ 90% of the BLASTN targeted loci.

Table 3.1: Primer pairs for molecular identification of fungal endophytes isolated from *C. aurea* subsp. *aurea* (*Ca*) tree samples obtained from Mt. Elgon Forest National Park in western Kenya

S/No.	Primer	Primer sequence	Target	Reference
1	ITS1 (F)	5-tccgtaggtgaacctgcgg-3	ITS 1	White *et al.*, 1990
2	ITS4 (R)	5-tcctccgcttattgatatgc-3	ITS 1	White *et al.*, 1990
3	EF-728 (F)	5-catcgagaagttcgagaagg)-3	eEF1α	Carbone *et al.*, 1999
4	EF-986 (R)	5-tacttgaaggaacccttacc-3	eEF1α	Carbone *et al.*, 1999
5	NL-1 (F)	5-gcatatcaataagcggaggaaaag-3	26S	O'Donnell, 1992
6	NL-4 (R)	5- ggtccgtgtttcaa-3	26S	O'Donnell, 1992
7	LR7 (R)	5- gacgg tactaccaccaagatct-3	26S	Vilgalys & Hester, 1990

The consensus ITS sequences obtained from this study and those obtained from GenBank (Appendix 165) were used to conduct phylogenetic analysis. These sequences were aligned using the Multiple Sequence Comparison by Log-Expectation (MUSCLE) (Edgar, 2004) alignment algorithm in Molecular Evolutionary Genetics Analysis (MEGA) version 11 (Tamura *et al.*, 2021). Maximum likelihood phylogenetic trees (Felsenstein & Churchill, 1996) with 1000 bootstrap analysis were constructed with MEGA version 11 (Tamura *et al.*, 2021) using the Kimura 2-parameter evolutionary model and gamma model of rate heterogeneity settings (K2 + G). Unordered characters, random taxon addition sequences, and gaps were treated as missing data. The basidiomycetes, *Corpinusradians,* and *Corprinopsis verticillata* were used as out-groups for the phylogenetic analysis. The tree was viewed in MEGA (Waterhouse *et al.*, 2009) and exported as PDF.

3.2.5 Screening Endophytes Anti-dermatophytic Activity

The dermatophytic strains *T. rubrum* (IDE 242), *T. interdigitalle* (LY34), *T. banhamiae* (IHEM 47010), *M. canis* (D106), and *N. gypsea* (SK2458120) were obtained as already prepared and fully characterized cultures from the institute of microbiology, Czech Academy of Sciences. These cultures were scrapped off a fully-grown plate and suspension prepared

using sterile distilled water. From the respective suspensions, cotton swabs were used to spread the strains on the Muller Hinton Agar (MHA) media in petri dishes and allowed to dry. Using a sterile cork borer, six-millimeter-diameter (6 mm) of 7-day-old mycelia plugs for each endophytic fungus were placed on plates inoculated with each dermatophyte. The plates were then incubated at ± 32°C for a period of 72 hours. For positive controls, the media was augmented with 1 mg/mL miconazole and 1.5 mg/mL voriconazole, which are the commercially available antidermatophytic drugs. Each treatment per experiment consisted of 3 plates, and three replicate experiments were carried out. The zone of inhibition was measured, and the average zone of inhibition was calculated to determine the most active endophyte isolate.

3.3 Results

3.3.1 Morphological Identification of Isolated Endophytes

A total of nineteen (19) distinct fungal endophytes were identified based on morphological characteristics. The morphology of the isolated species ranged from loosely textured white non-spore-forming species to yellow/green spore-forming species. Based on the colony characteristics, the 19 isolates were putatively grouped into six genera, namely *Aspergillus, Diaporthe, Talaromyces, Trametes, Penicillium,* and *Paraconiothyrium* (Table 3.2; Plate 3.1). The frequency of endophyte isolation from the tree parts was as follows: roots (11), stem bark (5), and leaves (3), representing 57.9, 26.3, and 15.7%, respectively.

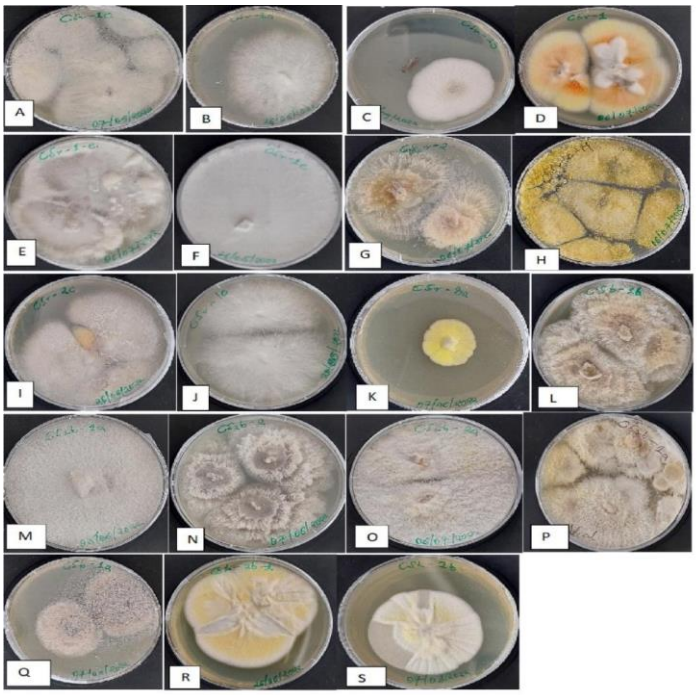

Plate 3.1: Morphological characteristics of the isolated fungal endophytes

Table 3.2: Morphological description of 19 axenic cultures of endophytic fungi isolated from *C. aurea* subsp. *aurea* roots, leaves and stem bark

Isolate Number	**Distinguishing morphological characteristics on PDA**
Csr-2C	Fast growing, loosely textured, lightly sporing, olive brown in color
Csb-1a	Fast growing, Yellowish- White with aerial mycelium, reverse buff with zonate and irregular lines
CsB-1b	Fast growing, white with aerial mycelium, reverse buff with zonate and irregular lines
Csr-1	Loosely textured, raised cultures, orange- green in color, lightly sporing
Csr-1a	White in color, very densely/ hairy hyphae, non- spore forming, Thick and tough flesh
Csr1c-2	White in color, very densely/ hairy hyphae, non- spore forming, thick and tough flesh
Csr-2	Fast growing, yellowish-white with aerial mycelium, reverse buff with zonate and irregular lines
Csl-2b	Light green aerial part, slightly loose spores,
Csr1e	White in color, very densely/ hairy hyphae, non- spore forming, thick and tough flesh
Csr1aN	Whitish in color with long hyphae
Csr3a	Yellow colony with white edges and sparingly loose spores
Cs2b-1a	Fast growing, White with aerial mycelium, reverse buff with zonate and irregular lines
Csl-1a	White-brown in color with fluffy appearance
Cs2b-2b	Olive brown in color with loose hyphae
Cs2b-2a	White-brown in color with fluffy appearance
Csr2b	Fast growing, grey with aerial mycelium, reverse buff with zonate and irregular lines
Csr-2	Fast growing, Yellow with aerial mycelium, reverse buff with zonate and
Csr1c-1	irregular lines
	Yellow/ orange in color with sparsely loose spores
Csl2b-1	Yellow whitish in color with sparsely loose spores

*Csr- roots isolates, Csl- leaf isolates, Csb- bark isolates

3.3.2 Molecular Characterization of Fungal Endophytes

The PCR amplification product resolved on 0.8 agarose gel revealed that the ITS amplicons obtained ranged between 500 and 700 bp, the LSU amplicons ranged between 635 and 651 bp and the elongation factor ranged between 700 and 770 bp. After sequencing the PCR amplicons, the actual size of the amplicon consensus sequences was within the ranges observed on 8% agarose gels (Appendix 169). All the samples were amplified using ITS primers (Plate 3.2 A) and the LSU primer set (Plate 3.2 B); however, only one sample was amplified by elongation factor primers (*TEF-1a*).

NCBI BLASTN targeted loci search using the ITS, LSU, and TEF-1α consensus sequences of the nineteen endophytes isolates reported in Section 3.4.1 revealed that 78.96% and 21.044% of the endophytes belong to the phylum Ascomycota and Basidiomycota, respectively. Furthermore, molecular identification based on BLASTN search revealed that the 19 endophyte isolates belong to the genera *Diaporthe* (36.7%), *Penicillium* (21.1%), and *Aspergillus* (10.5%). Other identified genera, which are rarely isolated, were *Talaromyces* and *Paraconiothyrum,* each representing 5.3% of the total isolates (Fig. 3.1). The genus *Trametes* was the only basidiomycetes isolated from this study, representing 21.1% of the total isolated fungal endophytes (Figure 3.2). Based on the explant source, molecular identification revealed that leaf isolates were identified as *Diaporthe velutina*, *Penicillium rubens,* and *Penicillium sp.* The stem and bark isolates were identified as *Diaporthe maritime, Diaporthe velutina, Paraconiothyrium hawaiiense, Diaporthe foeniculina,* and *Diaporthe foeniculina,* and the root isolates were *Talaromyces pinophilus, Trametes hirsute, Aspergillus flavus, Trametes hirsute, Penicillium rubens, Trametes hirsute, Diaporthe foeniculina, Trametes hirsute, Diaporthe ravennica, Aspergillus hancockii,* and *Penicillium manginii.*

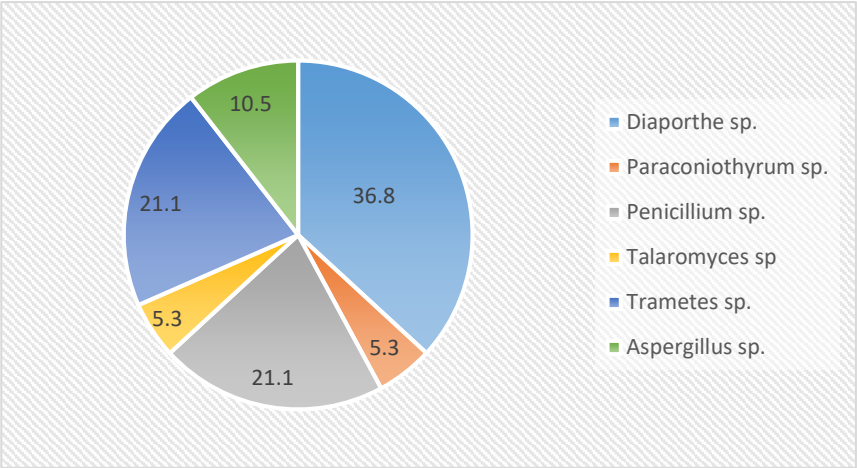

Figure 3.1: Species distribution (%) of 19 fungal endophytes isolated from leaves, roots and stems of *C. aurea* subsp. *aurea*

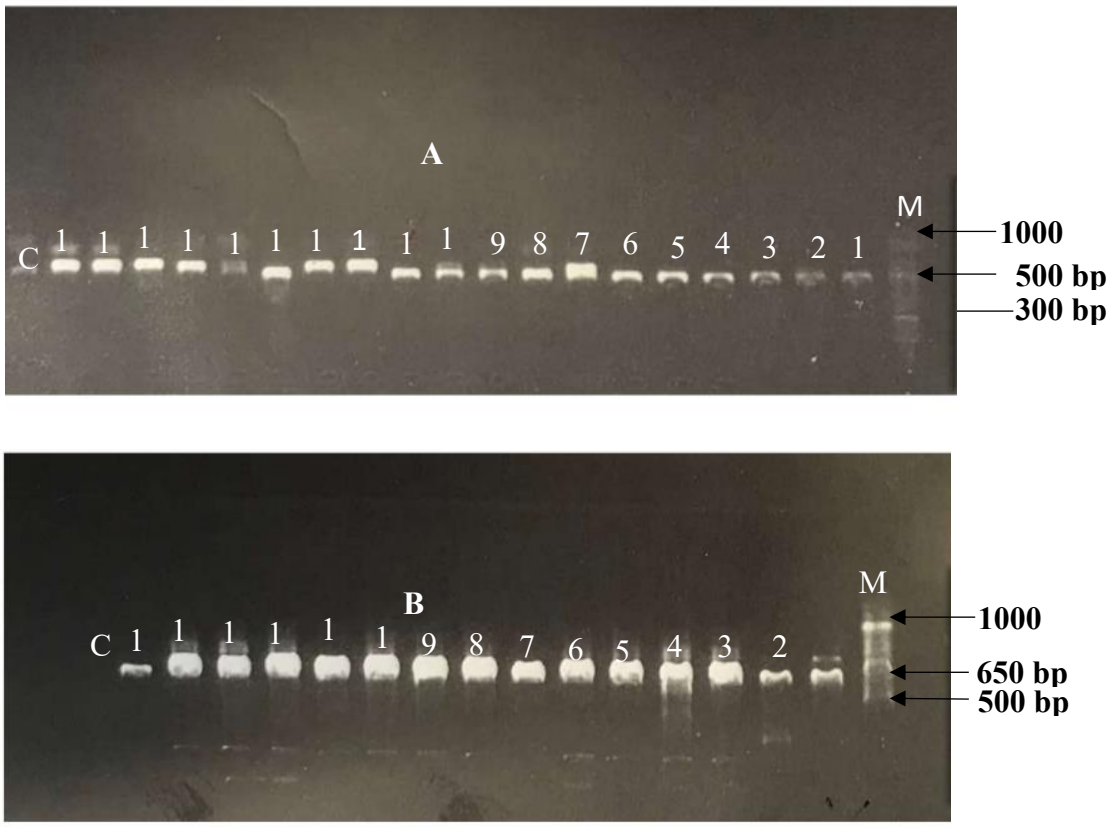

Plate 3.2 A: Gel electrophoresis image of the ITS amplicons. **B**: Gel electrophoresis image of the LSU amplicons**.** The molecular ladder used in the PCR amplification was 1000kb. The ITS amplicons had a molecular weight of approximately 530kb while the LSU amplicons were approximately 650kb.

1 (CsR-2C), 2 (Csb-1a), 3 (CsB-1b), 4 (CsR-1), 5 (CsR-1a), 6 (CsR1C-2), 7 (CsR-2), 8 (CsL-2b), 9 (CsR1e), 10 (CsR1aN),11 (CsR3a), 12 (Cs2b-1a), 13 (CsL-1a), 14 (Cs2b-2b), 15 (Cs2b-2a), 16 (CsR2b), 17 (CsR-2), 18 (CsR1C-1), 19 (CsL2b-1).

3.3.3 Phylogenetic Analysis of the Isolated Endophytes

To determine the phylogenetic relationship among the endophytic fungi from *Ca*, the ITS and LSU genes amplified from isolates and sequences were compared to the ones already deposited in the NCBI database. The identities of the isolates based on BLAST search as well as percentage similarities to previously deposited sequences were determined and tabulated (Appendix 165). The results revealed that all the isolates had 99% to 100% sequence similarities for both the ITS and LSU sequences with relevant sequences in the GenBank (Appendix 165). Phylogenetic analysis using the ITS region of the endophytic fungi is distributed into five clusters belonging to four different orders: *Eurotiales, Diaportharales, Sphaeropsidales,* and *Polyporales,;* the classes *Eurotiomycetes, Sordariomycetes, Coleomycetes,* and *Agariomycetes,* respectively, in the phylogenetic tree (Fig. 3.3). Further interpretation reveals that clusters A-D have strains that belong to the division Ascomycota, while the Basidiomycetes were in cluster E of the phylogenetic tree.

Further analysis of the tree showed that fungal endophytes from the three parts of *Ca* belonged to six genera. Clade A was comprised of six isolates belonging to the genera *Aspergillus, Penicillium,* and *Talaromyces*. Clade B had two isolates, which had close similarity with *Diaporthe canthii*. Five isolates were clustered in clade C, with two isolates showing a close relationship with *Diaporthe velutina* with a 90% bootstrap value and three isolates showing a close relationship with *Diaporthe foeniculina* with a 100% bootstrap value. Clade D was represented by one isolate, which showed a very high similarity to *Paraconithyrium haiwensii* with a 100% bootstrap value. The last clade E in the order *Polyporales* was composed of four singleton sequences, which strongly clustered to *Trameteshirsute* with 100% bootstrapping (Fig. 3.4). All these endophytes were subjected to antimicrobial activity against the available dermatophytes.

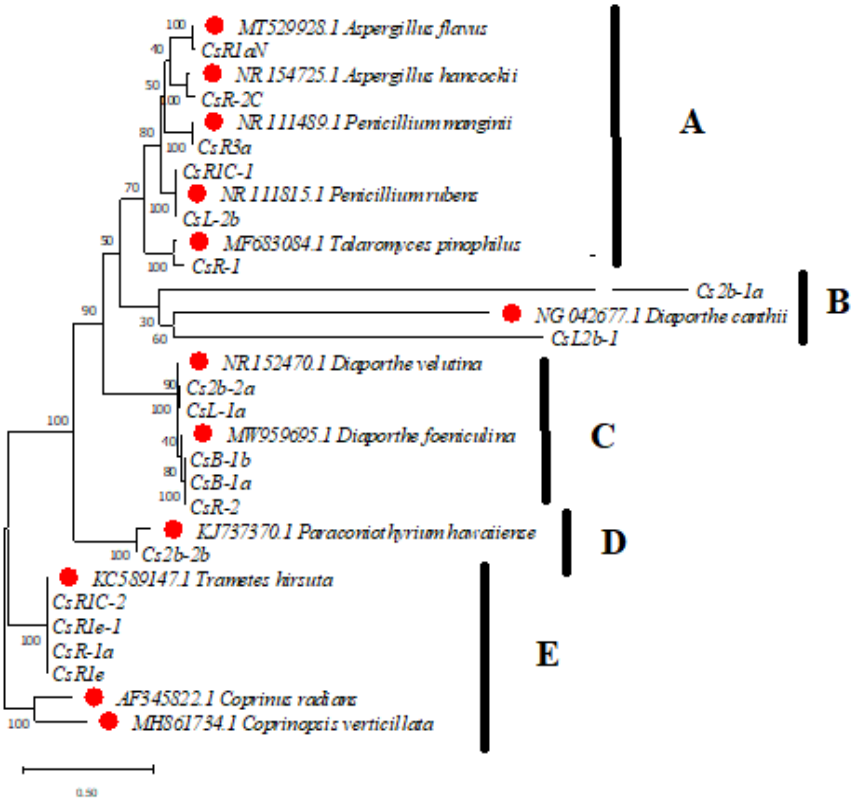

Figure 3.3: Phylogenetic tree of identified isolates associated with *C. aurea* subsp. *aurea*. The numbers at the nodes of the phylogenetic tree are percentages that indicate the levels of bootstrap support from 1000 replicates based on a neighbor joining analysis. The scale bar represents substitution per nucleotide position.

3.3.4 Antidermatophytic Activity of Isolated Endophytes

Out of the 19 endophytes, *P. hawaiiense* showed the greatest activity against all the dermatophytes, with a mean inhibition zone of 25±0.5 mm (Table 3.4; Plate 3.3). While endophytes identified as *D. maritima* and *A. flavus* exhibited activity against two dermatophytes. The isolates identified as *P. rubens*, *A. hancockii*, and *T. hirsuta* had activity against one dermatophyte each (Table 3.3).

Table 3.3: Antidermatophytic activities of the isolated fungal endophytes against disease causing dermatophytes

Endophyte Code	Identity	Test dermatophytes (Diameter in mm, n=3			
		T. benhamiae	*N. gypsea*	*T. interdigitalle*	*M. canis*
Cs2b-1a	*Diaporthe maritima*	0*	0	16 ± 0.5	15 ± 0.5
Cs2b-2a	*Diaporthe velutina*	0	0	0	0
Cs2b-2b	*Paraconiothyrium hawaiiense*	22.5 ± 0.5	20 ± 0.5	25 ± 0.5	25 ± 0.6
Csb-1a	*Diaporthe foeniculina*	0	0	0	0
Csb-1b	*Diaporthe foeniculina*	0	0	0	0
Csl-1a	*Diaporthe velutina*	0	0	0	0
Csl-2b	*Penicillium rubens*	20 ± 0.6	0	0	0
Csl2b-1	*Penicillium sp.*	0	0	0	0
Csr-1	*Talaromyces pinophilus*	0	0	0	0
Csr-1a	*Trametes hirsuta*	0	0	0	0
Csr1aN	*Aspergillus flavus*	23 ± 0.5	0	0	20 ± 0.6
Csr1c-1	*Penicillium rubens*	0	0	0	9 ± 0.5
Csr1c-2	*Trametes hirsuta*	0	0	0	0
Csr1e	*Trametes hirsuta*	9 ± 0.5	0	0	0
Csr1e-1	*Trametes hirsuta*	9 ± 0.5	0	0	0
Csr-2	*Diaporthe foeniculina*	0	0	0	0
Csr2b	*Diaporthe ravennica*	0	0	0	0
Csr-2c	*Aspergillus hancockii*	22 ± 0.8	0	0	0
Csr3a	*Penicillium manginii*	0	0	0	0
Positive control	Voriconazole (1.5 mg/ mL)	35.5 ± 0.5	28.5 ± 0.5	30.5 ± 0.5	32.5 ± 0.5
	Miconazole (1 mg/ mL)	25.6± 0.5	30.5± 0.5	28.5± 0.5	30.5± 0.5

* Values indicate zone of inhibition (mm) and are means of three replicate experiments followed by SD. *Csr- roots isolates, Csl- leaf isolates, Csb- bark isolates

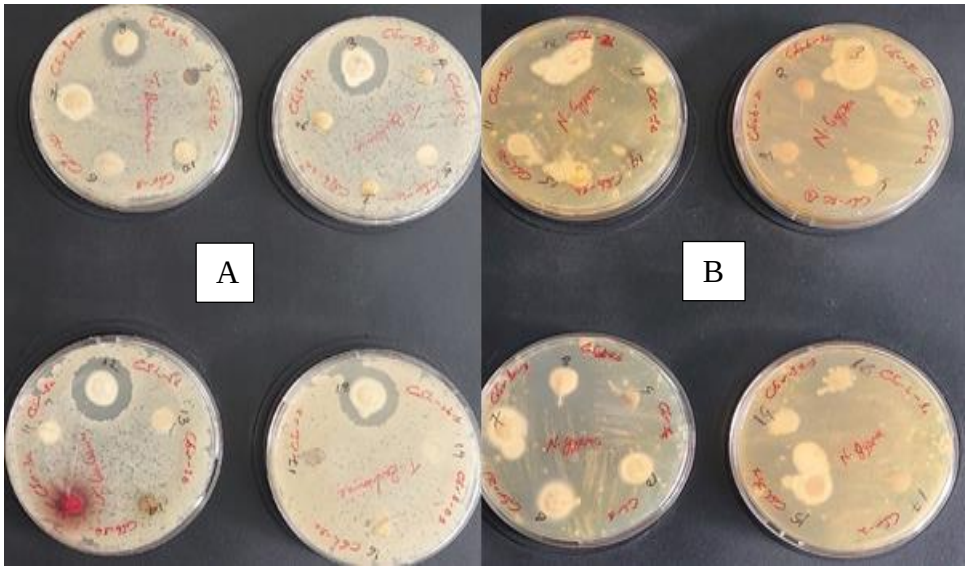

Plate 3.3: Dual culture assay of the isolated fungal endophytes against the test dermatophytes

Plate A: Antidermatophytic activities of *P. hawaiiense* (3), *P. rubens* (8), *A. flavus* (12) and *A. hancockii* (18) against *T. benhamiae*. Plate B: Antidermatophytic activities of *P. hawaiiense* (3), *P. rubens* (8), *A. flavus* (12) and *A. hancockii* (18) against *N. gypsea*.

3.4 Discussions

One of the major benefits of fungal endophytes is their capability to produce bioactive secondary metabolites with potential pharmaceutical benefits. However, isolation and characterization of the fungi are the most crucial stages in harnessing these secondary metabolites (Reis *et al.*, 2022). In this study, fungal endophytes were isolated from the leaves, stems, and roots of *Ca*. The choice of these explants was informed by literature reports indicating that fungal endophytes producing important metabolites obtained from higher plants are predominantly found in the selected tissues (Thi Hoa *et al.*, 2023). Endophytic fungi isolated from *Ca* tissues were first identified by morphological characteristics after being cultured on PDA media. However, many fungal endophytes, especially the non-sporing fungi, failed to present all the morphological characteristics required to facilitate exhaustive identification in artificial cultures, thus making their identification and classification difficult. Several reports, including Sun and Guo (2012), have highlighted similar challenges. Hence, DNA barcodes, such as ITS and LSU, were used for conclusive identification of these fungal endophytes, which is a recommended standard procedure (Xu, 2016).

PCR amplification and sequencing of the ITS fragments revealed that the majority of the endophytes isolated belonged to the phylum Ascomycota, and a few belonged to the phylum Basidiomycota. Notably, amplification was not achieved in 18 of the isolated strains apart from

Cs2b-1a when using *TEF-1α*. According to Mirhendi *et al.* (2015) and Porter & Golding (2012), TEF-1α was specifically designed to achieve a distinctive amplification of *Fusarium*, while LSU has a higher range of amplification across a wide range of Ascomycota fungal species; hence, it is the best choice for conclusive identification of fungal endophytes after ITS, as noted by Mirhendi *et al.* (2015). Additionally, a common trend that has been observed from various research studies involving isolation and diversity determination of fungal endophytes from medicinal plants, shrubs, and even grasses is that fungal endophytes belonging to the phylum Ascomycota had the highest rates of isolation as compared to those from the phylum Basidiomycota (Gakuubi *et al.,* 2021; Khalil *et al.,* 2021). The phylogenetic analysis based on ITS sequences of the isolated endophytes indicated that endophytic fungi belonging to the genus *Diaporthe* had the highest number of isolates obtained from *Ca*. Fungal endophytes from these genera have been reported as one of the most frequently encountered genera in several host plants (Botella *et al.,* 2011). Studies have shown that different species of *Diaporthe* have the capability of colonizing diverse host plants as opportunistic fungi, with several different species occurring concurrently on the same host or lesion (Crous & Groenewald, 2005). Interestingly, some species of *Diaporthe* can either be pathogenic or harmless endophytes depending on the host and its health; for instance, *D. phaseolurum* was found to be pathogenic to soybeans, while it is endophytic to *Laguncularia racemosa* mangroves (Santos *et al.,* 2011; Sebastianes *et al.,* 2012). The diverse fungal endophytes isolated from *Ca.* roots consisted of endophytes from the genus *Trametes,* with four isolates having a high similarity index to *T. hirsuta*. Fungal species *T. hirsuta* has been previously isolated as an endophytic fungus from diverse plant species such as *Podophyllum hexandrum* (Himalayan mayapple) and *Triticum aestivum* L. (Comby *et al.,* 2016; Puri *et al.,* 2006). Research shows that this species forms an important part of the root microbiota, and some of the benefits they provide to the host include acting as plant growth promoters, bio-control agents, and environmental stress regulators, and also offering protection to the host (Hardoim *et al.,* 2015; Mayerhofer *et al.,* 2013). The colonization capabilities of the endophytes in the root system are mainly determined by factors such as soil properties, root exudate traits, nutrient availability, and environmental conditions (Fang *et al.,* 2019; Maciá-Vicente *et al.,* 2008).

Another intriguing endophyte isolated from both the roots and the leaves was the *Penicillium* species. *Penicillium* is regarded as one of the most common fungi, colonizing all habitats and having a great economic impact on human life. It has both beneficial, harmful, and neutral interactions with plants and associates with them either as an epiphyte or endophyte. It's fascinating that many species of *Penicillium* have been shown to interact positively with

plant roots, helping plants grow by making it easier for them to take in nutrients like phosphorous and make plant growth regulators like gibberellic acid and acetic acid (Srinivasan *et al.,* 2020). Therefore, it is considered one of the agriculturally and economically significant fungi. *Penicillium*, just like other endophytic fungi, is regarded as pathogenic in most plants; however, this fungus has also been reported as endophytic with significant benefits in most plants, shrubs, and even grasses (Zakaria *et al.,* 2010). Additionally, *Talaromyces,* teleomorph of *Penicillium* was also isolated from the roots of *Ca*. The ITS phylogenetic analysis clustered these two species into a single clade, revealing their relationships. Researchers have isolated *T. pinophilus,* an endophytic fungus, from the aerial parts of *Salvia miltiorrhiza* and *Rosmarinus officinalis.* Interestingly, this endophytic fungus has also been shown to have phytoremediation properties as well as induction of growth in *Triticum aestivum* (El-Shahir *et al.,* 2021).

In the same clade A (Fig. 3.4), there was an Aspergillus species, which is also regarded as a synamorph of both *Penicillium* and *Talaromyces* species since they share the same ancestral characteristics with regard to reproducing capabilities. This relationship was shown in a phylogenetic analysis carried out by Houbraken *et al.* (2020). One isolate from the genus *Paraconiothyrium* was also obtained from this study as an endophytic fungus. Several fungal species from this genus have been isolated as endophytic fungi from various hosts and have demonstrated a great potential as a source of bio-control agents and antimicrobials (Wang *et al.,* 2021). This endophytic fungus has been isolated from various medicinal plants; interestingly, this is the first report on the isolation of endophytic fungi from *Ca*.

When subjected to an antidermatophytic assay against the disease-causing dermatophytes, the endophytic fungus *P. hawaiiense showed* great activity against all the test strains. Some of the secondary metabolites that have been isolated from *P. hawaiiense* include hawaiinolides E-G, diterpene lactones, and cleistanthane diterpenoid (Chen *et al.,* 2014), which have antibacterial, anticancer, antifungal, and antiviral properties (Wang *et al.,* 2021). Hence it is postulated that the presence of these secondary metabolites contributes to the bioactive activities in earlier reports as well as those shown in this study. However, the antidermatophytic capabilities of this endophytic fungus have received relatively little attention. Even though *Aspergillus* species have become a menace in the agricultural sector, endophytic fungi *A. flavus* and *A. hanckokii,* isolated in this study, exhibited antidermatophytic activity against *T. benhamiae* and *M. canis.* Endophytic fungi in the genus *Aspergillus* are considered a great source of novel secondary metabolites with promising biological activities. Different species have proved their ability to produce secondary metabolites such as alkaloids, butenolides,

terpenoids, phenalenones, cytochalasins, xanthones, streoles, and anthraquinone. These classes of compounds have been reported to have diverse biological activities such as antifungal, antibacterial, antiviral, anti-inflammatory, and anti-leishmanial activities (El-Hawary *et al.*, 2020); however, there are no reports on their antidermatophytic capabilities.

Economically, fungal species in this genus, *Diaporthe*, have been recognized as producers of interesting secondary metabolites with antimicrobial and anticancer properties, as well as enzymes that are commercially used (Elsässer *et al.*, 2005; Kumaran *et al.*, 2009). Furthermore, *Diaporthe* species have been reported to prevent herbivory, possess lignocellulosic activity, and can also be applied as bio-herbicides (Ash *et al.*, 2017; Jordaan *et al.*, 2006; Vesterlund *et al.*, 2011). In this study, *D. maritima* exhibited antidermatophytic activity against *T. interdigitalis* and *M. canis*, which is an additional contribution to the importance of endophytic fungi in this genus. In a study carried out by Malik *et al.* (2017), *T. hirsuta* was shown to be a great source of the anticancer and antimicrobial secondary metabolite podophyllotoxin (Puri *et al.*, 2006), hence making it an important source of novel antimicrobial secondary metabolites. From this study, this endophytic fungus exhibited weak antidermatophytic activity against *T. banhamiae*. This can be attributed to podophyllotoxins, alkaloids, and terpenes, which have antifungal activity against filamentous fungi (Pinar & Rodríguez-Couto, 2024). Interestingly, in research done by Dhinakaran *et al.* (2012), *Penicillium* species isolated from a mud volcano eruption exhibited antidermatophytic activity against *Epidermophyton floccosus*, *Microsprum gypseum*, *Tricophyton rubrum*, and *Tricophyton mentagr*ophytes. This is similar to the results obtained from this study where endophytic *Penicillium rubrum* exhibited antifungal activity against *T. benhamiae* and *M. canis*. This activity could be attributed to the production of mycophenolic acid (MPA) derivatives, which have been reported for their activity against most filamentous fungi. The antidermatophytic activities observed from the endophytic fungi isolated from *Ca*. suggest that these strains are potential sources of novel antimicrobial secondary metabolites.

3.5 Conclusion

The aim of this study was to isolate and identify endophytic fungi with antimicrobial activity from various parts of the medicinal plant. Based on their morphology, nineteen isolates were characterized and ITS molecular analysis, showing that 78.9% Ascomycota and 21.1% Basidiomycetes. Among them, *P. hawaiiense* showed strong antagonistic activity against *T. rubrum*, *T. interdigitalle*, *T. benhamiae*, *M. canis*, and *N. gypsea*, highlighting its potential as a source of novel antidermatophytic compounds. Other species, including *D. maritima*, *P.*

rubens, *A. flavus*, *A. hanckokii*, and *T. hirsute*, also exhibited inhibitory effects. This is the first report of endophytic fungi from *Ca* leaves, roots, and stem bark, highlighting their potential as sources of bio-active metabolites, though further large-scale metabolite characterization is needed.

CHAPTER FOUR

ISOLATION AND CHARACTERIZATION OF SECONDARY METABOLITES FROM *C. aurea* subsp. *aurea* LEAVES, STEM BARK AND ASSOCIATED FUNGAL ENDOPHYTES

Abstract

Secondary metabolites from medicinal plants and associated endophytic fungi have played a key role in the discovery and development of novel drugs through the isolation and characterization of the secondary metabolites within these sources. Medicinal plants and their associated endophytes have been one of the most sought-after sources of novel secondary metabolites for therapeutic use. Further analysis of *Ca*. and endophytic secondary metabolites that showed activity against selected dermatophytes in the pre-screening test conducted. The analysis focused on the secondary metabolites from the leaves and stem bark and endophyte *P. hawaiiense* which showed great activity as described in chapter 3. The leaves and the stem bark tissues were dried and extracted using methanol to obtain methanolic extract. On the other hand, the endophytic fungi was fermented on rice media and methanol crude extract prepared. These extracts were then portioned between hexane and ethyl acetate. The ethyl acetate extracts were then purified using reverse phase high performance liquid chromatography (HPLC) and, the purity and mass of the isolated compounds determined by liquid chromatography coupled with mass spectrometry (LC-MS). Using 1D and 2D NMR spectroscopy techniques, the structures of these compounds were determined. From the leaves and the stem bark of *C. aurea* subsp. *aurea*, eight (8) quinolizidine alkaloids and twelve (12) phenolic were isolated. Among the quinolizidine alkaloids isolated, four previously undescribed compounds were reported. From the endophytic fungi, *P. hawaiiense*, two compounds were isolated and characterized namely; Lactariolide (**67**), a macrolide and hydroxy- Euphorol E (**68**), a tirucallane triterpene, which is a previously undescribed compound. To the best of my knowledge, apart from compound **55** and **59** which had been previously reported from *Ca*., this this is the first report on the isolation of ten (**10**) phenolic compounds from *Ca*. Furthermore, this is the first report on the isolation of compounds **66** and **67** from the endophytic fungus *P. hawaiiense*. The isolation of novel compounds from this study enriches the natural products library, providing diverse lead compounds for developing next generation drugs with improved safety and efficacy.

4.1 Introduction

Natural products chemistry importance is usually experienced in the diversity of its sources. Animals, microorganisms and plants contain a wide quantity of bio-active compounds. Among the greatest aspects of biodiversity of nature is the numerous untapped opportunities to discover novel plant secondary metabolites. Natural products have contributed to the discovery and development of novel drugs (Dias *et al.*, 2012). As at the beginning of 21st century, approximately 11% of the 252 drugs that were considered basic and essential by the world health organization (WHO) were considered to be exclusively of plant origin (Veeresham, 2012). Plants specifically present great remedies for the treatment of various diseases in several continents around the globe (Brusotti *et al.*, 2014). Additionally, research shows that approximately 80% of the world's population depend on herbal medicine or plant extracts for treatment of various diseases as well as part of the primary healthcare systems (Bora *et al.*, 2011; Sen & Samanta, 2014). The search for novel therapeutics secondary metabolites from natural sources, has been on-going for centuries and has led to some great discoveries. For instance, isolation of morphine from *Papaver somniferum* L. (Opium poppy) which is an analgesic (Marderosian & Beutler, 2002). Another great discovery is acetylsalicylic acid, an anti-inflammatory agent commonly known as aspirin derived from salicin which is isolated from the bark of willow tree *Salix alba* L. Similarly, vincristine, an anticancer agent was isolated from *Caranthus roseus* and artemisinin an antimalarial drug isolated from *Artemisia annua* are some of the additional great discoveries from natural products. (Gerwick, 2013; Soares-Bezerra *et al.*, 2013).

Within the plant tissues are endophytes which are known to produce secondary metabolites which are helpful in coping with biotic and abiotic stress. These secondary metabolites include terpenoids, alkaloids, polyketides, flavonoids, phenols, phenolic acids and saponins (Jha *et al.,* 2023). The pharmaceutical and biochemical industries greatly rely on endophytic fungi as a source of new therapeutic bio-molecules that possess therapeutic properties such as immunosuppression, anticancer, antimicrobials (Singh & Kumar, 2023) among others. In order to obtain secondary metabolites from these endophytic fungi, one has to understand their ecology, capability of biotransformation of substrates and the bio-active components. The presence of bio-active components are tested using dual culture techniques (Chapter 3) in PDA slants as described by (Sharma *et al.*, 2016). The endophytic fungi are then subjected to an extended period of incubation. Since endophytic fungi tend to produce many biologically active metabolites, it is important to build a suitable cultivation system for commercial use (Singh & Kumar, 2023). Additionally, fermentation of these endophytes is

regarded as fruitful, environmentally friendly and a continuous process. These endophytes can be grown in solid state fermentation or liquid submerged system. Submerged culture process tend to produce mycelial biomass and bio-active metabolites faster however factors such as temperature, aeration, pH and agitation may affect secondary metabolites production and hence requires optimization for maximum yield (Brader *et al.,* 2014). Solid state fermentation of fungal cultures exhibits various advantages over submerged approach, since through this system, bio-active secondary metabolites can be manufactured in simple substrates such as rice, wheat, barley and malt. Furthermore, from this system there is an improved productivity, a high product concentration and it requires simple equipment for the fermentation process (Patil *et al.,* 2016).

Despite the availability of drugs from natural products, the use of plant and fungal extracts are on the rise due to their therapeutic effects such as anti-parasitic, anticancer, antidiabetic, antimicrobial, anti-fungal and anti-fertility (Anibogwu *et al.,* 2021; Navarrete-Carriola *et al.,* 2024). In most cases, the chemical composition of these extracts is usually unknown hence it is necessary to identify the secondary metabolites attributed for the specific therapeutic effects. In this case, different qualitative and quantitative studies of the secondary metabolite composition of the extracts from the natural products are undertaken to determine the appropriate extraction method (Smith, 2003). Different extraction methods have been used to obtain secondary metabolites. They are classified as either conventional methods; Soxhlet, hydro distillation and maceration or non-conventional methods such as; enzyme extraction, ultrasound assisted extraction, microwave assisted extraction, supercritical fluid extraction, pulsed electric field assisted extraction, and pressurized liquid extraction. Although some of the methods are regarded as very efficient, they tend to be very expensive hence the simplest and the most economical methods are used for extracting metabolites of interest (Navarrete-Carriola *et al.,* 2024). Identifying secondary metabolites from plant extracts is an important aspect in the study of traditional medicine. Different factors such as plant part properties, solvent, matrix, pressure, time and temperature are considered during the extraction process. These conditions must be optimized to obtain a high secondary metabolite yield (Azmir *et al.,* 2013; Sasidharan *et al.,* 2011). Once obtained, secondary metabolites from the extracts are structurally elucidated using chromatographic techniques such as gas chromatography- mass spectrometry (GC-MS), high performance liquid chromatography (HPLC), liquid chromatography- mass spectrometry and other spectroscopic techniques (Wangkheirakpam, 2018). Incorporation of MS into the chromatographic technique is very advantageous due to

its high sensitivity which allows the detection of low molecular weight compounds at a very low concentration such as nanogram per milliliter (Seger & Sturm, 2007).

Kenya is endowed with great ancestral traditions and richness in the use of herbal/traditional medicine. *Calpurnia aurea* (*Fabaceae*) has been used in the treatment of wounds, tinea infections, bacterial infections among others (Korir *et al.,* 2014). Phytochemical analysis of medicinal plants in the *Fabaceae* family consist majorly of flavonoids and quinolizidine alkaloids, hence these two classes of compounds are regarded as the phytochemical markers of this family (Korir *et al.,* 2014; De Nysschen *et al.,* 1998). Hence this study focused on the isolation and characterization of secondary metabolites from the leaves, stem bark and associated endophytes from this medicinal plant.

4.2 Materials and Methods

4.2.1 Site Description and Sample Collection

The leaves and stem bark samples were collected from Mt. Elgon National Park as described in chapter 3. The samples were placed in sacks and transported to the biotechnology lab at Egerton university where they were dried for 14 days under a shade to avoid photodecomposition.

4.2.2 General Experimental Procedures

The HR-ESIMS (High resolution electrospray ionization mass spectrometry) data was recorded on MaXis ESI-TOF (Electrospray Ionization-Time of Flight) mass spectrometer (Bruker Daltonics, Bremen, Germany). This machine was coupled to an Agilent 1260 series HPLC-UV system equipped with C18 Acquity UPLC BEH (Ultra performance Liquid chromatography) (Ethylene bridged hybrid) (waters) column. A diode array (DAD) UV detector was used with a wavelength detection range of 200-600 nm. The mobile phase was a mixture of Solvent A; Water (H_2O) supplemented with formic acid (0.1 %) and Solvent B; Acetonitrile (ACN) supplemented with 0.1% formic acid. The flow rate used was 0.6 mL/min at 40℃ gradient elution system with initial conditions being 5% B for 0.5 Min, increasing to 100% of solvent B in 19.5 minutes and holding at 100% for 5 minutes.

The HPLC-DAD/MS measurements were done in amazon speed ETD (electron transfer dissociation) ion trap mass spectrometer (Bruker Daltonics) and measured in both positive and negative modes simultaneously. The HPLC system consisted of a C18 Acquity UPLC BEH Column (Waters) with the mobile phase being solvent A; water (H_2O) supplemented with 0.1% formic acid and Solvent B being Acetonitrile (ACN) also supplemented with 0.1% formic acid. The gradient conditions were 5% solvent B for 0.5 Minutes increasing to 100% solvent B in

20 minutes, an isocratic condition was maintained at 100% B for 10 minutes with a flow rate 0.6 mL/ Minute. A UV/Vis detection was used with a wavelength range of 200-600 nm. Bruker Compass Data Analysis 4.4SR1 was used to analyze the data including determining the molecular formulae using the smart formulae algorithm (Bruker Daltonics).

Purification was done using a preparative HPLC system on an agilent 1100 series (Santa Clara, CA, USA) equipped with a 180-fraction collector binary pump and diode-array UV detector and the system was controlled by Chem station software. NMR spectra (1D and 2D) were measured on Avance III Bruker ^{1}H 700 MHz (^{1}H: 700 MH_Z, ^{13}C: 175 MH_Z) or Avance III 500 MHz (Bruker, ^{1}H 500 MHz, ^{13}C 125 MHz) spectrometer equipped with 5 mm TCI cryoprobe locked to the respective deuterium signal of the solvent. Chemical shifts are given in parts per million (ppm) and coupling constants in Hertz (Hz). The samples were dissolved in deuterated solvents and the residual proton signals of the respective deuterated solvent was used as reference for the calibration. The ^{1}HNMR chemical shifts with a value of 3.31ppm was referenced for deuterated methanol (CD_3OD) while the ^{13}CNMR chemicals shifts were also calibrated using the signal of the deuterated solvent and a reference value of 49.15 ppm for CD_3OD. The ^{1}HNMR chemical shifts were directly determined from the ^{1}HNMR spectra and/or the heteronuclear single quantum correlation (HSQC) spectra in case of overlapping. The HSQC spectra were recorded as multiplicity and used to assign the edited distortionless enhancement by polarization transfer (DEPT) and HSQC correlations. The multiplicities of carbon signals were determined from these experiments. Optical rotation data were measured in Anton Paar MCP-150 Polarimeter (Graz, Austria) with 100 mm path length and sodium D line at 589 nm. The UV spectra was measured on Shimadzu (Kyoto, Japan) UV/ Vis 2450 spectrophotometer using methanol (Uvasol, Merck, Darmstadt, Germany) as a solvent.

4.2.3 Extraction of Secondary Metabolites from Dried Plant Materials

Extraction for secondary metabolites from dried plant materials was separately carried out on the leaves and stem bark of *C. aurea* subsp *aurea*.

4.2.3.1 Extraction of Secondary Metabolites from the Leaves

The air-dried leaves were ground, and 1200 g of the powder was soaked in 2.5 L of methanol and extracted five times at room temperature. The methanol crude extract was concentrated under reduced pressure to yield brown residues weighing 200 g. A portion of the leaf extract/ residue (5 g) was analyzed using flash chromatography (Grace Reveleris®, Columbia, MD, USA) with a silica cartridge of 24 g sample weight. The mobile phase used in this analysis were solvent A consisting of a mixture of heptane and ethyl acetate in the ratio

of 9:1, solvent B was a mixture of ethyl acetate, heptane and methanol in the ratio of 6:3:1 respectively, while solvent C was 100% Ethyl acetate. The elution method was gradient that began with isocratic mixture of solvent A for 5 minutes then it gradually increases to 100 % of solvent B mixtures within 35 minutes of elution. This was finally held at 100 % of solvent C for 10 minutes. A total of fourteen fractions were collected which were later purified using a reverse phase preparative HPLC. Depending on the profile from mass analysis, fractions **2** (79.41 mg), **3** (70.02 mg) and **7** (140.05 mg) were further purified by preparative reverse phase- HPLC (RP-HPLC). The column used for preparative reverse phase- HPLC was a Synergi Polar RP-80 with the following dimensions: 250× 21.2 mm and 10 µm particle size. The mobile phase used was solvent A comprising of H_2O plus 0.1 % formic acid and Solvent B was acetonitrile (ACN) plus 0.1 % formic acid. The flow rate was 20 mL/min and UV detection were set at 210, 240, and 300 nm. The method used was a gradient elution that began with 5 % isocratic of solvent B for 5 minutes, followed by a gradual increase to 50 % of solvent B in 40 minutes and a final increase to 100 % solvent B in 10 minutes. This isocratic elution was later maintained for 10 minutes to afford **46** (22.8 mg; $_R$T= 12.2 min), **49** (4.64 mg; $_R$T = 9.3 min), **50** (3.02 mg; $_R$T= 8.4 min)**, 52** (23.2 mg; $_R$T = 7.52 min), **54** (3.6 mg; $_R$T = 22 min), **55** (4.15 mg; $_R$T= 25 min), **56** (6.41 mg $_R$T = 32 min) and **59** (4.15 mg; $_R$T = 34 min). Fraction 6 yielded yellowish crystals, which were not soluble in methanol, of **53** (40 mg) which formed after concentration in the rotary evaporator.

4.2.3.2 Extraction of Secondary Metabolites from Stem Bark

A portion (900 mg) of the stem bark methanol crude extract was suspended in water, partitioned between hexane and ethyl acetate to obtain 350 mg of ethyl acetate extract and 400 mg of hexane extract. The Ethyl acetate extract was further purified using reverse phase preparative HPLC on a Nucleodur C18 Htec column with the following dimensions, 250×40 mm and 10 µm particle size. The mobile phase used were solvent A; H_2O plus 0.1 % formic acid and solvent B; acetonitrile (ACN) plus 0.1 % formic acid. The flow rate was 40 mL/min and UV detection were set at 210, 240, and 300 nm wavelengths. The method of elution was gradient starting with 5 % solvent B in an isocratic mode for 5 minutes followed by an increase to 20 % solvent B in 20 minutes, and later to 50 % solvent B in 60 minutes and finally an increase to 100 % solvent B in 20 minutes which was maintained for 10 minutes to afford compounds; **47** (3.24 mg; $_R$T= 22.2 min), **48** (8.7 mg; $_R$T= 15.3 min), **51** (3.73 mg; $_R$T= 18.2 min), , **57** (7.2 mg; $_R$T= 21 min), **58** (3.15 mg; $_R$T= 22 min) **60** (6.2 mg; $_R$T= 28 min), **61** (2.96

mg; $_R$T= 23 min), 6**2** (2.07 mg; $_R$T=31.5 min), **63** (5.06 mg; 30 min), **64** (2.98 mg; 35 min) and **65** (1.53 mg; $_R$T= 32.5 min).

4.2.4 Extraction of Secondary Metabolites from Fungal Endophytes

Small scale and large scale fermentation of the fungal endophyte (*P. hawaiiense*) was done using rice media as described by Sum *et al.*,(2023). Ten plugs (5 mm diameter each) of fully grown specific endophytic fungi mycelia on a Yeast Malt agar plates were inoculated into 10 × 500 mL Erlenmeyer culture flasks, containing sterile rice media (Composed of 90 g of rice media in 90 mL of deionized water). These flasks were incubated at 24 °C in the dark for 45 days, after which secondary metabolites were extracted. Once ready, the cultures were Macerated in sterile condition by soaking in methanol for 24 hours with mild shaking at 120 rpm. The residues were then separated from methanol by filtration and the solvent evaporated. The semi-dried extract was reconstituted in distilled water to dissolve the sugars and partitioned with an equal amount of ethyl acetate according to the protocol described by (Chepkirui *et al.,* 2018). Briefly, the aqueous phase was extracted three times with ethyl acetate and later discarded whereas the organic phase was filtered through anhydrous sodium sulphate ($NaSO_4$) to remove water and evaporated under reduced pressure on a rotary evaporator (Heidolph) until dryness.

The ethyl acetate extract was further purified using reverse phase preparative HPLC on a Nucleodur C18 Htec column with the following dimensions, 250×40 mm and 10 μm particle size. The mobile phase used were solvent A; H_2O plus 0.1% formic acid and solvent B; acetonitrile (ACN) plus 0.1% formic acid. The flow rate was 40 mL/min and UV detection were set at 210, 240 and 300 nm wavelengths. The method of elution was gradient starting with 5 % solvent B in an isocratic mode for 5 minutes followed by an increase to 20 % solvent B in 20 minutes, and later to 50 % solvent B in 60 minutes and finally an increase to 100 % solvent B in 20 minutes which was maintained for 10 minutes to afford compound **66 (**1.25 mg; $_R$T= 35 min**)** and **67 (**1.88 mg; $_R$T= 32 min**).**

4.3 Results and Discussion

The medicinal plant under study, *C. aurea* subsp *aurea* is composed of a number of quinolizidine alkaloids and phenolic flavonoids (Korir *et al.,* 2014) which corresponded to those isolated in this study. From this study, purification of the leaf and stem bark extracts led to isolation of twenty (20) compounds; Compounds **46** – **53** were classified as quinolizidine alkaloids while compounds **54 – 65** were phenolic compounds. Additionally, from the endophytic fungi (*P. hawaiiense*) two (2) compounds were isolated: macrolide (**66**) and

triterpene (**67**). Herein are the description of all the isolated secondary metabolites using 1D and 2D spectrometric characteristics together with literature comparison.

4.3.1 Quinolizidine Alkaloids Isolated from the Leaves and Stem Bark

Compound **46** was isolated as a colorless solid with molecular formula $C_{21}H_{29}N_3O_4$ determined from its HRESIMS at *m/z* 388.2232 $[M + H]^+$ (calcd $C_{21}H_{30}N_3O_4$ for 388.2231) (Appendix 1 and 2). Other physiochemical parameters of this compound included an optical activity of $[\alpha]_D^{25}$ +7 (c 0.1, MeOH); UV (MeOH) λ_{max} (log ε) 265 (0.401), 228 (0.171), 202 (0.164) (Appendix 9); The ^1H and ^{13}C NMR data were measured in CD_3OD, 700 MHz, 175 MHz respectively (Table 4.1, Appendix 3 and 4); Assignment of NMR data was done using 1D and 2D NMR spectra and by comparison with quinolizidine alkaloids reported in literature (Asres *et al.,* 1986; Kubo *et al.,* 1984; Vermin *et al.,* 1979). The data (Table 4.1) suggested that **46** had the basic virgiline structure with methoxy and pyrrolylcarbonyl substituents. The presence of the pyrrolylcarbonyl substituent was confirmed by ^1H NMR data δ_H 6.91 (H-1′, dd, *J* = 1.53, 3.63 Hz), δ_H 6.20 (H-4′, dd, *J* = 2.58, 3.63 Hz), δ_H 6.99 (H-5′, dd, *J* = 1.53, 2.58 Hz) and ^{13}C NMR data, δc 123.4 (C-2′), δc 116.7 (C-3′), δc 110.6 (C-4′), δc 124.8 (C-5′), δc 161.7 (C-6′) (Asres *et al.,* 1986). The strong singlet at δ_H 3.20 corresponding to a carbon absorption signal at δc 55.0 was assigned to the methoxy group, whose protons had a strong HMBC correlation to the oxygenated methine carbon at δc 80.1 (C-2) confirming its position on ring A. These methoxy protons also showed NOESY (Appendix 8) correlations to H_2-8, H-9 and H_2-15 indicating that it has a β-orientation. The rest of the stereochemistry was assigned with the help of literature as reported by van Wyk *et al.* (1995) The other oxygenated methine proton at δ_H 5.36 (H-13) showed a strong HMBC correlation to the carbonyl carbon at δc 161.7 (C-6') indicating the attachment of the pyrrolylcarbonyl substituent on C-13. The presence of the other carbonyl group in ring B was confirmed by the HMBC correlations of H-6, H-7, H_2-8, H-9 and H-11 to C-10 (δc 175.3). This showed that **46** is of the virgiline type (Fig. 4.1). All other connectivities were confirmed by COSY and HMBC correlations (Appendix 6 and 7). Compound **46** was determined as previously undescribed and given the name 2β-Methoxy-13α-*O*-(2'-pyrrolylcarbonyl) virgiline.

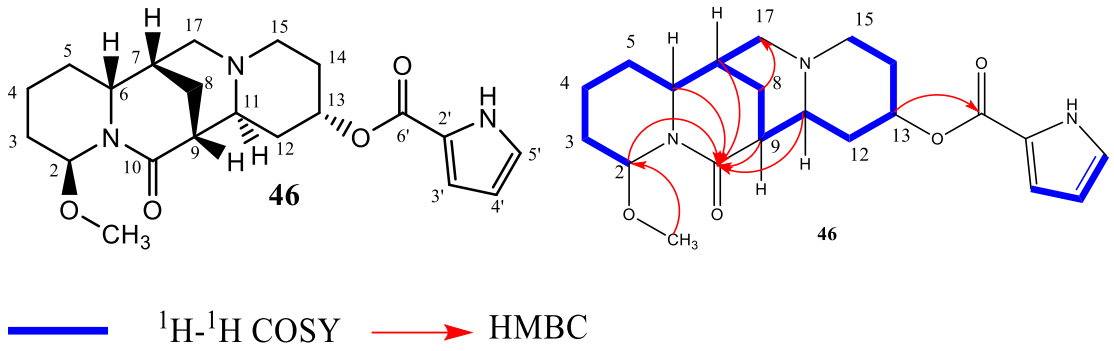

Figure 4.1: Structure, HMBC and COSY correlations of compound **46**

Table 4.1: The assignment of ^{13}CNMR, ^{1}HNMR, COSY and HMBC of compound 46

No.	^{13}CNMR δ_C	TYPE/ DEPT	^{1}HNMR (δ_H, mult. *J* in Hz)	COSY	HMBC
1	N		-	-	-
2	80.1	CH	5.80 (m)	3,	3, 4, 6, 10
3	30.1	CH_2	1.60 (m), 1.90 (m)	2,4	2, 4
4	19.5	CH_2	1.65 (m), 1.87 (m)	3,5	2, 3
5	29.6	CH_2	1.66 (m)	6	6
6	54.6	CH	3.71 (m)	5,7	4, 5, 7, 10, 17
7	32.8	CH	2.17 (m)	6, 17	6, 9
8	22.4	CH_2	1.80 (m), 2.11 (m)	9	6, 7, 9, 10, 17
9	44.1	CH	2.44 (m)	8, 11	8, 10, 11, 12
10	175.3	Cq	-	-	-
11	54.7	CH	3.73 (m)	9	9, 10, 12, 15, 17
12	27.5	CH_2	1.62 (m), 2.41 (m)	13	9
13	69.2	CH	5.36 (m)	12, 14	6′, 11, 12, 14,
14	23.4	CH_2	1.61 (m), 2.11 (m)	13,15	15, 13, 15
15	49.5	CH_2	2.82 (m), 3.41 (m)	14	11, 13, 14, 17
16	N		-	-	-
17	46.6	CH_2	2.87 (m), 3.34 (m)	7	6, 7, 8, 15
1′	N		-	-	-
2′	123.4	Cq	-	-	-
3′	116.7	CH	6.91 (dd, *J* = 3.8, 1.5 Hz,	4′	2′, 4′, 5′, 6′

			1H)		
No.	^{13}CNMR δ_C	TYPE/ DEPT	^{1}HNMR ($\delta_{H,}$ mult. *J* in Hz)	COSY	HMBC
4′	110.6	CH	6.21 (dd, *J* = 3.7, 2.5 Hz, 1H)	3′, 5′	2′, 3′, 5′, 6′
5′	124.8	CH	6.99 (dd, *J* = 2.5, 1.5 Hz, 1H)	4′	2′, 3′ ,4′, 6′
6′	161.7	C_q	-	-	-
2-OCH_3	55.0	OCH_3	3.20, s	-	2

*Recorded in CD_3OD at 700 MH_Z and 175 MH_Z

Compound **47** was isolated as a colourless solid with molecular formula $C_{21}H_{29}N_3O_4$ as determined from the HRESIMS at *m/z* 388.2222 for $[M+H]^+$ (calcd for $C_{21}H_{30}N_3O_4$, 388.2231) (Appendix 10 and 11). Other physio-chemical characteristics measured for this compound were: optical activity $[\alpha]_D^{25}$ -7 (c 0.1, MeOH); UV (MeOH) λ_{max} (log ε) 265 (0.107), 211 (0.106), 199 (-0.027) (Appendix 18); The ^{1}H and ^{13}C NMR data were both measured in chloroform (CD_3OD) at 700 MH_Z and 175 MH_Z respectively (Table 4.2, Appendix 12 and 13); This compound had the same molecular formula with compound **46** and with a slight difference in elution time in the HPLC. The ^{1}H and ^{13}C NMR data of **47** were very similar to those of **46** (Table 4.2; Appendix 14, 15, 16 and 17). The difference between **46** and **47** was the optical activity whereby **46** had an optical activity of $[\alpha]_D^{25}$ values of +7 and while 47 had an optical activity of $[\alpha]_D^{25}$ -7 (Fig. 4.2). The structure of **47** was determined as the enantiomer of **46** and given the name 2α-Methoxy-13β-*O*-(2′-pyrrolylcarbonyl) virgiline which was reported as a previously undescribed compound.

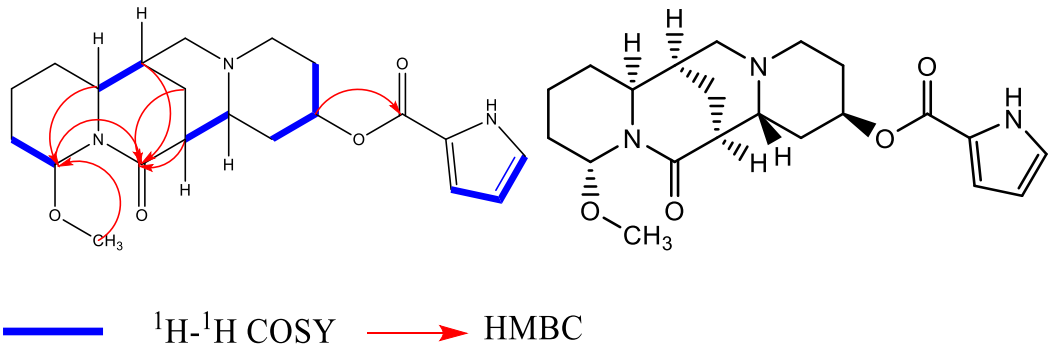

Figure 4.2: Structure, HMBC and COSY correlations of compound **47**

Table 4.2: The assignment of ^{13}CNMR, ^{1}HNMR, COSY and HMBC of compound **47**

No.	δ_C	TYPE/ DEPT	^{1}HNMR (δ_H, mult. *J* in Hz)	COSY	HMBC
1	N	-	-	-	-
2	79.0	CH	5.83, m	3	3, 4, 6, 10
3	29.2	CH2	1.60, 1.92, m	2, 4	2, 4
4	18.3	CH2	1.67, 1.89, m	3, 5	2, 3
5	28.4	CH2	1.67, m	6	6
6	53.4	CH	3.69, m	5, 7	4, 5, 7, 10, 17
7	31.7	CH	2.14, m	6, 17	6, 9
8	21.4	CH2	1.79, 2.10, m	9	6, 7, 9, 10, 17
9	43.3	CH	2.41, m	8, 11	8, 10, 11, 12
10	174.7	Cq	-	-	-
11	53.2	CH	3.68, m	9	9, 10, 12, 15, 17
12	25.9	CH2	1.55, 2.40, m	13	9
13	68.8	CH	5.38, m	12, 14	6′, 11, 12, 14, 15
14	22.1	CH2	1.54, 2.11, m	13, 15	13, 15
15	48.1	CH2	2.75, 3.37, m	14	11, 13, 14, 17
16	N	-	-	-	-
17	45.4	CH2	2.78, 3.27, m	7	6, 7, 8, 15
1′	N	-	-	-	-
2′	122.3	Cq	-	-	-
3′	115.4	CH	6.92, dd (1.53, 3.67)	4′	2′, 4′, 5′, 6′
4′	109.3	CH	6.22, dd (2.49, 3.67)	3′, 5′	2′, 3′, 5′, 6′
5′	123.4	CH	6.99, dd (1.53, 2.49)	4′	2′, 3′ ,4′, 6′
6′	160.5	Cq	-	-	-
2-OCH_3	53.6		3.22, s	-	2

*Recorded in CD_3OD at 700 MH_Z and 175 MH_Z

Compound **48** was isolated as a colorless solid and gave a molecular ion at *m/z* 472.2460 for $[M+H]^+$ (calcd for $C_{25}H_{34}N_3O_6$, 472.2442) (Appendix 19 and 20). Other physio-chemical characteristics of this compound were; optical activity $[\alpha]_D^{25}$ -61 (c 0.1, MeOH); UV (MeOH) λ_{max} (log ε) 265 (0.174), 210 (0.232), 193 (0.204) (Appendix 27); ^{1}H and ^{13}C NMR data (CD_3OD, 700 MH_Z, 175 MH_Z) data (Table 4.3, Appendix 21 and 22). The ^{1}H and ^{13}C NMR data of **48** was comparable to that of **46** and **47** indicating that it also has a virgiline

skeleton with a pyrrolylcarbonyl substituent. However, the major difference was presence of an extra oxygenated methine δc 70.6 (C-3) in addition to the ones at δc 71.3 (C-2) and δc 66.9 (C-13). COSY and HMBC (Fig. 4.3, Appendix 24 and 25) correlations indicated that it was adjacent to C-2 which has a hydroxyl group. The ^{13}C NMR and HSQC spectra (Appendix 23) shows presence of another substituent that consisted of two methyls, one methine and two quaternary carbons at δc 14.5 (C-1″), 138.1 (C-2″), 127.6 (C-3″), 167.3 (C-4″) and 19.2 (C-5″). These data indicated that unlike **46** and **47**, compound **48** possessed either angelate or tiglate ester groups. The absence of a NOESY correlation between the protons of the two methyl groups (C-1″ and C-5″) showed that they are *trans* to each other and therefore the substituent was determined as angelate ester. The HMBC correlation (Appendix 24) of H-3 to C-4″ confirmed its attachment to C-3. The $^{3}J_{H\text{-}2\text{-}H\text{-}3}$ of 10 Hz is indicative of a *trans* conformation of the hydroxyl and angelate ester groups with the former in a β-orientation. This α-orientation of the angelate ester group is supported by the absence of any NOESY correlations with H-6, H-7, H_2-8 and H-9 (Appendix 26). Thus, compound (**48**) was identified as 3α-*O*-Angelate-2β-hydroxy-13α-*O*-(2′-pyrrolylcarbonyl) virgiline which was also reported as a previously undescribed.

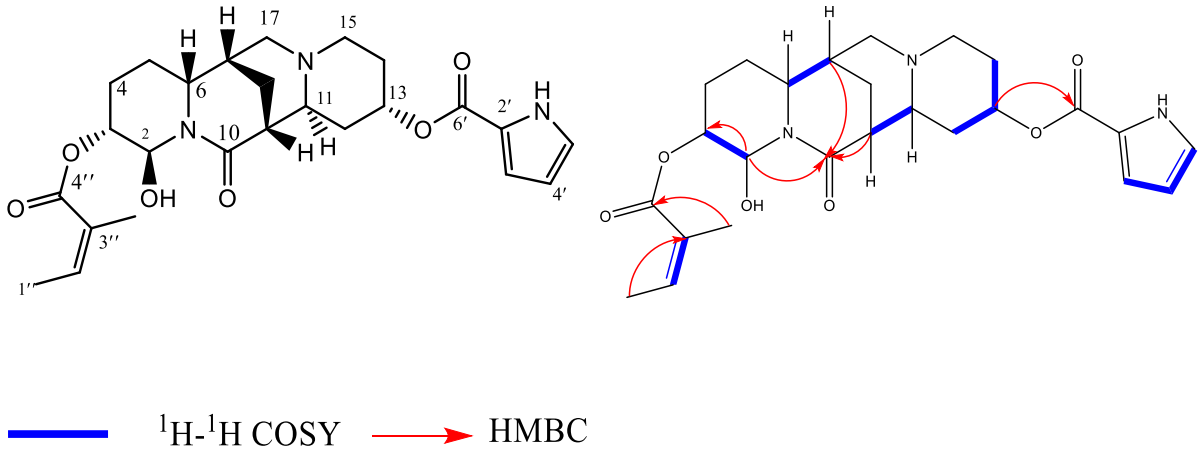

Figure 4.3: Structure, HMBC and COSY correlations of compound **48**

Table 1.3: The assignment of ^{13}CNMR, ^{1}HNMR, COSY and HMBC of compound **48**

	δ_C	TYPE/ DEPT	^{1}HNMR (δ_H, mult. *J* in Hz)	COSY	HMBC
1	N	-	-	-	-
2	71.3	CH	4.30 (d, *J* = 10.1)	3	3, 4, 5, 10
3	70.6	CH	5.08, m	2	2, 4, 5, 4″,
4	30.2	CH_2	1.92, 2.25, m		2, 3, 5, 6
5	22.9	CH_2	2.06, 2.48, m		3, 4, 6, 7,
6	56.9	CH	3.66, m		2, 4, 5, 10, 17
7	32.9	CH	1.97, m		5, 6, 8, 9, 17
8	24.3	CH_2	1.70, 2.25, m		6, 7, 9, 10, 11, 17
9	31.6	CH	2.21, m		7, 8, 10, 11, 12
10	172.1	Cq	-	-	-
11	58.0	CH	3.24, m		9, 10, 12, 15
12	28.5	CH_2	1.35, m		9, 11, 13, 14
13	66.9	CH	5.27, m		11, 12, 14, 15, 6′
14	25.0	CH_2	2.01, 2.12, m		12, 13, 15
15	49.2	CH_2	3.11, 3.27, m		11, 13, 14, 17
16	N	-	-	-	-
17	46.8	CH_2	2.92, 4.36, m		7, 8, 11, 15
1′	N	-	-	-	-
2′	122.1	Cq	-	-	-
3′	115.6	CH	6.93 (dd, *J* = 3.7, 1.6)	4′	2′, 4′, 5′
4′	109.4	CH	6.21, dd (*J* = 2.50, 3.57)	3′, 5′	3′, 5′, 6′
5′	123.6	CH	7.01, br s	4′	2′, 3′, 4′,
6′	160.4	Cq	-	-	-
1″	14.5	CH_3	2.0, d (*J* = 7.24)	2″	2″, 3″, 5″
2″	138.1	CH	6.16, q (*J* = 7.24)	1″	1″, 3″, 4″ 5″
3″	127.6	Cq	-	-	-
4″	167.3	Cq	-	-	-
5″	19.2	CH_3	1.91, s		2″, 3″, 4″

*Recorded in CD_3OD at 700 MH_Z and 175 MH_Z

Compound **49** was isolated as a colorless solid with molecular formula $C_{15}H_{22}N_2O_2$ determined from its HRESIMS at *m/z* 263.1758 for $[M+H]^+$ (Calcd for $C_{15}H_{22}N_2O_2$, 263.1754)

(Appendix 28 and 29). Other physiochemical parameters measured included: optical activity $[\alpha]_D^{25}$ -39 (c 0.1, MeOH); UV (MeOH) λ_{max} (log ε) 230 (0.172), 195 (0.168) (Appendix 36); ^{1}H and ^{13}C NMR data (CD_3OD, 700 MH_Z, 175 MH_Z) data (Table 4.4, Appendix 30 and 31). A total of 15 carbons were observed in the ^{13}C NMR spectrum (Table 4.4). In general, the NMR data pointed to a virgiline carbon skeleton with a double bond due to the presence of sp^2 carbons at δc 123.3 (C-2) and 110.9 (C-3). The HMBC correlations (Fig. 4.4, Appendix 33) of H-6, H-7, H_2-8, H-9 and H-10 to the carbonyl group at δc 171.3 confirmed the virgiline structure. The COSY correlations (Appendix 34) of H-2 to H-3, H-3 to H-3 to H_2-4, H_2-4 to H_2-5 and H_2-5 to H-6 (Fig. 4.4) identified the connectivity's in A and the HMBC correlation of H-2 to C-10 confirmed the position of the double bond. These data indicated that **49** is a dehydro derivative of virgiline (Asres *et al.*, 1986) and was identified as 2, 3-Deydro-virgiline and report as a previously reported compound.

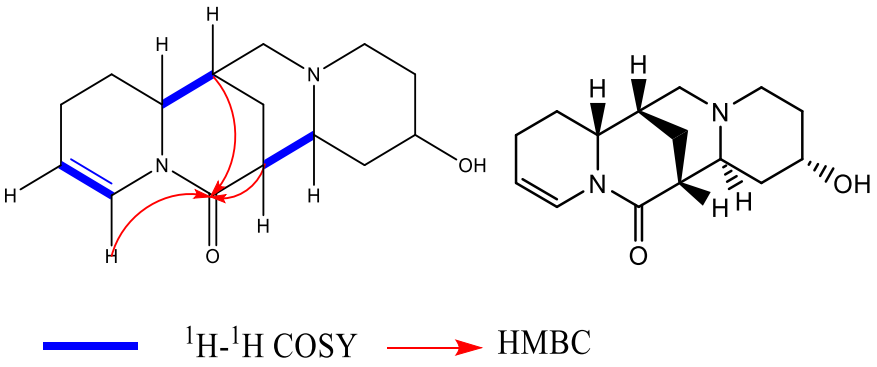

Figure 4.4: Structure, HMBC and COSY correlations of compound **49**

Compound **50** was isolated as a colorless solid with molecular formula $C_{20}H_{27}N_3O_3$ determined from its HRESIMS at *m/z* 358.2132 for $[M+H]^+$ (Calcd for $C_{20}H_{27}N_3O_3$, 358.2086) (Appendix 37 and 38). Other physiochemical parameters measured included: optical activity $[\alpha]_D^{25}$ -29 (c 0.1, MeOH); UV (MeOH) λ_{max} (log ε) 265 (0.656), 239 (0.249), 206 (0.483) (Appendix 43); ^{1}H and ^{13}C NMR data (CD_3OD, 700 MH_Z, 175 MH_Z) data (Table 4.5, appendix 39 and 40). Assignment of NMR data was done using 1D and 2D NMR spectra suggested that **50** just like the already described alkaloids had the basic structure of virgiline with pyrrolylcarbonyl substituent. The presence of the pyrrolylcarbonyl substituent was confirmed by ^{1}H NMR data [δ_H 6.91 H5′ (dd, J = 2.5, 1.5 Hz), 6.11 H4′ (dd, J = 3.8, 2.5 Hz, 6.84 H3′ (dd, J = 3.7, 1.5 Hz) and ^{13}C NMR data, δc 123.9 (C-2′), 116.1 (C-3′), 109.6 (C-4′), 123.9 (C-5′), 167.6 (C-6′) (Asres *et al.*, 1986).

The other oxygenated methine proton at δ_H 5.36 (H-13) showed a strong HMBC correlation (Fig. 4.5, Appendix 41) to the carbonyl carbon at δc 167.6 (C-6') indicating the attachment of the pyrrolylcarbonyl substituent on C-13. The presence of the other carbonyl group in ring B was confirmed by the HMBC correlations of H-6, H-7, H2-8, H-9 and H-11 to C-10 (δc 173.7). This showed that **50** is of the virgiline type. All other connectivities were confirmed by COSY, ^{1}H-^{1}H (Fig. 4.5, Appendix 42) correlation which displayed that the virgiline portion possessed a continuous spin system. These connectivities were also confirmed by HMBC correlations. From comparison with literature **50** was determined as 13α-*O*-(2'-pyrrolylcarbonyl) virgiline (Kubo *et al.*, 1984).

Table 4.4: The assignment of ^{13}CNMR, ^{1}HNMR, COSY and HMBC of compound **49**

NO	δ_C	TYPE/ DEPT	^{1}HNMR (δ_H, mult. *J* in Hz)	COSY	HMBC
1	N		-	-	-
2	123.3	CH	7.05, d (8.31)	3	3, 4, 6, 10
3	110.9	CH	5.07, m	2	2, 4, 5,
4	22.6	CH_2	2.10, m	3, 5	2, 3, 5, 6
5	25.2	CH_2	1.64, m	4, 6	3, 6, 7,
6	57.7	CH	3.49, m	5, 7	2, 4, 7, 8, 17
7	32.0	CH	2.01, m	6, 8, 17	5, 6, 8, 9, 17
8	21.7	CH_2	1.73, 1.93, m	9	7, 9, 10
9	43.0	CH	2.13, m	8, 11	8, 10, 11
10	171.3	Cq	-	-	-
11	53.5	CH	3.37, m	9, 12	9, 10, 12, 13, 15, 17
12	28.8	CH_2	28.8, m	12, 13	9, 13, 14
13	64.8	CH	4.04, m	12, 14	11, 15,
14	24.6	CH_2	1.07, 1.79, m	15	12, 13, 15,
15	47.9	CH_2	2.40, 3.07, m	14	11, 13, 14, 17
16	N	-	-	-	-
17	45.1	CH_2	2.54, 3.08, m	-	6, 7, 8, 11, 15

***** Recorded in CD_3OD at 700 MH_Z and 175 MH_Z

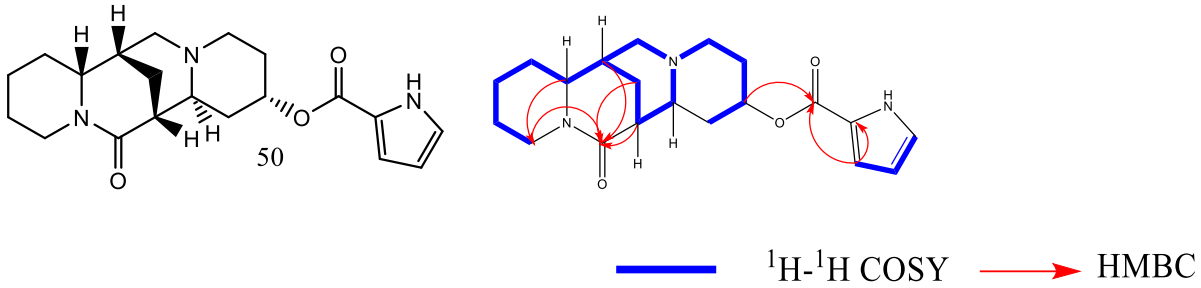

Figure 4.5: Structure, HMBC and COSY correlations of compound **50**

Table 4.5: The assignment of ^{13}CNMR, ^{1}HNMR, COSY and HMBC of compound **50**

No.	^{13}CNMR δ_C	TYPE/ DEPT	^{1}HNMR (δ_H, mult. *J* in Hz)	COSY	HMBC
1	N		-	-	-
2	49.6	CH2	3.13 (m), 2.77 (m)	3,	3, 4, 6, 10
3	32.1	CH_2	2.36	2,4	2, 4
4	18.9	CH_2	1.59 (m), 1.78 (m)	3,5	2, 3
5	29.6	CH_2	1.66 (m)	6	6
6	54.6	CH	3.71 (m)	5,7	4, 5, 7, 10, 17
7	32.8	CH	2.17 (m)	6, 17	6, 9
8	22.4	CH_2	1.80 (m), 2.11 (m)	9	6, 7, 9, 10, 17
9	44.1	CH	2.44 (m)	8, 11	8, 10, 11, 12
10	173.7	Cq	-	-	-
11	58.9	CH	3.02 (m)	9	9, 10, 12, 15, 17
12	26.6	CH_2	1.80 (m), 1.51 (m)	13	9
13	65.2	CH	5.17 (m)	12, 14	6′, 11, 12, 14, 15,
14	24.3	CH_2	1.61 (m), 2.13 (m)	13,15	13, 15
15	49.8	CH_2	2.79 (m), 3.43 (m)	14	11, 13, 14, 17
16	N		-	-	-
17	46.0	CH_2	2.67 (m), 4.43 (m)	7	6, 7, 8, 15
1′	N		-	-	-
2′	121.7	Cq	-	-	-
3′	116.1	CH	6.84 (dd, *J* = 3.7, 1.5 Hz)	4′	2′, 4′, 5′, 6′
4′	109.6	CH	6.11 (dd, *J* = 3.8, 2.5 Hz)	3′, 5′	2′, 3′, 5′, 6′
5′	123.9	CH	6.91 (dd, *J* = 2.5, 1.5 Hz)	4′	2′, 3′ ,4′, 6′
6′	167.6	Cq	-	-	-

***** Recorded in CD_3OD at 700 MH_Z and 175 MH_Z

Compound **51** was isolated as a colorless solid with molecular formula $C_{20}H_{27}N_3O_3$ determined from its HRESIMS at *m/z* 358.2122 for $[M+H]^+$ (Calcd for $C_{20}H_{27}N_3O_3$, 358.2086) (Appendix 44 and 45). Other physiochemical parameters measured included: optical activity $[\alpha]_D^{25}$ +30 (c 0.1, MeOH); UV (MeOH) λ_{max} (log ε) 265 (0.656), 239 (0.249), 200 (0.483) (Appendix 50); ^{1}H and ^{13}C NMR data (CD_3OD, 700 MHz, 175 MHz) data (Table 4.6, Appendix 46 and 47). Assignment of NMR data was done using 1D and 2D NMR spectra suggested that **51** just like the already described alkaloids had the basic structure of virgiline with pyrrolylcarbonyl substituent. The presence of the pyrrolylcarbonyl substituent was confirmed by ^{1}H NMR data [δ_H 6.91 H5′ (dd, *J* = 2.5, 1.5 Hz), 6.11 H4′ (dd, *J* = 3.8, 2.5 Hz, 6.84 H3′ (dd, *J* = 3.7, 1.5 Hz) and ^{13}C NMR data, δc 123.9 (C-2′), 116.1 (C-3′), 109.6 (C-4′), 123.9 (C-5′), 167.6 (C-6′) (Asres *et al.*, 1986). The other oxygenated methine proton at δ_H 5.36 (H-13) showed a strong HMBC correlation (Appendix 48) to the carbonyl carbon at δc 167.6 (C-6’) indicating the attachment of the pyrrolylcarbonyl substituent on C-13. The presence of the other carbonyl group in ring B was confirmed by the HMBC correlations of H-6, H-7, H2-8, H-9 and H-11 to C-10 (δc 173.7). This showed that **51** is of the virgiline type. All other connectivities were confirmed by COSY, ^{1}H-^{1}H correlations (Fig. 4.6, Appendix 49) which displayed that the virgiline portion possessed a continuous spin system. These connectivities were also confirmed by HMBC correlations. The data indicated above were the same as those of compound **50**, however, these two compounds differed in their optical activity in which this compound had an optical activity $[\alpha]_D^{25}$ +30 which was different from **50** which was $[\alpha]_D^{25}$ – 30. From comparison with literature **51** was determined as 13β-*O*-(2’-pyrrolylcarbonyl) virgiline (Kubo *et al.*, 1984).

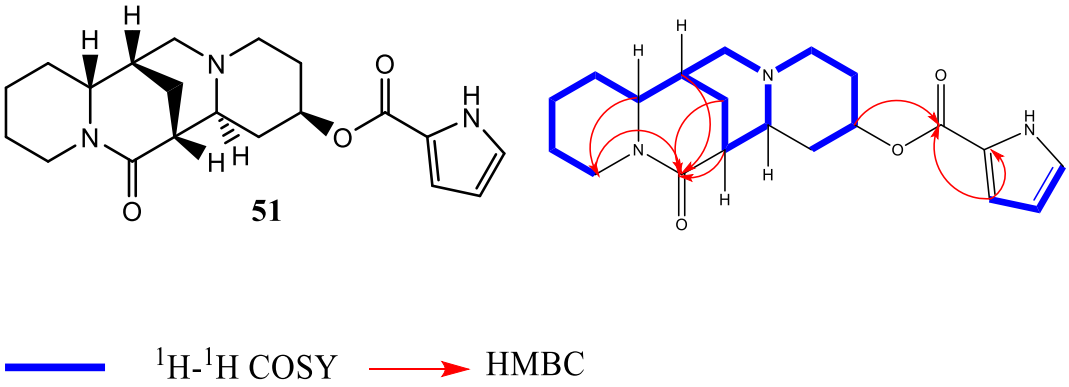

Figure 4.6: Structure, HMBC and COSY correlations of compound **51**

Compound **52** was isolated as a colourless solid with molecular formula $C_{20}H_{27}N_3O_3$ determined from its HRESIMS at *m/z* 354.1867 for $[M-H]^+$ (Calcd for $C_{20}H_{27}N_3O_3$, 356.1929) (Appendix 51 and 52). Other physiochemical parameters measured included: optical activity $[\alpha]_D^{25}$ + 43 (c 0.1, MeOH); UV (MeOH) λ_{max} (log ε) 261 (0.395), 239 (0.249), 195 (0.045); ^{1}H and ^{13}C NMR data (CD_3OD, 700 MHz, 175 MHz) data (Table 4.7). A total of 20 carbons were observed in the ^{13}C NMR spectrum (Table 4.7, Appendix 53 and 54).

Table 4.6: The assignment of ^{13}CNMR, ^{1}HNMR, COSY and HMBC of compound **51**

No.	^{13}CNMR δ_C	TYPE/ DEPT	^{1}HNMR (δ_H, mult. *J* in Hz)	COSY	HMBC
1	N		-	-	-
2	49.6	CH_2	3.37 (m), 2.79 (m)	3,	3, 4, 6, 10
3	33.4	CH_2	2.12	2,4	2, 4
4	22.7	CH_2	1.59 (m), 1.78 (m)	3,5	2, 3
5	29.6	CH_2	1.66 (m)	6	6
6	54.6	CH	3.71 (m)	5,7	4, 5, 7, 10, 17
7	32.8	CH	2.17 (m)	6, 17	6, 9
8	22.4	CH_2	1.80 (m), 2.11 (m)	9	6, 7, 9, 10, 17
9	44.1	CH	2.44 (m)	8, 11	8, 10, 11, 12
10	173.7	Cq	-	-	-
11	58.9	CH	3.02 (m)	9	9, 10, 12, 15, 17
12	26.6	CH_2	1.80 (m), 1.51 (m)	13	9
13	65.2	CH	5.17 (m)	12, 14	6′, 11, 12, 14, 15,
14	24.3	CH_2	1.61 (m), 2.13 (m)	13,15	13, 15
15	49.8	CH_2	2.79 (m), 3.43 (m)	14	11, 13, 14, 17
16	N		-	-	-
17	46.0	CH_2	2.67 (m), 4.43 (m)	7	6, 7, 8, 15
1′	N		-	-	-
2′	121.7	Cq	-	-	-
3′	116.1	CH	6.84 (dd, *J* = 3.7, 1.5 Hz)	4′	2′, 4′, 5′, 6′
4′	109.6	CH	6.11 (dd, *J* = 3.8, 2.5 Hz)	3′, 5′	2′, 3′, 5′, 6′
5′	123.9	CH	6.91 (dd, *J* = 2.5, 1.5 Hz)	4′	2′, 3′ ,4′, 6′
6′	167.6	C_q	-	-	-

***** Recorded in CD_3OD at 700 MHz and 175 MHz

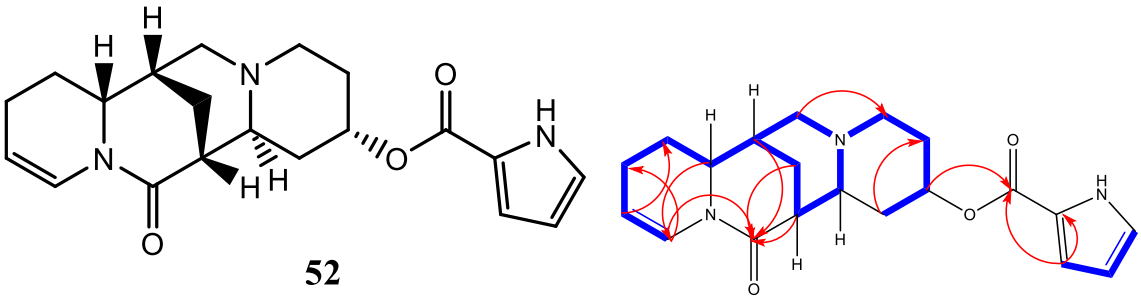

52

Figure 4.7: Structure, HMBC and COSY correlations of compound **52**

In general, the NMR data pointed to a virgiline carbon skeleton with a double bond due to the presence of sp2 carbons at δc 123.3 (C-2) and 110.9 (C-3). The HMBC correlations (Appendix 55) of H-6, H-7, H_2-8, H-9 and H-10 to the carbonyl group at δc 171.3 confirmed the virgiline structure. The COSY correlations (Appendix 56) of H_2-2 to H_2-3, H_2-3 to H_2-4, H_2-4 to H_2-5 and H_2-5 to H-6 identified the connectivities in A and the HMBC correlation of H-2 to C-10 confirmed the position of the double bond. In addition to that, the presence of a pyrrolylcarbonyl substituent was confirmed by ^{1}H NMR data [δ_H 6.92 (dd, *J* = 3.8, 1.5 Hz), 6.20 (dd, *J* = 3.7, 2.5 Hz), 7.10 (dt, *J* = 8.4, 2.0 Hz) and ^{13}C NMR data, δc 123.9 (C-2′), 116.1 (C-3′), 109.6 (C-4′), 123.9 (C-5′), 167.6 (C-6′) (Asres *et al.*, 1986). The other oxygenated methine proton at δ_H 5.37 (H-13) showed a strong HMBC correlation (Fig. 4.7, Appendix 55) to the carbonyl carbon at δc 167.6 (C-6') indicating the attachment of the pyrrolylcarbonyl substituent on C-13. These data together with those from literature indicated that **52** was as 2, 3-Dehydro-13α-*O*-(2'-pyrrolylcarbonyl) virgiline (Kubo *et al.*, 1984).

Compound **53** was isolated as yellow crystals with a molecular formula of $C_{20}H_{27}N_3O_3$ determined from its HRESIM at *m/z* 358.2052 for $[M+H]^+$ (Calcd for $C_{20}H_{27}N_3O_3$, 358.2076) (Appendix 57 and 58). Other physiochemical parameters measured included: optical activity $[\alpha]_D^{25}$ -11 (c 0.1, MeOH); UV (MeOH) λ_{max} (log ε) 265.5 (0.180), 239.5 (0.083), 208.5 (0.138), 199.5 (0.005) (Appendix 63); ^{1}H and ^{13}C NMR data (CD_3OD, 700 MH_Z, 175 MH_Z) data (Table 4.8, Appendix 58 and 59). Assignment of NMR data was done using 1D and 2D NMR spectra and by comparison with quinolizidine alkaloids reported in literature. The data (Table 4.8) suggested that **53** had the basic structure of lupanine with a pyrrolylcarbonyl substituents.

Table 4.7: The assignment of ^{13}CNMR, ^{1}HNMR, COSY and HMBC of compound **52**

NO	δ_C	TYPE/ DEPT	^{1}HNMR (δ_H, mult. *J* in Hz)	COSY	HMBC
1	N	-	-	-	-
2	123.5	CH	7.05, d (8.31)	3	3, 4, 6, 10
3	111.2	CH	5.25, m	2	2, 4, 5,
4	22.3	CH_2	2.09, 1.58, m	3, 5	2, 3, 5, 6
5	25.3	CH_2	1.88, m	4, 6	3, 6, 7,
6	57.7	CH	3.67, m	5, 7	2, 4, 7, 8, 17
7	31.9	CH	2.19, m	6, 8, 17	5, 6, 8, 9, 17
8	21.5	CH_2	2.14, 1.88, m	9	7, 9, 10
9	42.7	CH	2.40, m	8, 11	8, 10, 11
10	170.9	Cq	-	-	-
11	54.3	CH	3.65, m	9, 12	9, 10, 12, 13, 15, 17
12	26.3	CH_2	2.40, 1.61, m	12, 13	9, 13, 14
13	68.6	CH	5.37, m	12, 14	6′, 11, 12, 14, 15,
14	24.6	CH_2	1.07, 1.79, m	15	12, 13, 15,
15	47.9	CH_2	2.40, 3.07, m	14	11, 13, 14, 17
16	N	-	-	-	-
17	45.1	CH_2	2.54, 3.08, m	-	6, 7, 8, 11, 15
1′	N	-	-	-	-
2′	121.7	Cq	-	-	-
3′	116.1	CH	6.92 (dd, *J* = 3.8, 1.5 Hz)	4′	2′, 4′, 5′, 6′
4′	109.6	CH	6.20 (dd, *J* = 3.7, 2.5 Hz)	3′, 5′	2′, 3′, 5′, 6′
5′	123.9	CH	7.10 (dt, *J* = 8.4, 2.0 Hz)	4′	2′, 3′ ,4′, 6′
6′	167.6	Cq	-	-	-

***** Recorded in CD_3OD at 700 MH_Z and 175 MH_Z

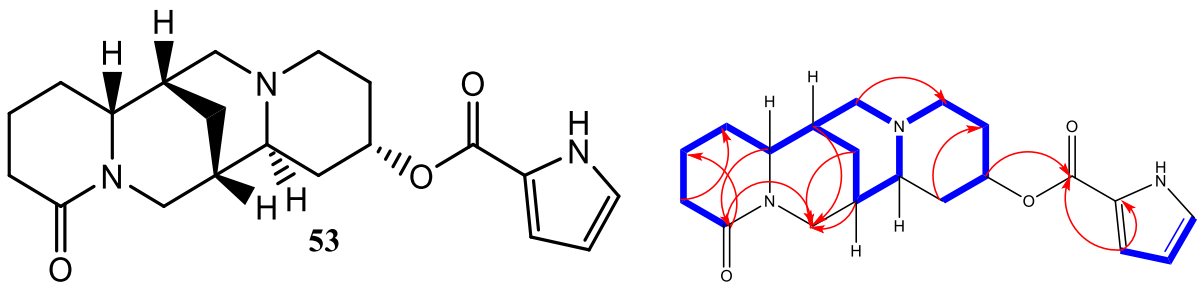

Figure 4.8: Structure, HMBC and COSY correlations of compound **53**

The presence of the pyrrolylcarbonyl substituent was confirmed by ^{1}H NMR data [δ_H 6.82 (H-3′ (ddd, *J* = 3.9, 2.4, 1.5 Hz), 6.17 (H-4′, dt, J = 2.33, 3.7 Hz), 7.01 (H-5′, td, J = 1.5, 2.7 Hz) and ^{13}C NMR data, δc 122.7 (C-2′), 115.7 (C-3′), 110.0 (C-4′), 124.3 (C-5′), 160.1 (C-6′). The presence of the carbonyl group was confirmed by a strong HMBC correlation between H-2, H-3, and H-10 to C-2 (δ 170.8) carbonyl substituents in ring A showing that **53** is of the lupanine type. The rest of the stereochemistry was assigned with the help of literature. The oxygenated methine proton at δ_H 5.29 (H-13) showed a strong HMBC correlation to the carbonyl carbon at δc 160.1 (C-6') indicating the attachment of the pyrrolylcarbonyl substituent on C-13. All other connectivities were confirmed by COSY (Appendix 62) and HMBC correlations (Fig. 4.8, Appendix 61). After comparison with literature, compound **53** was determined as 13α-*O*-(2′-pyrrolylcarbonyl) lupanine (Lindner *et al.*, 1976)**.**

Table 4.8: The assignment of ^{13}CNMR, ^{1}HNMR, COSY and HMBC of compound **53**

NO	δ_C	TYPE/ DEPT	^{1}HNMR (δ_H, mult. *J* in Hz)	COSY	HMBC
1	N	-	-	-	-
2	170.8	Cq	-	-	-
3	29.2	CH2	1.57, 1.45, m	2	2, 4, 5,
4	22.4	CH_2	1.84, 1.58, m	3, 5	2, 3, 5, 6
5	24.8	CH_2	1.80, 1.38, m	4, 6	3, 6, 7,
6	58.8	CH	3.26, m	5, 7	2, 4, 7, 8, 17
7	32.2	CH	1.97, m	6, 8, 17	5, 6, 8, 9, 17
8	22.6	CH_2	1.97, 1.25, m	9	7, 9, 10
9	43.1	CH	2.12, m	8, 11	8, 10, 11
10	41.9	CH_2	4.57 (ddt, *J* = 13.0, 4.1, 1.9 Hz, 1H), 2.31, m	-	-
11	52.3	CH	3.39, m	9, 12	9, 10, 12, 13, 15, 17
12	25.6	CH_2	1.60, 1.18, m	12, 13	9, 13, 14
13	69.0	CH	5.29 (q, *J* = 3.0 Hz, 1H)	12, 14	6′, 11, 12, 14, 15,
14	26.0	CH_2	2.12, 1.26, m	15	12, 13, 15,

NO	δ_C	TYPE/ DEPT	^{1}HNMR (δ_H, mult. *J* in Hz)	COSY	HMBC
15	48.2	CH_2	3.26, 2.54, m	14	11, 13, 14, 17
16	N	-	-	-	-
17	45.8	CH_2	2.55, 3.04, m	-	6, 7, 8, 11, 15
1′	N	-	-	-	-
2′	122.7	Cq	-	-	-
3′	115.7	CH	6.82 (ddd, *J* = 3.9, 2.4, 1.5 Hz, 1H)	4′	2′, 4′, 5′, 6′
4′	110.0	CH	6.17 (dt, *J* = 3.7, 2.3 Hz, 1H)	3′, 5′	2′, 3′, 5′, 6′
5′	124.3	CH	7.01 (td, *J* = 2.7, 1.5 Hz, 1H)	4′	2′, 3′ ,4′, 6′
6′	160.1	Cq	-	-	-

*Recorded in CD_3OD at 700 MH_Z and 175 MH_Z

4.3.2 Phenolic Compounds Isolated from the Leaves and Stem Bark

Twelve (12) phenolic compounds were isolated from the stem bark and leaves of *C. aurea* subsp. *aurea* and characterized based on their spectral data and physiochemical properties. Although previously isolated from other medicinal plants and apart from compounds **55** and **59** which have been reported from this plant, this is the first report on the isolation of remaining 10 phenolic compounds from the leaves and stem bark of *C. aurea* subsp. *aurea*. The chemical structures were determined based on the spectral data and literature comparison.

Compound **54** was isolated as a yellow amorphous powder (MeOH); UV spectral analysis showed absorption bands at λ_{max} (logε) (MeOH); 331(1,504), 268 (1.576), 205 (3.250) nm (Appendix 71). Its positive HRESIMS showed a peak at *m/z* 579.1711 $[M + H]^+$ corresponding to the molecular formula $C_{27}H_{30}O_{14}$ (calculated for 578.1669) (Appendix 64 and 65). ^{1}H and ^{13}C NMR data (CD_3OD, 700 MH_Z, 175 MH_Z) (Table 4.9, Appendix 66 and 67). The NMR data assignment was done by analysis of 1D and 2D NMR spectra and by comparison with already isolated flavonoids reported in literature. This compound had an apigenin core structure which was shown by both ^{13}C and ^{1}H spectra (Appendix 66 and 67). The proton spectrum ^{1}H revealed the presence of a pair of meta coupled aromatic protons (δ_H 6.77/6.45, doublets) with lower coupling constant values *J* = 2.2 Hz in ring A, a very distinguished aromatic singlet (δ_H 6.65) with one integration in ring C, and two doublets at δ_H 7.87 and δ_H 6.92 ppm with the same coupling constants *J* = 8.8 Hz, calculated for the two doublets with an integration 2H and 2H, which indicates the presence of ortho protons in ring

B. The most common up-field hydrogen bonded phenolic proton in ring B with carbonyl group on ring C at 12ppm in flavonoids was missed due to deuterium exchange from the deuterated methanol. In combination with the ^{13}C NMR data which showed signals for a carbonyl group at δ_C 182.6 (C-4), five oxygenated quaternary carbons, δ_C; 165.3 (C-2), 157.5 (C-5), 163.0 (C-7), 161.5 (C8a), and 163.0 (C-4′), two sp2 quaternary carbons δ_C 105.6 (C-4a) and δ_C 121.6 (C-1′),and seven sp2 tertiary carbons (methines) δ_C 94.5 (C-6), δ_C 99.6 (C-8), δ_C 102.7 (C-3), δ_C 115.7 (C3′and 5′), and δ_C 128.2 (C2′ and 6′). Additionally, the ^{1}H NMR (appendix 67) spectrum displayed signals at δ_H 5.20 (d, *J* = 7.6 Hz) which indicated the presence of a glucose anomeric proton and overlapping signals of between δ_H 3.40 – 3.95. The ^{13}CNMR showed signals δ_C 100.4 (C-1"), δ_C 77.6 (C-2"), δ_C 77.5 (C-3"), δ_C 76.9.7 (C-4"), δ_C 72.5 (C-5"), 61.1 (C6 ″)] indicating the presence of a glucosyl moiety. Additionally, the presence of a rhamnosyl group was shown by the proton signals at δ_H 5.29 (C1‴), a methyl proton δ_H 1.33 (3H, d, *J* = 6.2 Hz) which is characteristic of a rhamnosyl sugar, and other overlapping signals of between δ_H 3.41- 3.94. The ^{13}CNMR showed signals δ_C 98.4 (C-1‴), δ_C 70.0 (C-2"), δ_C 70.8 (C-3"), δ_C 72.5 (C-4"), δ_C 68.6 (C-5"), 16.8 (Rham, CH_3, C6 ″). The HMBC correlations (Appendix 69) from anomeric proton of α-rhamnosyl at δ_H at 5.29 to 77.6 (C2″) and anomeric proton of β-glucosyl at δ_H 5.20 to δ_C 163.0 (C-7), clarified the presence of neohesperidose attachment at position 7 of the apigenine core structure. After comparison with literature, compound **54** was determined as rhoifolin.

Compound **55** was isolated as a yellow amorphous powder (MeOH); UV (MeOH), λ_{max} 325, 268, 210 nm; HRESIMS *m/z* 433.1127 $[M + H]^+$ corresponding to the molecular formula of $C_{21}H_{20}O_{10}$ (Calculated for 433.1090) (Appendix 72 and 73). The ^{1}H and ^{13}C NMR data were measured in CD_3OD, 700 MH_Z, 175 MH_Z. The NMR data assignment was done by analysis of 1D and 2D NMR spectra (Table 4.9, Appendix 74 and 75) and by literature comparison. This compound had the same apigenin core structure as **54.** This was revealed by the ^{1}H spectra (Appendix 74) which showed the presence of meta-coupled aromatic protons δ_H 6.83 (d, *J* = 2.2 Hz, H-6) and δ_H 6.51 (d, *J* = 2.1 Hz, 1H, H-8) in ring A, an aromatic singlet 6.67 (s, 1H, H-3) with a single integration in ring C and two doublets with 2H integrations (δ_H 7.90 (d, *J* = 8.9 Hz, 1H, H2′, H6′) and δ_H 6.94 (d, *J* = 8.8 Hz, 2H, H3′, H5′). The higher coupling constants of these protons indicated the presence of *ortho* coupling in ring B. Just like shown in **54,** the up-field hydrogen bonded phenolic proton in ring B with carbonyl group in ring C at 12ppm was missing due to deuterium exchange from the deuterated methanol. The ^{13}C NMR spectra (Appendix 75) also showed signals for a carbonyl δ_C 182.7 (C-4), five oxygenated quaternary carbons δ_C; (165.4 (C-2), 157.5 (C-5), 163.4 (C-7), 161.5(C-8a) and 163.0 (C4′)); two sp2

quaternary carbons; δ_C 105.7 (C-4a) and δ_C 121.5, (C-1′) and seven methines groups δ_C 94.7 (C-6), 99.7 (C-8), 102.8 (C-3), 115.7 (C3′, C5′) and 128.3 (C2′, C6′). Unlike **54** which had a neohesperidose attachement, **55** had a glucosyl attachment at position 7 of the apigenin core. This was justified by the presence on an anomeric proton δ_H 5.07 (d, *J* = 7.1 Hz, 1H, glu H-1) which had an HMBC correlation (Appendix 76) to δ_C 163.4 (C-7). Another proton signal resonated at δ_H 3.50 (d, *J* = 3.6 Hz, H-2,) 3.40 (glu H-3), 3.55 (Glu H-4), 3.97 (Glu H-5), 3.92 and 3.70 glu H-6). Glucose carbon signals resonated at δ_C 101.6, δ_C 73.4 (Glu C-2), δ_C 69.9 (glu C-3), δ_C 76.9 (glu C-4), δ_C 68.3 (glu C-5), δ_C 61.0 (glu C-6). After comparison with literature this compound was determined as apigenin 7-*O*-glucoside

Compound **56** was isolated as a yellow (MeOH); UV (MeOH), λ_{max} 334 (0.931), 268 (1.322), 206 (3.739) nm; HRESIMS *m/z* 449.1080 $[M + H]^+$ corresponding to the molecular formula of $C_{21}H_{20}O_{11}$ (calculated for 449.1039) (Appendix 79 and 80). The ^1H and ^{13}C NMR data were measured in CD_3OD at 700 MHz and 175 MHz respectively. ^{13}CNMR data of this compound showed that it had 21 carbon atoms (Table 4.9, Appendix 82 and 83) of which 6 belong to the glycosyl moiety while 15 belong to the aglycone compound luteolin by comparing the ^1H and ^{13}C NMR data with literature. The core compound luteolin had proton peaks resonating at δ_H 6.80 (d, *J* = 2.2 Hz, H6) and δ_H 6.50 (d, *J* = 2.2 Hz, H-8) (Table 4.9, Appendix 81) indicating the presence of meta-coupled aromatic protons in Ring A. A very distinct aromatic singlet at δ_H 6.66 (s, 1H, H-3) with a single integration in ring C was also seen (Fig 4.9). Unlike **55** ring B of **56** had an ABC coupled aromatic protons resonating at δ_H 7.43 (d, *J* = 8.3, 2.2 Hz, 1H, H6′), 7.40 (d, *J* = 2.2 Hz, H2′), 6.91 (d, *J* = 8.3 Hz, H-5′). The ^{13}C NMR data showed peaks resonating at δ_C 182.6 (C-4) for the carbonyl, six oxygenated quaternary carbons; δ_C; 165.4 (C-2), 157.6 (C-5), 163.4 (C-7), 161.5 (C-8a), 145.7 (C-3′), 149.8 (C-4′); two sp2 quaternary carbons δ_C 105.7 (C-4a) and δ_C 122.1 (C-1′); six methines δ_C 95.9 (C-6), 101.0 (C-8), 104.0 (C-3), 114.2 (C2′), 119.1(C-5′), 116.7 (C-6′). The attachment of the glycosyl group at position 7 of the aglycone was shown by HMBC correlation (Appendix 83) of the anomeric proton δ_H 5.07 (d, *J* = 7.2 Hz) to δ_C 163.4 (C-7). Other proton signals of the glycosyl group resonated between δ_H 3.40-3.92 (glu H2-H6) while the ^{13}C signals had a resonance of δ_C 101.5 (anomeric), δ_C 74.7 (Glu C-2), δ_C 71.9 (glu C-3), δ_C 77.8 (glu C-4), δ_C 69.2 (glu C-5), δ_C 62.3 (glu C-6). After comparison with literature, compound **56** was determined as luteolin-7-*O*-glucoside (Lin *et al.,* 2015).

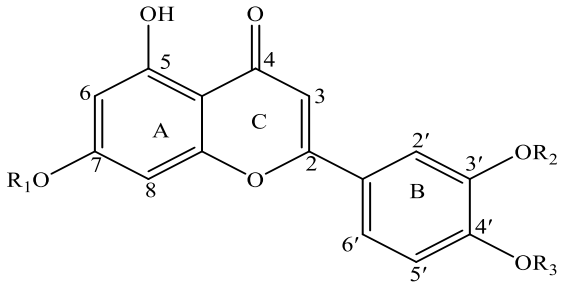

54: R1=neohesperidose, R2= H, R3= OH
55: R1= Glysosyl, R2= H, R3= OH
56: R1= Glycosyl, R2= OH, R3= OH

Figure 4.9: Chemical structures of compounds **54**, **55**, and **56**

Table 4.9*:* The assignment of ^{13}CNMR, ^{1}HNMR, COSY and HMBC of compound **54, 55 and 56**

No.	**54**		**55**		**56**	
	δ_C	δ_H, mult. (*J* in Hz)	δ_C	δ_H, mult. (*J* in Hz)	δ_C	δ_H, mult. (*J* in Hz)
1	-	-	-	-	-	-
2	165.3	-	165.4	-	165.4	-
3	102.7	6.65, s	102.8	6.67 s, 1H,	104.0	6.66 s, 1H,
4	182.6	-	182.67	-	182.6	-
4a	105.6	-	105.7	-	105.7	-
5	157.5	-	157.5	-	157.6	-
6	94.5	6.45, d, *J* = 2.2 Hz,	94.7	6.83 d, *J* = 2.2 Hz,	95.9	6.80 (d, *J* = 2.2 Hz, H6)
7	163.0	-	163.4	-	163.4	-
8	99.6	6.77, d, *J* = 2.2 Hz	99.7	6.51 d, *J* = 2.1 Hz,	101.0	6.50 (d, *J* = 2.2 Hz,
8a	161.5	-	161.5	-	161.5	-
1′	121.6	-	121.5	-	122.1	-
2′	128.2	6.92, 2H, d, *J* = 8.9 Hz	128.3	7.90 d, *J* = 8.9 Hz, 1H	114.2	7.40 d, *J* = 2.2 Hz,
3′	115.7	7.87, 2H, d, *J* = 8.8 Hz	115.7	6.94 (d, *J* = 8.8 Hz, 2H	145.7	-
4′	161.5	-	163.0	-	149.8	-
5′	115.7	7.87 (2H, d, *J* =	115.7	6.94 (d, *J* = 8.8	119.1	7.43 d, *J* = 8.3,

		8.8 Hz		Hz, 2H		2.2
No.	**54**		**55**		**56**	
	δ_C	δ_H, mult. (*J* in Hz)	δ_C	δ_H, mult. (*J* in Hz)	δ_C	δ_H, mult. (*J* in Hz)
6′	128.2	6.92 (2H, d, *J* = 8.9 Hz	128.3	7.90 d, *J* = 8.9 Hz, 1H	116.7	6.91 d, *J* = 8.3 Hz
Gluc-anomeric	98.4	5.20 d, *J* = 7.6 Hz,	101.6	5.07 (d, *J* = 7.1 Hz, 1H,	101.5	5.07 (d, *J* = 7.2 Hz, 1H),
C2 ″	77.6	[a]3.40-3.95, m	73.4	[a]3.40-3.97, m	74.7	[a]3.40-3.92, m
C3 ″	77.5	[a]3.40-3.95, m	69.9	[a]3.40-3.97, m	71.9	[a]3.40-3.92, m
C4 ″	76.9	[a]3.40-3.95, m	76.9	[a]3.40-3.97, m	77.8	[a]3.40-3.92, m
C5 ″	72.5	[a]3.40-3.95, m	68.3	[a]3.40-3.97, m	69.2	[a]3.40-3.92, m
C6 ″	61.1	[a]3.40-3.95, m	61.0	[a]3.40-3.97, m	62.3	[a]3.40-3.92, m
Rham- C1′ ″	101.1	5.29 (rha anomeric, H),	-	-	-	-
C2 ‴	70.0	[a]3.55-3.95, m	-	-	-	-
C3 ‴	70.8	[a]3.55-3.95, m	-	-	-	-
C4 ‴	72.5	[a]3.55-3.95, m	-	-	-	-
C5 ‴	68.6	[a]3.55-3.95, m	-	-	-	-
Rha- CH_3	16.8	1.33 (3H, d, *J* = 6.2 Hz	-	-	-	-
OCH_3	-	-	-	-	-	-
OCH_3	-	-	-	-	-	-

aSignals without multiplicity are overlapping signals deduced from the HSQC spectrum;* Recorded in CD_3OD at 700 MH_Z and 175 MH_Z

Compound **57** was isolated as a yellow gel (MeOH); UV (MeOH), λ_{max} 265, 305, nm; HRESIMS *m/z* 431.1339 $[M + H]^+$ corresponding to the molecular formula of $C_{22}H_{22}O_9$ (calculated for 431.1297) (Appendix 86 and 87). The ^1H and ^{13}C NMR data were measured in CD_3OD, at 700 MH_Z, 175 MH_Z respectively. This compound had an isoflavone skeleton which was shown by both the ^{1}HNMR, ^{13}CNMR and HSQC spectra (Appendix 88, 89 and 90). The proton NMR spectra (^1H NMR) showed the presence of a tri-substitution in ring A; δ_H 8.18 (d, *J* = 8.9 Hz, 1H, H-5) which was *ortho* coupled to δ_H 7.22 (dd, *J* = 8.9, 2.3 Hz, 1H, H-6) and

meta coupled to δ_H 7.26 (d, *J* = 2.3 Hz, 1H, H-8) (Table 4.10). From this substitution, together with ^{1}H- ^{1}H COSY correlations and HMBC correlations, the presence of the hydroxyl group was confirmed at position 7 of ring A. A singlet was seen in ring C resonating at δ_H 8.24 (s, 1H, H-2) while in ring B there was seen two doublets with 2H integrations δ_H 7.49 (d, *J* = 8.9 Hz, 2H, H3′ H5′) and δ_H 6.99 (d, *J* = 8.8 Hz, 2H, H2′, H6′) with ortho coupling. The ^{13}C NMR spectra also showed signals for carbonyl group δ_C 176.5 (C-4), oxygenated quaternary carbons δ_C; 163.4 (C-7), δ_C 159.1 (C-8a), two sp2 quaternary carbons δ_C; 120.1 (C-4a) and 124.9 (C-1′), seven methines resonating at δ_C ; 128.2 (C-5), 104.9 (C-8), 117.0 (C-6), 130.0 (C-2′, 6′), and 113.5 (C3′, 5′) and an oxygenated methine δ_C 153.9 (C-2). An extra methoxy group connecting at C-4′ was deduced by HMBC correlation between OCH_3 δ_H 3.83 (3H, s) (δ_C 54.3) and C-4′ δ_C 161.0. The remaining data showed the presence of gluco-pyranosyl group δ_H (5.11, d, *J* = 7.4 Hz, H-1″) and other protons resonating between δ_H: 3.41-3.94 (6H, H-2″-6″). The ^{13}C NMR data were δ_C; 100.4 (glu anomeric), 73.3 (glu C-2), 69.8 (glu C-3), 76.5 (glu C-4), 76.7 (glu C-5), 61.0 (glu, C-6). The HMBC correlation between the anomeric proton and C-7 of the isoflavone confirmed the glucopyranosyl attachment to the isoflavone core compound. After comparison with literature compound **57** was determined as ononin (Lee *et al.,* 2006; Nakanishi *et al.,* 1985)

Compound **58** was isolated as a yellow amorphous powder (MeOH); UV (MeOH), λ_{max} 268, 206 nm; HRESIMS *m/z* 269.0805 $[M + H]^+$corresponding to the molecular formula of $C_{16}H_{12}O_4$; calculated for 269.0769 (Appendix 93 and 94). The ^{1}H and ^{13}C NMR data were measured in CD_3OD at 700 MH_Z, 175 MH_Z respectively. This compound is a fragment of **57** without the glucopyranosyl moiety and with an isoflavone core. Ring A was tri-substituted as shown in the ^{1}H NMR resonating at δ_H 6.97 (dd, *J* = 8.8, 2.3 Hz, 1H, H-6), 8.08 (d, *J* = 8.8 Hz, 1H, H-5) 6.87 (d, *J* = 2.2 Hz, 1H, H-8) (Table 4.10, Appendix 95). Ring C was characterized by the presence of a singlet resonating at δ_H 8.26 (s, 1H, H-2) while ring B was characterized by the presence of *ortho* coupled doublets with 2H integrations resonating at δ_H 6.98 (dd, *J* = 8.9, 2.0 Hz, 2H, H2′, H6′) and δ_H 7.48 (d, *J* = 8.5, H3′, H5′). The ^{13}C NMR spectra (Appendix 96 and 97) showed carbonyl signals at δ_C 178.0 (C-4), oxygenated quaternary carbons δ_C; 159.9 (C-2), 164.6 (C), 159.1 (C-9), three sp2 quaternary carbons δ_C; 118.1(C-10), 125.5 (C-3), 125.3 (C-1′) and seven methines resonating at δ_C; 128.4 (C-5), 116.3 (C-6), 103.5 (C-8), 131.3 (C2′, 6′) and 114.7 (C-3′, 5′) and an oxygenated methine δ_C 154.5 (C-2). An additional methoxy group connecting at C-4′ was confirmed by HMBC correlation between OCH_3 δ_H 3.83 (δ_C 55.0) and δ_C 161.0 (C-4′). After comparison with literature, compound **58** was determined as formononetin (Lanisnik Rizner *et al.,* 2019; Vetter, 1995)

Table 4.10: The assignment of ^{13}CNMR, ^{1}HNMR, COSY and HMBC of compound **57** and **58**

No.	**57**		**58**	
	δ_C	δ_H, mult. (*J* in Hz)	δ_C	δ_H, mult. (*J* in Hz)
1	-	-	-	-
2	153.9	8.24 s, 1H	154.5	8.26 s, 1H
3	125.9	-	125.5	-
4	176.5	-	178.0	-
5	128.2	8.16 (d, *J* = 8.9 Hz, 1H	128.4	8.08 (d, *J* = 8.9 Hz, 1H
6	117.0	7.22 (dd, *J* = 8.9, 2.3 Hz, 1H)	116.3	6.97 (dd, *J* = 8.9, 2.3 Hz, 1H)
7	163.4	-	164.6	-
8	104.9	7.26, d, *J* = 2.3 Hz	103.1	6.87, d, *J* = 2.3 Hz
9	159.1	-	159.1	-
10	120.1	-	118.1	-
1′	124.9	-	125.3	-
2′	130.0	7.48 d, *J* = 8.5, 2H	131.3	7.48 d, *J* = 8.5,
3′	113.5	6.99 (d, *J* = 8.8 Hz, 2H	114.7	6.98 dd, *J* = 8.9, 2.0 Hz, 2H
4′	159.9	-	161.0	-
5′	113.5	6.99 d, *J* = 8.8 Hz, 2H,	114.7	6.98, dd, *J* = 8.9, 2.0 Hz, 2H
6′	130.0	7.48 d, *J* = 8.5, H3′	131.3	7.48 d, *J* = 8.5
Gluc-anomeric	100.4	5.11	-	-
C2 ″	73.3	[a]3.41- 3.94	-	-
C3 ″	69.8	[a]3.41- 3.94	-	-
C4 ″	76.5	[a]3.41- 3.94	-	-
C5 ″	76.7	[a]3.41- 3.94	-	-
C6 ″	61.0	[a]3.41- 3.94	-	-
OCH_3	54.3	3.83, s	55.0	3.83

*[a]Signals without multiplicity are overlapping signals deduced from the HSQC spectrum; *Recorded in CD_3OD at 700 MH_Z and 175 MH_Z

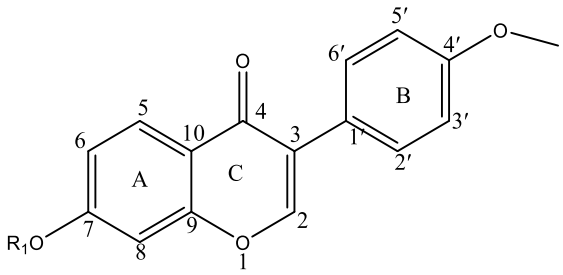

57: R1= glucopyranosyl
58: R1= H

Figure 4.10: Chemical structures of compounds **57** and **58**

Compound **59** was isolated as a white needle (MeOH); UV (MeOH), λ_{max} 251 (2.839), 209 (4.4.516) nm; HRESIMS *m/z* 299.0912 $[M + H]^+$ corresponding to a molecular formula of $C_{17}H_{14}O_5$ (calculated for 299.0875) (Appendix 100 and 101); ^1H and ^{13}C NMR data were recorded in CD_3OD, 700 MH_Z, 175 MH_Z respectively. From the 1D and 2D NMR analysis, this compound contained one hydroxyl and two methoxyl groups, and a singlet at δ_H 8.26 (s, 1H, H2) in ring C a characteristic of an isoflavonoid. The aromatic proton signal comprised of an signal resonating at δ_H 7.83 (d, *J* = 8.9 Hz, 1H, H5) and δ_H 7.01 (d, *J* = 8.8 Hz, 2H, H6), that were *ortho* coupled given their high coupling constants (*J* = 8.9 Hz) in ring A. Ring B was characterized by the presence of *ortho* coupled doublets with 2H integrations resonating at δ_H 7.48 (d, *J* = 8.8 Hz, 2H, H2′, 6′), 6.99 (d, *J* = 8.7 Hz, 2H, H3′, H5′) (Table 4.11, Appendix 102). The ^{13}CNMR spectra (Appendix 103 and 104) showed carbonyl signal at δ_C 177.9 (C-4), oxygenated quaternary carbon δ_C; 156.5 (C-7) and 152.7 (C-9), methines δ_C; 115.2 (C-6), 122.2 (C-5), 154.5 (C-2), 130.1 (C2′, C6′), 113.5 (C3′, C5′), two sp2 quaternary carbons δ_C; 118.9 (C-4a) 125.9 (C-3) and 124.8 (C-1′) (Table 12). Additionally, HMBC correlations were used to determine the attachment of methoxy groups at position 8 and 4′. The singlet 3.97 (s, 1H) (δ_C 61.7) had a correlation with the carbon resonating at δ_C; 135.2 (C-8), in ring A while the singlet resonating at δ_H 3.83 (s, 1H) (δ_C 55.6) had a correlation with carbon at C-4′ resonating at δ_C 160.1 in ring B. After comparison with literature, compound **59** was determined as 8-*O*-methylretusin (Sichaem *et al.*, 2018).

Compound **60** was isolated as a white amorphous powder (MeOH); UV (MeOH), λ_{max} 330 (1.025), 254 (1.496), 204 (2.655) nm (Appendix 113); HRESIMS *m/z* 461.1444 $[M + H]^+$ corresponding to a molecular formula of $C_{23}H_{24}O_{10}$ calculated for 461.1403 (Appendix 107 and 108); The ^1H and ^{13}C NMR data were recorded in CD_3OD, 700 MH_Z, 175 MH_Z

respectively. From the 1D and 2D NMR analysis, compound **60** was like compound **59** with an extra glycosyl group which was also observed in the mass spectra fragmentation of 298.99 $[M + H]^+$ and 461.13 $[M + H]^+$. The core compound contained one hydroxyl and two methoxyl groups, and a singlet at δ_H 8.29 (s, 1H, H2), in ring C a characteristic of an isoflavonoid. The aromatic proton signal comprised of an signal resonating at δ_H 7.93 (d, *J* = 9.1 Hz, 1H, H5), and δ_H 7.40 (d, *J* = 9.2 Hz, 1H, H6), that were *ortho* coupled given their high coupling constants (*J* = 9.2 Hz) in ring A. Ring B was characterized by the presence of *ortho* coupled doublets with 2H integration resonating at δ_H 7.51 (d, *J* = 8.8 Hz, 2H, H2′, 6′), δ_H 7.00 (d, *J* = 8.9 Hz, 2H, H3′, H5′) (Table 4.11, Appendix 109). The ^{13}CNMR spectra showed carbonyl signal at δ_C 177.8 (C-4), oxygenated quaternary carbon δ_C; 155.7 (C-7) and δ_C 152.3 (C10), methines δ_C; 115.5 (C-6), 121.9 (C-5), 155.2 (C-2), 131.3 (C2′, C6′), 114.7 (C3′, C5′), three sp2 quaternary carbons δ_C; 118.9 (C-4a) 125.9 (C-3) and 124.8 (C-1′). Additionally, HMBC correlations (Appendix 111) were used to determine the attachment of methoxy groups at position 8 and 4′. The singlet δ_H 4.03 (s, 1H) (δ_C 62.2) had a correlation with the carbon resonating at δ_C; 138.8 (C-8), in ring A while the singlet resonating at δ_H 3.83 (s, 1H) (δ_C 55.6) had a correlation with carbon at C-4′ resonating at δ_C; 161.0 in ring B. The attachment of the glycosyl moiety at position 7 of the isoflavonoid core structure was determined by HMBC correlation between the anomeric proton δ_H 5.15 (d, *J* = 7.6 Hz, 1H) to carbon 155.7 (C-7). Other glycosyl protons resonated between δ_H 3.43-3.92 (glu H2-H6) while the resonance of the carbon atoms was δ_C; 102.1 (glu anomeric), 74.8 (glu, C2), 77.9 (glu C3), 71.1 (glu C4), 78.1 (glu C5), 62.3 (glu, C6) (Table 4.11). The HSQC correlations (Appendix 110) was used to determine the protons that are directly attached to carbon atoms (CH, CH_2 and CH_3) with their respective resonance and the ^{1}H-^{1}H COSY spectra (Appendix 112) were used to determine the correlation between protons on adjacent carbon atoms. The quaternary carbon atoms were determined from the correlations on the HMBC spectra. After comparison with literature, compound **60** was determined as 8-*O*-methylretusin-7-*O*-β-D-glucopyranoside (Sichaem *et al*., 2018).

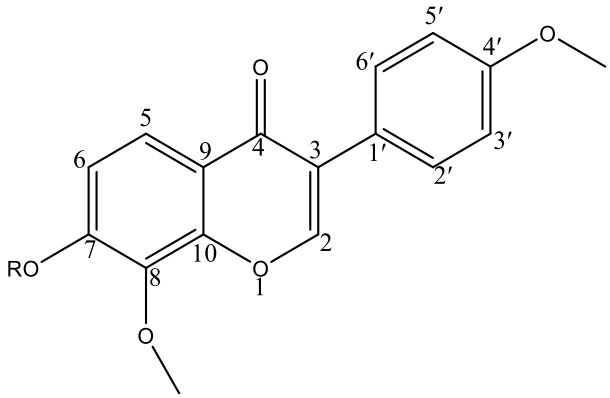

59: R= H
60: R= Glucopyranosyl

Figure 4.11: Chemical structures of compounds **59** and **60**

Compound **61** was isolated as a yellow amorphous powder (MeOH); UV spectral analysis showed absorption bands at λ_{max} (logε) (MeOH); 330 (1,504), 268 (1.576), 205 (3.250) nm (Appendix 120). Its positive HRESIMS showed a peak at *m/z* 581.1864 $[M + H]^+$ corresponding to the molecular formula $C_{27}H_{32}O_{14}$ (calculated for 581.1826) (Appendix 114 and 115). The ^1H and ^{13}C NMR data were measured in CD_3OD, 700 MH_Z, 175 MH_Z, respectively (Appendix 117 and 118). The NMR data assignment was done by analysis of 1D and 2D NMR spectra (Table 4.12) and by comparison with already isolated flavonoids reported in literature. This compound was a flavanone derivative observed by both ^{13}C and ^1H spectra. The proton spectrum ^1H revealed the presence of a pair of meta coupled aromatic protons δ_H 6.11 (1H, d, *J* = 2.2 Hz, H8), δ_H 6.08 (1H, d, *J* = 2.2 Hz, H6), with lower coupling constant values *J* = 2.2 Hz in ring A and two doublets at δ_H 7.32 (2H, d, *J* = 8.8 Hz, H-2′, H6′), δ_H 6.80 (2H, d, *J* = 8.9 Hz, H3′, H5′) with the same coupling constants *J* = 8.8 Hz, calculated for the two doublets with an integration 2H and 2H, which indicates the presence of ortho protons in ring B. Ring C was characterized by the presence of a oxygenated methine proton resonating at δ_H 5.56 (d, *J* = 3.4 Hz, 1H), methylene protons δ_H 2.72 (dd, *J* = 5.6, 3.0 Hz, H-2), δ_H 3.38 (dd, *J* = 5.6, 3.0 Hz, H-2).

In combination with the ^{13}C NMR data which showed signals for a carbonyl group at δ_C 197.4 (C-4), four oxygenated quaternary carbons, δ_C; 157.5 (C-5), 163.0 (C-7), 165.1 (C-8a), and 158.1 (C- 4′), two sp2 quaternary carbons δ_C 103.6 (C-4a), and δ_C 121.6 (C-1′), six sp2 tertiary carbons (methines) δ_C; 96.8 (C-6), 95.6 (C-8), 115.8 (C3′and 5′), and 128.9 (C2′, C6′), oxygenated methine δ_C 79.0 (C-2) and methylene carbon δ_C 42.6 (C-3).

Table 4.11: The assignment of ^{13}CNMR, ^{1}HNMR, COSY and HMBC of compound **59 and 60**

No.	**59**		**60**	
	δ_C	δ_H, mult. (*J* in Hz)	δ_C	δ_H, mult. (*J* in Hz)
1	-	-	-	-
2	154.5	8.26 (s,)	155.2	8.29 (s,
3	152.7	-	152.1	-
4	177.9	-	177.8	-
5	122.2	7.83 (d, *J* = 8.9 Hz	121.9	7.93 (d, *J* = 9.1 Hz
6	115.2	7.01 (d, *J* = 8.8 Hz	115.5	7.40 (d, *J* = 9.2 Hz,
7	160.1	-	155.7	-
8	135.2	-	138.8	-
9	152.7	-	152.3	-
10	125.3	-	122.1	-
1′	124.5	-	124.8	-
2′	130.1	6.99 (d, *J* = 8.7 Hz	131.3	7.00 (d, *J* = 8.9 Hz
3′	113.5	7.48 (d, *J* = 8.8 Hz	114.7	7.51 (d, *J* = 8.8 Hz
4′	160.1	-	161.0	-
5′	113.5	7.48 (d, *J* = 8.8 Hz,	114.7	7.51 (d, *J* = 8.8 Hz
6′	130.1	6.99 (d, *J* = 8.7 Hz,	131.3	7.00 (d, *J* = 8.9 Hz
Gluc- anomeric	-	-	102.1	5.15 (d, *J* = 7.6 Hz
C2 ″	-	-	74.8	[a]3.43-3.92, m
C3 ″	-	-	77.9	[a]3.43-3.92, m
C4 ″	-	-	71.1	[a]3.43-3.92, m
C5 ″	-	-	78.1	[a]3.43-3.92, m
C6 ″	-	-	62.3	[a]3.43-3.92, m
OCH_3	54.4	3.97 (s)	55.6	4.03 (s)
OCH_3	60.5	3.83 (s)	62.2	3.83 (s)

*[a]Signals without multiplicity are overlapping signals deduced from the HSQC spectrum; *Recorded in CD_3OD at 700 MHz and 175 MHz

Additionally, the ^{1}H NMR (appendix 116) spectrum displayed signals at δ_H 5.20 (d, *J* = 7.6 Hz, glc anomeric H), which indicated the presence of a glucose anomeric proton and

overlapping signals of between δ_H 3.40 – 3.95. The ^{13}C NMR showed signals δ_C 97.9 (C-1"), δ_C 77.6 (C-2"), δ_C 77.5 (C-3"), δ_C 76.9.7 (C-4"), δ_C 72.5 (C-5"), δ_C 61.1 (C6 ″)] indicating the presence of a glucosyl moiety. Additionally, the presence of a rhamnosyl group was shown by the proton signals at δ_H 5.29 (C1‴), a methyl proton δ_H 1.04 (3H, d, *J* = 6.2 Hz, rha CH_3); which is characteristic of a rhamnosyl sugar, and other overlapping signals of between δ_H 3.41-3.94. The ^{13}C NMR showed signals δ_C 101.0 (C-1"'), δ_C 70.0 (C-2"), δ_C 70.8 (C-3"), δ_C 72.5 (C-4"), δ_C 68.6 (C-5"), δ_C 18.5 (Rham, CH_3, C6 ″). The HMBC correlations (Appendix 118) from anomeric proton of α-rhamnosyl at δ_H at 5.29 to 77.6 (C2″) and anomeric proton of β-glucosyl at δ_H 5.20 to δ_C 163.0 (C-7), clarified the presence of neohesperidose attachment at position 7 of the flavanone core structure. After comparison with literature, compound **61** was determined as naringin.

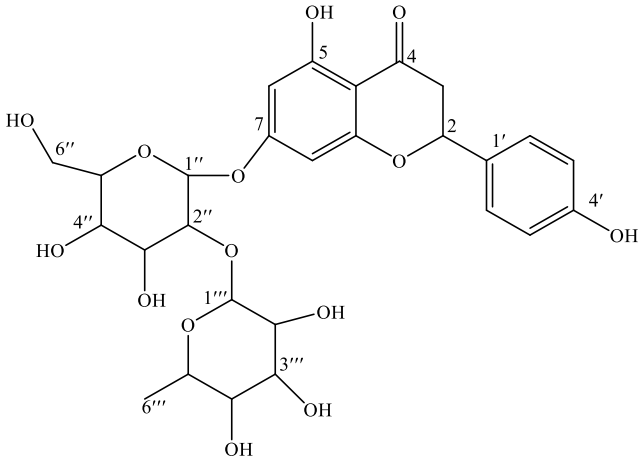

Figure 4.12: Chemical structure of compounds **61**

Compound **62** was isolated as a colourless oil (MeOH); UV (MeOH), λ_{max} 309 (1.696), 286 (1.406), 205 (5.000) nm (Appendix 127); HRESIMS *m/z* 285.0754 $[M + H]^+$ corresponding to a molecular formula of $C_{16}H_{12}O_5$ calculated for 285.0718 (appendix 121 and 122); The ^1H and ^{13}C NMR data were measured in CD_3OD, 700 MHz, 175 MHz respectively. The ^1H NMR spectrum (Appendix 123) showed a characteristic set of peaks corresponding to a pterocarpan skeleton as suggested by (Mizuno *et al.*, 1990) δ_H; 3.47 (ddd, *J* = 10.6, 7.0, 4.8 Hz, H6a), δ_H 3.56 (t, *J* = 10.7 Hz, H6), δ_H 4.23 (m, H6) and δ_H 5.45 (d, *J* = 6.9 Hz, H11a) (Table 4.13).

Table 4.12: The assignment of ^{13}CNMR, ^{1}HNMR, COSY and HMBC of compound **61**

No.	δ_C	δ_H, mult. (*J* in Hz)
1	-	-
2	79.0	5.50 (H-2)
3	42.6	3.35,2.73 (H-3),
4	197.4	-
4a	121.6	-
5	157.5	-
6	96.8	6.08 (1H, d, *J* = 2.2 Hz
7	163.0	-
8	95.6	6.11 (1H, d, *J* = 2.2 Hz
8a	161.5	-
1′	121.6	-
2′	115.8	7.32 (2H, d, *J* = 8.8 Hz
3′	128.9	6.80 (2H, d, *J* = 8.9 Hz
4′	158.1	-
5′	128.9	6.80 (2H, d, *J* = 8.9 Hz
6′	115.8	7.32 (2H, d, *J* = 8.8 Hz
Gluc- anomeric	97.9	5.20 (d, *J* = 7.6 Hz
C2 ″	77.6	[a]3.40-3.95, m
C3 ″	77.6	[a]3.40-3.95, m
C4 ″	76.9	[a]3.40-3.95, m
C5 ″	72.5	[a]3.40-3.95, m
C6 ″	61.1	[a]3.40-3.95, m
Rham- C1′ ″	101.0	5.29 (rha anomeric, H),
C2 ‴	70.0	[a]3.55-3.95, m
C3 ‴	70.8	[a]3.55-3.95, m
C4 ‴	72.5	[a]3.55-3.95, m
C5 ‴	68.6	[a]3.55-3.95, m
Rha- CH_3	18.5	1.04 (3H, d, *J* = 6.2 Hz,

*[a]Signals without multiplicity are overlapping signals deduced from the HSQC spectrum;

*Recorded in CD_3OD at 700 MH_Z and 175 MH_Z

The ^{1}H NMR spectrum also showed a methylenedioxy functional group indicated by a two-proton doublet of doublet at δ_H 5.87 (dd, *J* = 13.0, 1.2 Hz, H1′). The protons in the aromatic ring A had a resonance of δ_H 7.26 (dd, *J* = 8.4, 0.6 Hz, H1) which was *ortho* coupled to δ_H 6.48 (dd, *J* = 8.4, 2.4 Hz, H2) while H-2 was meta coupled to δ_H 6.30 (d, *J* = 2.4 Hz, H4). This pattern ascertained that the hydroxyl group was attached at position 3 of aromatic ring A while the methylenedioxy was attached to ring D. Two singlets / Parasubstituted aromatic protons δ_H 6.80 (d, *J* = 0.6 Hz, 1H, H7) and δ_H 6.37 (s, H10), were assigned to ring D. The assignment of ^{13}C NMR chemical shifts was subject to analysis of HSQC and HMBC spectra (appendix 124 and 124) which included; five methine carbons with a resonance of δ_C ;133.1 (C-1), 110.6 (C-2), 104.0 (C-4), 105.9 (C-7), 94.1 (C-10), five oxygenated aromatic carbon δ_C ; 160.1 (C-3), 149.4 (C-9), 143.0 (C-8), 155.5 (C-10a), 157.9 (C-4a), two oxygenated methylene δ_C 67.3 (C-6) and δ_C 102.3 (C1′), one oxygenated methine δ_C 79.9 (C-11a) and methine 40.2 (C-6a) and one sp2 hybridized carbon δ_C 119.8 (C-6b). Additionally, the signal δ_H 5.87 (OCH_2O) showed a long-range correlation with C-8 and C-9 δ_C 143.0, 149.4 respectively confirming the attachment of methylenedioxy to ring D. After comparison with literature, compound **62** was determined as Maackiain (Mizuguchi *et al.,* 2015; Mizuno *et al.,* 1990).

Compound **63** was isolated as a colourless crystals (MeOH); UV (MeOH), λ_{max} 286, 214 nm (Appendix 134); HRESIMS *m/z* 447.1278 $[M + H]^+$ corresponding to a molecular formula of $C_{22}H_{22}O_{10}$ calculated for 447.1247 (Appendix 128 and 129); The ^{1}H and ^{13}C NMR data were measured in CD_3OD, 700 MH_Z, 175 MH_Z respectively). This compound was like **61** apart from the additional gluco-pyranosly moiety. The ^{1}H NMR spectrum showed a characteristic set of peaks corresponding to a pterocarpan skeleton as suggested by Mizuno *et al.* (1990); δ_H 3.53 (dd, *J* = 6.8, 4.5 Hz, H6a), δ_H 4.26 (dd, *J* = 10.9, 4.7 Hz, H6), δ_H 3.60 (t, *J* = 10.6 Hz, H6) and δ_H 5.49 (d, *J* = 7.0 Hz, H11a) (Table 4.13, Appendix 130). The ^{1}H NMR spectrum also showed a methylenedioxy functional group indicated by a two-proton doublet of doublet at δ_H 5.87 (d, *J* = 12.9 Hz, H1′). The protons in the aromatic ring A had a resonance of δ_H 7.38 (d, *J* = 8.5 Hz, H1), which was *ortho* coupled to δ_H 6.79 (dd, *J* = 8.5, 2.5 Hz, H2), while H-2 was meta coupled to δ_H 6.64 (d, *J* = 2.4 Hz, H4). This pattern ascertained that the hydroxyl group was attached at position 3 of aromatic ring A while the methylenedioxy was attached to ring D. Two singlets / parasubstituted aromatic protons δ_H 6.81 (s, H7), δ_H 6.38 (s, H10), were assigned to ring D. The assignment of ^{13}C NMR chemical shifts was subject to analysis of HSQC and HMBC spectra (Appendix 131 and 132) which included; five methine carbons with a resonance of δ_C ;132.9 (C-1), 111.5 (C-2), 105.5 (C-4), 105.8 (C-7), 94.0 (C-10), five oxygenated aromatic carbon δ_C ; 160.1 (C-3), 149.9 (C-9), 143.0 (C-8), 155.4 (C-10a), 157.7

(C-4a), two oxygenated methylene δ_C 67.4 (C-6) and δ_C 102.2 (C1′), one oxygenated methine δ_C 79.5 (C-11a) and methine δ_C 41.5 (C-6a) and one sp2 hybrdized carbon δ_C 119.5 (C-6b). Additionally, the signal δ_H 5.87 (OCH_2O) showed a long-range correlation with C-8 and C-9 δ_C 143.0, δ_C 149.9 respectively confirming the attachment of methylenedioxy to ring D. The presence of the glucopyranosyl moiety was confirmed by the presence of anomeric proton δ_H 4.90 (d, *J* = 7.2 Hz, 1H, glu anomeric) which had an HMBC correlation with δ_C 160.1 (C-3) hence confirming its attachment to ring A of the pterocarpan core. Other proton correlations for the sugar moiety ranged between δ_H 3.45-3.87(glu H2-H6) while the ^{13}C NMR chemical shifts were δ_C; 101.9 (glu anomeric), 74.7 (glu C-2), 77.9 (glu C-3), 71.3 (glu C-4), 71.1 (glu C-5), 62.3 (glu C-6). After comparison with literature, compound **63** was determined as trifolirhizin (Aratanechemuge *et al.*, 2004).

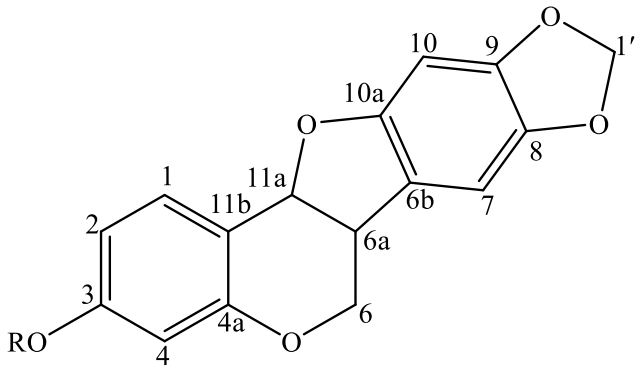

62: R=H
63: R= glucopyranosyl

Figure 4.13: Chemical structure of compounds **62** and **63**

Compound **64** was isolated as pale-yellow crystals (MeOH); UV (MeOH), λ_{max} 286 (1.736), 214(4.366) nm (appendix 141); HRESIMS *m/z* 271.0964 $[M + H]^+$corresponding to a molecular formula of $C_{16}H_{14}O_4$ calculated for 279.0926 (appendix 135 and 136); The ^1H and ^{13}C NMR data were measured in CD_3OD, 700 MH_Z, 175 MH_Z respectively. This compound was similar to **61** however instead of a methylenedioyx, it had a methoxy attachment in ring D. The ^1H NMR spectrum (appendix 137) showed a characteristic set of peaks corresponding to a pterocarpan skeleton as suggested by (Mizuno *et al.*, 1990); δ_H 3.53 (dd, *J* = 6.8, 4.5 Hz, H6a), δ_H 4.24 (dd, *J* = 10.9, 4.7 Hz, H6), δ_H 3.55 (t, *J* = 10.6 Hz, H6) and δ_H 5.49 (d, *J* = 7.0 Hz, H11a) (Table 4.13). The protons in the aromatic ring A had a resonance of δ_H 7.31 (d, *J* = 8.4 Hz, H1), which was ortho coupled to δ_H 6.51 (dd, *J* = 8.4, 2.5 Hz, H2), while H-2 was meta coupled to δ_H 6.32 (d, *J* = 2.4 Hz, H4). This pattern, together with $^1H - ^1H$ COSY (appendix

140) and HMBC correlation (appendix 139) ascertained that the hydroxyl group was attached at position 3 of aromatic ring A. Ring D was characterized by the presence of a doublet δ_H 7.19 (d, *J* = 8.2 Hz, H7) which was *ortho* coupled to a doublet of doublet peak at δ_H 6.47 (dd, *J* = 8.2, 2.3 Hz, H8) and an additional meta coupled peak at δ_H 6.40 (d, *J* = 2.2 Hz, H10). This peak sequence, together with $^1H - ^1H$ COSY and HMBC correlations were used to ascertained the attachment of the methoxy group at position 9 of ring D. The assignment of ^{13}C NMR chemical shifts was subject to analysis of HSQC and HMBC spectra (appendix 138 and 139) which included; six methine carbons with a resonance of δ_C ;133.1 (C-1), 110.6 (C-2), 104.0 (C-4), 129.5 (C-7), 107.1 (C-8), 97.5 (C-10), four oxygenated aromatic carbon δ_C ; 160.1 (C-3), 162.6 (C-9), 161.9 (C-10a), 157.9 (C-4a), one oxygenated methylene δ_C 67.4 (C-6), one oxygenated methine δ_C 80.0 (C-11a) and methine δ_C 40.7 (C-6a) and two sp2 hybridized carbon δ_C 120.7 (C-7a), 112.8 (C11b). A methoxy singlet δ_H 3.76 (s, OCH_3), (δ_C 56.0), had direct correlation with C-9 162.6 (C-9) indicating its attachment at that position in ring D. After comparison with literature, compound **64** was determined as medicarpin (Martínez-Sotres *et al.*, 2012).

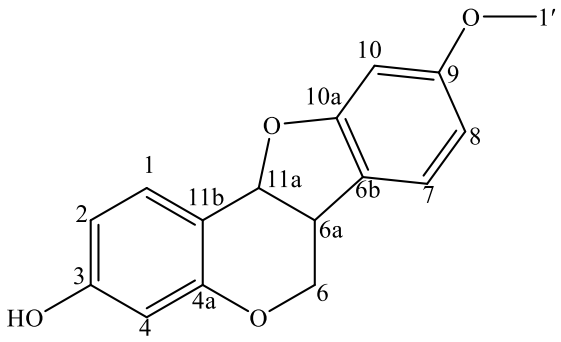

Figure 4.14: Chemical structure of compounds **64**

Table 4.13: The assignment of ^{13}CNMR, ^{1}HNMR, COSY and HMBC of compound **62**, **63** and **64**

Compound	**62**		**63**		**64**	
No	δ_C	δ_H, mult. (*J* in Hz)	δ_C	δ_H, mult. (*J* in Hz)	δ_C	δ_H, mult. (*J* in Hz)
1	133.1	7.26 (d, *J* = 8.4	132.9	7.38 d, *J* = 8.5 Hz	133.1	7.31 d, *J* = 8.4 Hz
2	110.6	6.48 (dd, *J*= 8.4, 2.4 Hz	111.5	6.79 dd, *J* = 8.5, 2.5 Hz	110.6	6.51 dd, *J* = 8.4, 2.4 Hz
3	160.1	-	160.1	-	160.1	-
4	104.0	6.30 (d, *J* = 2.4 Hz,	105.5	6.64 (d, *J* = 2.4 Hz	104.0	6.32 d, *J* = 2.4 Hz
4a	157.9	-	157.7	-	157.9	-
5	-	-	-	-	-	-
6	67.3	4.23 ,3.56 (t, *J* =	67.4	4.26, 3.60 (	67.4	4.24 (m, H6),
6a	40.2	10.7 Hz 3.47 ddd, *J* = 10.6, 7.0, 4.8 Hz,	41.5	dd, *J* = 10.9, 4.7 Hz 3.53 dd, *J* = 6.8, 4.5 Hz	40.7	3.55 (m) 3.53 (m)
7a	119.8	-	119.5	-	120.7	
7	105.9	6.80 d, *J* = 0.6 Hz	105.8	6.81 (s)	125.9	7.19 d, *J* = 8.2 Hz
8	149.4	-	149.4	6.47 dd, *J* = 8.2,	107.1	6.47 dd, *J* =
9	143.0	-	143.0	2.3 Hz	162.6	8.2, 2.3 Hz -
10	94.1	6.37 (s)	94.0	6.38 (s)	97.5	6.40 (d, *J* = 2.2 Hz
10a	155.5	-	155.4	-	161.9	-
11	-	-	-	-	-	-
11a	79.9	5.45 d, *J* = 6.9 Hz	79.5	5.49 (d, *J* = 7.0 Hz	80.0	5.49 d, *J* = 6.3 Hz
C1′	102.3	5.87 (dd, *J* = 13.0, 1.2 Hz, H1′)	102.2	5.87 d, *J* = 12.9 Hz		

Compound	**62**		**63**		**64**	
No.	δ_C	δ_H, mult. (*J* in Hz)	δ_C	δ_H, mult. (*J* in Hz)	δ_C	δ_H, mult. (*J* in Hz)
Gluc-anomeric	-	-	101.9	4.90 (d, *J* = 7.2 Hz	-	-
C2 ″	-	-	74.7	a3.45-3.87	-	-
C3 ″	-	-	77.9	[a]3.41- 3.94	-	-
C4 ″	-	-	71.3	[a]3.41- 3.94	-	-
C5 ″	-	-	71.1	[a]3.41- 3.94	-	-
C6 ″	-	-	62.3	[a]3.41- 3.94	-	-
OCH_3 (C1″)	-	-	-	-	56.0	3.76, (s)

*[a]Signals without multiplicity are overlapping signals deduced from the HSQC spectrum; *Recorded in CD_3OD at 700 MH_Z and 175 MH_Z

Compound **65** was isolated as a colorless crystals (MeOH); UV (MeOH), λ_{max} 302 (1.297), 204 (2.832) nm (appendix 148); HRESIMS *m/z* 253.1066 $[M + H]^+$ corresponding to a molecular formula of $C_{13}H_{16}O_5$ (calculated for 253.1031) (appendix 142 and 143). The ^1H and ^{13}C NMR data were measured in CD_3OD, 700 MH_Z, 175 MH_Z respectively (Table 4.14, Appendix 144 and 145). The aliphatic chain was characteristic of doublet peaks with chemical shifts δ_H 7.63 (d, *J* = 15.9 Hz, H1′) and δ_H 6.49 (d, *J* = 16.0 Hz, H2′). The high coupling constant, *J* = 16.0 Hz between the olefinic protons suggested their *trans* relationship.

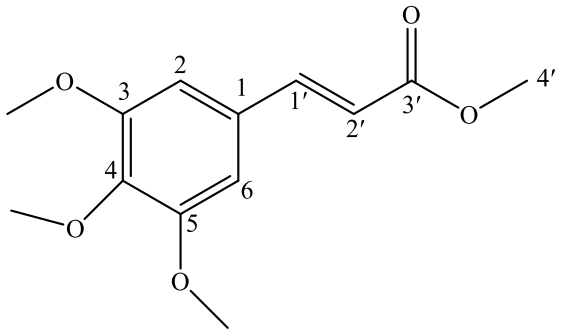

Figure 4.15: Chemical structure of compounds **65**

Table 4.14: The assignment of ^{13}CNMR, ^{1}HNMR, COSY and HMBC of compound **65**

Compound	**65**	
No	δ_C	$\delta_{H,}$ mult. (*J* in Hz)
1	131.3	-
2	106.5	6.93 (s,)
3	154.5	
4	147.0	-
5	154.5	-
6	106.5	6.93 (s,)
C1′	145.9	7.63 (d, *J* = 15.9 Hz, H1′),
C2′	117.8	6.49 (d, *J* = 16.0 Hz, H2′)
C3′	168.9	-
OCH_3 (4′)	56.5	3.78 (s)
OCH_3 (C2″)	61.0	3.87, 6H (s,)
OCH_3 (C3″)	56.5	3.87, 6H (s,)
OCH_3 (C4′)	51.5	3.79 (s)

*[a]Signals without multiplicity are overlapping signals deduced from the HSQC spectrum; *Recorded in CD_3OD at 700 MH_Z and 175 MH_Z

A singlet at δ_H 3.78 (s, 1H) (δ_C 51.8) had an HMBC correlation with an α, β- unsaturated carbonyl group δ_C 168.9 (C-3′) on the same chain. The aromatic region was characterized by two aromatic protons, as two proton singlets at δ_H 6.93 (s, 2H) with the corresponding carbon (δ_C 106.5) at position H2 and H6). Additionally, three methoxyl groups were identified to be attached to this aromatic region as singlet at δ_H 3.79 (s, 1H) (δ_C 61.0) which had a correlation with δ_C 141.2 (C-4) and a high intensity at δ_H 3.87 (s, 6H) (δ_C 56.5) representing two methoxyl peaks which had HMBC correlations with two aromatic quaternary carbons δ_C 154.5 (C-3) and δ_C 154.5 (C-5) (appendix 146). After comparison with literature, compound **65** was determined methyl (*E*)-3,4,5-trimethoxycinnamate (Corothie & Ilija, 1975; Hai *et al.,* 2002).

4.3.3 Compounds Isolated from Endophytic Fungi *P. hawaiiense*

Two compounds were isolated from the endophytic fungus *P. hawaiiense* after solid state fermentation on rice media. Compound **66** was a known compound namely; Lactariolide

1 while compound **67** was confirmed as a previously undescribed compound and was given the name hydroxy-Euphorol E.

Compound **66** was obtained as white crystals. It had a molecular formula of $C_{18}H_{30}O_2$ as shown by HRESIMS *m/z* 279.2320 $[M + H]^+$, calcd. 279.2279 (Appendix 149 and 150). The ^{13}CNMR (Table 4.15; Appendix 152) indicated the presence of an ester group and two double bonds as shown in the following absorbance δ_C; 178.2, 137.5, 133.1, 129.6, 126.7 which in addition to the molecular formula indicated the presence of one ring. Additionally, the ^{1}HNMR spectrum (Appendix 151) indicated the presence of the double methylene group (C-12), which was shown to be bearing an oxygenated methylene (C-13) by two signals; δ_H 5.62 (dd, $J_{12,\ 11}$ = 15.2, $J_{12,\ 13}$= 6.8 Hz, 1H) and δ_H 4.07 (d, $J_{\ 13\text{-}12}$= 6.7 Hz, 1H). The ^{13}CNMR spectrum also confirmed the presence of one tertiary carbon linked to an oxygen atom δ_C 73.6.

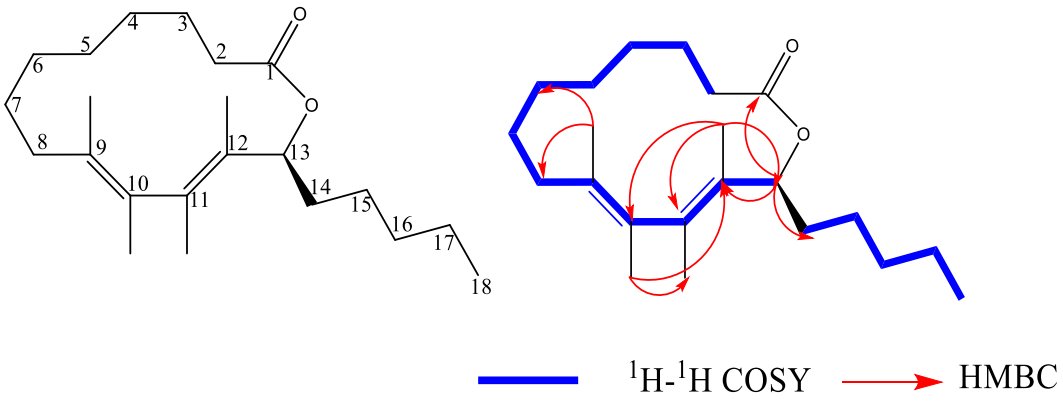

Figure 4.16: Structure, HMBC and COSY correlations of compound **66**

As compared with the literature (Zhang & Feng, 1997), it was ascertained that the oxygenated methylene group must be linking to the tertiary olefinic carbon and methylene groups respectively which enhanced the splitting of the quaternary peaks by nearly equivalent coupling constants of the three hydrogen atoms (C_{12}-H, C_{14}- H2). Together with HMBC, COSY and HSQC correlations (Appendix 153- 155), this structure was confirmed to be a 14 membered lactone ring with saturated side chains (C_5H_{11}). The high values observed in the NMR coupling constants (J=15.2) indicated that the double bonds were both in *trans* configurations.

Table 4.15: The assignment of 13CNMR, 1HNMR, COSY and HMBC of compound **66**

No.	δ_C	TYPE/ DEPT	^{1}HNMR (δ_H, mult. *J* in Hz)	COSY	HMBC
1	178.2	Cq	-	-	-
2	35.4	CH_2	2.27 (t, *J* = 7.4 Hz)	3	1, 3, 4
3	26.4	CH_2	1.61	2, 4	1, 2, 4, 5
4	30.6	CH_2	1.36	3, 5	2, 3, 5, 6
5	30.4	CH_2	1.39	4, 6	4, 6, 7
6	30.3	CH_2	1.39	5, 7	5, 7, 8
7	30.9	CH_2	1.41		5, 6, 8, 9
8	28.8	CH_2	2.21 (m)	9	6, 7, 9, 10
9	129.6	CH	6.00 (dd, *J* = 15.2, 11.1, 1H)	8, 10	7, 8, 10, 11
10	126.7	CH	5.62 (dd, *J* = 15.2, 6.8 Hz, 1H)	9, 11	8, 9, 11, 12
11	133.1	CH	5.54 (dd, *J* = 15.2,	10, 12	9, 10, 12, 13
12	137.5	CH	7.0, 1H)	11, 13	10, 11, 13, 14
			5.62 (dd, *J* = 15.2, 6.8 Hz, 1H)		
13	73.6	CH	4.07 (d, *J* = 6.7 Hz, 1H)	12, 14	1, 12, 14, 15
14	38.6	CH_2	1.49	13	13, 15, 16
15	33.2	CH_2	1.34	16	13, 14, 16, 17
16	26.5	CH_2	1.33	15	14, 15, 17
17	23.9	CH_2	1.35	18	15, 16, 18
18	14.6	CH_3	0.93	17	16, 17

*Recorded in CD_3OD at 700 MH_Z and 175 MH_Z

The configuration of this compound was confirmed by the NOESY spectra (Appendix 156) which showed that this compound had the R- configuration. From the comparison from the available literature, this compound was confirmed to be Lactariolide which has been isolated from the fruit bodies of *Lactarius subvellereus* and *Shiraia* sp, endophytic fungi isolated from *Selaginella delicatula* (Chen *et al.*, 2022; Zhang & Feng, 1997).

Compound **67** was isolated as a white amorphous powder. It had a molecular formula of $C_{31}H_{50}O_4$ as shown by HRESIMS *m/z* 487.3784 $[M + H]^+$, calcd. 487.3743 (Appendix 157 and 158). The molecular formula indicated the presence of seven degrees of unsaturation. The ^{1}HNMR (700 MHz, CD_3OD) and ^{13}CNMR (175 MHz, CD_3OD) spectra (Table 4.16, Appendix 159 and 160) exhibited the presence of five tertiary methyl groups (δ_H 0.91, 0.97, 0.83, 1.05, 1.42), three secondary methyls (δ_H 1.04, 1.03, 0.83) and three oxymethines (δ_H 4.60 d, *J* = 7.1 Hz; 3.23 dd, *J* = 11.9, 4.2 Hz; δ_H 4.41 td, *J* = 8.0, 5.7 Hz). One terminal CH_2 group at C-24 (δ_H 4.70, m; δ_C 106.8, 158.3) and an α, β unsaturated ketone moiety; δ_C 203.6, 140.0, 166.8 were also characterized. The remaining signals were assigned to seven methylene carbons, four methine carbones and four quaternary carbons. The gross structure of **67** was deduced from the HSQC, HMBC and COSY data (Appendix 161, 162 and 163).

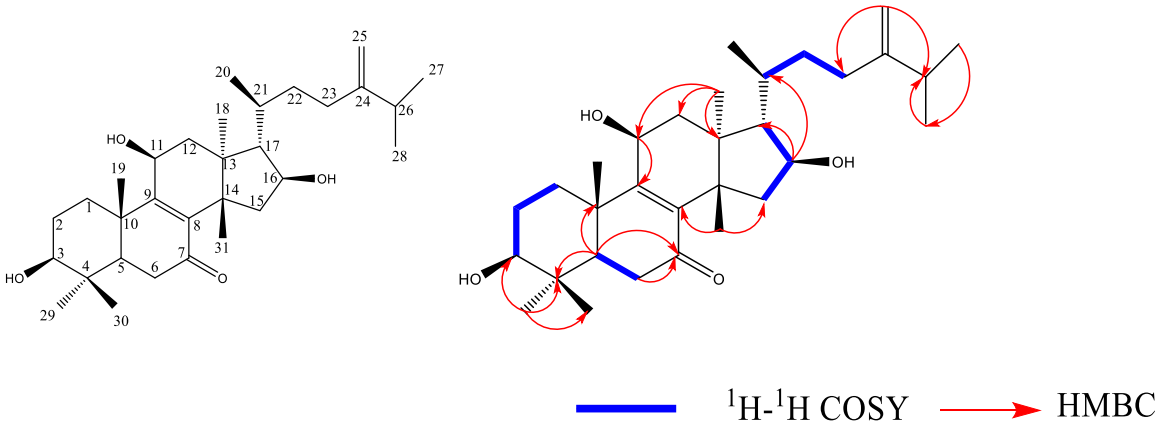

Figure 4.17: Structure, HMBC and COSY correlations of compound **67**

Table 4.16: The assignment of 13CNMR, 1HNMR, COSY and HMBC of compound **67**

No.	δ_C	TYPE/ DEPT	^{1}HNMR (δ_H, mult. *J* in Hz)	COSY	HMBC
1	35.0	CH_2	2.63		3, 5, 9, 10
2	28.4	CH_2	1.78		3, 4, 10
3	79.0	CH	3.23 (dd, *J* = 11.9, 4.2 Hz, 1H)		2, 4, 5,
4	40.4	Cq	-		-
5	52.6	CH	1.61		4, 6, 10, 21, 29, 28
6	37.8	CH_2	2.60, 2.36		4, 5, 7, 8, 10
7	203.6	Cq	-		-
8	140.0	Cq	-		-
9	166.8	Cq	-		-
10	41.8	Cq	-		-
11	67.2	CH	4.60 (d, *J* = 7.1 Hz, 1H)		8, 9, 12, 13
12	44.1	CH_2	1.98, 2.19		13, 14, 18, 20
13	44.8	Cq	-		-
14	48.1	Cq	-		-
15	36.7	CH_2	1.88, 1.17		13, 14, 16, 17, 19
16	73.9	CH	4.41 (td, *J* = 8.0, 5.7 Hz, 1H)		14, 15, 17, 18
17	32.1	CH	1.88		16, 18, 22, 31,
18	18.4	CH_3	1.05		12, 13, 14, 18
19	19.9	CH_3	1.42		1, 5, 9, 10
20	54.1	CH	1.54		13, 17, 22, 23, 20
21	26.6	CH_3	0.83		8, 12, 13, 14, 15, 20
22	32.9	CH_2	2.19, 2.01		22, 23, 25, 26
23	46.4	CH_2	2.69, 1.80		22, 24, 25
24	158.3	Cq	-		-
25	106.8	CH_2	4.70		24, 25, 27, 28
27	35.2	CH_2	2.29		25, 26, 28, 29
28	22.5	CH_2	1.04		25, 26,27, 29
29	16.3	CH_3	0.91		25, 26, 28,
30	28.3	CH_3	0.97		3, 4, 5, 10, 31
31	22.6	CH_3	1.03		3, 4, 5, 10, 30

*Recorded in CD_3OD at 700 MH_Z and 175 MH_Z

The HMBC spectrum showed correlations, the two germinal CH_3-28 and CH_3-29 groups correlations with C-3, C-4 and C-5; H-11 cross peaks with C-9, C-10 and C-12; H-16 peaks with C-15, C-17 and C-20 respectively which indicated three hydroxyl groups (δ_H 3.23 dd, *J* = 11.9, 4.2 Hz; δ_C 79.0) at C- 3; δ_H 4.60 d, *J* = 7.1 Hz; δ_C 67.2 at C-11 and δ_H 4.41 td, *J* = 8.0, 5.7 Hz; δ_C 73.9 at C-16. The HMBC cross peaks between CH_3-19 and C-9; CH_3- 30 and C- 8; H- 6 and C- 7 further confirmed the presence of an 8-ene-7 ketone moiety. The CH_2-24 correlations with C-23, C-26 and C-27 revealed the presence of a terminal bond unit at C-24. Additionally, the HMBC spectrum showed cross peaks between CH_3-21 and C-17, C-20 and C-22; between CH_3- 18 and C-12, C-13, C-14 and C-17; between H-17 and C-16 and C-20; and between H-5 and C-3, C-4, C-6, C-7 and C-10. The relative configuration was established by comparison from literature, extensive analyses of the ^{1}HNMR (appendix 159) and NOESY correlations (Appendix 164). The coupling constants of H-3 (δ_H 3.23 dd, *J* = 11.9, 4.2 Hz) clearly indicated that the 3-hydroxy group was in equatorial β- position (Ahmed *et al.*,2006). The relative configuration of H-11 in the equatorial β- configuration was deduced by the multiplicities of its signals 4.60 d, *J* = 7.1 Hz which was further backed by NOESY correlations H-11/H-1α and H-11/CH3-18. Additionally, the relative configuration of H-16 in the β-position was deduced by the multiplicities of its signals 4.41 td, *J* = 8.0, 5.7 Hz, which was also backed by NOESY correlation between H-16/H-15α, H16/23a. Lack of NOESY correlation between CH_3-18/CH_3-21 and CH_3-21/H12 confirmed that this molecule was a tirucallane triterpene. Thus compound **67** was elucidated to be a previously undescribed compound, tirucalla-24-methylene-8-ene-3β,11β,16β-triol-7-one a derivative of Euphorol E which has been isolated from *Euphorbia resinifera* Berg (Wang *et al.*, 2016) hence given the trivial name 16-hydroxy- Euphorol E.

4.4 Conclusion

The aim of this study was to isolate and characterize secondary metabolites from the leaves, stem bark and associated endophytic fungi. Twenty-two (22) compounds were isolated from this study, those from the plant tissues that belonged to two main classes; quinolizidine alkaloids (**46- 53)** and phenolic compounds **(54-65)**. Four previously undescribed quinolizidine alkaloids were reported namely; 2β-Methoxy-13α-*O*-(2'-pyrrolylcarbonyl) virgiline (**46)** 2α-Methoxy-13β-*O*-(2′-pyrrolylcarbonyl) virgiline (**47)** 3α-*O*-Angelate-2β-hydroxy-13α-*O*-(2′-pyrrolylcarbonyl) virgiline (**48)** and 2, 3-Deydro-virgiline (**49)**. The phenolic compounds were grouped as flavones, flavanones, isoflavones, pterocarpan flavonoids and cinnamic acids depending of their chemical properties and structures. This is the first report of **10** phenolic

compounds (apart from compound **55** and **59**) from *C. aurea* susp. *aurea* while the quinolizine alkaloids have previously been reported from this medicinal plant apart from compounds **46-49** which are regarded as being reported for the first time. Compounds **66** and **67** were isolated from the endophytic fungi *P. hawaiinse* for the first time. Compound **66** was confirmed as a macrolide known as Lactariolide I while compound **67** is a previously undescribed triterpenoid given the trivial name hydroxy- Euphorol E. These results indicate the potential of *C. aurea* and its associated endophytic fungi as a source of novel secondary metabolites. However further studies should be done on isolation and characterization of novel quinolizidine alkaloids and phenolic compounds from the leaves and stem bark of this medicinal plant based on the LC-MS profile. Additionally, more work needs to be done on characterization of secondary metabolites from the endophytic fungi in this study which was hindered by the low number of extracts obtained from fermentation of the fungal endophyte under study.

CHAPTER FIVE

DETERMINATION OF ANTIMICROBIAL, ANTIDERMATOPHYTIC, ANTIPROLIFERATIVE AND CYTOTOXIC POTENTIAL OF THE CRUDE EXTRACTS AND PURE COMPOUNDS

Abstract

The rise in fungal and bacterial infections, particularly those contracted in healthcare settings, has resulted in increased resistance to synthetic antimicrobial agents. Additionally, cancer incidences are on the rise while the available pharmaceutical treatments are only partially effective and are associated with adverse side effects in patients from radiation and chemotherapy. This has necessitated the need to explore alternative sources for antimicrobial and anticancer agents, particularly those of natural origin. Crude extracts of methanol, ethyl acetate, and hexane were obtained from the leaves, stem bark, and specific fungal endophytes of *Calpurnia aurea* subsp. *aurea* (*Ca*). The extracts were assessed for antidermatophytic, antimicrobial, antiproliferative, and cytotoxic properties. Furthermore, all of the aforementioned biological bioassays were performed on pure compounds that were isolated from the leaves and stem bark of *Ca*. Antimicrobial and antifungal assays were conducted on selected clinically significant pathogens, while cytotoxicity was assessed using the MTT assay on KB3.1 and L929 cell lines. All extracts demonstrated antidermatophytic activity against the test strains, with the exception of the leaf extracts, which showed no activity against *Trichophyton interdigitale*. The pure compounds demonstrated antidermatophytic activity against *Trichophyton rubrum*, *T. interdigitale*, *Trichophyton benhamiae*, *Microsporum canis*, and *Nannizzia gypsea*, with MIC values ranging between 6.6 µg/mL and 300 µg/mL. Furthermore, several phenolic compounds including **54**, **58**, **60**, **62**, and **64** demonstrated antifungal activity against *Mucor hiemalis* and *Schizosaccharomyces pombe*, with a minimum inhibitory concentration (MIC) of 66.6 µg/mL. Compound **65** demonstrated antibacterial activity against *Bacillus subtilis* (DSM 10), with a minimum inhibitory concentration (MIC) of 16.6 µg/mL, comparable to the positive control Oxytetracycline (MIC 16.6 µg/mL). Simmilarly, these phenolic compounds also demonstrated cytotoxic and antiproliferative activities, with IC_{50} values ranging from 15 µg/mL to 24 µg/mL against the KB3.1 and L929 cell lines. The compounds derived from the fungal endophytes (**66** and **67**) were present in minimal quantities, preventing any assessment of their biological activity. This study's findings indicate that both crude and pure compounds isolated from *Ca*. may serve as significant sources

of novel metabolites for drug development. Additional validation is required for further studies on the structure-activity relationship of the reported active compounds.

5.1 Introduction

High mortality and morbidity in developing countries has been linked to infectious diseases: hence they are of great concern to public health. Despite the great number of antibiotics available, the emergence and extent of antimicrobial resistance due to misuse is a worrying trend. Hence there is a need to urgently find new molecules for treatment of infectious diseases (Alanis, 2005; Brown & Wright, 2016). An interesting strategy for finding such molecules would be to test plants used to treat infectious diseases in traditional healing systems, since these plants have been used as a source of many pharmaceutical drugs for a range of diseases, including bacterial, viral, fungal, and protozoal infections, as well as cancer cases (Gurib-Fakim, 2006; Harvey, 2008). On the other hand, the side effects and consequences of using synthetic chemicals in the fight against diseases, calls for safer alternatives, particularly natural products (Yessoufou *et al.,* 2015). These natural products are sources of phenolic, alkaloid and terpenoid compounds that suppress free radical production, delay oxidative stress reactions, and play an important role in cancer management (Bray *et al.,* 2021). Research shows that carcinogenesis, which includes three main stages namely, initiation, promotion and progression, could be prevented by using natural products as a chemoprevention tool (Ma *et al.,* 2021).

Medicinal plants are a source of more than 50% of all drugs and are known to contribute to approximately 70% of the small molecules of therapeutic drugs (Dzobo, 2022; Newman & Cragg, 2007; 2016). They are regarded as natural, readily available, and they have relatively fewer side effects compared to synthetic drugs. One such important plant is *C. aurea* subsp. *aurea* (*Ca.),* that has been reported to have various therapeutic properties such as antibacterial, antioxidant (Adedapo *et al.,* 2008), wound healing and anti-inflammatory (Ayal *et al.,* 2019), antidiarrheal (Damtie, 2023) and antidiabetic (Belayneh *et al.,* 2019). In a study done by (Mulata *et al.,* 2015), *Ca* seed extracts were effective countermeasure for the toxic hematopoietic effects of highly active antiretroviral therapy (HAART) on rats, but cause hematotoxicity. The activity was attributed to the presence of phytochemicals such as flavonoids, terpenoids, and tannins. These phytochemicals were able to slow down the death of hematopoietic cells caused by HAART in both the bone marrow and the peripheral blood.

Dermatophytes are a group of clinically significant fungi that infect keratinized tissues such as skin, nails, and hair. These pathogens are a major cause of superficial infections, also

known as dermatophytosis or tinea infections (Arenas *et al.*, 2017). Besides dermatophytes, yeast strains like *Mucor hiemalis, Candida albicans, Pichia anomala,* and *Schizosaccharomyces pombe* are also considered clinically important. They cause fungal infections like fungemia, candidiasis, and mucormycosis, which can be fatal for people with weak immune systems (Gnat *et al.,* 2021). Additionally, gram-positive and gram-negative bacterial strains such as *S. aureus, B. subtilis, E. coli,* and *P. aeruginosa* are great concern, since they are responsible for nosocomial infections (Parasuraman *et al.,* 2024). Discovery of novel secondary metabolites from natural sources would play a significant role towards management of infections in humans and animals. This chapter focused on determination of the antidermatophytic, antimicrobial, antiproliferative, and cytotoxic activities of the extracts and the pure secondary metabolites isolated from the leaves, stem bark, and endophytic fungi of *Ca.*

5.2 Materials and Methods

5.2.1 Description of Test Extracts and Compounds

The bioactivity of three crude extracts (methanol, ethyl acetate, and hexane) derived from the leaves and stem bark of *Ca* were examined through bioassays. Additionally, pure substances categorized as quinolizidine alkaloids (**46-53**) and phenolic compounds (**54-65**) were also evaluated. The extraction of crude extracts and purification of pure compounds is outlined in Chapter 4, section 4.3.2, while characterization and description of quinolizidine alkaloids and phenolic compounds is detailed in Chapter 4, sections 4.4.1 and 4.4.2, respectively.

5.2.2 Antidermatophytic Assays

Five dermatophytic strains were used in the study; *T. rubrum* (IDE 242), *T. interdigitalle* (LY34), *T. banhamiae* (IHEM 47010), *M. canis* (D106), and *N. gypsea* (SK2458120). The strains were obtained from the Institute of Microbiology, Czech Academy of Sciences, Czech Republic. The minimum inhibitory concentration (MIC) of the methanolic, hexane, ethyl acetate and pure compounds isolated were evaluated using a broth micro-dilution assay in accordance with the Clinical and Laboratory Standards Institute (CLSI) M38-A2 guidelines (Wayne, 2010), with minor modifications. The inoculum suspension for each test dermatophyte isolate was prepared by scraping the surface of 10-day-old cultures and suspending the material in sterile 0.1% (v/v) Tween 80 in PBS to create the stock solution. One mL of the stock solution was diluted in 60 mL of yeast malt broth (YMB). Colony forming units (CFU/mL) were confirmed microscopically using a hemocytometer by counting the

colonies that emerged from 10 mL of the prepared suspension. Spore suspension (150 µL) containing 10^5 of each dermatophyte was inoculated into 96-well microdilution plates. In the first row of each plate, 130 µl of YMB and 20 µl of the test compounds consisting of crude and pure extracts separately, at a concentration of 4.5 mg/mL were added in duplicate and mixed thoroughly. Methanol served as negative control, whereas Voriconazole (1.5 mg/mL) and Miconazole (1 mg/mL) were used as positive controls. The mixture underwent serial dilution by transferring 150 µL from each row to the next until the final row, where the remaining 150 µL was discarded after the last mixing. The resulting final concentrations were 2.3, 4.7, 9.4, 18.8, 37.5, 75, 150, and 300 µg/mL. The mixture was incubated at ±30 °C for 3–7 days, while growth was continuously monitored. The minimum concentration at which no visible growth was observed was defined as the MIC and reported in µg/mL. The assay was carried out in triplicate.

5.2.3 Antimicrobial Activity

The antimicrobial bioassay was conducted following the protocol established by Becker *et al.* (2020). All crude and purified compounds were dissolved in methanol at a concentration of 1 mg/mL. Stock solutions of the test micro-organisms were prepared by culturing the organisms overnight in 50 mL shaking flasks containing 25 mL of yeast malt broth (YMB) growth medium at 140 rpm. The growth of the microorganism was assessed by measuring the optical density (OD) at 600 nm for bacteria and 548 nm for fungi. The *M. smegmatis* strain was obtained from aliquots that had been previously stored at -80 ℃ in 25% glycerol. Before utilizing *M. smegmatis*, the aliquots were thawed, and the optical density of the suspension was measured and adjusted accordingly. The optical density at 600 nm was adjusted to 0.01, and at 548 nm to 0.1, through dilution with the YMB growth medium. In a 96-well microtiter plate (one plate per test strain), 150 µL of the adjusted test organism suspensions were added to each well. Furthermore, 130 µL of YMB growth medium was added into row A of the microtiter plate, followed by the addition of 20 µL of test compounds (1 mg/mL) in the same row, yielding a total volume of 300 µL. The positive control was positioned in the final column of row A. The contents of the first row (A) were mixed thoroughly, after which 150 µL of the mixture was transferred to row B and mixed thoroughly again. This process was repeated for the subsequent rows until row H, at which point the excess 150 µL was discarded. This produced a serial dilution ranging from 66.6 µg/mL in row A to 0.52 µg/mL in row H. The plates were incubated in a microtiter plate shaker at 800 rpm at 30 °C (for fungi) or 37 °C (for bacteria) for a duration of 18 to 24 hours, dependent upon the test strains. Following the designated

incubation period, the plates were assessed visually for evidence of growth inhibition. The minimum inhibitory concentration (MIC) was identified as the lowest concentration at which growth inhibition became evident. *E. coli* (DSM 1116), *S. aureus* (DSM 346), *A. baumanii* (DSM 30008), *C. violaceum* (DSM 30191), *B. subtilis* (DSM 10), *P. aeruginosa* (PA14), and *M. smegmatis* (ATCC 700084) were the bacterial test organisms utilized in this assay. The fungal strains screened included *C. albicans* (DSM 1665), *S. pombe* (DSM 70572), *M. hiemalis* (DSM 2656), *P. anomala* (DSM 6766), and *R. glutinis* (DSM 10134). The negative control comprised methanol, while the positive controls included Oxytetracycline (1 mg/mL), Ciprofloxacin (2.54 mg/mL), Gentamycin (1 mg/mL), and Kanamycin (1 mg/mL) for bacterial assays. The antifungal control utilized was Nystatin (1 mg/mL). The assay was carried out in triplicate.

5.2.4 Antiproliferative and Cytotoxicity Assay

The cytotoxicity of the crude and pure compounds was assessed using the MTT assay against mouse fibroblast L-929 and human endocervical adenocarcinoma KB-3.1 cell lines (obtained from Helmholtz center for infectious diseases, Braunschweig Germany), following the procedure described by Becker *et al.* (2020). The cell lines were incubated in Gibco™ DMEM medium (Thermo Fisher Scientific, Waltham, MA, USA) under conditions of 10 % CO_2, a temperature of 37 ℃, and supplemented with 10 % Fetal Bovine Serum (FBS). In a microtiter plate, 120 µL of a suspension containing approximately 50,000 cells/mL was added to each well. In a fresh microtiter plate, 100 µL of growth medium was added in each well. In the first column of the fresh plate, 50 µL (1 mg/mL) of the test compounds were added in duplicate (one compound per row). The solution was serially diluted beginning with the first column, where 50 µL was transferred to the next column and mixed thoroughly, continuing this process until the final column, where the remaining 50 µL was discarded after the last mixing step. This resulted in a serial dilution from 333 µg/mL to 1.9×10^-3 µg/mL. Sixty microliters of solution mixtures with concentrations from 111 µg/mL to 1.9×10^-3 µg/mL were transferred from this plate to the first plate containing 120 µL of cell suspension, excluding the highest concentration of 333 µg/mL. The final concentration of the test crude and pure compounds ranged from 37 µg/mL to 0.6×10^-3 µg/mL. The cell lines were incubated for five days in a 96-well flat-bottom microtiter plate with serially diluted compounds. In this experiment, cells devoid of additives and methanol served as the negative-control.

Upon completion of the incubation period, the cells were subjected to staining with 3-(4,5-dimethyl-2-thiazolyl)-2,5-diphenyl-2H-tetrazolium bromide (MTT) and monitored for

color changes. Twenty microliters of a 5 mg/mL MTT solution were added to each well and incubated for 2 hours at 37°C. The microtiter plate was subsequently centrifuged at 3000 rpm for 5 minutes, and the supernatant was discarded by inverting the plate and gently shaking. The wells are subsequently washed with 100 µL of phosphate buffered saline (PBS), centrifuged, and the supernatant is discarded. Subsequently, 100 µL of Isopropanol: HCl solution (1 L isopropanol + 4 mL HCl 37% w/v) was added to the wells and incubated for 10 minutes at ambient temperature. The optical density was assessed at 595 nm using an Infinite® 200 Pro microplate reader (TECAN, Männedorf, Schweiz), from which the half-maximum inhibitory concentration (IC_{50}) in µM was determined. The assays were performed in three independent experiments in duplicates.

5.2.5 Statistical Analysis

The test results were presented as the mean ± standard deviation (SD). The MIC values were reported as the mean of three consistent replicates. Statistical analysis was conducted using SPSS version 27.0, and treatment comparisons were executed via one-way analysis of variance (ANOVA). A post hoc test, Tukey's test (assuming equal variance), was conducted to identify which extract yielded a significant result. P value <0.05 was considered statistically significant.

5.3 Results

5.3.1 Antidermatophytic Activity of the Methanolic, Hexane and Ethyl Acetate Extracts

The fungistatic characteristics of the extracts are dependent upon the solvent employed for extraction and the specific test microorganism involved. Table 5.1 illustrates that all the plant extracts demonstrated inhibitory activity against *T. benhamiae*, *T. rubrum*, *T. interdigitale*, *N. gypsea,* and *M. canis*. In comparing the leaf and stem bark, it was observed that the extracts from the stem bark demonstrated an inhibitory effect on all tested strains, whereas the leaf extracts showed no activity against *T. interdigitale*. Among these extracts, the ethyl acetate fraction derived from the stem bark exhibited a more pronounced inhibitory activity against all tested organisms, with a zone of inhibition ranging from 20.0 to 26.0 mm, in contrast to the methanol crude and hexane extracts obtained from both the leaves and stem bark. The findings further underscore the variations in susceptibility among the tested dermatophyte strains in relation to the same extract. This study used miconazole and voriconazole as the positive controls for all antidermatophytic assays, yielding zones of

inhibition ranging from 30.0 to 38.0 mm and 20.0 to 25.0 mm, respectively, across all test organisms (Table 5.1).

Table 5.1: Antidermatophytic activity of the crude, ethyl acetate and hexane extract of *Calpurnia aurea* obtained from the leaves and the stem bark against dermatophytic fungi

Extracts	Test Organisms/ Zone of inhibition in millimeters, n= 3				
	T. benhamiae	*N. gypsea*	*T. interdigitale*	*M. canis*	*T. rubrum*
CaB Crude	16 ±1	18 ± 0.5	12.5 ± 0.5	16±1	15.5 ± 1
CaB Ethyl acetate	26 ± 1	24 ± 1	25.3 ± 0.6	20 ± 1	21.5 ± 0.5
CaB Hexane	23 ± 0.5	14 ± 1	21 ± 1	16.3 + 0.3	16 ± 1
CaL Crude	12 ± 1	16.5 ± 0.5	n.i	8.5 ± 0.5	14.5 ± 0.5
CaL Ethyl acetate	19 ± 0.5	18 ± 0.5	n.i	12.3 ± 0.6	18.5± 0.5
CaL Hexane	15± 0.5	12.5 ± 0.5	n.i	10 ± 1	15 ± 1
Voriconazole	35± 0.5	38± 1	34 ±1	30 ±1	32 ±0.5
Miconazole	20 ± 0.5	22 ± 0.5	25 ± 0.5	21 ± 0.5	28 ± 0.5

*CaB- *Calpurnia aurea* Bark, *CaL- *Calpurnia aurea* leaf, *n.i- No inhibition; *The values are expressed as mean ± standard deviation (SD) (n = 3).

5.3.2 Antidermatophytic Activity of Quinolizidine Alkaloids

The antifungal activity of quinolizidine alkaloids against five dermatophytic species demonstrated that *N. gypsea* showed greater susceptibility to all tested alkaloids, with a minimum inhibitory concentration (MIC) range of 37.5 – 150 µg/mL, in contrast to *M. canis*, which was also susceptible to all test compounds, exhibiting a MIC range of 75 – 300 µg/mL. Conversely, *T. benhamiae* exhibited resistance to five of the eight compounds (**46**, **47**, **48**, **50**, and **52**). Compared to the positive controls, miconazole (0.260 µg/mL) and voriconazole (0.390 µg/mL), compounds **51** and **52** exhibited an activity of 37.5 µg/mL against *N. gypsea*, whereas the other compounds demonstrated a minimum inhibitory concentration (MIC) range of 75 – 300 µg/mL against the other dermatophytes (Table 5.2).

Table 5.2*:* Antidermatophytic activity of quinolizidine alkaloids obtained from leaves and stem bark of *Calpurnia aurea* against disease causing dermatophytes

Test compounds	MIC Concentration (µg/mL)/Test Organisms, n= 3				
	T. rubrum	*T. interdigitale*	*T. benhamiae*	*M. canis*	*N. gypsea*
46	150	300	n.i	150	150
47	n.i	300	n.i	300	150
48	300	300	n.i	150	75
49	150	n.i	300	150	75
50	150	n.i	n.i	75	75
51	300	150	300	300	37.5
52	150	300	n.i	300	37.5
53	150	150	300	150	75
Miconazole	0.260	0.260	0.260	0.260	0.260
Voriconazole	0.390	0.390	0.390	0.390	0.390

*n.i- No inhibition; *The values are expressed as mean of three consistent replicates.

5.3.3 Antidermatophytic Activity of the Isolated Phenolic Compounds

The results obtained from the phenolic compounds demonstrated variability in inhibitory effects, dependent upon the class of phenolic compounds and the type of test dermatophytic strain. For instance, *T. intedigitale* demonstrated the greatest susceptibility to the flavones (compounds **54**, **55**, and **56**), with a minimum inhibitory concentration (MIC) of 75 µg/mL. Other strains, *T. benhamiae, M. canis,* and *N. gypsea*, demonstrated sensitivity to these phenolic compounds, with a minimum inhibitory concentration (MIC) between 150 µg/mL and 300 µg/mL while *T. rubrum* demonstrated resistance to all flavones. Among the four isoflavone phenolic compounds (**57**, **58**, **59**, and **60**), compound **59** demonstrated the highest inhibitory activity, with a minimum inhibitory concentration (MIC) range of 6.6 – 75 µg/mL. In contrast, compound **58** exhibited the lowest activity, with a MIC range of 35 – 300 µg/mL. Among the test strains, *T. interdigitale* exhibited greater susceptibility to the isoflavone, whereas *M. canis* demonstrated lower susceptibility to the isoflavones (Table 5.3).

Table 5.3: Antidermatophytic activity of phenolic compounds isolated from the leaves and stem bark of *Calpurnia aurea* subsp. *aurea*

Compounds	MIC concentration (µg/mL)/ Test organisms				
	T. rubrum	*T. interdigitale*	*T. benhamiae*	*M. canis*	*N. gypsea*
54	n.i	75	300	150	n.i
55	n.i	75	300	300	150
56	n.i	75	300	300	150
57	150	35	75	75	75
58	n.i	35	300	300	150
59	35	35	75	75	6.6
60	150	75	75	150	75
61	300	150	300	300	n.i
62	75	6.6	6.6	16.6	16.6
63	300	150	300	150	150
64	35	16.6	35	75	75
65	300	150	300	300	33.3
Miconazole	**0.260**	**0.260**	**0.260**	**0.260**	**0.260**
Voriconazole	**0.390**	**0.390**	**0.390**	**0.390**	**0.390**

*n.i- No inhibition; *The values are expressed as mean of three consistent replicates.

5.3.4 Antimicrobial Activity of the Isolated Pure Compounds

In this study, quinolizidine alkaloids (**46-53**) demonstrated no activity against the test strains, whereas the phenolic compounds (**54-65**) displayed a varying activity against the test organisms (Table 5.4). As illustrated in Table 5.4, six compounds (**54**, **55**, **56**, **59**, **62**, and **64**) exhibited activity against *M. hiemalis* with an MIC of 66.6 µg/mL while compounds **56**, **59**, **62** and **64** showing the same range of inhibition against *S. pombe* compared to Nystatin which had an MIC of 8.3 µg/mL against both fungal strains. Additionally, compared to oxytetracycline

(MIC 16.6 µg/mL) which was used positive control, compound **65** demonstrated antibacterial activity against *B. subtilis*, with a minimum inhibitory concentration (MIC) of 16.6 µg/mL (Table 5.4).

Table 5.4: Antibacterial and antifungal activity of the isolated compounds against selected clinically important pathogens

	MIC Concentration (µg/mL)/ Test Organisms			
Compounds	***S. pombe***	***Pichia anomala***	***Mucor hiemalis***	***Bacillus subtilis***
54	n.i.	n.i.	**66.6**	n.i.
55	n.i.	n.i.	**66.6**	n.i.
56	**66.6**	n.i.	**66.6**	n.i.
57	n.i.	n.i.	n.i.	n.i.
58	n.i.	n.i.	n.i.	n.i.
59	**66.6**	n.i.	**66.6**	n.i.
60	n.i.	n.i.	n.i.	n.i.
61	n.i.	n.i.	n.i.	n.i.
62	**66.6**	n.i.	**66.6**	n.i.
63	n.i.	n.i.	n.i.	n.i.
64	**66.6**	n.i.	**66.6**	n.i.
65	n.i.	n.i.	n.i.	**16.6**
Reference	**20µl (N) 8.3**	**20µl (N) 8.3**	**20µl (N)8.3**	**20µl (O)16.6**

*n.i: No inhibition, N: Nystatin (1mg/mL), O: Oxytetracycline (1mg/mL); *The was no activity against test strains that are not represented on this table. * The values are expressed as mean of three consistent replicates.

5.3.5 Cytotoxic and Anti-proliferative Activity of the Isolated Compounds

The quinolizidine alkaloids exhibited no antiproliferative or cytotoxic activity against the KB3.1 and L929 cell lines. In contrast, the phenolic compounds displayed varying degrees of antiproliferative and cytotoxic activity against these cell lines, as shown in Table 5.5. Most phenolic compounds demonstrated antiproliferative and cytotoxic activity against the studied cell lines, with the exception of compounds **60**, **61**, and **63**. A notable trend was observed in which glycosylated flavonoids demonstrated no activity relative to non-glycosylated compounds, with the exception of compound **54**, which displayed cytotoxic activity against the

KB3.1 cell line despite its glycosylation. Compound **65** demonstrated significant cytotoxic activity, exhibiting an IC_{50} of 18 µg/mL against the L929 cell line.

Table 5.5: Cytotoxicity and antiproliferative assay results of the Phenolic compounds against KB3.1 and L929 cell lines

Compounds	**Cell lines /IC_{50} values in** µg/mL	
	L929	**KB3.1**
54	*	23
55	**	**
56	**	**
57	*	**
58	*	**
59	24	15
60	*	*
61	*	*
62	**	24
63	*	*
64	**	20
65	18	**
Epithilone B	**0.00068**	**0.000029**

*No altered cells, No cytotoxic effect ** No altered cells, No cytotoxic effect, Proliferative inhibition; * The values are expressed as mean of three consistent replicates.

As illustrated in Table 5.5 above, the cytotoxicity results did not demonstrate statistical significance when compared to the IC_{50} values obtained from the positive control epithilone B, which exhibited IC_{50} values of 0.00068 µg/mL and 0.000029 µg/mL against the L929 and KB3.1 cell line, respectively. Compounds **66** and **67** were not evaluated for biological activity due to insufficient isolation quantities.

5.4 Discussion

Kenya is a tropical nation notable for its significant biodiversity of flora and fauna, which serve as important sources of natural products that may aid in the discovery and development of new antifungal, antimicrobial, and cytotoxic agents (Zhou *et al.,* 2017) . This study assessed the antidermatophytic, antimicrobial, and cytotoxic effects of crude extracts and

pure compounds on major clinical microbial pathogens. The cytotoxic and antiproliferative properties of the compounds were further examined. According to Prasad *et al.* (2004) and Coker *et al.* (2016), plant extracts from the *Fabaceae* family, such as *Psoralea coylifolia* and *Daniella oliveri*, have shown antidermatophytic activity against *T. rubrum*, *Microsporum gypseum*, *Trichophyton schoenleinii*, *Epidermatophyton floccosum*, and *T. mentagrophytes*. The antidermatophytic activity of crude extracts in this study against the test strains were in line with the previous reports on the activity of medicinal plants in this family. In contrast to the ethyl acetate extracts, the methanol crude extract had comparatively less antidermatophytic action against the dermatophytic strains. Research by Abu *et al.* (2017), Nakamura *et al.* (2017), and Suhaimy *et al.* (2017) shows that the high activity in ethyl acetate extracts as opposed to methanol extracts is caused by the phenomenon of crude extract being partitioned using ethyl acetate, which enhances the selection of more soluble phenolic and alkaloid compounds in comparison to the larger array of molecules found in the methanol crude extract.

Phytochemical constituents such as flavonoids, anthocyanins, tannins, saponins, alkaloids, anthraquinones, glycosides, and free quinones derived from plants in the *Fabaceae* family are recognised for their antidermatophytic activity (Issakou *et al.,* 2022). Following purification, the flavonoids and quinolizidine alkaloids obtained from *Ca.* showed antidermatophytic efficacy against the studied dermatophytes. The activity was partially attributed to the ethyl acetate fraction of the leaf and stem bark extracts. Apart from the antidermatophytic action of *Ca* extracts, associated to its high flavonoid profile (Prasad *et al.,* 2004), the quinolizidine alkaloids that were identified also showed antidermatophytic activity against the test strains. It has been demonstrated that quinolizidine alkaloids from *Genistoid* taxa (*Fabaceae*) exhibit antifungal effects on *Fusarium oxysporum* (Cely-Veloza, *et al.,* 2023), however, this is the first study to demonstrate that this class of secondary metabolites from *Ca* has antidermatophytic effects.

The bacterial and fungal test strains used in this study exhibited resistance to the antimicrobial effects of the quinolizidine alkaloids. The report by Hammouche-Mokrane *et al.* (2017), however, indicated that sparteine quinolizidine alkaloids do exhibit antibacterial properties against various bacteria and phytopathogenic fungi. Additionally, pure quinolizidine alkaloids extracted from *Lipinus angustifolius* var. *mirela* (*Fabaceae*), including lupanine, 13-hydroxylupanine, sparteine, and angustifoline, demonstrated bacteriostatic effects against *B. subtilis, S. aureus, E. coli, B. thuringiensis*, and *P. aeruginosa*, as well as fungistatic activity against phytopathogenic fungi (Cely-Veloza *et al.,* 2023; Liu *et al.,* 2014; Tyski *et al.,* 1988). The aglycone (non-glycosylated flavonoids) exhibited antimicrobial activity against the

selected test strains, in contrast to the glycosylated flavonoids. This findings aligns with a study by Sudheeran *et al.* (2020), indicating that flavonoid aglycones exhibit superior antifungal and antibacterial properties compared to glycosylated flavonoids. The glycosylation of flavonoids reduces their antibacterial efficacy by hindering their ability to penetrate bacterial and fungal cell walls, thereby diminishing their interaction with microbial membranes (Aboody & Mickymaray, 2020; Shamsudin *et al.*, 2022). The antibacterial action of cinnamic acid (**65**) against *B. subtilis aligns* with the findings of Mingoia *et al.* (2022), which demonstrated that cinnamic acids and their derivatives exhibit significant antibacterial properties. This is attributed to their capacity to disrupt bacterial membrane, leading to bacterial lysis and subsequent leakage of intracellular contents (Korkut *et al.*, 2025).

The absence of cytotoxic and antiproliferative activity in the quinolizidine alkaloids isolated in this study may be attributed to the specific types that were isolated. The antiproliferative and cytotoxic properties of alkaloids are largely contingent upon their specific type, as detailed by Cely-Veloza *et al.* (2023). The matrine type of quinolizidine alkaloids, exhibiting an average IC_{50} value exceeding 50 µM, demonstrated cytotoxic activity against various human cancer cell lines, including HepG-2 (hepatoma), MCF-7 (breast), HL-60 (leukemia), and A549 (lung adenocarcinoma) (Lei *et al.*,2014; Liu *et al.*,2014; Rong *et al.*, 2022; Tan *et al.*, 2017; Xu *et al.*, 2017; Zhang *et al.*, 2009). Additionally, Lupanine and cytosine, types of quinolizidine alkaloids, exhibited significant cytotoxic effects against HepG-2 cell lines, MCF-7, and glioma stem cells (GSC-3, GSC-12, and GSC-18), with an IC_{50} range of 117–20 µM (Aly *et al.*, 2022; Hirasawa *et al.*, 2014; Hirasawa *et al.*,2003; Li *et al.*, 2022; Pouny *et al.*, 2021; Pan *et al.*, 2016; Raub *et al.*,1991). In comparing these three types of quinolizidine alkaloids with the sparteine type identified in *Ca* extracts, it is clear that they exhibit potential cytotoxic activity.

The cytotoxic and antiproliferative properties of flavonoids of all types and cinnamic acids have been documented (Bhuia *et al.*, 2023; Gong *et al.*, 2024; Nolasco-Quintana *et al.*, 2023; Refaat *et al.*, 2015; Şirin *et al.*, 2020; Ye *et al.*, 2022; Zhao *et al.*, 2019;). For *Ca*, the flavones, isoflavones, flavanones, pterocarpan flavonoids, and cinnamic acids exhibited cytotoxic and antiproliferative activities, with the exception of the glycosylated compounds **60**, **61**, and **63**. There are reports indicating that *O*-glycosylation of flavonoids tends to diminish their bioactivity *in vitro* (Godinho *et al.*, 2021; Slika *et al.*, 2022; Yang *et al.*, 2018), thus elucidating the observed inactivity observed for these compounds. Furthermore, it has been shown that the glycosyl moiety reduces the cytotoxic and antiproliferative effects of these compounds (Huang *et al.*, 2016). In contrast to these accounts, the glycosylated compounds

54, **55**, and **56** exhibited activity against the cell lines under investigation. Rhoifolin (54) which has been identified as a potent cytotoxic flavonoid found in nature, has also been reported by Refaat *et al.* (2015, as cytotoxic and antiproliferative against various cell lines. Apigenin 7-O-glucoside (**55**) has been documented for its cytotoxic and antiproliferative effects on HeLa cell lines (Liu *et al.*,2020). Similarly, Emad *et al.* (2020) reported the cytotoxic and antiproliferative properties of luteolin 7-O-glycoside (**56**), with an IC_{50} value of 18 µg/mL. Thus, the bioactivity of some flavonoids as demonstrated in this work may not be influenced by the presence or absence of a glycosyl moiety rather their activity may be attributed to their core structures as shown by phenolic compounds with an apigenin nucleus (**54**, **55** and **56**) (Şirin *et al.*, 2020).

5.5 Conclusion

This study assessed the antidermatophytic, antimicrobial, antiproliferative, and cytotoxic properties of the crude extracts, as well as the isolated pure flavonoids and quinolizidine alkaloids. The plant extracts demonstrated antidermatophytic activities against the examined strains. The ethyl acetate extract demonstrated superior antidermatophytic activity relative to the other extracts. All quinolizidine alkaloids demonstrated antidermatophytic activity against the test strains, with minimum inhibitory concentrations (MIC) varying from 37.5 µg/mL to 300 µg/mL; compounds 52 and 53 displayed the lowest activity at 37.5 µg/mL against *N. gypsea*. The quinolizidine alkaloids showed no antimicrobial, antiproliferative, or cytotoxic activity against the test strains. The phenolic compounds displayed varying levels of activity against the test strains and cell lines. Compounds **54**, **55**, **56**, **59**, **62**, and **64** demonstrated activity against *M. hiemalis*, with a minimum inhibitory concentration (MIC) of 66.6 µg/mL. Additionally, compounds **56**, **59**, **62**, and 64 exhibited comparable inhibition against *S. pombe*. Cinnamic acid (**65** demonstrated antibacterial efficacy against *B. subtilis*, with a minimum inhibitory concentration (MIC) of 16.6 µg/mL, comparable to the positive control oxytetracycline (MIC 16.6 µg/mL). The glycosylated flavonoids showed no activity against the KB3.1 and L929 cell lines, apart from compounds **54**, **55**, and **56**. The cinnamic acid **65** exhibit significant activity, with an IC_{50} value of 18 µg/mL.

The results indicate that both crude and pure compounds derived from *Ca* represent a substantial source of novel secondary metabolites with potential applications in drug development for various bacterial, fungal, and inflammatory conditions. Additional studies on the structure-activity relationship of the identified active compounds are required to confirm their biological relevance in treating various diseases. This study contributes to the ethnobotanical and pharmacological knowledge of *C. aurea* subsp. *aurea* as the first

investigation of the antidermatophytic, antiproliferative, and cytotoxic action of the pure compounds and crude extracts derived from the species.

CHAPTER SIX

GENERAL DISCUSSION, CONCLUSIONS AND RECCOMENDATIONS

6.1 General Discussion

The study reported herein this thesis evaluated the antimicrobial, antidermatophytic, antiproliferative, and cytotoxicity of crude and pure secondary of metabolites extracted or isolated from *Ca* and its associated endophytes. Leaves and stem bark of the plants were collected from Mt. Elgon National Park for the isolation of fungal endophytes and secondary metabolites. The isolated pure compounds were characterized using 1D and 2D spectrometric and spectroscopic data. This study predominantly identified and characterized endophytic fungi as Ascomycetes, with a smaller proportion classified as Basidiomycetes. This trend is commonly noted in research studies that focus on the isolation and characterization of endophytic fungi (Rungjindamai & Jones, 2024). Ascomycota are widely acknowledged as prevalent endophytes, demonstrating a markedly higher occurrence than other taxonomic groups. The restricted isolation of endophytic Basidiomycota can be ascribed to factors including isolation techniques, media choice, incubation time, and temperature conditions. No standardized isolation procedure for endophytic fungi has been documented (Gupta *et al.,* 2019). However, a study by Yu *et al.* (2022) indicates that varying conditions for surface sterilization are essential for stem, leaf, and root tissues, with mature stem and root tissues necessitating higher concentrations and extended exposure times for thorough sterilization. This differs from the methodology used in this study, where all tissues underwent the same conditions of isolation and exposure duration. The formulation of culture media can enhance the growth of certain fungi while suppressing others. This study used PDA media exclusively as the isolation medium, highlighting a notable gap in the research. PDA is recommended as a sole culture medium for research focused on particular groups of readily cultivable fungal endophytes (Ibrahim *et al.,* 2021). To investigate the diversity of fungal endophytes, the primary focus of this study, it is recommended to employ at least two mycological media in addition to PDA (Pinruan *et al.,* 2010). Extended incubation periods and lower temperatures are optimal for isolating slow-growing endophytes, as demonstrated by (Doust *et al.,* 2019) who successfully isolated a diverse range of fungal endophytes at 4ºC over a period of up to 6 weeks, contrasting with the incubation conditions utilized in this study.

Two pure compounds were isolated from the fungal endophytes *P. hawaiiense* in small amounts, resulting in the absence of biological activity assessments (Chapter 4). This does not

accurately represent the phytochemical compositions of this strain. Studies indicate that enhancing fermentation parameters, including temperature and NaCl addition, increases the likelihood of detecting additional bio-active metabolites from the strains (Bills *et al.,* 2008). The research herein primarily concentrated on solid state fermentation utilizing rice media, which may facilitate the isolation of several secondary metabolites from this strain. The extraction of quinolizidine alkaloids and phenolic compounds from *Ca*., as discussed in chapter 4, aligns with previously published findings (Korir *et al.,* 2014). However, the bioactivity of the quinolizidine alkaloids obtained from this study does not correlate with the published results (chapter 5). For instance, Sparteine quinolizidine alkaloids have been documented for their antibacterial, cytotoxic and antiproliferative activity (Hammouche-Mokrane *et al.,* 2017). However, the sparteine type isolated in this study did not demonstrate these biological activities, except for antidermatophytic effects. This underscores the necessity for additional research on the structure-activity relationship of the isolated compounds. The bioactivity of the phenolic compounds isolated in this study aligns with previously published findings (Khan *et al.,* 2024; Mans *et al.,* 2022; Morante-Carriel *et al.,* 2024). This study was unable to determine the structure-activity relationships of the compounds; therefore, further research is necessary, particularly on those compounds identified as antibacterial, antidermatophytic, antiproliferative, and cytotoxic.

6.2 Conclusions

i. Isolation and Characterization of Endophytic Fungi

A total of 19 fungal endophytes were isolated from the leaves, stem bark, and roots of Ca, based on morphological and molecular analysis. The endophytes demonstrated antifungal activity against *T. rubrum, T. interdigitalle, T. benhamiae, M. canis,* and *N. gypsea*, with *P. Hawaiiense* showing the most effective activity against these strains.

ii. Isolation and Characterization of Secondary Metabolites

Twenty-two (22) pure compounds were isolated from the leaves, stem bark, and associated fungal endophytes of *P. hawaiiense*. Four previously undescribed quinolizidine alkaloids were reported: 2β-methoxy-13α-*O*-(2′- pyrrolylcarbonyl) virgiline (**46**), 2α-methoxy-13β-*O*-(2′-pyrrolylcarbonyl) virgiline (**47**), 3α-*O*-angelate-2β-hydroxy-13α-*O*-(2′-pyrrolylcarbonyl) virgiline (**48**), and 2,3-dehydro-virgiline (**49**). Two pure compounds were isolated from the fungal endophytes (*P. hawaiiense*); Lactorilide (**66**) and a previously undescribed compound (**67**).

iii. Antimicrobial, Antidermatophytic, Antiproliferative and Cytotoxic Activity of the Isolated Compound and Endophytic Fungi

Quinolizidine alkaloids demonstrated antidermatophytic activity against the selected strains; however, this class of compounds did not show antimicrobial, antiproliferative, or cytotoxic activities. The phenolic compounds exhibited anidermatophytic, antimicrobial, antiproliferative, and cytotoxic activities

6.3 Recommendations

i. Isolation and characterization of endophytic fungi

The methods employed for isolating endophytic fungi primarily focused on the rapid growth characteristics of certain species. Therefore, significant focus must be directed towards the isolation of slow-growing strains to expand the range of beneficial strains that can be isolated. Furthermore, expanding the selection of media is essential to enhance the range of fungal species isolation. This study utilized a single medium (PDA) for isolation, which may have limited the scope of isolation. Additional biological activities ought to be conducted on the isolated fungal endophytes, as this study primarily concentrated on antidermatophytic activities alone.

ii. Isolation and characterization of secondary metabolites

A greater number of secondary metabolites, particularly the quinolizidine alkaloids, ought to be isolated, as most of this class of compounds remains largely unexamined from this medicinal plant. Some of these compounds were detected in the crude extracts during the LC-MS analysis; however, their isolation was not feasible in this study because of time and resource limitations. The LC-MS spectrum analysis indicated that the quantity of these additional compounds was minimal for further spectroscopic and spectrometric examination. Furthermore, because of fermentation and extraction limitations, only two compounds were isolated from the fungal endophytes, which does not accurately reflect the phytochemical composition of the extracts from *P. Hawaiiense*. Consequently, further analysis is required on the phytochemical composition of this fungal endophyte.

iii. Antimicrobial, antidermatophytic, antiproliferative and cytotoxic activity of the isolated compound and endophytic fungi

The obtained compounds were evaluated for antibacterial activity *in vitro*; however, their low isolation quantities precluded *in vivo* investigations. Therefore, there are alternative approaches to increase their yield with the aim of conductinge *in vivo* investigations, particularly on the compounds that demonstrated favorable outcomes in antidermatophytic,

antimicrobial, and antifungal, as reported herein. Furthermore, a selectivity test should be conducted on the phenolic compounds that demonstrate cytotoxic effects. Subsequently, additional research on the structure-activity relationship of the identified active compounds is necessary to substantiate their biological significance in addressing diverse disorders.

6.4 Further Research Directions

As illustrated from the results obtained from this study, *Calpurnia aurea* subsp. *aurea* is a potent medicinal plant that contains mainly flavonoids and quinolizidine alkaloids classes of compounds that exhibit significant antidermatophytic, antimicrobial, antiproliferative and cytotoxic activities. However, despite these ethnopharmacological importance, research on the isolation and structural characterization of its metabolites, and particularly those synthesized by axenic endophytic fungi, remains limited. Therefore, future studies should adopt integrative and technology-driven strategies to fully exploit the plant–endophyte metabolic potential. Additionally, advanced metabolomic studies using high-resolution LC–MS/MS can enhance rapid dereplication of known molecules and identification of novel secondary metabolites for purification and structure elucidation using NMR spectroscopy. The cryptic or silent pathways of these endophytic fungi can be activated using one-strain–many-compounds (OSMAC) cultivation strategies/ approach, co-culturing with other fungi or bacteria, or treatment with epigenetic modifiers that can induce secondary metabolism. Moreover, spatial metabolomics approaches, such as MALDI-MS imaging, can further enhance localization of metabolites within plant tissues, distinguishing between host derived and fungus derived secondary metabolites/ compounds and offering insight into their ethnobotanical importance and ecological functions. Finally, ethical and sustainable bioprospecting must accompany these recomedations, including fair benefit-sharing and potential biotechnological production through fermentation of endophytic gene clusters or heterologous expression. Application of a combination of metabolomic and genomic knowledge of this medicinal plant will assist in briding the gap between the ethnobotanical knowledge and the scientific validation of its traditional uses.

REFERENCES

Aamir, M., Rai, K. K., Zehra, A., Kumar, S., Yadav, M., Shukla, V., & Upadhyay, R. S. (2020). Fungal endophytes: Classification, diversity, ecological role, and their relevance in sustainable agriculture. *Microbial Endophytes: Prospects for Sustainable Agriculture*, 291–323. https://doi.org/10.1016/b978-0-12-818734-0.00012-7

Aboody, M. S. Al, & Mickymaray, S. (2020). Anti-Fungal Efficacy and Mechanisms of Flavonoids. *Antibiotics (Basel, Switzerland)*, *9*(2), 45. https://doi.org/10.3390/antibiotics9020045

Abu, F., Mat Taib, C. N., Mohd Moklas, M. A., & Mohd Akhir, S. (2017). Antioxidant properties of crude extract, partition extract, and fermented medium of *Dendrobium sabin* flower. *Evidence-Based Complementary and Alternative Medicine*, *2017*(1), 2907219. https://doi.org/10.1155/2017/2907219

Abubakar, E. M. M. (2009). The use of *Psidium guajava* Linn. in treating wound, skin and soft tissue infections. *Scientific Research and Essay*, *4*(6), 605–611. https://doi.org/10.1002/0471701343.sdp21680

Adedapo, A. A., Jimoh, F. O., Koduru, S., Afolayan, A. J., & Masika, P. J. (2008). Antibacterial and antioxidant properties of the methanol extracts of the leaves and stems of *Calpurnia aurea*. *BMC Complementary and Alternative Medicine*, *8*(1), 1–8. https://doi.org/10.1186/1472-6882-8-53

Adeleke, B. S., & Babalola, O. O. (2021). Pharmacological Potential of Fungal Endophytes Associated with Medicinal Plants: A Review. *Journal of Fungi*, *7*(2), 147. https://doi.org/10.3390/jof7020147

Adhikari, P., Joshi, K., & Pandey, A. (2023). Taxus associated fungal endophytes: anticancerous to other biological activities. *Fungal Biology Reviews*, *45*, 100308. https://doi.org/10.1016/j.fbr.2023.100308

Adler, N. E., & Newman, K. (2002). Socioeconomic disparities in health: pathways and policies. *Health affairs*, *21*(2), 60-76. https://doi.org/10.1377/hlthaff.21.2.60

Afsar, F. S. (2010). Skin infections in developing countries. *Current Opinion in Pediatrics*, *22*(4), 459–466. https://doi.org/10.1097/mop.0b013e32833bc468

Ahmad, F., Anwar, F., & Hira, S. (2016). Review on medicinal importance of *Fabaceae* family. *Pharmacologyonline*, *3*, 151-157.

Ahmed, E., Malik, A., Ferheen, S., Afza, N., Lodhi, M. A., & Choudhary, M. I. (2006). Chymotrypsin inhibitory triterpenoids from *Silybum marianum*. *Chemical and pharmaceutical bulletin*, *54*(1), 103-106. https://doi.org/10.1248/cpb.54.103

Akash, M. S. H., Ibrahim, M., Hameed, A., Rehman, K., Niazi, M. S. K., Farooq, T., & Qadir, M. I. (2016). Antiretroviral Agents: Looking for the Best Possible Chemotherapeutic Options to Conquer HIV. *Critical Reviews™ in Eukaryotic Gene Expression*, *26*(4), 363–381. https://doi.org/10.1615/critreveukaryotgeneexpr.2016018255

Akshatha, V. J., Nalini, M. S., D'Souza, C., & Prakash, H. S. (2014). *Streptomycete* endophytes from anti-diabetic medicinal plants of the Western Ghats inhibit alpha-amylase and promote glucose uptake. *Letters in Applied Microbiology*, *58*(5), 433–439. https://doi.org/10.1111/lam.12209

Al-Khikani, F. (2020). Dermatophytosis a worldwide contiguous fungal infection: Growing challenge and few solutions. *Biomedical and Biotechnology Research Journal*, *4*(2), 117–122. https://doi.org/10.4103/bbrj.bbrj_1_20

Alam, M. M., Islam, M., Wahab, A., & Billah, M. (2019). Antimicrobial Resistance Crisis and Combating Approaches. *Journal of Medicine*, *20*(1), 38–45. https://doi.org/10.3329/jom.v20i1.38842

Alanis, A. J. (2005). Resistance to Antibiotics: Are We in the Post-Antibiotic Era? *Archives of Medical Research*, *36*(6), 697–705. https://doi.org/10.1016/j.arcmed.2005.06.009

Alfouzan, W., Al-Balushi, Z., Al-Maslamani, M., Al-Rashed, A., Al-Sabah, S., Al-Salman, J., Baguneid, M., Khamis, F., Habashy, N., Kurdi, A., & Eckmann, C. (2021). Antimicrobial Management of Complicated Skin and Soft Tissue Infections in an Era of Emerging Multi-Drug Resistance: Perspectives from 5 Gulf Countries. *Journal of Acute Care Surgery*, *11*(3), 89–101. https://doi.org/10.17479/jacs.2021.11.3.89

Aly, S. H., Elissawy, A. M., Allam, A. E., Farag, S. M., Eldahshan, O. A., Elshanawany, M. A., & Singab, A. N. B. (2022). New quinolizidine alkaloid and insecticidal activity of *Sophora secundiflora* and *Sophora tomentosa* against *Culex pipiens* (Diptera: Culicidae). *Natural Product Research*, *36*(11), 2722–2734. https://doi.org/10.1080/14786419.2021.1919108

Amirthalingam, S., Yi, K. S., Ching, L. T., & Mun, N. Y. (2015). Topical Antibacterials and Global Challenges on Resistance Development. *Tropical Journal of Pharmaceutical Research*, *14*(5), 919–924. https://doi.org/10.4314/tjpr.v14i5.24

Anibogwu, R., De Jesus, K., Pradhan, S., Pashikanti, S., Mateen, S., & Sharma, K. (2021). Extraction, Isolation and Characterization of Bioactive Compounds from *Artemisia* and Their Biological Significance: A Review. *Molecules*, *26*(22), 6995. https://doi.org/10.3390/molecules26226995

Aratanechemuge, Y., Hibasami, H., Katsuzaki, H., Imai, K., & Komiya, T. (2004). Induction

of apoptosis by maackiain and trifolirhizin (maackiain glycoside) isolated from sanzukon (*Sophora Subprostrate* Chen et T. Chen) in human promyelotic leukemia HL-60 cells. *Oncology Reports*, *12*(6), 1183–1188. https://doi.org/10.3892/or.12.6.1183/html

Arenas, R., Del Rocío Reyes-Montes, M., Duarte-Escalante, E., Frías-De-León, M. G., & Martínez-Herrera, E. (2017). Dermatophytes and Dermatophytosis. *Current Progress in Medical Mycology*, 381–425. https://doi.org/10.1007/978-3-319-64113-3_13

Arif, N., Yousfi, S., & Vinnard, C. (2016). Deaths from necrotizing fasciitis in the United States, 2003–2013. *Epidemiology & Infection*, *144*(6), 1338–1344. https://doi.org/10.1017/s0950268815002745

Arnold, A. E., & Lutzoni, F. (2007). Diversity and host range of foliar fungal endophytes: are tropical leaves biodiversity hotspots? *Ecology*, *88*(3), 541–549. https://doi.org/10.1890/05-1459

Arnold, A. E., Zuleyka, M., & Gilbert, G. S. (2001). Fungal endophytes in dicotyledonous neotropical trees: patterns of abundance and diversity. *Mycological Research*, *105*(12), 1502–1507. https://doi.org/10.1017/s0953756201004956

Ash, G. J., Stodart, B., Sakuanrungsirikul, S., Anschaw, E., Crump, N., Hailstones, D., & Harper, J. D. (2010). Genetic characterization of a novel *Phomopsis* sp., a putative biocontrol agent for Carthamus lanatus. *Mycologia*, *102*(1), 54-61. https://doi.org/10.3852/08-198

Asres, K., Gibbons, W. A., Phillipson, J. D., & Mascagni, P. (1986). Alkaloids of ethiopian *Calpurnia aurea* subsp. *aurea*. *Phytochemistry*, *25*(6), 1443–1447. https://doi.org/10.1016/s0031-9422(00)81306-0

Ateba, J. E. T., Toghueo, R. M. K., Awantu, A. F., Mba'ning, B. M., Gohlke, S., Sahal, D., Rodrigues-Filho, E., Tsamo, E., Boyom, F. F., Sewald, N., & Lenta, B. N. (2018). Antiplasmodial Properties and Cytotoxicity of Endophytic Fungi from *Symphonia globulifera* (*Clusiaceae*). *Journal of Fungi*, *4*(2), 70. https://doi.org/10.3390/jof4020070

Ayal, G., Belay, A., & Kahaliw, W. (2019). Evaluation of wound healing and anti-inflammatory activity of the leaves of *Calpurnia aurea* (Ait.) Benth (*fabaceae*) in mice. *Wound Medicine*, *25*(1), 100151. https://doi.org/10.1016/j.wndm.2019.100151

Azani, N., Babineau, M., Bailey, C. D., Banks, H., Barbosa, A. R., Pinto, R. B., ... & Zimmerman, E. (2017). A new subfamily classification of the Leguminosae based on a taxonomically comprehensive phylogeny: The Legume Phylogeny Working Group (LPWG). *Taxon*, *66*(1), 44-77. https://doi.org/10.12705/661.3

Azmir, J., Zaidul, I. S. M., Rahman, M. M., Sharif, K. M., Mohamed, A., Sahena, F., ... &

Omar, A. K. (2013). Techniques for extraction of bioactive compounds from plant materials: A review. *Journal of food engineering*, *117*(4), 426-436. https://doi.org/10.1016/j.jfoodeng.2013.01.014

Ballus, J., Lopez-Delgado, J. C., Sabater-Riera, J., Perez-Fernandez, X. L., Betbese, A. J., & Roncal, J. A. (2015). Surgical site infection in critically ill patients with secondary and tertiary peritonitis: Epidemiology, microbiology and influence in outcomes. *BMC Infectious Diseases*, *15*(1), 1–6. https://doi.org/10.1186/s12879-015-1050-5/tables/2

Baquero, F., Saralegui, C., Marcos-Mencía, D., Ballestero, L., Vañó-Galván, S., Moreno-Arrones, Ó. M., & del Campo, R. (2021). Epidermis as a Platform for Bacterial Transmission. *Frontiers in Immunology*, *12*, 774018. https://doi.org/10.3389/fimmu.2021.774018

Bartlett, J. G., Gilbert, D. N., & Spellberg, B. (2013). Seven Ways to Preserve the Miracle of Antibiotics. *Clinical Infectious Diseases*, *56*(10), 1445–1450. https://doi.org/10.1093/cid/cit070

Beaumont, A. J., Beckett, R. P., Edwards, T. J., & Stirton, C. H. (1999). Revision of the genus *Calpurnia* (*Sophoreae*: *Leguminosae*). *Bothalia*, *29*(1), 5–23. https://doi.org/10.4102/abc.v29i1.568

Becker, K., Wessel, A. C., Luangsa-Ard, J. J., & Stadler, M. (2020). Viridistratins A−C, Antimicrobial and Cytotoxic Benzo[j]fluoranthenes from Stromata of *Annulohypoxylon viridistratum* (*Hypoxylaceae*, Ascomycota). *Biomolecules*, *10*(5), 805. https://doi.org/10.3390/biom10050805

Beddok, A., Cottu, P., Fourquet, A., & Kirova, Y. (2021). Combination of Modern Radiotherapy and New Targeted Treatments for Breast Cancer Management. *Cancers*, *13*(24), 6358. https://doi.org/10.3390/cancers13246358

Belayneh, Y. M., Birru, E. M., & Ambikar, D. (2019). Evaluation of hypoglycemic, antihyperglycemic and antihyperlipidemic activities of 80% methanolic seed extract of *calpurnia aurea* (Ait.) benth. (*fabaceae*) in mice. *Journal of Experimental Pharmacology*, *11*, 73–83. https://doi.org/10.2147/jep.s212206

Bernard, P. (2008). Management of common bacterial infections of the skin. *Current Opinion in Infectious Diseases*, *21*(2), 122–128. https://doi.org/10.1097/qco.0b013e3282f44c63

Bhargavan, B., Singh, D., Gautam, A. K., Mishra, J. S., Kumar, A., Goel, A., ... & Sanyal, S. (2012). Medicarpin, a legume phytoalexin, stimulates osteoblast differentiation and promotes peak bone mass achievement in rats: evidence for estrogen receptor β-mediated osteogenic action of medicarpin. *The Journal of nutritional biochemistry*, *23*(1), 27-38.

https://doi.org/10.1016/j.jnutbio.2010.11.002

Bhuia, M. S., Aktar, M. A., Chowdhury, R., Ferdous, J., Rahman, M. A., Hasan, M. S. Al, & Islam, M. T. (2023). Therapeutic potentials of ononin with mechanistic insights: A comprehensive review. *Food Bioscience*, *56*, 103302. https://doi.org/10.1016/j.fbio.2023.103302

Bills, G. F., Platas, G., Fillola, A., Jiménez, M. R., Collado, J., Vicente, F., Martín, J., González, A., Bur-Zimmermann, J., Tormo, J. R., & Peláez, F. (2008). Enhancement of antibiotic and secondary metabolite detection from filamentous fungi by growth on nutritional arrays. *Journal of Applied Microbiology*, *104*(6), 1644–1658. https://doi.org/10.1111/j.1365-2672.2008.03735.x

Birhanu, M. Y., Temesgen, H., Ketema, D. B., Desta, M., Getaneh, T., Bekele, G. M., Zeleke, B., & Jemberie, S. S. (2023). Tinea capitis among schoolchildren in Ethiopia: A systematic review and meta analysis. *PLOS ONE*, *18*(2), e0280948. https://doi.org/10.1371/journal.pone.0280948

Bishwabidyalay, W. G., Sultana, R., & Wahiduzzaman, M. (2019). Emerging threat in antifungal resistance on superficial dermatophyte infection. *Bangladesh Medical Journal Khulna*, *51*(1-2), 21-24. https://doi.org/10.3329/bmjk.v51i1-2.40469

Blanco Carcache, P. J., Addo, E. M., & Kinghorn, A. D. (2021). Higher plant sources of cancer chemotherapeutic agents and the potential role of biotechnological approaches for their supply. *Medicinal plants: domestication, biotechnology and regional importance* (pp. 545-581). https://doi.org/10.1007/978-3-030-74779-4_17

Boakye-Yiadom, E., Odoom, A., Osman, A. H., Ntim, O. K., Kotey, F. C. N., Ocansey, B. K., & Donkor, E. S. (2024). Fungal Infections, Treatment and Antifungal Resistance: The Sub-Saharan African Context. *Therapeutic Advances in Infectious Disease*, *11*. https://doi.org/10.1177/20499361241297525

Bodey, G. P. (2000). Unusual presentations of infection in neutropenic patients. *International Journal of Antimicrobial Agents*, *16*(2), 93–95. https://doi.org/10.1016/S0924-8579(00)00241-7

Bora, K. S., & Sharma, A. (2011). The genus *Artemisia*: a comprehensive review. *Pharmaceutical biology*, *49*(1), 101-109. https://doi.org/10.3109/13880209.2010.497815

Borelli, C., Merk, K., Schaller, M., Jacob, K., Vogeser, M., Weindl, G., Berger, U., & Plewig, G. (2006). *In vivo* porphyrin production by *P. acnes* in untreated acne patients and its modulation by acne treatment. *Acta Dermato-Venereologica*, *86*(4), 316–319.

https://doi.org/10.2340/00015555-0088

Botella, L., & Diez, J. J. (2011). Phylogenic diversity of fungal endophytes in Spanish stands of Pinus halepensis. *Fungal Diversity*, *47*(1), 9-18. https://doi.org/10.1007/s13225-010-0061-1

Brader, G., Compant, S., Mitter, B., Trognitz, F., & Sessitsch, A. (2014). Metabolic potential of endophytic bacteria. *Current Opinion in Biotechnology*, *27*, 30–37. https://doi.org/10.1016/j.copbio.2013.09.012

Bray, F., Laversanne, M., Weiderpass, E., & Soerjomataram, I. (2021). The ever-increasing importance of cancer as a leading cause of premature death worldwide. *Cancer*, *127*(16), 3029–3030. https://doi.org/10.1002/cncr.33587

Breyre, A., & Frazee, B. W. (2018). Skin and Soft Tissue Infections in the Emergency Department. *Emergency Medicine Clinics of North America*, *36*(4), 723–750. https://doi.org/10.1016/j.emc.2018.06.005

Brook, I., Frazier, E. H., & Yeager, J. K. (1997). Microbiology of Nonbullous Impetigo. *Pediatric Dermatology*, *14*(3), 192–195. https://doi.org/10.1111/j.1525-1470.1997.tb00235.x

Brown, E. D., & Wright, G. D. (2016). Antibacterial drug discovery in the resistance era. *Nature*, *529*(7586), 336–343. https://doi.org/10.1038/nature17042

Brown, G. D., Denning, D. W., Gow, N. A. R., Levitz, S. M., Netea, M. G., & White, T. C. (2012). Hidden killers: Human fungal infections. *Science Translational Medicine*, *4*(165). https://doi.org/10.1126/scitranslmed.3004404

Brusotti, G., Cesari, I., Dentamaro, A., Caccialanza, G., & Massolini, G. (2014). Isolation and characterization of bioactive compounds from plant resources: the role of analysis in the ethnopharmacological approach. *Journal of pharmaceutical and biomedical analysis*, *87*, 218-228. https://doi.org/10.1016/j.jpba.2013.03.007

Burstein, V. L., Beccacece, I., Guasconi, L., Mena, C. J., Cervi, L., & Chiapello, L. S. (2020). Skin Immunity to Dermatophytes: From Experimental Infection Models to Human Disease. *Frontiers in Immunology*, *11*, 605644. https://doi.org/10.3389/fimmu.2020.605644

Cely-Veloza, W., Kato, M. J., & Coy-Barrera, E. (2023). Quinolizidine-Type Alkaloids: Chemodiversity, Occurrence, and Bioactivity. *ACS Omega*, *8*(31), 27862–27893. https://doi.org/10.1021/acsomega.3c02179

Cely-Veloza, W., Yamaguchi, L., Quiroga, D., Kato, M. J., & Coy-Barrera, E. (2023). Antifungal activity against *Fusarium oxysporum* of quinolizidines isolated from three

controlled-growth *Genisteae* plants: structure–activity relationship implications. *Natural Products and Bioprospecting*, *13*(1), 1–11. https://doi.org/10.1007/s13659-023-00373-4

Chen, D., Zhang, S., Kuang, M., Peng, W., Tan, J., Wang, W., Kang, F., Zou, Z., & Xu, K. (2022). A New Benzophenone Derivative from the Endophyte Shiraia sp. BYJB-1. *Records of Natural Products*, *16*, 471–476. https://doi.org/10.25135/rnp.306.2111.2265

Chen, K., Wu, W., Hou, X., Yang, Q., & Li, Z. (2021). A review: antimicrobial properties of several medicinal plants widely used in Traditional Chinese Medicine. *Food Quality and Safety*, *5*. https://doi.org/10.1093/fqsafe/fyab020

Chen, S., Zhang, Y., Zhao, C., Ren, F., Liu, X., & Che, Y. (2014). Hawaiinolides E–G, cytotoxic cassane and cleistanthane diterpenoids from the entomogenous fungus *Paraconiothyrium hawaiiense*. *Fitoterapia*, *99*(1), 236–242. https://doi.org/10.1016/j.fitote.2014.09.021

Chepkirui, C., Yuyama, K. T., Wanga, L. A., Decock, C., Matasyoh, J. C., Abraham, W. R., & Stadler, M. (2018). Microporenic Acids A-G, Biofilm Inhibitors, and Antimicrobial Agents from the Basidiomycete Microporus Species. *Journal of Natural Products*, *81*(4), 778–784. https://doi.org/10.1021/acs.jnatprod.7b00764

Chokshi, A., Sifri, Z., Cennimo, D., & Horng, H. (2019). Global contributors to antibiotic resistance. *Journal of global infectious diseases*, *11*(1), 36-42. https://doi.org/10.4103/jgid.jgid_110_18

Christenhusz, M. J., & Byng, J. (2016). The number of known plants species in the world and its annual increase. *Phytotaxa*, *261*(3), 201-217. https://doi.org/10.11646/phytotaxa.261.3.1

Cock, I. E., & Van Vuuren, S. F. (2020). A review of the traditional use of southern African medicinal plants for the treatment of fungal skin infections. *Journal of Ethnopharmacology*, *251*, 112539. https://doi.org/10.1016/j.jep.2019.112539

Coker, Ogundele, M. E. &, & S., O. (2016). Evaluation of the anti-fungal properties of extracts of *Daniella oliveri*. *African Journal of Biomedical Research*, *19*(1), 55–60. https://doi.org/10.4314/njpr.v16i2.8s

Comby, M., Lacoste, S., Baillieul, F., Profizi, C., & Dupont, J. (2016). Spatial and temporal variation of cultivable communities of co-occurring endophytes and pathogens in wheat. *Frontiers in microbiology*, *7*, 403. https://doi.org/10.3389/fmicb.2016.00403/bibtex

Corothie, E., & Ilija, H. (1975). Studies on the neutral constituents of *Aragoa lucidula*. *Planta Medica*, *27*(2), 182–184. https://doi.org/10.1055/s-0028-1097783

Crous, P. W., & Groenewald, J. Z. (2005). Hosts, species and genotypes: Opinions versus data - Presented as a keynote address at the 15th Biennial Conference of the Australasian Plant Pathology Society, Geelong, Australia, 26-29 September 2005. *Australasian Plant Pathology*, *34*(4), 463–470. https://doi.org/10.1071/ap05082/metrics

Currò, D. (2018). The role of gut microbiota in the modulation of drug action: a focus on some clinically significant issues. *Expert Review of Clinical Pharmacology*, *11*(2), 171–183. https://doi.org/10.1080/17512433.2018.1414598

Daksa Ejeta, D., & Abdisa, Z. (2018). Antioxidant Activity Assessment of *Calpurnia aurea* Root Extract, *6*(307), 2. https://doi.org/10.4172/2329-6836.1000307

Damtie, D. (2023). Review of Medicinal Plants Traditionally Used to Treat Diarrhea by the People in the Amhara Region of Ethiopia. *Evidence-Based Complementary and Alternative Medicine*, *2023*(1), 8173543. https://doi.org/10.1155/2023/8173543

Darade, R. B., Zambare, K. K., Jaiswal, N. R., & Kaware, A. A. (2020). An overview on pharmacotherapy of jock itch (Tinea cruris). *World Journal of Pharmaceutical Research*, *9*. https://doi.org/10.20959/wjpr20201-16505

De Nysschen, A. M., Van Wyk, B. E., & Van Heerden, F. R. (1998). Seed flavonoids of the *Podalyrieae* and *Liparieae* (*Fabaceae*). *Plant Systematics and Evolution*, *212*(1–2), 1–11. https://doi.org/10.1007/bf00985218

Deckert, R. J., Melville, L. H., & Peterson, R. L. (2001). Structural features of a Lophodermium endophyte during the cryptic life-cycle phase in the foliage of Pinus strobus. *Mycological Research*, *105*(8), 991-997. https://doi.org/10.1017/S0953756201004373

Dhinakaran, A., Kalaiselvam, M., Sekar, V., & Sethubathi, G. V. B. (2012). Isolation of *Penicillium* sp. and its antagonistic activity against dermatophytes from volcano soil of Baratang Island, Andaman. *International Journal of Pharmaceutical Sciences and Research*, *3*(2), 564–568. https://doi.org/10.26452/ijrps.v11i1.1784

Dias, D. A., Urban, S., & Roessner, U. (2012). A Historical Overview of Natural Products in Drug Discovery. *Metabolites 2*(2), 303–336. https://doi.org/10.3390/metabo2020303

dos Reis, J. B. A., Lorenzi, A. S., & do Vale, H. M. M. (2022). Methods used for the study of endophytic fungi: a review on methodologies and challenges, and associated tips. *Archives of Microbiology*, *204*(11), 1–30. https://doi.org/10.1007/s00203-022-03283-0

Doust Hagh, N., Safaie, N., Schmitt, I., Otte, J., & Bálint, M. (2019). Culture-based methods using low-temperature incubation revealed cold-adapted fungal endophytes from semiarid forests. *Forest Pathology*, *49*(3), e12515. https://doi.org/10.1111/efp.12515

Dropulic, L. K., & Lederman, H. M. (2016). Overview of Infections in the

Immunocompromised Host. *Diagnostic Microbiology of the Immunocompromised Host*, 1–50. https://doi.org/10.1128/9781555819040.ch1

Druzhinina, I. S., Kopchinskiy, A. G., Komoń, M., Bissett, J., Szakacs, G., & & Kubicek, C. P. (2005). An oligonucleotide barcode for species identification in *Trichoderma* and *Hypocrea*. *Fungal Genetics and Biology*, *42*(10), 813–828. https://doi.org/10.1016/j.fgb.2005.06.007

Dryden, M. S. (2014). Novel antibiotic treatment for skin and soft tissue infection. *Current Opinion in Infectious Diseases*, *27*(2), 116–124. https://doi.org/10.1097/qco.0000000000000050

Dudeja, S. S., & Giri, R. (2014). Beneficial properties, colonization, establishment and molecular diversity of endophytic bacteria in legumes and non legumes. *African Journal of Microbiology Research, 8*(15), 1562-1572. https://doi.org/10.5897/ajmr2013.6541

Dzobo, K. (2022). The Role of Natural Products as Sources of Therapeutic Agents for Innovative Drug Discovery. *Comprehensive Pharmacology*, *2*, 408. https://doi.org/10.1016/b978-0-12-820472-6.00041-4

European Centre for Disease Prevention and Control. (2019). Surveillance of antimicrobial resistance in Europe 2018. *Stockholm: ECDC.* https://www.ecdc.europa.eu/en/publications-data/surveillance-antimicrobial-resistance-europe-2018

Edgar, R. C. (2004). MUSCLE: multiple sequence alignment with high accuracy and high throughput. *Nucleic Acids Research*, *32*(5), 1792–1797. https://doi.org/10.1093/nar/gkh340

Egbuta, M. A., Mwanza, M., & Babalola, O. O. (2017). Health Risks Associated with Exposure to Filamentous Fungi. *International Journal of Environmental Research and Public Health, 14*(7), 719. https://doi.org/10.3390/ijerph14070719

El-Gowelli, H. M., & El-Mas, M. M. (2015). Central modulation of cyclosporine-induced hypertension. *Naunyn-Schmiedeberg's Archives of Pharmacology*, *388*(3), 351–361. https://doi.org/10.1007/s00210-014-1074-1

El-Hawary, S. S., Moawad, A. S., Bahr, H. S., Abdelmohsen, U. R., & Mohammed, R. (2020). Natural product diversity from the endophytic fungi of the genus Aspergillus. *RSC Advances*, *10*(37), 22058. https://doi.org/10.1039/d0ra04290k

El-Shahir, A. A., El-Tayeh, N. A., Ali, O. M., Abdel Latef, A. A. H., & Loutfy, N. (2021). The Effect of Endophytic Talaromyces pinophilus on Growth, Absorption and Accumulation of Heavy Metals of Triticum aestivum Grown on Sandy Soil Amended by Sewage Sludge.

Plants, *10*(12). https://doi.org/10.3390/plants10122659

Elsässer, B., Krohn, K., Flörke, U., Root, N., Aust, H. J., Draeger, S., Schulz, B., Antus, S., & Kurtán, T. (2005). X-ray Structure Determination, Absolute Configuration and Biological Activity of Phomoxanthone A. *European Journal of Organic Chemistry*, *2005*(21), 4563–4570. https://doi.org/10.1002/ejoc.200500265

Emad, F., Khalafalah, A. K., El Sayed, M. A., Mohamed, A. E. H., Stadler, M., & Helaly, S. E. (2020). Three new polyacetylene glycosides (PAGs) from the aerial part of Launaea capitata (Asteraceae) with anti-biofilm activity against *Staphylococcus aureus*. *Fitoterapia*, *143*, 104548. https://doi.org/10.1016/j.fitote.2020.104548

Esposito, S., Noviello, S., & Leone, S. (2016). Epidemiology and microbiology of skin and soft tissue infections. *Current Opinion in Infectious Diseases*, *29*(2), 109–115. https://doi.org/10.1097/qco.0000000000000239

Evolution, R. A. F., & Woods, R. J. (2014). Antibiotic resistance management. *Evolution, medicine, and public health*, *2014*(1), 147. https://doi.org/10.1093/emph/eou024

Fadiji, A. E., & Babalola, O. O. (2020). Elucidating Mechanisms of Endophytes Used in Plant Protection and Other Bioactivities With Multifunctional Prospects. *Frontiers in Bioengineering and Biotechnology*, *8*, 532550. https://doi.org/10.3389/fbioe.2020.00467/bibtex

Fang, K., Miao, Y. F., Chen, L., Zhou, J., Yang, Z. P., Dong, X. F., & Zhang, H. B. (2019). Tissue-Specific and Geographical Variation in Endophytic Fungi of *Ageratina adenophora* and Fungal Associations With the Environment. *Frontiers in Microbiology*, *10*. https://doi.org/10.3389/fmicb.2019.02919

Felsenstein, J., & Churchill, G. A. (1996). A Hidden Markov Model approach to variation among sites in rate of evolution. *Molecular Biology and Evolution*, *13*(1), 93–104. https://doi.org/10.1093/oxfordjournals.molbev.a025575

Fill, T. P., Da Silva, B. F., & Rodrigues-Fo, E. (2010). Biosynthesis of phenylpropanoid amides by an endophytic Penicillium brasilianum found in root bark of Melia azedarach. *Journal of Microbiology and Biotechnology*, *20*(3), 622-629. https://doi.org/10.4014/jmb.0908.08018

Frings, M., Lakes, T., Müller, D., Khan, M. M. H., Epprecht, M., Kipruto, S., Galea, S., & Gruebner, O. (2018). Modeling and mapping the burden of disease in Kenya. *Scientific Reports*, *8*(1), 1–9. https://doi.org/10.1038/s41598-018-28266-4

Gakuubi, M. M., Ching, K. C., Munusamy, M., Wibowo, M., Liang, Z. X., Kanagasundaram, Y., & Ng, S. B. (2022). Enhancing the Discovery of Bioactive Secondary Metabolites

From Fungal Endophytes Using Chemical Elicitation and Variation of Fermentation Media. *Frontiers in Microbiology*, *13*, 898976. https://doi.org/10.3389/fmicb.2022.898976/bibtex

Gakuubi, M. M., Munusamy, M., Liang, Z. X., & Ng, S. B. (2021). Fungal Endophytes: A Promising Frontier for Discovery of Novel Bioactive Compounds. *Journal of Fungi*, *7*(10). https://doi.org/10.3390/jof7100786

Ganaie, H. A., & Wani, M. A. (2021). Candidiasis and Dermatophytosis: Infections and Their Prevention. *Fungal Diseases in Animals: From Infections to Prevention* (pp. 35-47). https://doi.org/10.1007/978-3-030-69507-1_3

Gaytán, Á., Bergsten, J., Canelo, T., Pérez-Izquierdo, C., Santoro, M., & Bonal, R. (2020). DNA Barcoding and geographical scale effect: The problems of undersampling genetic diversity hotspots. *Ecology and Evolution*, *10*(19), 10754–10772. https://doi.org/10.1002/ece3.6733

Gazis, R., Rehner, S., & Chaverri, P. (2011). Species delimitation in fungal endophyte diversity studies and its implications in ecological and biogeographic inferences. *Molecular ecology*, *20*(14), 3001-3013. https://doi.org/10.1111/j.1365-294x.2011.05110.x

Gazis, Romina, & Chaverri, P. (2010). Diversity of fungal endophytes in leaves and stems of wild rubber trees (*Hevea brasiliensis*) in Peru. *Fungal Ecology*, *3*(3), 240–254. https://doi.org/10.1016/j.funeco.2009.12.001

Gemechu, A., Giday, M., Worku, A., & Ameni, G. (2013). In vitro Anti-mycobacterial activity of selected medicinal plants against *Mycobacterium tuberculosis* and *Mycobacterium bovis* Strains. *BMC Complementary and Alternative Medicine*, *13*(1), 1–6. https://doi.org/10.1186/1472-6882-13-291

Gerwick, W. H. (2013). Plant Sources of Drugs and Chemicals. *Encyclopedia of Biodiversity: Second Edition*, 129–139. https://doi.org/10.1016/b978-0-12-384719-5.00111-8

Gezici, S., & Şekeroğlu, N. (2019). Current Perspectives in the Application of Medicinal Plants Against Cancer: Novel Therapeutic Agents. *Anti-Cancer Agents in Medicinal Chemistry*, *19*(1), 101–111. https://doi.org/10.2174/1871520619666181224121004

Ghasemnezhad, A., Frouzy, A., Ghorbanpour, M., & Sohrabi, O. (2021). *Microbial Endophytes: New Direction to Natural Sources*, 123–155. https://doi.org/10.1007/978-3-030-65447-4_6

Gilaberte, Y., Prieto-Torres, L., Pastushenko, I., & Juarranz, Á. (2016). Anatomy and Function of the Skin. *Nanoscience in Dermatology*, 1–14. https://doi.org/10.1016/b978-0-12-802926-8.00001-x

Gill, E. E., Franco, O. L., & Hancock, R. E. W. (2015). Antibiotic Adjuvants: Diverse Strategies for Controlling Drug-Resistant Pathogens. *Chemical Biology & Drug Design*, *85*(1), 56–78. https://doi.org/10.1111/cbdd.12478

Gnat, S., Łagowski, D., Nowakiewicz, A., & Dyląg, M. (2021). A global view on fungal infections in humans and animals: opportunistic infections and microsporidioses. *Journal of Applied Microbiology*, *131*(5), 2095–2113. https://doi.org/10.1111/jam.15032

Gnat, Sebastian, Łagowski, D., Nowakiewicz, A., & Dyląg, M. (2020). Unusual dermatomycoses caused by *Nannizzia nana*: the geophilic origin of human infections. *Infection*, *48*(3), 429–434. https://doi.org/10.1007/s15010-020-01416-5

Godinho, P. I., Soengas, R. G., & Silva, V. L. (2021). Therapeutic potential of glycosyl flavonoids as anti-coronaviral agents. *Pharmaceuticals*, *14*(6), 546. https://doi.org/10.3390/ph14060546

Gong, G., Wan, Y., Liu, Y., Zhang, Z., & Zheng, Y. (2024). Ononin triggers ferroptosis-mediated disruption in the triple negative breast cancer both in vitro and in vivo. *International Immunopharmacology*, *132*, 111959. https://doi.org/10.1016/j.intimp.2024.111959

Gouda, S., Das, G., Sen, S. K., Shin, H. S., & Patra, J. K. (2016). Endophytes: A treasure house of bioactive compounds of medicinal importance. *Frontiers in Microbiology*, *7*, 219261. https://doi.org/10.3389/fmicb.2016.01538/bibtex

Gupta, S., Chaturvedi, P., Kulkarni, M. G., & Van Staden, J. (2020). A critical review on exploiting the pharmaceutical potential of plant endophytic fungi. *Biotechnology advances*, *39*, 107462. https://doi.org/10.1016/j.biotechadv.2019.107462

Gupta, Shubhpriya, Chaturvedi, P., Kulkarni, M. G., & Van Staden, J. (2020). A critical review on exploiting the pharmaceutical potential of plant endophytic fungi. *Biotechnology Advances*, *39*, 107462. https://doi.org/10.1016/j.biotechadv.2019.107462

Gurib-Fakim, A. (2006). Medicinal plants: traditions of yesterday and drugs of tomorrow. *Molecular aspects of Medicine*, *27*(1), 1-93. https://doi.org/10.1016/j.mam.2005.07.008

Hai, L. Q., Liang, H., Zhao, Y. Y., & Du, N. S. (2002). Studies on chemical constituents in the root of *Hedysarum polybotrys*. *Zhongguo Zhongyao Zazhi*, *27*(11), 845. https://doi.org/10.4268/cjcmm20111710

Hall, T. (2013). BioEdit, version 7.2. 5. *Ibis Biosciences, Carlsbad, CA, USA*.

Hammouche-Mokrane, N., León-González, A. J., Navarro, I., Boulila, F., & Martín-Cordero, C. (2017). Phytochemical Profile and Antibacterial Activity of *Retama raetam* and *R.*

sphaerocarpa cladodes from Algeria. *NPC Natural Product Communications*, *12*, 1857–1860. https://doi.org/10.1177/1934578x1701201211

Hardoim, P. R., van Overbeek, L. S., Berg, G., Pirttilä, A. M., Compant, S., Campisano, A., Döring, M., & Sessitsch, A. (2015). The Hidden World within Plants: Ecological and Evolutionary Considerations for Defining Functioning of Microbial Endophytes. *Microbiology and Molecular Biology Reviews*, *79*(3), 293–320. https://doi.org/10.1128/mmbr.00050-14

Harvey, A. L. (2008). Natural products in drug discovery. *Drug Discovery Today*, *13*(19–20), 894–901. https://doi.org/10.1016/j.drudis.2008.07.004

Hassanzadeh Rad, B., Hashemi, S. J., Farasatinasab, M., & Atighi, J. (2018). Epidemiological Survey of Human Dermatophytosis due to Zoophilic Species in Tehran, Iran. *Iranian Journal of Public Health*, *47*(12), 1930. /pmc/articles/pmc6379625/

Hatlen, T. J., & Miller, L. G. (2021). Staphylococcal Skin and Soft Tissue Infections. *Infectious Disease Clinics*, *35*(1), 81–105. https://doi.org/10.1016/j.idc.2020.10.003

Hay, R. J., Johns, N. E., Williams, H. C., Bolliger, I. W., Dellavalle, R. P., Margolis, D. J., ... & Naghavi, M. (2014). The global burden of skin disease in 2010: an analysis of the prevalence and impact of skin conditions. *Journal of investigative dermatology*, *134*(6), 1527-1534. https://doi.org/10.1038/jid.2013.446

Hebert, P., & Cywinska, A., Ball, S. L., & DeWaard, J. R. (2003). Biological identifications through DNA barcodes. *Proceedings of the Royal Society of London.*, *270*(1512), 313–321. https://doi.org/10.1098/rspb.2002.2218

Hirasawa, Y., Kato, Y., Wong, C. P., Uchiyama, N., Goda, Y., Hadi, A. H. A., Ali, H. M., & Morita, H. (2014). Hupermine A, a novel C16N2-type Lycopodium alkaloid from *Huperzia phlegmaria*. *Tetrahedron Letters*, *55*(11), 1902–1904. https://doi.org/10.1016/j.tetlet.2014.01.141

Hirasawa, Y., Morita, H., & Kobayashi, J. (2003). Senepodines B–E, new C22N2 alkaloids from *Lycopodium chinense*. *Tetrahedron*, *59*(20), 3567–3573. https://doi.org/10.1016/S0040-4020(03)00545-3

Hiruy, B., & Getu, E. (2018). Efficacy of solvent extracts of *Calpurnia aurea* (Ait.) Benth and *Milletia ferruginea* (Hochest) Baker leaves against maize weevils, Sitophilus zeamais (Motsch.) of stored maize in Ethiopia. *Journal of Stored Products and Postharvest Research*, *9*(3), 27-35. https://doi.org/10.5897/jsppr2018.0259

Hollestein, L. M., & Nijsten, T. (2014). An Insight into the Global Burden of Skin Diseases. *Journal of Investigative Dermatology*, *134*(6), 1499–1501.

https://doi.org/10.1038/jid.2013.513

Houbraken, J., Kocsubé, S., Visagie, C. M., Yilmaz, N., Wang, X. C., Meijer, M., Kraak, B., Hubka, V., Bensch, K., Samson, R. A., & Frisvad, J. C. (2020). Classification of *Aspergillus*, *Penicillium*, *Talaromyces* and related genera (*Eurotiales*): An overview of families, genera, subgenera, sections, series and species. *Studies in Mycology*, *95*, 5–169. https://doi.org/10.1016/j.simyco.2020.05.002

Huang, D., Zhou, X., Si, J., Gong, X., & Wang, S. (2016). Studies on cellulase-ultrasonic assisted extraction technology for flavonoids from *Illicium verum* residues. *Chemistry Central Journal*, *10*(1), 1–9. https://doi.org/10.1186/s13065-016-0202-z

Ibrahim, M., Oyebanji, E., Fowora, M., Aiyeolemi, A., Orabuchi, C., Akinnawo, B., & Adekunle, A. A. (2021). Extracts of endophytic fungi from leaves of selected Nigerian ethnomedicinal plants exhibited antioxidant activity. *BMC Complementary Medicine and Therapies*, *21*(1), 98. https://doi.org/10.1186/s12906-021-03269-3

Indrianingsih, A. W., & Tachibana, S. (2017). α-Glucosidase inhibitor produced by an endophytic fungus, *Xylariaceae* sp. QGS 01 from *Quercus gilva* Blume. *Food Science and Human Wellness*, *6*(2), 88–95. https://doi.org/10.1016/j.fshw.2017.05.001

Ismail Suhaimy, N. W., Noor Azmi, A. K., Mohtarrudin, N., Omar, M. H., Tohid, S. F. M., Cheema, M. S., Teh, L. K., Salleh, M. Z., & Zakaria, Z. A. (2017). Semipurified Ethyl Acetate Partition of Methanolic Extract of *Melastoma malabathricum* Leaves Exerts Gastroprotective Activity Partly via Its Antioxidant-Antisecretory-Anti-Inflammatory Action and Synergistic Action of Several Flavonoid-Based Compounds. *Oxidative Medicine and Cellular Longevity*, 6542631. https://doi.org/10.1155/2017/6542631

Issakou, B.-V., Payang, Y. P., Christophe, D., Alio, H. M., Otchom, B. B., Valéry, M. B., Tidjani, A., Issakou, B.-V., Payang, Y. P., Christophe, D., Alio, H. M., Otchom, B. B., Valéry, M. B., & Tidjani, A. (2022). Antidermatophyte activity of ethanolic extracts of *Daniellia oliveri* (*Fabaceae*) and *Parinari curatellifolia* (*Chrysobalanaceae*) in Chad. *GSC Advanced Research and Reviews*, *13*(2), 170-179. https://doi.org/10.30574/gscarr.2022.13.2.0299

Jabborova, D., Davranov, K., & Egamberdieva, D. (2019). Antibacterial, antifungal, and antiviral properties of medical plants. *Medically Important Plant Biomes: Source of Secondary Metabolites*, 51-65. https://doi.org/10.1007/978-981-13-9566-6_3

Jansen, P. C. M. (1981). Spices, condiments and medicinal plants in Ethiopia, their taxonomy and agricultural significance. *Wageningen University and Research*. https://doi.org/10.18174/201964

Jha, P., Kaur, T., Chhabra, I., Panja, A., Paul, S., Kumar, V., & Malik, T. (2023). Endophytic fungi: hidden treasure chest of antimicrobial metabolites interrelationship of endophytes and metabolites. *Frontiers in Microbiology, 14*. https://doi.org/10.3389/fmicb.2023.1227830

Jordaan, A., Taylor, J. E., & Rossenkhan, R. (2006). Occurrence and possible role of endophytic fungi associated with seed pods of *Colophospermum mopane* (*Fabaceae*) in Botswana. *South African Journal of Botany*, *72*(2), 245-255. https://doi.org/10.1016/j.sajb.2005.09.007

Julien, G. A., Adiyaga, W. C., Saaka, R. A.-E., Sunyazi, S. S., Batuiamu, A. T., Abugri, D., & Abugri, J. (2021). Dermatophytic Diseases: A Review of Tinea Pedis. *medRxiv*, *2021*(6). https://doi.org/10.1101/2021.06.28.21259664

Kalagouda, R., Kabera, B., Muia, C. K., Ale, B. M., & Kalagouda Patil, R. (2022). Hospital acquired infections in a private paediatric hospital in Kenya: a retrospective cross-sectional study. *Pan African Medical Journal*, *41*(1). https://doi.org/10.11604/pamj.2022.41.28.25820

Karimi, A., Majlesi, M., & Rafieian-Kopaei, M. (2015). Herbal versus synthetic drugs; beliefs and facts. *Journal of Nephropharmacology*, *4*(1), 27. http://doi.org/pmc/articles/pmc5297475/

Kaul, S., Gupta, S., Ahmed, M., & Dhar, M. K. (2012). Endophytic fungi from medicinal plants: A treasure hunt for bioactive metabolites. *Phytochemistry Reviews*, *11*(4), 487–505. https://doi.org/10.1007/s11101-012-9260-6

Kaur, V., Kumar, M., Kumar, A., Kaur, K., Dhillon, V. S., & Kaur, S. (2018). Pharmacotherapeutic potential of phytochemicals: Implications in cancer chemoprevention and future perspectives. *Biomedicine & Pharmacotherapy*, *97*, 564–586. https://doi.org/10.1016/j.biopha.2017.10.124

Kaushik, B., Sharma, J., Yadav, K., Kumar, P., & Shourie, A. (2021). Phytochemical Properties and Pharmacological Role of Plants: Secondary Metabolites. *Biosciences biotechnology research asia*, *18*(1), 23–35. https://doi.org/10.13005/bbra/2894

Kelly, K. A., Balogh, E. A., Kaplan, S. G., Feldman, S. R., Kelly, K. A. ;, Balogh, E. A. ;, & Fernández-Bustos, G. (2021). Skin Disease in Children: Effects on Quality of Life, Stigmatization, Bullying, and Suicide Risk in Pediatric Acne, Atopic Dermatitis, and Psoriasis Patients. *Children*, *8*(11), 1057. https://doi.org/10.3390/children8111057

Kenicer, G. (2005). Legumes of the World. *Edinburgh Journal of Botany, 62*((3),), 195-196. https://cir.nii.ac.jp/crid/1130282268638128000

Keshri, P. K., Rai, N., Verma, A., Kamble, S. C., Barik, S., Mishra, P., Singh, S. K., Salvi, P., & Gautam, V. (2021). Biological potential of bioactive metabolites derived from fungal endophytes associated with medicinal plants. *Mycological Progress 20*(5), 577–594. https://doi.org/10.1007/S11557-021-01695-8

Khalil, A. M. A., Hassan, S. E. D., Alsharif, S. M., Eid, A. M., Ewais, E. E. D., Azab, E., Gobouri, A. A., Elkelish, A., & Fouda, A. (2021). Isolation and Characterization of Fungal Endophytes Isolated from Medicinal Plant *Ephedra pachyclada* as Plant Growth-Promoting. *Biomolecules*, *11*(2), 1–18. https://doi.org/10.3390/biom11020140

Khameneh, B., Diab, R., Ghazvini, K., & Fazly Bazzaz, B. S. (2016). Breakthroughs in bacterial resistance mechanisms and the potential ways to combat them. *Microbial Pathogenesis*, *95*, 32–42. https://doi.org/10.1016/j.micpath.2016.02.009

Khan, S., Al-Qurainy, F., Al-hashimi, A., Nadeem, M., Tarroum, M., Gaafar, A. R. Z., Shaikhaldein, H. O., Salih, A. M., & Karuppiah, P. (2024). Molecular phylogeny, phenolics content, and antimicrobial activity of some potential medicinal plant species of the *Fabaceae* family collected from different geographical regions of Saudi Arabia. *Plant Biosystems - An International Journal Dealing with All Aspects of Plant Biology*, *158*(6), 1482–1492. https://doi.org/10.1080/11263504.2024.2424247

Khan, S. S., Hay, R. J., & Saunte, D. M. L. (2022). A Review of Antifungal Susceptibility Testing for Dermatophyte Fungi and It's Correlation with Previous Exposure and Clinical Responses. *Journal of Fungi*, *8*(12), 1290. https://doi.org/10.3390/JOF8121290

Kim, E. Y., & Moudgil, K. D. (2017). Immunomodulation of autoimmune arthritis by pro-inflammatory cytokines. *Cytokine*, *98*, 87–96. https://doi.org/10.1016/j.cyto.2017.04.012

Koekemoer, M., Steyn, H. M., & Bester, S. P. (2013). Guide to plant families of southern Africa. *Guide to Plant Families of Southern Africa.* (pp. iv+-296). https://doi.org/10.1640/0002-8444-103.1.57

Kolařík, M., Vrublevskaya, M., Kajzrová, S., Kulišová, M., & Kolouchová, I. J. (2023). Taxonomic analysis reveals host preference of rare fungi in endophytes of *Vitis vinifera* from the Czech Republic. *Folia Microbiologica*, *68*(6), 961–975. https://doi.org/10.1007/s12223-023-01066-8

Kolarsick, P. A. J., Kolarsick, M. A., & Goodwin, C. (2011). Anatomy and Physiology of the Skin. *Journal of the Dermatology Nurses' Association*, *3*(4), 203–213. https://doi.org/10.1097/jdn.0b013e3182274a98

Korir, E., Kiplimo, J. J., Crouch, N. R., Moodley, N., & Koorbanally, N. A. (2014). Isoflavones from *Calpurnia aurea* subsp. *aurea* and their Anticancer Activity. *African Journal of*

Traditional, Complementary and Alternative Medicines, *11*(5), 33–37. https://doi.org/10.4314/ajtcam.v11I5.5

Korkut, A., Gül, S. Ö., Aydemir, E., Er, H., & Köse, E. O. (2025). Cinnamic Acid Compounds (p-Coumaric, Ferulic, and p-Methoxycinnamic Acid) as Effective Antibacterial Agents Against Colistin-Resistant *Acinetobacter baumannii*. *Antibiotics*, *14*(1), 71. https://doi.org/10.3390/antibiotics14010071

Kubo, I., Matsumoto, T., Kozuka, M., Chapya, A., & Naoki, H. (1984). Quinolizine Alkaloids from the African Medicinal Plant *Calpurnia aurea*: Molluscicidal Activity and Structural Study by 2D-NMR. *Agricultural and Biological Chemistry*, *48*(11), 2839–2841. https://doi.org/10.1271/bbb1961.48.2839

Kubo, I., Matsumoto, T., Kozuka, M., Chapya, A., & Naoki, H. (2014). Agricultural and Biological Chemistry Quinolizine Alkaloids from the African Medicinal Plant Calpurnia aurea: Molluscicidal Activity and Structural Study by 2D-NMR. *Agricultural and biological chemistry*, *48*(11), 2839-2841. https://doi.org/10.1080/00021369.1984.10866598

Kumar, G., Chandra, P., & Choudhary, M. (2017). Endophytic Fungi: A Potential Source of Bioactive Compounds. *Chemical Science Review and Letters*, *6*(24), 2373–2381. https://doi.org/10.1007/978-981-15-9371-0_12

Kumaran, R. S., & Hur, B. K. (2009). Screening of species of the endophytic fungus *Phomopsis* for the production of the anticancer drug taxol. *Biotechnology and Applied Biochemistry*, *54*(1), 21-30. https://doi.org/10.1042/ba20080110

Kumarihamy, M., Ferreira, D., Croom, E. M., Sahu, R., Tekwani, B. L., Duke, S. O., Khan, S., Techen, N., & Dhammika Nanayakkara, N. P. (2019). Antiplasmodial and Cytotoxic Cytochalasins from an Endophytic Fungus, *Nemania* sp. UM10M, Isolated from a Diseased *Torreya taxifolia* Leaf. *Molecules* *24*(4), 777. https://doi.org/10.3390/molecules24040777

Lacap, D. C., Hyde, K. D., & Liew, E. C. Y. (2003). An evaluation of the fungal'morphotype'concept based on ribosomal DNA sequences. *Fungal Diversity*.

Lanisnik Rizner, T., Krenn, L., Goh, B.-H., Teng-Hern Tan, L., Chan, K.-G., Tay, K.-C., Kei Chan, C., Lai Hong, S., Hsum Yap, W., Pusparajah, P., & Lee, L.-H. (2019). Formononetin: A Review of Its Anticancer Potentials and Mechanisms. *Frontiers in Pharmacology*, *10*, 457757. https://doi.org/10.3389/fphar.2019.00820

Lawal, B., Shittu, O. K., Oibiokpa, F. I., Berinyuy, E. B., & Mohammed, H. (2016). African natural products with potential antioxidants and hepatoprotectives properties: a review.

Clinical Phytoscience, *2*(1), 1–66. https://doi.org/10.1186/s40816-016-0037-0

Lee, H. J., Lee, O. K., Kwon, Y. H., Choi, D. H., Kang, H. Y., Lee, H. Y., Paik, K. H., & Lee, H. J. (2006). Isoflavone glycosides from the bark of *Amorpha fruticosa*. *Chemistry of Natural Compounds*, *42*(4), 415–418. https://doi.org/10.1007/s10600-006-0169-4

Lei, W., Xing-De, W., Juan, H., Gen-Tao, L., Li-Yan, P., Yan, L., Liu-Dong, S., & Qin-Shi, Z. (2014). A new quinolizidine alkaloid from *Sophora flavescens*. *Chemistry of Natural Compounds*, *50*(5), 876–879. https://doi.org/10.1007/s10600-014-1104-8

Leistner, O. A. (2000). Seed plants of southern Africa: families and genera. *Seed Plants of Southern Africa: Families and Genera.* (pp. 775-pp). https://doi.org/10.1142/9789814354318_0001

Leroy, C., Rigot, J. M., Leroy, M., Decanter, C., Le Mapihan, K., Parent, A. S., Le Guillou, A. C., Yakoub-Agha, I., Dharancy, S., Noel, C., & Vantyghem, M. C. (2015). Immunosuppressive drugs and fertility. *Orphanet Journal of Rare Diseases*, *10*(1), 1–15. https://doi.org/10.1186/s13023-015-0332-8

Letourneau, A., Seena, S., Marvanová, L., & Bärlocher, F. (2010). Potential use of barcoding to identify aquatic hyphomycetes. *Fungal Diversity*, *40*, 51–64. https://doi.org/10.1007/S13225-009-0006-8

Li, J. C., Zhang, Z. J., Liu, D., Jiang, M. Y., Li, R. T., & Li, H. M. (2022). Quinolizidine alkaloids from the roots of *Sophora flavescens*. *Natural Product Research*, *36*(7), 1781–1788. https://doi.org/10.1080/14786419.2020.1817011

Lin, L. C., Pai, Y. F., & Tsai, T. H. (2015). Isolation of Luteolin and Luteolin-7-*O*-glucoside from *Dendranthema morifolium* Ramat Tzvel and Their Pharmacokinetics in Rats. *Journal of Agricultural and Food Chemistry*, *63*(35), 7700–7706. https://doi.org/10.1021/jf505848z

Lin, R., Kim, H., Hong, J., & Li, Q. J. (2014). Biological evaluation of subglutinol a as a novel immunosuppressive agent for inflammation intervention. *ACS Medicinal Chemistry Letters*, *5*(5),485–490. https://doi.org/10.1021/ml4004809

Lindner, E., Kaiser, I., & Schacht, U. (1976). Hypotensive and antiarrhythmic effects of a new alkaloid, the 13-hydroxylupanine-2-pyrrolcarbonic acid ester, from the Madagascan plant *Cadia ellisiana*. *Arzneimittel-Forschung*, *26*(9), 1651–1657. https://doi.org/10.1016/b978-0-08-021308-8.50911-x

Lipsky, Z. W., Patsy, M., Marques, C. N. H., & German, G. K. (2022). Mechanisms and Implications of Bacterial Invasion across the Human Skin Barrier. *Microbiology Spectrum*, *10*(3). https://doi.org/10.1128/spectrum.02744-21

Liu, J., Nagabhyru, P., & Schardl, C. L. (2017). Epichloë festucae endophytic growth in florets, seeds, and seedlings of perennial ryegrass (*Lolium perenne*). *Mycologia*, *109*(5), 691–700. https://doi.org/10.1080/00275514.2017.1400305

Liu, M. M., Ma, R. H., Ni, Z. J., Thakur, K., Cespedes-Acuña, C. L., Jiang, L., & Wei, Z. J. (2020). Apigenin 7-*O*-glucoside promotes cell apoptosis through the PTEN/PI3K/AKT pathway and inhibits cell migration in cervical cancer HeLa cells. *Food and Chemical Toxicology*, *146*, 111843. https://doi.org/10.1016/j.fct.2020.111843

Liu, S. S., Jiang, J. X., Huang, R., Wang, Y. T., Jiang, B. G., Zheng, K. X., & Wu, S. H. (2019). A new antiviral 14-nordrimane sesquiterpenoid from an endophytic fungus *Phoma* sp. *Phytochemistry Letters*, *29*, 75–78. https://doi.org/10.1016/j.phytol.2018.11.005

Liu, Y., Xu, Y., Ji, W., Li, X., Sun, B., Gao, Q., & Su, C. (2014). Anti-tumor activities of matrine and oxymatrine: Literature review. *Tumor Biology*, *35*(6), 5111–5119. https://doi.org/10.1007/s13277-014-1680

Lloyd, D. H., & Patel, A. (2012). Structure and function of the skin. *BSAVA Manual of Canine and Feline Dermatology*, 1–11. https://doi.org/10.22233/9781905319886.1

Louis, S., Delobel, B., Gressent, F., Duport, G., Diol, O., Rahioui, I., Charles, H., & Rahbé, Y. (2007). Broad screening of the legume family for variability in seed insecticidal activities and for the occurrence of the A1b-like knottin peptide entomotoxins. *Phytochemistry*, *68*(4), 521–535. https://doi.org/10.1016/j.phytochem.2006.11.032

Ludwig-Müller, J. (2015). Plants and endophytes: equal partners in secondary metabolite production? *Biotechnology Letters*, *37*(7), 1325–1334. https://doi.org/10.1007/s10529-015-1814-4

Ma, L., Zhang, M., Zhao, R., Wang, D., Ma, Y., & Ai, L. (2021). Plant Natural Products: Promising Resources for Cancer Chemoprevention. *Molecules*, *26*(4), 933. https://doi.org/10.3390/molecules26040933

Maciá-Vicente, J. G., Jansson, H. B., Mendgen, K., & Lopez-Llorca, L. V. (2008). Colonization of barley roots by endophytic fungi and their reduction of take-all caused by *Gaeumannomyces graminis* var. *tritici*. *Canadian Journal of Microbiology*, *54*(8), 600–609. https://doi.org/10.1139/w08-047

Mahé, A., Faye, O., Thiam N'Diaye, H., Ly, F., Konaré, H., Kéita, S., Traoré, A. K., & Hay, R. (2005). Definition of an algorithm for the management of common skin diseases at primary health care level in sub-Saharan Africa. *Transactions of the Royal Society of Tropical Medicine and Hygiene*, *99*(1), 39–47. https://doi.org/10.1016/j.trstmh.2004.03.008/2/m_99-1-39

Maina, E. K., Kiiyukia, C., Wamae, C. N., Waiyaki, P. G., & Kariuki, S. (2013). Characterization of methicillin-resistant *Staphylococcus aureus* from skin and soft tissue infections in patients in Nairobi, Kenya. *International Journal of Infectious Diseases*, *17*(2), e115–e119. https://doi.org/10.1016/j.ijid.2012.09.006

Maina, M., Mwaniki, P., Odira, E., Kiko, N., McKnight, J., Schultsz, C., English, M., & Tosas-Auguet, O. (2020). Antibiotic use in Kenyan public hospitals: Prevalence, appropriateness and link to guideline availability. *International Journal of Infectious Diseases*, *99*, 10–18. https://doi.org/10.1016/j.ijid.2020.07.084

Malik, A., Butt, T. A., Naqvi, S. T. A., Yousaf, S., Qureshi, M. K., Zafar, M. I., ... & Iqbal, M. (2020). Lead tolerant endophyte Trametes hirsuta improved the growth and lead accumulation in the vegetative parts of *Triticum aestivum* L. *Heliyon*, *6*(7). https://doi.org/10.1016/j.heliyon.2020.e04188

Mans, D. R., Friperson, P., Pawirodihardjo, J., & Djotaroeno, M. (2022). Phenolic compounds and antioxidant activities of eight species of *fabaceae* that are commonly used in traditional medical practices in the republic of Suriname. *Medicinal Plants*. IntechOpen. https://doi.org/10.5772/intechopen.106076

Marderosian, D. A., & Beutler, J. A. (2002). The review of natural products: the most complete source of natural product information. *No*. 3, (xii+-869).

Maroyi, A. (2017). Diversity of use and local knowledge of wild and cultivated plants in the Eastern Cape province, South Africa. *Journal of Ethnobiology and Ethnomedicine*, *13*(1). https://doi.org/10.1186/s13002-017-0173-8

Maroyi, A. (2023). Medicinal Uses of the *Fabaceae* Family in Zimbabwe: A Review. *Plants 2023*, *12*(6), 1255. https://doi.org/10.3390/plants12061255

Martínez-Sotres, C., López-Albarrán, P., Cruz-de-León, J., García-Moreno, T., Rutiaga-Quiñones, J. G., Vázquez-Marrufo, G., Tamariz-Mascarúa, J., & Herrera-Bucio, R. (2012). Medicarpin, an antifungal compound identified in hexane extract of *Dalbergia congestiflora* Pittier heartwood. *International Biodeterioration & Biodegradation*, *69*, 38–40. https://doi.org/10.1016/j.ibiod.2011.11.016

Mayerhofer, M. S., Kernaghan, G., & Harper, K. A. (2013). The effects of fungal root endophytes on plant growth: A meta-analysis. *Mycorrhiza*, *23*(2), 119–128. https://doi.org/10.1007/s00572-012-0456-9

McGuire, S. (2016). World Cancer Report 2014. Geneva, Switzerland: World Health Organization, International Agency for Research on Cancer, WHO Press, 2015. *Advances in Nutrition*, *7*(2), 418. https://doi.org/10.3945/an.116.012211

Govindappa, M. (2015). A review on role of plant (s) extracts and its phytochemicals for the management of diabetes. *Journal of Diabetes Metabolism*, *6*(7), 1-38. https://doi.org/10.4172/2155-6156.1000565

Mengistu, A. A. (2020). Endophytes: colonization, behaviour, and their role in defense mechanism. *International Journal of Microbiology*, *2020*(1), 6927219. https://doi.org/10.1155/2020/6927219

Miller, L. G., Eisenberg, D. F., Liu, H., Chang, C. L., Wang, Y., Luthra, R., Wallace, A., Fang, C., Singer, J., & Suaya, J. A. (2015). Incidence of skin and soft tissue infections in ambulatory and inpatient settings, 2005-2010. *BMC Infectious Diseases*, *15*(1), 1–8. https://doi.org/10.1186/s12879-015-1071-0

Mingoia, M., Conte, C., Di Rienzo, A., Dimmito, M. P., Marinucci, L., Magi, G., Turkez, H., Cufaro, M. C., Del Boccio, P., Di Stefano, A., & Cacciatore, I. (2022). Synthesis and Biological Evaluation of Novel Cinnamic Acid-Based Antimicrobials. *Pharmaceuticals*, *15*(2), 228. https://doi.org/10.3390/ph15020228/S1

Mirhendi, H., Makimura, K., De Hoog, G. S., Rezaei-Matehkolaei, A., Najafzadeh, M. J., Umeda, Y., & Ahmadi, B. (2015). Translation elongation factor 1-α gene as a potential taxonomic and identification marker in dermatophytes. *Medical Mycology*, *53*(3), 215–224. https://doi.org/10.1093/mmy/myu088

Mizuguchi, H., Nariai, Y., Kato, S., Nakano, T., Kanayama, T., Kashiwada, Y., Nemoto, H., Kawazoe, K., Takaishi, Y., Kitamura, Y., Takeda, N., & Fukui, H. (2015). Maackiain is a novel antiallergic compound that suppresses transcriptional upregulation of the histamine H1 receptor and interleukin-4 genes. *Pharmacology Research & Perspectives*, *3*(5), e00166. https://doi.org/10.1002/prp2.166

Mizuno, M., Tanaka, T., Katsuragawa, M., Saito, H., & Iinuma, M. (1990). A new pterocarpan from the heartwood of *cladrastis platycarpa*. *Journal of Natural Products*, *53*(2), 498–499. https://doi.org/10.1021/np50068a037

Molares, S., & Ladio, A. (2012). The usefulness of edible and medicinal *Fabaceae* in Argentine and Chilean Patagonia: environmental availability and other sources of supply. *Evidence-Based Complementary and Alternative Medicine*, *2012*(1), 901918. https://doi.org/10.1155/2012/901918

Monod, M. (2008). Secreted proteases from dermatophytes. *Mycopathologia*, *166*(5–6), 285–294. https://doi.org/10.1007/s11046-008-9105-4

Monteiro-Riviere, N. A. (2010). Structure and function of skin. *Toxicology of the Skin* (pp. 15-32). CRC Press. https://doi.org/10.1201/9780203020821.ch1

Morales-Alvarez, M. C. (2020). Nephrotoxicity of Antimicrobials and Antibiotics. *Advances in Chronic Kidney Disease*, *27*(1), 31–37. https://doi.org/10.1053/j.ackd.2019.08.001

Morante-Carriel, J., Nájera, H., Samper-Herrero, A., Živković, S., Martínez-Esteso, M. J., Martínez-Márquez, A., Sellés-Marchart, S., Obrebska, A., & Bru-Martínez, R. (2024). Therapeutic Potential of Prenylated Flavonoids of the *Fabaceae* Family in Medicinal Chemistry: An Updated Review. *International Journal of Molecular Sciences*, *25*(23), 13036. https://doi.org/10.3390/ijms252313036

Morgan, D. J., Okeke, I. N., Laxminarayan, R., Perencevich, E. N., & Weisenberg, S. (2011). Non-prescription antimicrobial use worldwide: a systematic review. *The Lancet Infectious Diseases*, *11*(9), 692–701. https://doi.org/10.1016/s1473-3099(11)70054-8

Moto, J. N., Maingi, J. M., & Nyamache, A. K. (2015). Prevalence of Tinea capitis in school going children from Mathare, informal settlement in Nairobi, Kenya. *BMC Research Notes*, *8*(1), 1–4. https://doi.org/10.1186/s13104-015-1240-7

Motyka, S., Jafernik, K., Ekiert, H., Sharifi-Rad, J., Calina, D., Al-Omari, B., Szopa, A., & Cho, W. C. (2023). Podophyllotoxin and its derivatives: Potential anticancer agents of natural origin in cancer chemotherapy. *Biomedicine & Pharmacotherapy*, *158*, 114145. https://doi.org/10.1016/j.biopha.2022.114145

Mousa, W. K., & Raizada, M. N. (2013). The diversity of anti-microbial secondary metabolites produced by fungal endophytes: an interdisciplinary perspective. *Frontiers in Microbiology*, *4*, 44840. https://doi.org/10.3389/fmicb.2013.00065

Mulata, H., Gnanasekaran, N., Melaku, U., & Daniel, S. (2015). Effect of *Calpurnia aurea* Seed Extract on HAART Induced Haematotoxicity in Albino Wistar Rats. *International Blood Research & Reviews*, *3*(2), 66–75. https://doi.org/10.9734/ibrr/2015/15888

Mulatu, G. (2020). Antibacterial activities of Calpurnia aurea against selected animal pathogenic bacterial strains. *Advances in Pharmacological and Pharmaceutical Sciences*, *2020*(1), 8840468. https://doi.org/10.1155/2020/8840468

Murphy, B. R., Doohan, F. M., & Hodkinson, T. R. (2014). Yield increase induced by the fungal root endophyte *Piriformospora indica* in barley grown at low temperature is nutrient limited. *Symbiosis*, *62*(1), 29–39. https://doi.org/10.1007/s13199-014-0268-0

Mussin, J., Robles-Botero, V., Casañas-Pimentel, R., Rojas, F., Angiolella, L., San Martín-Martínez, E., & Giusiano, G. (2021). Antimicrobial and cytotoxic activity of green synthesis silver nanoparticles targeting skin and soft tissue infectious agents. *Scientific Reports*, *11*(1), 1–12. https://doi.org/10.1038/s41598-021-94012-y

Mutisya, E., & Yarime, M. (2011). Understanding the Grassroots Dynamics of Slums in

Nairobi: The Dilemma of Kibera Informal Settlements. *International Transaction Journal of Engineering*, *2*(2). http://tuengr.com/v02/197-213

Nakamura, M., Ra, J. H., Jee, Y., & Kim, J. S. (2017). Impact of different partitioned solvents on chemical composition and bioavailability of Sasa quelpaertensis Nakai leaf extract. *Journal of Food and Drug Analysis*, *25*(2), 316–326. https://doi.org/10.1016/j.jfda.2016.08.006

Nakanishi, T., Inada, A., Kambayashi, K., & Yoneda, K. (1985). Flavonoid glycosides of the roots of *Glycyrrhiza uralensis*. *Phytochemistry*, *24*(2), 339–341. https://doi.org/10.1016/S0031-9422(00)83548-7

Nalin Rathnayake, G. R., Savitri Kumar, N., Jayasinghe, L., Araya, H., & Fujimoto, Y. (2019). Secondary Metabolites Produced by an Endophytic Fungus *Pestalotiopsis microspora*. *Natural Products and Bioprospecting*, *9*(6), 411–417. https://doi.org/10.1007/S13659-019-00225-0

Nalini, M. S., & Prakash, H. S. (2017). Diversity and bioprospecting of actinomycete endophytes from the medicinal plants. *Letters in Applied Microbiology*, *64*(4), 261–270. https://doi.org/10.1111/lam.12718

Nana, P. (2010). Potential of Integrating Calpurnia aurea with Entomopathogenic Fungus Metarhizium anisopliae for the Control of *Rhipicephalus appendiculatus* and *Rhipicephalus pulchellus* (Doctoral dissertation, Jomo Kenyatta University of Agriculture and Technology). http://localhost:8080/xmlui/handle/123456789/243

Navarrete-Carriola, D. V., Paz-González, A. D., Vázquez-Jiménez, L. K., De Luna-Santillana, E., Cruz-Hernández, M. A., Bandyopadhyay, D., & Rivera, G. (2024). Comparative Analysis of a Secondary Metabolite Profile from Roots and Leaves of *Iostephane heterophylla* by UPLC-MS and GC-MS. *ACS Omega*, *9*(5), 5429–5439. https://doi.org/10.1021/acsomega.3c06800

Newman, D. J., & Cragg, G. M. (2007). Natural products as sources of new drugs over the last 25 years. *Journal of Natural Products*, *70*(3), 461–477. https://doi.org/10.1021/NP068054V

Newman, D. J., & Cragg, G. M. (2016). Natural Products as Sources of New Drugs from 1981 to 2014. *Journal of Natural Products*, *79*(3), 629–661. https://doi.org/10.1021/acs.jnatprod.5B01055

Nilsson, R. H., Ryberg, M., Abarenkov, K., Sjökvist, E., & & Kristiansson, E. (2009). The ITS region as a target for characterization of fungal communities using emerging sequencing technologies. *FEMS Microbiology Letters*, *296*(1), 97–101.

https://doi.org/10.1111/j.1574-6968.2009.01618.x

Nolasco-Quintana, N. Y., González-Maya, L., Razo-Hernández, R. S., & Alvarez, L. (2023). Exploring the Gallic and Cinnamic Acids Chimeric Derivatives as Anticancer Agents over HeLa Cell Line: An *in silico* and *in vitro* Study. *Molecular Informatics*, *42*(1), 2200016. https://doi.org/10.1002/minf.202200016

Nonyelum, C., Aritetsoma, H., & Author, C. (2015). Blood glucose lowering activity of five Nigerian medicinal plants in alloxan-induced diabetic wistar albino rats. *Animal Research International*, *12*(2), 2150–2158. https://www.ajol.info/index.php/ari/article/view/130559

Obistioiu, D., Cocan, I., Tîrziu, E., Herman, V., Negrea, M., Cucerzan, A., Neacsu, A. G., Cozma, A. L., Nichita, I., Hulea, A., Radulov, I., & Alexa, E. (2021). Phytochemical profile and microbiological activity of some plants belonging to the *fabaceae* family. *Antibiotics*, *10*(6), 662. https://doi.org/10.3390/antibiotics10060662/S1

Oguzkaya Artan, M., Koc, A. N., Baykan, Z., & Buldu, H. (2013). Prevalence of tinea capitis in primary school children. *International Journal of Medical Investigation*, *2*(2), 0–0. http://intjmi.com/article-1-35-en.html

Pan, Q. M., Zhang, G. J., Huang, R. Z., Pan, Y. M., Wang, H. S., & Liang, D. (2016). Cytisine-type alkaloids and flavonoids from the rhizomes of *Sophora tonkinensis*. *Journal of Asian Natural Products Research*, *18*(5), 429–435. https://doi.org/10.1080/10286020.2015.1131680

Parasuraman, P., Busi, S., & Lee, J.-K. (2024). Standard Microbiological Techniques (Staining, Morphological and Cultural Characteristics, Biochemical Properties, and Serotyping) in the Detection of ESKAPE Pathogens. *ESKAPE Pathogens*, 119–155. https://doi.org/10.1007/978-981-99-8799-3_4

Parthasarathi, S., Sathya, S., Bupesh, G., Samy, R. D., Mohan, M. R., Kumar, G. S., ... & Balakrishnan, K. (2012). Isolation and characterization of antimicrobial compound from marine *Streptomyces hygroscopicus* BDUS 49. *World J Fish Mar Sci*, *4*(3), 268-277. https://doi.org/10.5829/idosi.wjfms.2012.04.03.5658

Patil, R. H., Patil, M. P., & Maheshwari, V. L. (2016). Bioactive Secondary Metabolites From Endophytic Fungi: A Review of Biotechnological Production and Their Potential Applications. *Natural Products Chemistry*, *49*, 189–205. https://doi.org/10.1016/b978-0-444-63601-0.00005-3

Peterson, C. T., Sharma, V., Uchitel, S., Denniston, K., Chopra, D., Mills, P. J., & Peterson, S. N. (2018). Prebiotic potential of herbal medicines used in digestive health and disease.

Journal of Alternative and Complementary Medicine, *24*(7), 656–665. https://doi.org/10.1089/acm.2017.0422

Pinar, O., & Rodríguez-Couto, S. (2024). Biologically active secondary metabolites from white-rot fungi. *Frontiers in Chemistry*, *12*, 1363354. https://doi.org/10.3389/fchem.2024.1363354

Pinruan, U., Rungjindamai, N., Choeyklin, R., Lumyong, S., Hyde, K. D., & Jones, E. B. G. (2010). Occurrence and diversity of basidiomycetous endophytes from the oil palm, Elaeis guineensis in Thailand. *Fungal Diversity*, *41*, 71–88. https://doi.org/10.1007/s13225-010-0029-1

Porter, T. M., & Golding, G. B. (2012). Factors That Affect Large Subunit Ribosomal DNA Amplicon Sequencing Studies of Fungal Communities: Classification Method, Primer Choice, and Error. *PLoS ONE*, *7*(4), 35749. https://doi.org/10.1371/journal.pone.0035749

Potshangbam, M., Indira Devi, S., Sahoo, D., & Strobel, G. A. (2017). Functional characterization of endophytic fungal community associated with *Oryza sativa* L. and *Zea mays* L. *Frontiers in Microbiology*, *8*, 325. https://doi.org/10.3389/fmicb.2017.00325

Poulakou, G., Lagou, S., & Tsiodras, S. (2019). What's new in the epidemiology of skin and soft tissue infections in 2018? *Current Opinion in Infectious Diseases*, *32*(2), 77–86. https://doi.org/10.1097/qco.0000000000000527

Pouny, I., Long, C., Batut, M., Aussagues, Y., Jean Valère, N., Achoundong, G., David, B., Lavaud, C., & Massiot, G. (2021). Quinolizidine Alkaloids from *Cylicomorpha solmsii*. *Journal of Natural Products*, *84*(4), 1198–1202. https://doi.org/10.1021/acs.jnatprod.0c01261

Prestinaci, F., Pezzotti, P., & Pantosti, A. (2015). Antimicrobial resistance: A global multifaceted phenomenon. *Pathogens and Global Health*, *109*(7), 309–318. https://doi.org/10.1179/2047773215y.0000000030

Puri, A., Padda, K. P., & Chanway, C. P. (2016). Evidence of nitrogen fixation and growth promotion in canola (Brassica napus L.) by an endophytic diazotroph *Paenibacillus polymyxa* P2b-2R. *Biology and Fertility of Soils*, *52*(1), 119–125. https://doi.org/10.1007/s00374-015-1051-y

Puri, S. C., Nazir, A., Chawla, R., Arora, R., Riyaz-Ul-Hasan, S., Amna, T., Ahmed, B., Verma, V., Singh, S., Sagar, R., Sharma, A., Kumar, R., Sharma, R. K., & Qazi, G. N. (2006). The endophytic fungus *Trametes hirsuta* as a novel alternative source of podophyllotoxin and related aryl tetralin lignans. *Journal of Biotechnology*, *122*(4), 494–510. https://doi.org/10.1016/j.jbiotec.2005.10.015

Raekiansyah, M., Mori, M., Nonaka, K., Agoh, M., Shiomi, K., Matsumoto, A., & Morita, K. (2017). Identification of novel antiviral of fungus-derived brefeldin A against dengue viruses. *Tropical Medicine and Health*, *45*(1), 1–7. https://doi.org/10.1186/s41182-017-0072-7

Rai, N., Kumari Keshri, P., Verma, A., Kamble, S. C., Mishra, P., Barik, S., Kumar Singh, S., & Gautam, V. (2021). Plant associated fungal endophytes as a source of natural bioactive compounds. *Mycology*, *12*(3), 139–159. https://doi.org/10.1080/21501203.2020.1870579

Rajendra Prasad, N., Anandi, C., Balasubramanian, S., & Pugalendi, K. V. (2004). Antidermatophytic activity of extracts from *Psoralea corylifolia* (*Fabaceae*) correlated with the presence of a flavonoid compound. *Journal of Ethnopharmacology*, *91*(1), 21–24. https://doi.org/10.1016/j.jep.2003.11.010

Rajivgandhi, G. N., Vimala, R. T. V., Ramachandran, G., Kanisha, C. C., Manoharan, N., & Li, W. J. (2022). An overview on natural product from endophytic actinomycetes. *Natural Products from Actinomycetes: Diversity, Ecology and Drug Discovery*, 151–165. https://doi.org/10.1007/978-981-16-6132-7_6

Ramos-e-Silva, M., Lima, C. M. O., Schechtman, R. C., Trope, B. M., & Carneiro, S. (2010). Superficial mycoses in immunodepressed patients (AIDS). *Clinics in Dermatology*, *28*(2), 217–225. https://doi.org/10.1016/j.clindermatol.2009.12.008

Raub, M. F., Cardellina, J. H., Choudhary, M. I., Ni, C. Z., Clardy, J., & Alley, M. C. (1991). Clavepictines A and B: Cytotoxic Quinolizidines from the *Tunicate Clavelina* Picta. *Journal of the American Chemical Society*, *113*(8), 3178–3180. https://doi.org/10.1021/ja00008A060

Refaat, J., Yehia, S. Y., Kamel, M. S., Ramadan, A., Desoukey, S. Y., & Ramadan, M. A. (2015). Rhoifolin: a review of sources and biological activities. *International Journal of Pharmacognosy*, *2*(3), 102–109. https://doi.org/10.13040/ijpsr.0975-8232.ijp.2(3).102-09

Rong, Z. J., Gao, X. X., Hu, G. S., Yan, T., Jia, J. M., & Wang, A. H. (2022). A novel alkaloid from the seeds of *Sophora alopecuroides* L. *Natural Product Research*, *36*(7), 1864–1869. https://doi.org/10.1080/14786419.2020.1824226

Roy, S., & Banerjee, D. (2018). Diversity of endophytes in tropical forests. *Endophytes of forest trees: biology and applications* (pp. 43-62). https://doi.org/10.1007/978-3-319-89833-9_3.

Ruchti, F., & LeibundGut-Landmann, S. (2023). New insights into immunity to skin fungi shape our understanding of health and disease. *Parasite Immunology*, *45*(2), e12948. https://doi.org/10.1111/pim.12948

Rungjindamai, N., & Jones, E. B. G. (2024). Why Are There So Few Basidiomycota and Basal Fungi as Endophytes? A Review. *Journal of Fungi*, *10*(1), 67. https://doi.org/10.3390/jof10010067

Sagar, S., Kaistha, S., Das, A. J. J., & Kumar, R. (2019). Antibiotic resistant bacteria: A challenge to modern medicine. *Antibiotic Resistant Bacteria: A Challenge to Modern Medicine*, 1–179. https://doi.org/10.1007/978-981-13-9879-7

Sanders, K., Moran, Z., Shi, Z., Paul, R., & Greenlee, H. (2016). Natural Products for Cancer Prevention: Clinical Update 2016. *Seminars in Oncology Nursing*, *32*(3), 215–240. https://doi.org/10.1016/j.soncn.2016.06.001

Santamaría, J., & Bayman, P. (2005). Fungal epiphytes and endophytes of coffee leaves (*Coffea arabica*). *Microbial ecology*, *50*(1), 1-8. https://doi.org/10.1007/s00248-004-0002-1

Santos, J. M., Vrandečić, K., Ćosić, J., Duvnjak, T., & Phillips, A. J. L. (2011). Resolving the Diaporthe species occurring on soybean in Croatia. *Persoonia-Molecular Phylogeny and Evolution of Fungi*, *27*(1), 9-19. https://doi.org/10.3767/003158511x603719

Santoyo, G., Moreno-Hagelsieb, G., del Carmen Orozco-Mosqueda, M., & Glick, B. R. (2016). Plant growth-promoting bacterial endophytes. *Microbiological Research*, *183*, 92–99. https://doi.org/10.1016/j.micres.2015.11.008

Sardana, K., Gupta, A., Sadhasivam, S., Gautam, R. K., Khurana, A., Saini, S., Gupta, S., & Ghosh, S. (2021). Checkerboard Analysis To Evaluate Synergistic Combinations of Existing Antifungal Drugs and Propylene Glycol Monocaprylate in Isolates from Recalcitrant Tinea Corporis and Cruris Patients Harboring Squalene Epoxidase Gene Mutation. *Antimicrobial Agents and Chemotherapy*, *65*(8). https://doi.org/10.1128/aac.00321-21

Sasidharan, S., Chen, Y., Saravanan, D., Sundram, K. M., & Latha, L. Y. (2011). Extraction, isolation and characterization of bioactive compounds from plants' extracts. *African journal of traditional, complementary and alternative medicines*, *8*(1). https://www.ajol.info/index.php/ajtcam/article/view/60483

Schneider, P., Misiek, M., & Hoffmeister, D. (2008). In vivo and in vitro production options for fungal secondary metabolites. *Molecular Pharmaceutics*, *5*(2), 234-242. https://doi.org/10.1021/mp7001544

Schulz, B., & Boyle, C. (2007). What are Endophytes? *Microbial Root Endophytes*, 1–13. https://doi.org/10.1007/3-540-33526-9_1

Sebastianes, F. L. S., Lacava, P. T., Fávaro, L. C. L., Rodrigues, M. B. C., Araújo, W. L., Azevedo, J. L., & Pizzirani-Kleiner, A. A. (2012). Genetic transformation of Diaporthe

phaseolorum, an endophytic fungus found in mangrove forests, mediated by Agrobacterium tumefaciens. *Current Genetics*, *58*(1), 21–33. https://doi.org/10.1007/S00294-011-0362-2

Seger, C., & Sturm, S. (2007). Analytical aspects of plant metabolite profiling platforms: Current standings and future aims. *Journal of Proteome Research*, *6*(2), 480–497. https://doi.org/10.1021/pr0604716

Semenya, S. S., & Maroyi, A. (2018). Ethnomedicinal Uses of Fabaceae Species for Respiratory Infections and Related Symptoms in the Limpopo Province, South Africa. *Journal of Pharmacy and Nutrition Sciences*, *8*(4), 219–229. https://doi.org/10.29169/1927-5951.2018.08.04.10

Sen, T., & Samanta, S. K. (2014). Medicinal plants, human health and biodiversity: A broad review. *Advances in Biochemical Engineering/Biotechnology*, *147*, 59–110. https://doi.org/10.1007/10_2014_273

Shahabudin, S., Azmi, N. S., Lani, M. N., Mukhtar, M., & Hossain, M. S. (2024). *Candida albicans* skin infection in diabetic patients: An updated review of pathogenesis and management. *Mycoses*, *67*(6), e13753. https://doi.org/10.1111/myc.13753

Shamsudin, N. F., Ahmed, Q. U., Mahmood, S., Shah, S. A. A., Khatib, A., Mukhtar, S., Alsharif, M. A., Parveen, H., & Zakaria, Z. A. (2022). Antibacterial Effects of Flavonoids and Their Structure-Activity Relationship Study: A Comparative Interpretation. *Molecules*, *27*(4), 1149. https://doi.org/10.3390/molecules27041149

Shankarnarayan, S. A., Shaw, D., Sharma, A., Chakrabarti, A., Dogra, S., Kumaran, M. S., Kaur, H., Ghosh, A., & Rudramurthy, S. M. (2020). Rapid detection of terbinafine resistance in Trichophyton species by Amplified refractory mutation system-polymerase chain reaction. *Scientific Reports*, *10*(1), 1–6. https://doi.org/10.1038/s41598-020-58187-0

Shapiro, C. L. (2016). Highlights of Recent Findings on Quality-of-Life Management for Patients With Cancer and Their Survivors. *JAMA Oncology*, *2*(11), 1401–1402. https://doi.org/10.1001/jamaoncol.2016.3620

Sharma, A., Flores-Vallejo, R. del C., Cardoso-Taketa, A., & Villarreal, M. L. (2017). Antibacterial activities of medicinal plants used in Mexican traditional medicine. *Journal of Ethnopharmacology*, *208*, 264–329. https://doi.org/10.1016/J.JEP.2016.04.045

Sharma, D., Pramanik, A., & Agrawal, P. K. (2016). Evaluation of bioactive secondary metabolites from endophytic fungus Pestalotiopsis neglecta BAB-5510 isolated from leaves of *Cupressus torulosa* D. Don. *3 Biotech*, *6*(2), 210.

https://doi.org/10.1007/s13205-016-0518-3

Shipunov, A., Newcombe, G., Raghavendra, A. K. H., & Anderson, C. L. (2008). Hidden diversity of endophytic fungi in an invasive plant. *American Journal of Botany*, *95*(9), 1096–1108. https://doi.org/10.3732/ajb.0800024

Shrestha, P., Cooper, B. S., Coast, J., Oppong, R., Do Thi Thuy, N., Phodha, T., Celhay, O., Guerin, P. J., Wertheim, H., & Lubell, Y. (2018). Enumerating the economic cost of antimicrobial resistance per antibiotic consumed to inform the evaluation of interventions affecting their use. *Antimicrobial Resistance and Infection Control*, *7*(1). https://doi.org/10.1186/s13756-018-0384-3

Shukla, S., & Mehta, A. (2015). Anticancer potential of medicinal plants and their phytochemicals: a review. *Revista Brasileira de Botanica*, *38*(2), 199–210. https://doi.org/10.1007/s40415-015-0135-0

Sichaem, J., Ruksilp, T., Sawasdee, P., Khumkratok, S., & Tip-pyang, S. (2018). Chemical Constituents of the Stems of Spatholobus parviflorus and Their Cholinesterase Inhibitory Activity. *Chemistry of Natural Compounds*, *54*(2), 356–357. https://doi.org/10.1007/s10600-018-2344-9

Singh, B., & Kaur, A. (2016). Antidiabetic potential of a peptide isolated from an endophytic Aspergillus awamori. *Journal of Applied Microbiology*, *120*(2), 301–311. https://doi.org/10.1111/jam.12998

Singh, V. K., & Kumar, A. (2023). Secondary metabolites from endophytic fungi: Production, methods of analysis, and diverse pharmaceutical potential. *Symbiosis (Philadelphia, Pa.)*, *90*(2), 1. https://doi.org/10.1007/s13199-023-00925-9

Şirin, N., Elmas, L., Seçme, M., & Dodurga, Y. (2020). Investigation of possible effects of apigenin, sorafenib and combined applications on apoptosis and cell cycle in hepatocellular cancer cells. *Gene*, *737*, 144428. https://doi.org/10.1016/j.gene.2020.144428

Slika, H., Mansour, H., Wehbe, N., Nasser, S. A., Iratni, R., Nasrallah, G., Shaito, A., Ghaddar, T., Kobeissy, F., & Eid, A. H. (2022). Therapeutic potential of flavonoids in cancer: ROS-mediated mechanisms. *Biomedicine & Pharmacotherapy*, *146*, 112442. https://doi.org/10.1016/j.biopha.2021.112442

Smith, R. M. (2003). Before the injection - Modern methods of sample preparation for separation techniques. *Journal of Chromatography A*, *1000* (1–2), 3–27. https://doi.org/10.1016/s0021-9673(03)00511-9

Soares-Bezerra, R. J., Calheiros, A. S., da Silva Ferreira, N. C., da Silva Frutuoso, V., & Alves,

L. A. (2013). Natural products as a source for new anti-inflammatory and analgesic compounds through the inhibition of purinergic P2X receptors. *Pharmaceuticals*, *6*(5), 650-658. https://doi.org/10.3390/ph6050650

Sobel, J. D. (2007). Vulvovaginal candidosis. *The Lancet*, *369*(9577), 1961–1971. https://doi.org/10.1016/s0140-6736(07)60917-9

Son, S. R., Yoon, Y. S., Hong, J. P., Kim, J. M., Lee, K. T., & Jang, D. S. (2022). Chemical Constituents of the Roots of *Polygala tenuifolia* and Their Anti-Inflammatory Effects. *Plants*, *11*(23), 3307. https://doi.org/10.3390/plants11233307/s1

Song, X., Tu, R., Mei, X., Wu, S., Lan, B., Zhang, L., Luo, X., Liu, J., & Luo, M. (2020). A mycophenolic acid derivative from the fungus Penicillium sp. SCSIO sof101. *Natural Product Research*, *34*(9), 1206–1212. https://doi.org/10.1080/14786419.2018.1553881

Sprent, J. I. (2008). 60Ma of legume nodulation. What's new? What's changing? *Journal of Experimental Botany*, *59*(5), 1081–1084. https://doi.org/10.1093/jxb/erm286

Sprent, J. I., Ardley, J., & James, E. K. (2017). Biogeography of nodulated legumes and their nitrogen-fixing symbionts. *New Phytologist*, *215*(1), 40–56. https://doi.org/10.1111/nph.14474

Srinivasan, R., Prabhu, G., Prasad, M., Mishra, M., Chaudhary, M., & Srivastava, R. (2020). Penicillium. *Beneficial Microbes in Agro-Ecology: Bacteria and Fungi*, 651–667. https://doi.org/10.1016/b978-0-12-823414-3.00032-0

Stępniewska, Z., & Kuåniar, A. (2013). Endophytic microorganisms - Promising applications in bioremediation of greenhouse gases. *Applied Microbiology and Biotechnology*, *97*(22), 9589–9596. https://doi.org/10.1007/s00253-013-5235-9/figures/3

Stevens, D. L., Bisno, A. L., Chambers, H. F., Dellinger, E. P., Goldstein, E. J. C., Gorbach, S. L., Hirschmann, J. V., Kaplan, S. L., Montoya, J. G., & Wade, J. C. (2014). Practice Guidelines for the Diagnosis and Management of Skin and Soft Tissue Infections: 2014 Update by the Infectious Diseases Society of America. *Clinical Infectious Diseases*, *59*(2), e10–e52. https://doi.org/10.1093/cid/ciu296

Stierle, A., Strobel, G., & Stierle, D. (1993). Taxol and Taxane Production by Taxomyces andreanae, an Endophytic Fungus of Pacific Yew. *Science*, *260*(5105), 214–216. https://doi.org/10.1126/science.8097061

Strobel, G. (2018). The Emergence of Endophytic Microbes and Their Biological Promise. *Journal of Fungi*, *4*(2), 57. https://doi.org/10.3390/jof4020057

Sudheeran, P. K., Ovadia, R., Galsarker, O., Maoz, I., Sela, N., Maurer, D., Feygenberg, O., Oren Shamir, M., & Alkan, N. (2020). Glycosylated flavonoids: fruit's concealed

antifungal arsenal. *New Phytologist*, *225*(4), 1788–1798. https://doi.org/10.1111/nph.16251

Sum, W. C., Ebada, S. S., Kirchenwitz, M., Wanga, L., Decock, C., Stradal, T. E. B., Matasyoh, J. C., Mándi, A., Kurtán, T., & Stadler, M. (2023). Neurite Outgrowth-Inducing Drimane-Type Sesquiterpenoids Isolated from Cultures of the Polypore Abundisporus violaceus MUCL 56355. *Journal of Natural Products*, *86*(11), 2457–2467. https://doi.org/10.1021/acs.jnatprod.3c00525

Sun, X, Guo, L., & Diversity, K. H. (2014). Community composition of endophytic fungi in Acer truncatum and their role in decomposition. *Fungal Diversity*, *47*, 85–95. https://doi.org/10.1007/s13225-010-0086-5

Sun, Xiang, & Guo, L. D. (2012). Endophytic fungal diversity: review of traditional and molecular techniques. *Mycology*, *3*(1), 65–76. https://doi.org/10.1080/21501203.2012.656724

Suroowan, S., Javeed, F., Ahmad, M., Zafar, M., Noor, M. J., Kayani, S., Javed, A., & Mahomoodally, M. F. (2017). Ethnoveterinary health management practices using medicinal plants in South Asia – a review. *Veterinary Research Communications*, *41*(2), 147–168. https://doi.org/10.1007/s11259-017-9683-z

Tadeg, H., Mohammed, E., Asres, K., & Gebre-Mariam, T. (2005). Antimicrobial activities of some selected traditional Ethiopian medicinal plants used in the treatment of skin disorders. *Journal of Ethnopharmacology*, *100*(1–2), 168–175. https://doi.org/10.1016/j.jep.2005.02.031

Tamura, K., Stecher, G., & Kumar, S. (2021). MEGA11: molecular evolutionary genetics analysis version 11. *Molecular biology and evolution*, *38*(7), 3022-3027. https://doi.org/10.1093/molbev/msab120

Tan, C. J., Liu, L. N., & Zhao, B. Y. (2017). A New Quinolizidine Alkaloid from Oxytropis ochrocephala. *Chemistry of Natural Compounds*, *53*(2), 322–324. https://doi.org/10.1007/s10600-017-1979-2

Taylor, T. & E. T. (2000). The rhynie chert ecosystem: a model for understanding fungal interactions. *Microbial Endophytes*, 45–62. https://doi.org/10.1201/9781482277302-2

Tenover, F. C. (2006). Mechanisms of Antimicrobial Resistance in Bacteria. *The American Journal of Medicine*, *119*(6), S3–S10. https://doi.org/10.1016/j.amjmed.2006.03.011

Hoa, T. T., Giang, N. T., Ha, N. T. H., Huyen, T. T., Phat, D. T., Ha, C. H., ... & Quang, T. H. (2023). Diversity of endophytic fungi from medicinal plants *Dysosma difformis* (Hemsl & EH Wilson) TH Wang collected in Ha Giang and Lai Chau. *Vietnam Journal of*

Biotechnology, *21*(2), 365-373. https://doi.org/10.15625/1811-4989/18344

Turcotte, L. M., Liu, Q., Yasui, Y., Arnold, M. A., Hammond, S., Howell, R. M., ... & Neglia, J. P. (2017). Temporal trends in treatment and subsequent neoplasm risk among 5-year survivors of childhood cancer, 1970-2015. *Jama*, *317*(8), 814-824. https://doi.org/10.1001/jama.2017.0693

Tyski, S., Markiewicz, M., Gulewicz, K., & Twardowski, T. (1988). The effect of lupin alkaloids and ethanol extracts from seeds of Lupinus angustifolius on selected bacterial strains. *Journal of plant physiology*, *133*(2), 240-242. https://doi.org/10.1016/s0176-1617(88)80144-5

Umer, S., Tekewe, A., & Kebede, N. (2013). Antidiarrhoeal and antimicrobial activity of Calpurnia aurea leaf extract. *BMC Complementary and Alternative Medicine*, *13*(1), 1–5. https://doi.org/10.1186/1472-6882-13-21

Usman, M., Khan, W. R., Yousaf, N., Akram, S., Murtaza, G., Kudus, K. A., Ditta, A., Rosli, Z., Rajpar, M. N., & Nazre, M. (2022). Exploring the Phytochemicals and Anti-Cancer Potential of the Members of *Fabaceae* Family: A Comprehensive Review. *Molecules*, *27*(12), 3863. https://doi.org/10.3390/molecules27123863

Uzma, F., Mohan, C. D., Hashem, A., Konappa, N. M., Rangappa, S., Kamath, P. V., Singh, B. P., Mudili, V., Gupta, V. K., Siddaiah, C. N., Chowdappa, S., Alqarawi, A. A., & Abd-Allah, E. F. (2018). Endophytic fungi-alternative sources of cytotoxic compounds: A review. *Frontiers in Pharmacology*, *9*, 328484. https://doi.org/10.3389/fphar.2018.00309

Uzor, P. F., Osadebe, P. O., & Nwodo, N. J. (2017). Antidiabetic Activity of Extract and Compounds from an Endophytic Fungus Nigrospora oryzae. *Drug Research*, *67*(5), 308–311. https://doi.org/10.1055/s-0042-122777/id/r2016-10-1300-0010

Van Wyk, B. E. (2019). The diversity and multiple uses of southern African legumes. *Australian Systematic Botany*, *32*(6), 519–546. https://doi.org/10.1071/sb19028

Vasundhara, M., Baranwal, M., & Kumar, A. (2016). Fusarium tricinctum, An Endophytic Fungus Exhibits Cell Growth Inhibition and Antioxidant Activity. *Indian Journal of Microbiology*, *56*(4), 433–438. https://doi.org/10.1007/s12088-016-0600-x

Veeresham, C. (2012). Natural products derived from plants as a source of drugs. *Journal of Advanced Pharmaceutical Technology and Research*, *3*(4), 200–201. https://doi.org/10.4103/2231-4040.104709

Vélëz, H., Gauchan, D. P., & García-Gil, M. del R. (2022). Taxol and β-tubulins from endophytic fungi isolated from the Himalayan Yew, *Taxus wallichiana* Zucc. *Frontiers in Microbiology*, *13*, 956855. https://doi.org/10.3389/fmicb.2022.956855

Vermin, W. J., De Kok, A. J., Romers, C., Radema, M. H., & Van Eijk, J. L. (1979). Calpurmenin and its 13α-(2'-pyrrolecarboxylic acid) ester. *Structural Science*, *35*(8), 1839-1842. https://doi.org/10.1107/s0567740879007871

Vesterlund, S. R., Helander, M., Faeth, S. H., Hyvönen, T., & Saikkonen, K. (2011). Environmental conditions and host plant origin override endophyte effects on invertebrate communities. *Fungal Diversity*, *47*, 109–118. https://doi.org/10.1007/s13225-011-0089-x

Vetter, J. (1995). Isoflavones in Different Parts of Common Trifolium Species. *Journal of Agricultural and Food Chemistry*, *43*(1), 106–108. https://doi.org/10.1021/jf00049a020

Vialle, A., Feau, N., Allaire, M., Didukh, M., Martin, F., Moncalvo, J. M., & Hamelin, R. C. (2009). Evaluation of mitochondrial genes as DNA barcode for Basidiomycota. *Molecular Ecology Resources*, *9*, 99-113. https://doi.org/10.1111/j.1755-0998.2009.02637.x

Wamalwa, R. (2019). Fungal tinea capitis and associated risk factors in school going children aged 3-14 years in Kakamega Central sub- county;Kenya. Dissertation. https://repository.maseno.ac.ke/handle/123456789/1300

Wang, H., Naghavi, M., Allen, C., Barber, R. M., Carter, A., Casey, D. C., Charlson, F. J.,… & Zuhlke, L. J. (2016). Global, regional, and national life expectancy, all-cause mortality, and cause-specific mortality for 249 causes of death, 1980–2015: a systematic analysis for the Global Burden of Disease Study 2015. *The Lancet*, *388*(10053), 1459–1544. https://doi.org/10.1016/S0140-6736(16)31012-1

Wang, Jihua, Lou, J., Luo, C., Zhou, L., Wang, M., & Wang, L. (2012). Phenolic Compounds from *Halimodendron halodendron* (Pall.) Voss and Their Antimicrobial and Antioxidant Activities. *International Journal of Molecular Sciences*, *13*(9), 11349–11364. https://doi.org/10.3390/ijms130911349

Wang, Junfei, Shao, S., Liu, C., Song, Z., Liu, S., & Wu, S. (2021). The genus *Paraconiothyrium*: species concepts, biological functions, and secondary metabolites. *Critical Reviews in Microbiology*, *47*(6), 781–810. https://doi.org/10.1080/1040841x.2021.1933898

Wang, L. W., Wang, J. L., Chen, J., Chen, J. J., Shen, J. W., Feng, X. X., Kubicek, C. P., Lin, F. C., Zhang, C. L., & Chen, F. Y. (2017). A novel derivative of (-)mycousnine produced by the endophytic fungus *Mycosphaerella nawae*, exhibits high and selective immunosuppressive activity on T cells. *Frontiers in Microbiology*, *8*, 265023. https://doi.org/10.3389/fmicb.2017.01251

Wang, S., Liang, H., Zhao, Y., Wang, G., Yao, H., Kasimu, R., ... & Wang, J. (2016). New triterpenoids from the latex of *Euphorbia resinifera* Berg. *Fitoterapia*, *108*, 33-40. https://doi.org/10.1016/j.fitote.2015.11.009

Wanga, L., & Nyamboki, K. (2023). Medicinal Plants Used in the Management of Skin Disorders in Kenya: A Review. *Pharmacognosy Reviews*, *17*(33), 69–103. https://doi.org/10.5530/097627870276

Wangkheirakpam, S. (2018). Traditional and Folk Medicine as a Target for Drug Discovery. *Natural Products and Drug Discovery: An Integrated Approach*, 29–56. https://doi.org/10.1016/b978-0-08-102081-4.00002-2

Wasihun, Y., Alekaw Habteweld, H., & Dires Ayenew, K. (2023). Antibacterial activity and phytochemical components of leaf extract of Calpurnia aurea. *Scientific Reports*, *13*(1), 1–7. https://doi.org/10.1038/s41598-023-36837-3

Waterhouse, A. M., Procter, J. B., Martin, D. M. A., Clamp, M., & Barton, G. J. (2009). Jalview Version 2—a multiple sequence alignment editor and analysis workbench. *Bioinformatics*, *25*(9), 1189–1191. https://doi.org/10.1093/bioinformatics/btp033

Wayne, P. A. (2011). Clinical and laboratory standards institute. Performance standards for antimicrobial susceptibility testing. https://www.nih.org.pk/wp-content/uploads/2021/02/CLSI-2020.pdf

World Health Organisation (WHO). (2018). Antimicrobial resistance and primary health care. *World Health Organization. WHO core package of interventions to support national action plans*. World Health Organization. https://doi.org/10.2471/blt.11.088435

World Health Organization, W. (2015). Global dermatophyte resistance and use surveillance system report 2014. https://doi.org/10.2471/blt.11.088535

World Health Organization. (2022). Global antimicrobial resistance and use surveillance system (GLASS) report 2022. World Health Organization. https://www.who.int/publications/i/item/9789240062702

Xu, J. (2016). Fungal DNA barcoding1. *Genome*, *59*(11), 913–932. https://doi.org/10.1139/gen-2016-0046

Xu, Z., Zhang, F., Bai, C., Yao, C., Zhong, H., Zou, C., & Chen, X. (2017). Sophoridine induces apoptosis and S phase arrest via ROS-dependent JNK and ERK activation in human pancreatic cancer cells. *Journal of Experimental and Clinical Cancer Research*, *36*(1), 1–10. https://doi.org/10.1186/s13046-017-0590-5

Xue, Y., Zhou, J., Xu, B. N., Li, Y., Bao, W., Cheng, X. L., He, Y., Xu, C. P., Ren, J., Zheng, Y. rong, & Jia, C. Y. (2022). Global Burden of Bacterial Skin Diseases: A Systematic

Analysis Combined With Sociodemographic Index, 1990–2019. *Frontiers in Medicine*, *9*, 861115. https://doi.org/10.3389/fmed.2022.861115

Yan, D. H., Song, X., Li, H., Luo, T., Dou, G., & Strobel, G. (2018). Antifungal Activities of Volatile Secondary Metabolites of Four Diaporthe Strains Isolated from *Catharanthus roseus*. *Journal of Fungi 2018*, *4*(2), 65. https://doi.org/10.3390/jof4020065

Yang, B., Liu, H., Yang, J., Gupta, V. K., & Jiang, Y. (2018). New insights on bioactivities and biosynthesis of flavonoid glycosides. *Trends in Food Science and Technology*, *79*, 116–124. https://doi.org/10.1016/j.tifs.2018.07.006

Ye, B., Ma, J., Li, Z., Li, Y., & Han, X. (2022). Ononin Shows Anticancer Activity Against Laryngeal Cancer via the Inhibition of ERK/JNK/p38 Signaling Pathway. *Frontiers in Oncology*, *12*, 939646. https://doi.org/10.3389/fonc.2022.939646

Yeshitila, H. & Getu, E (2018). Status, Species Composition and Management of Stored Maize Grain Insect Pests in Hadiya and Silte zones of Southern Ethiopia. (Doctoral dissertation, Department of Zoological Sciences, Addis Ababa University).

Yessoufou, K., Elansary, H. O., Mahmoud, E. A., & Skalicka-Woźniak, K. (2015). Antifungal, antibacterial and anticancer activities of Ficus drupacea L. stem bark extract and biologically active isolated compounds. *Industrial Crops and Products*, *74*, 752–758. https://doi.org/10.1016/j.indcrop.2015.06.011

Yineger, H., & Yewhalaw, D. (2007). Traditional medicinal plant knowledge and use by local healers in Sekoru District, Jimma Zone, Southwestern Ethiopia. *Journal of Ethnobiology and Ethnomedicine*, *3*(1), 1–7. https://doi.org/10.1186/1746-4269-3-24

Yineger, H., Yewhalaw, D., & Teketay, D. (2008). Ethnomedicinal plant knowledge and practice of the Oromo ethnic group in southwestern Ethiopia. *Journal of Ethnobiology and Ethnomedicine*, *4*(1), 1–10. https://doi.org/10.1186/1746-4269-4-11

Yu, Y., Chen, Z., Xie, H., Feng, X., Wang, Y., & Xu, P. (2022). Overhauling the Effect of Surface Sterilization on Analysis of Endophytes in Tea Plants. *Frontiers in Plant Science*, *13*. https://doi.org/10.3389/fpls.2022.849658

Zakaria, L., Yaakop, A. S., Salleh, B., & Zakaria, M. (2010). Endophytic Fungi from Paddy. *Tropical Life Sciences Research*, *21*(1), 101. http//doi.org/pmc/articles/PMC3819061

Zembower, T. R. (2014). Epidemiology of infections in cancer patients. *Cancer Treatment and Research*, *161*, 43–89. https://doi.org/10.1007/978-3-319-04220-6_2

Zhang & Feng, X. Z. (1997). Lactariolide, a new 14-membered-ring compound from *Lactarius Subvellereus*. 中国化学快报, *8*(02), 135-136. https://doi.org/10.1002/chin.199750185

Zhang, Q. Y., Wang, F. X., Jia, K. K., & Kong, L. D. (2018a). Natural product interventions for chemotherapy and radiotherapy-induced side effects. *Frontiers in Pharmacology*, *9*, 415590. https://doi.org/10.3389/fphar.2018.01253

Zhang, Y., Zhang, H., Yu, P., Liu, Q., Liu, K., Duan, H., Luan, G., Yagasaki, K., & Zhang, G. (2009). Effects of matrine against the growth of human lung cancer and hepatoma cells as well as lung cancer cell migration. *Cytotechnology*, *59*(3), 191–200. https://doi.org/10.1007/s10616-009-9211-2

Zhao, P., Luo, J., & Zhuang, W. Y. (2011). Practice towards DNA barcoding of the nectriaceous fungi. *Fungal Diversity*, *46*(1), 183–191. https://doi.org/10.1007/s13225-010-0064-y

Zhao, Z., Song, H., Xie, J., Liu, T., Zhao, X., Chen, X., He, X., Wu, S., Zhang, Y., & Zheng, X. (2019). Research progress in the biological activities of 3,4,5-trimethoxycinnamic acid (TMCA) derivatives. *European Journal of Medicinal Chemistry*, *173*, 213–227. https://doi.org/10.1016/j.ejmech.2019.04.009

Zhou, G., Shi, Q. S., Huang, X. M., & Xie, X. B. (2015). The Three Bacterial Lines of Defense against Antimicrobial Agents. *International Journal of Molecular Sciences*, *16*(9), 21711–21733. https://doi.org/10.3390/ijms160921711

Zhou, S., Nagel, J. L., Kaye, K. S., LaPlante, K. L., Albin, O. R., & Pogue, J. M. (2021). Antimicrobial Stewardship and the Infection Control Practitioner: A Natural Alliance. *Infectious Disease Clinics of North America*, *35*(3), 771–787. https://doi.org/10.1016/j.idc.2021.04.011

Zhou, Y., Liu, B., Mbuni, Y., Yan, X., Mwachala, G., Hu, G., & Wang, Q. (2017). Vascular flora of Kenya, based on the Flora of Tropical East Africa. *PhytoKeys*, *90*(90), 113. https://doi.org/10.3897/phytokeys.90.20531

Zishan, M., Saidurrahman, S., Anayatullah, A., Azeemuddin, A., Ahmad, Z., & Hussain, M. W. (2017). Natural products used as anti-cancer agents. *Journal of Drug Delivery and Therapeutics*, *7*(3), 11–18. https://doi.org/10.22270/jddt.v7i3.1443

Zorloni, A., Penzhorn, B. L., & Eloff, J. N. (2010). Extracts of *Calpurnia aurea* leaves from southern Ethiopia attract and immobilise or kill ticks. *Veterinary Parasitology*, *168*(1–2), 160–164. https://doi.org/10.1016/j.vetpar.2009.10.026

APPENDICES

Appendix 1: H RT. 2:64-3:00 matogram of compound **46**.

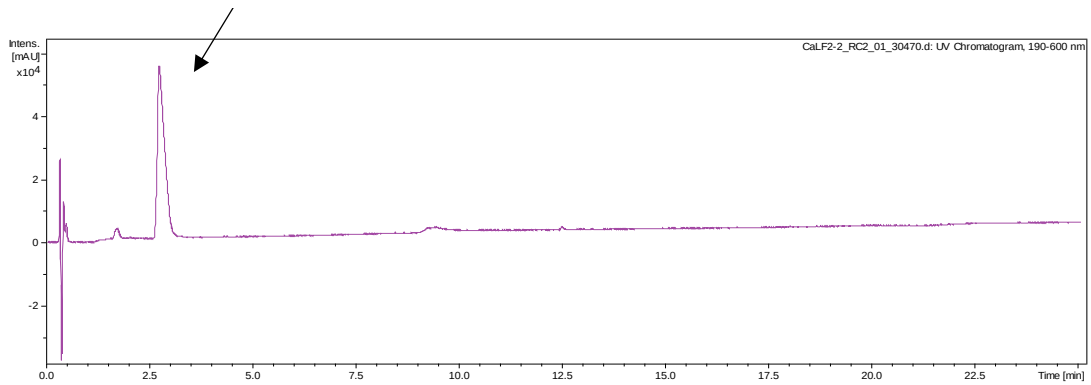

Appendix 2: HR-(+) ESIMS spectrum of compound **46**.

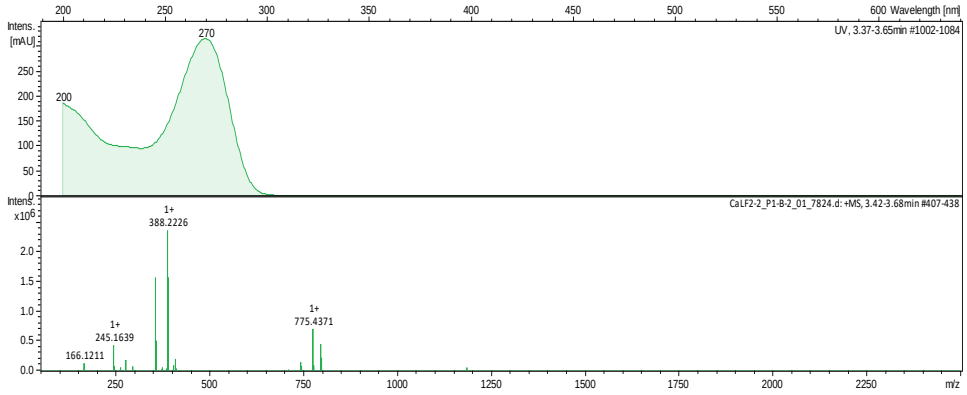

Appendix 3: ^{1}H NMR spectrum (700 MHz, CD_3OD) of compound **46**.

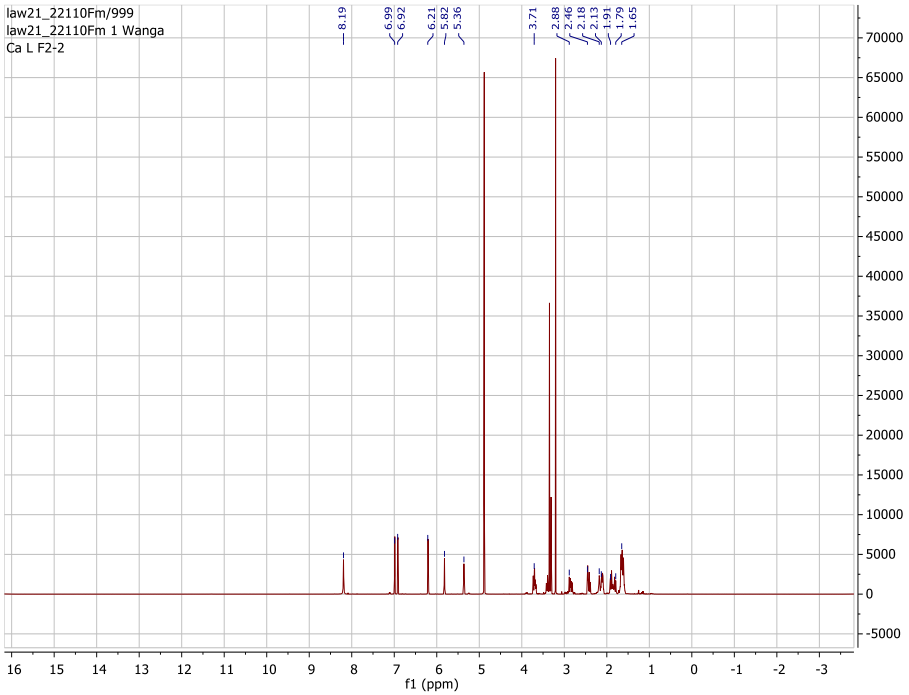

Appendix 4: ^{13}C NMR spectrum (700 MHz, CD_3OD) of compound **46**.

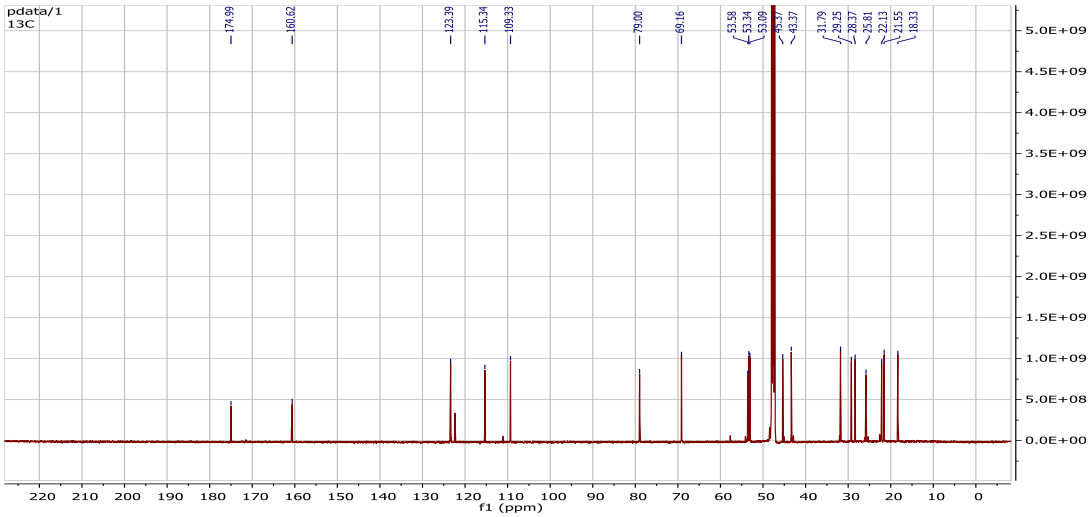

Appendix 5: ^{1}H, ^{13}C HSQC-DEPT spectrum (500 MHz, CD_3OD) of compound **46**.

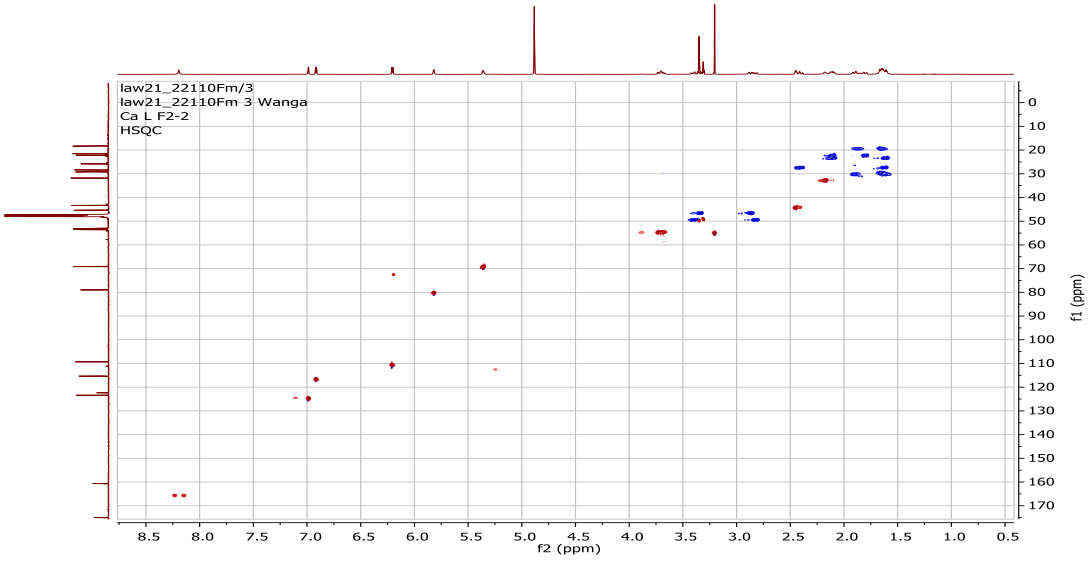

Appendix 6: ^{1}H, ^{13}C HMBC spectrum (500 MHz, CD_3OD) of compound **46**.

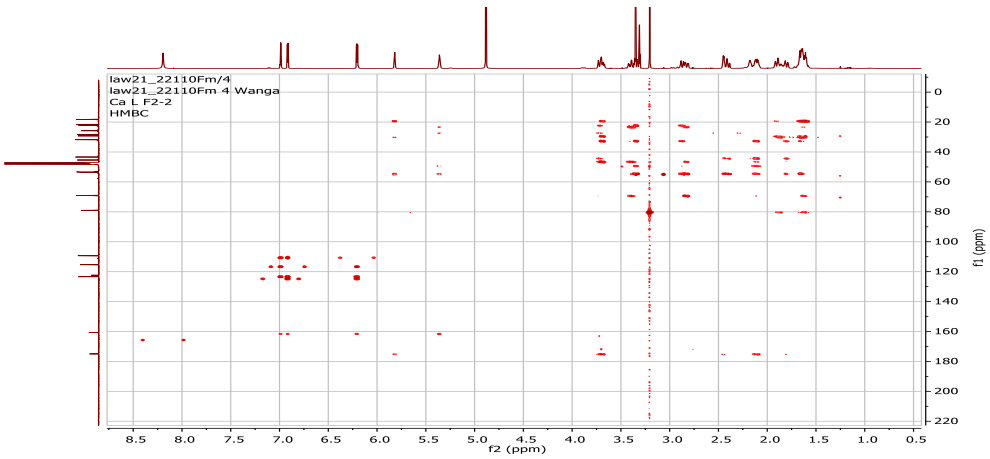

Appendix 7: ^{1}H- ^{1}H COSY spectrum (500 MHz, CD_3OD) of compound **46**.

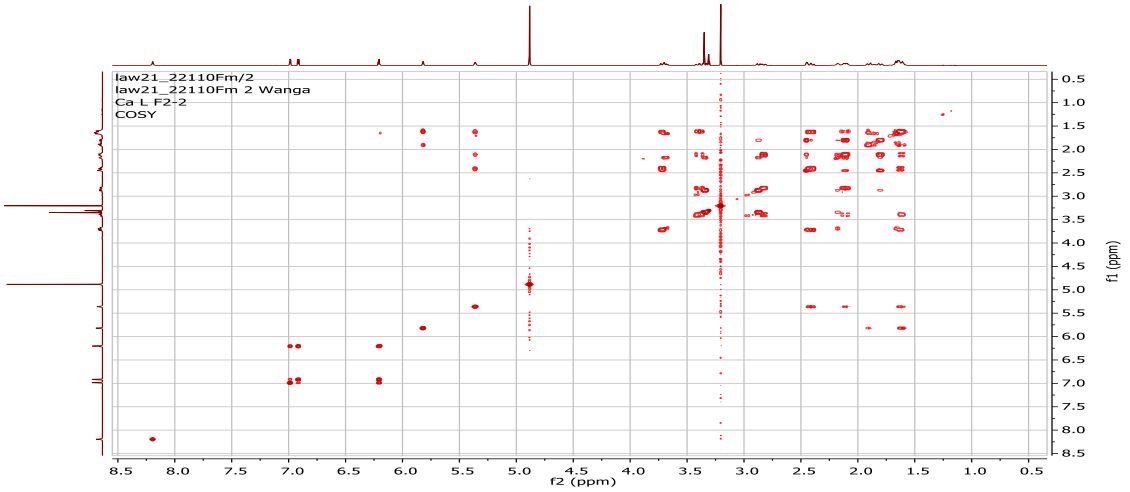

Appendix 8: ^{1}H, ^{1}H NOESY spectrum (500 MHz, CD_3OD) of compound **46**.

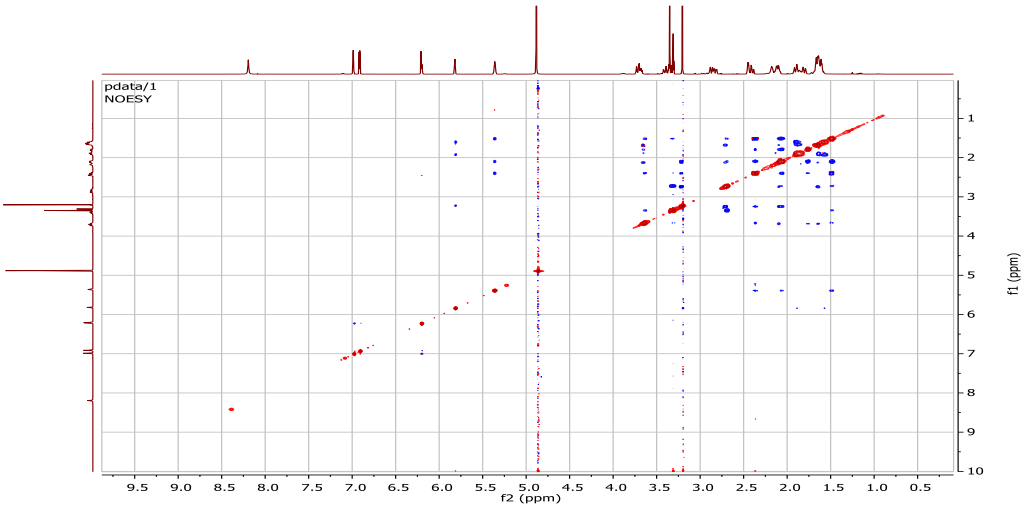

Appendix 9: UV/Vis spectrum of compound **46** in MeOH.

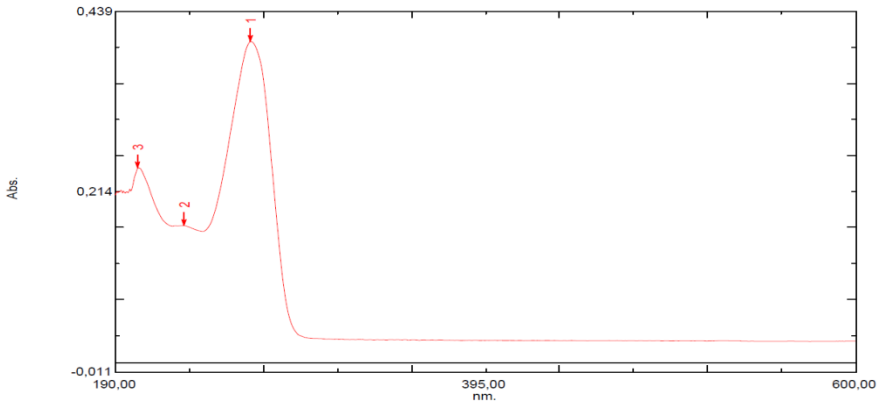

Appendix 10: HPLC-DAD chromatogram of compound **47**.

RT: 3:18-3:44

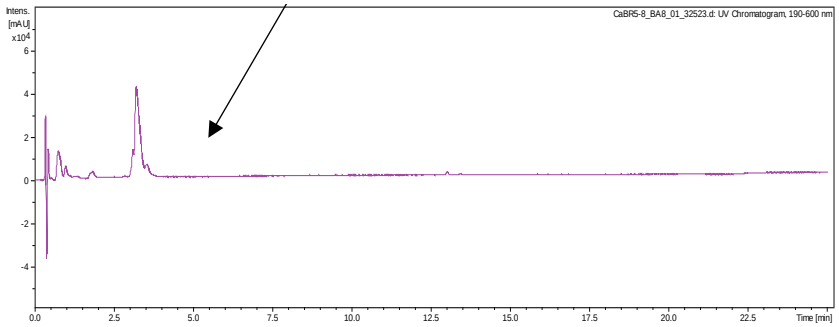

Appendix 11: HR-(+) ESIMS spectrum of compound **47**.

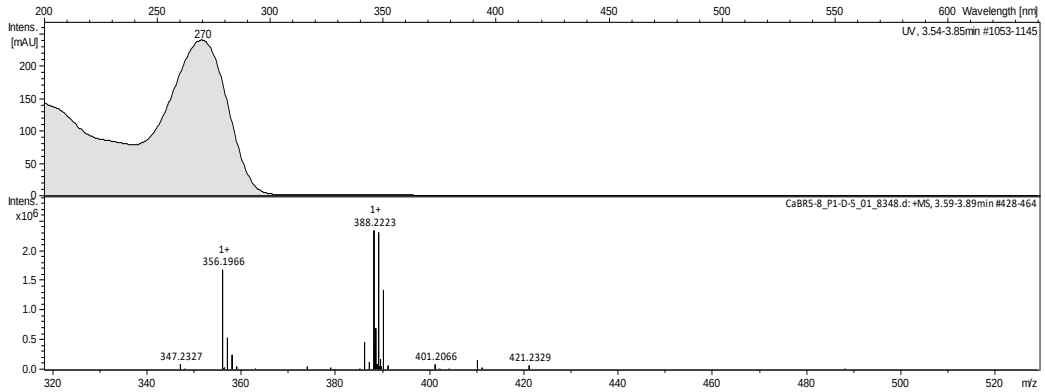

Appendix 12: ^{1}H NMR spectrum (500 MHz, CD_3OD) of compound **47**.

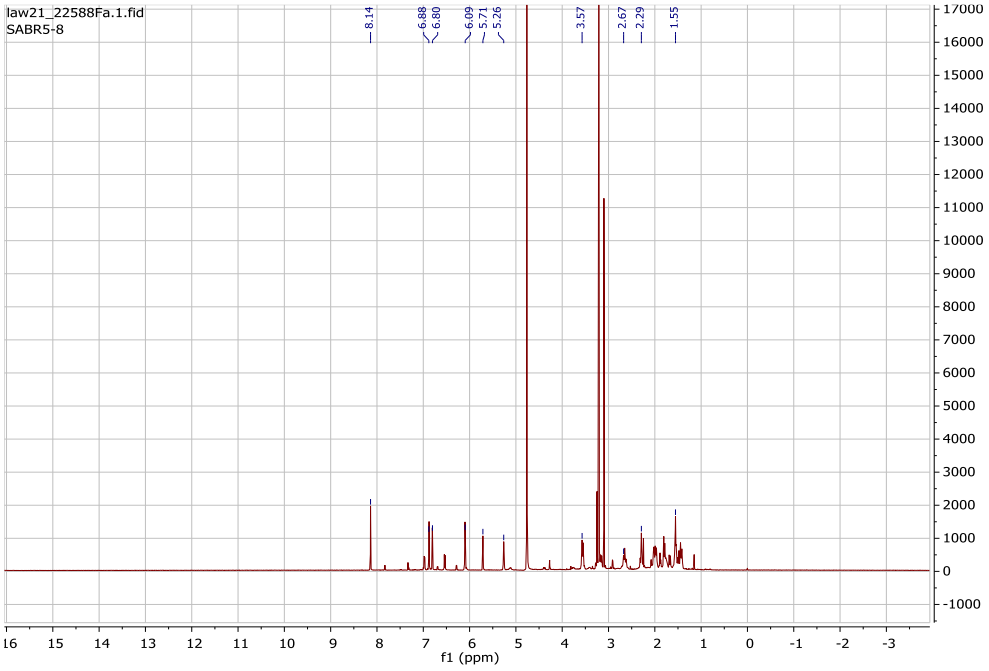

Appendix 13: ^{13}C NMR spectrum (500 MHz, CD_3OD) of compound **47**.

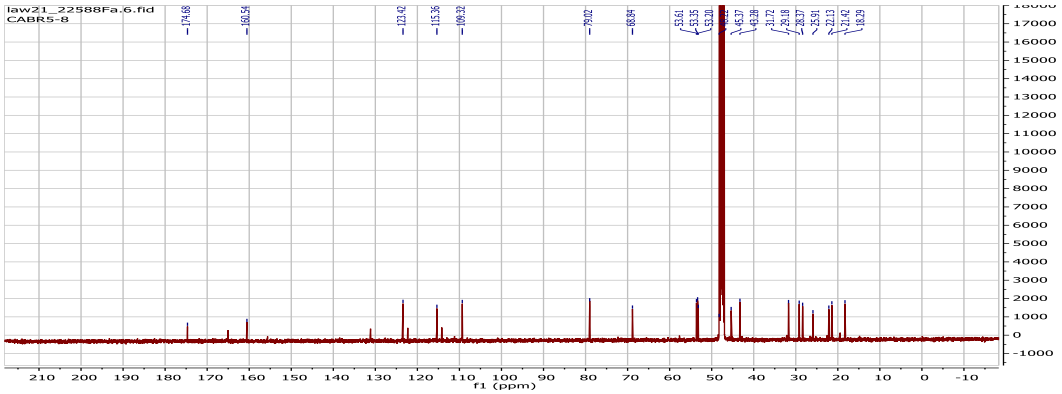

Appendix 14: ^{1}H, ^{13}C HSQC-DEPT spectrum (500 MHz, CD_3OD) of compound **47**.

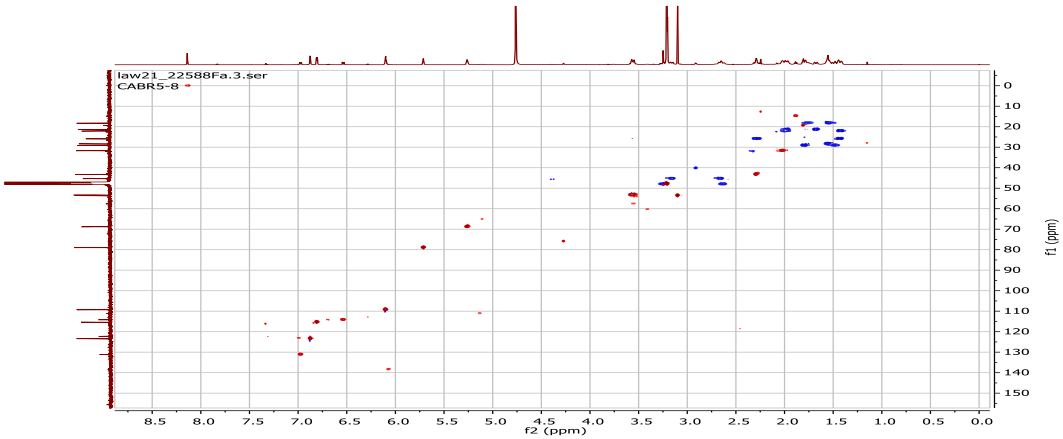

Appendix 15: ^{1}H, ^{13}C HMBC spectrum (500 MHz, CD_3OD) of compound **47**.

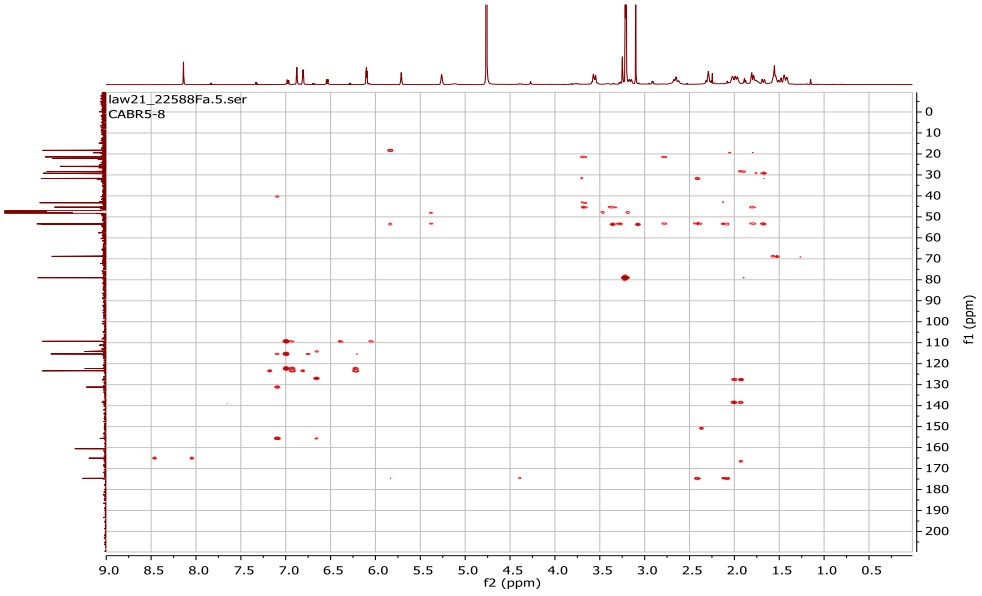

Appendix 16: ^{1}H- ^{1}H COSY spectrum (500 MHz, CD_3OD) of compound **47**

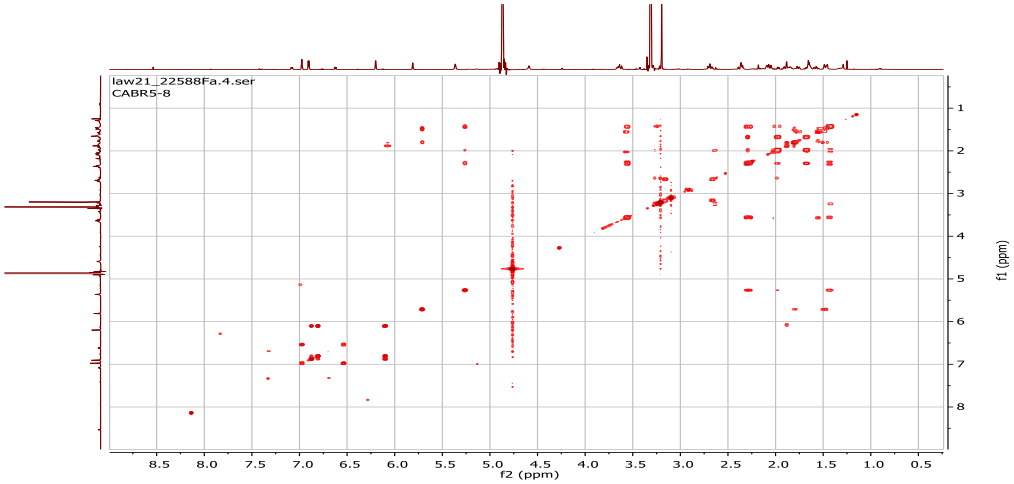

Appendix 17: ^{1}H- ^{1}H NOESY spectrum (500 MHz, CD_3OD) of compound **47**.

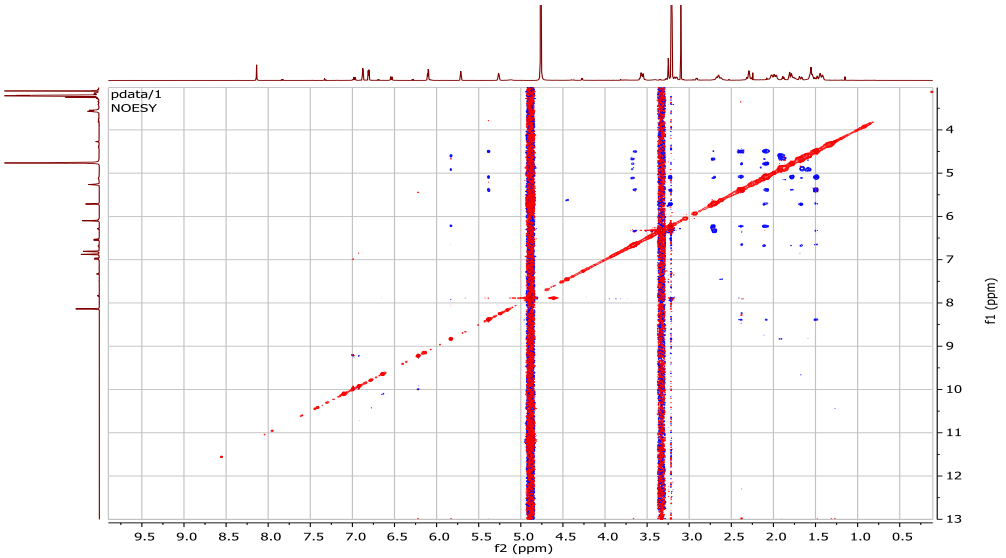

Appendix 18: UV/Vis spectrum of compound **47** in MeOH.

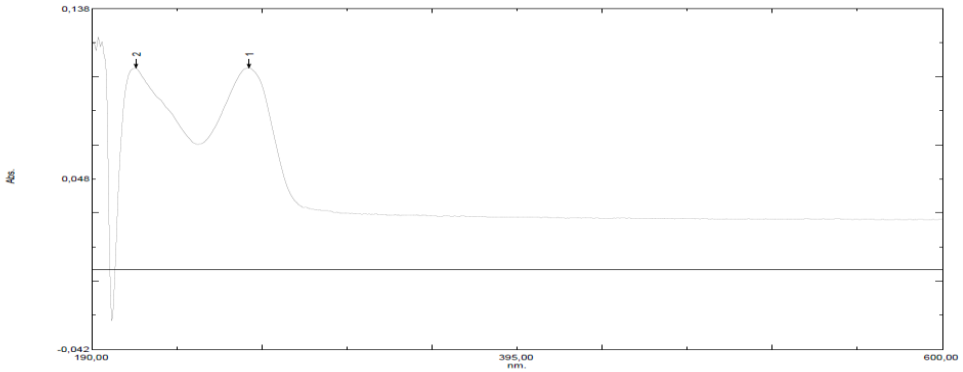

Appendix 19: HPLC-DAD chromatogram of compound **48**.

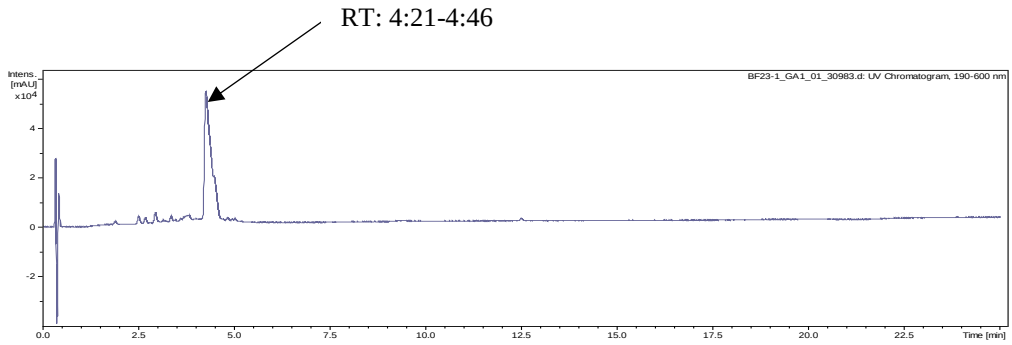

Appendix 20: HR-(+) ESIMS spectrum of compound **48**.

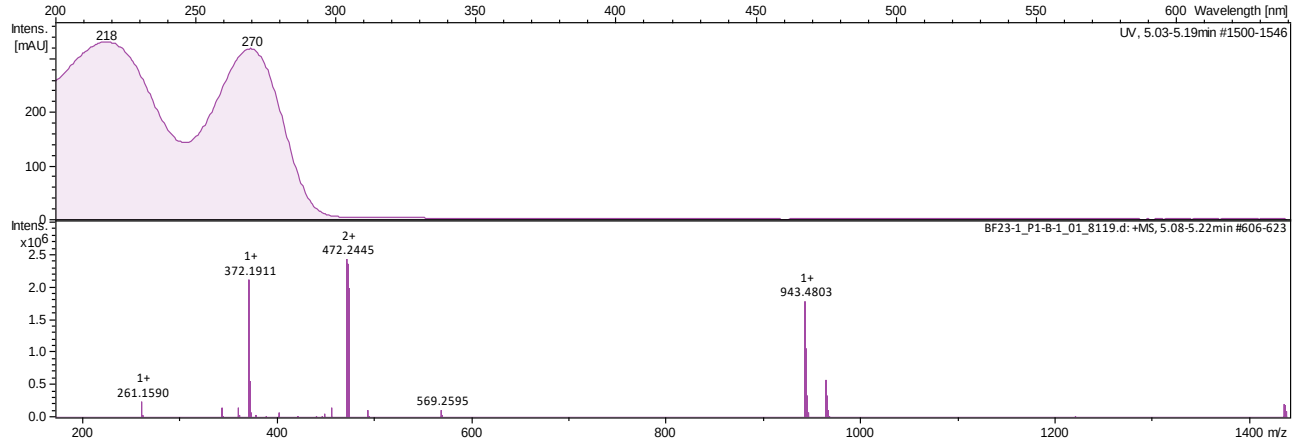

Appendix 21: ^{1}H NMR spectrum (500 MHz, CD_3OD) of compound **48.**

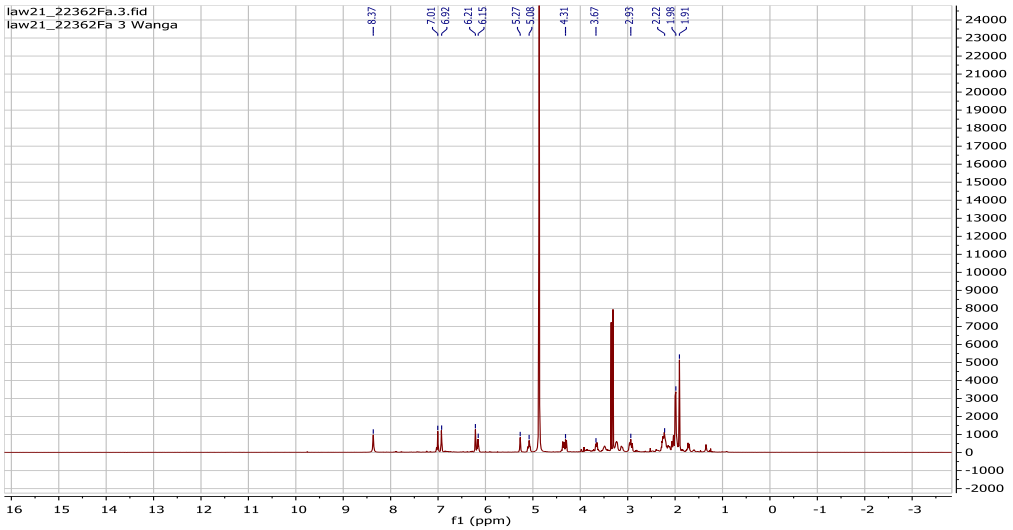

Appendix 22: ^{13}C NMR spectrum (500 MHz, CD_3OD) of compound **48**

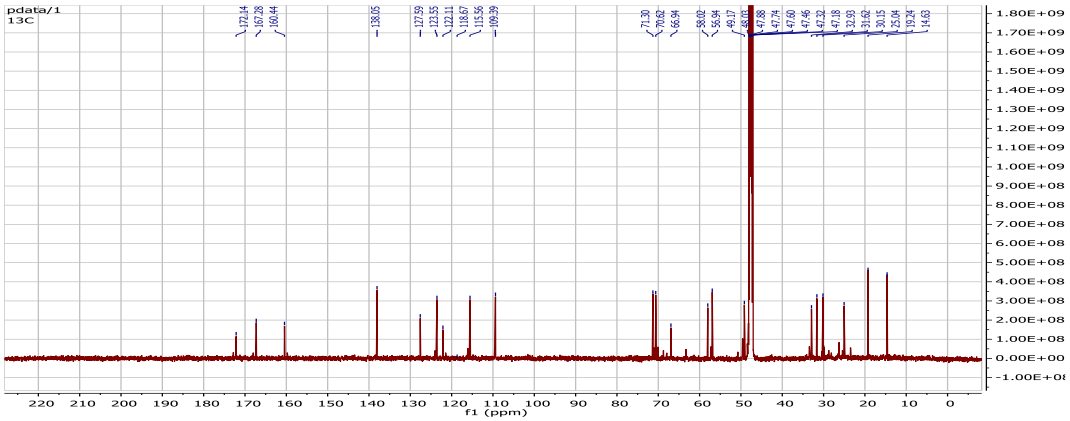

Appendix 23: ^{1}H, ^{13}C HSQC-DEPT spectrum (500 MHz, CD_3OD) of compound **48**.

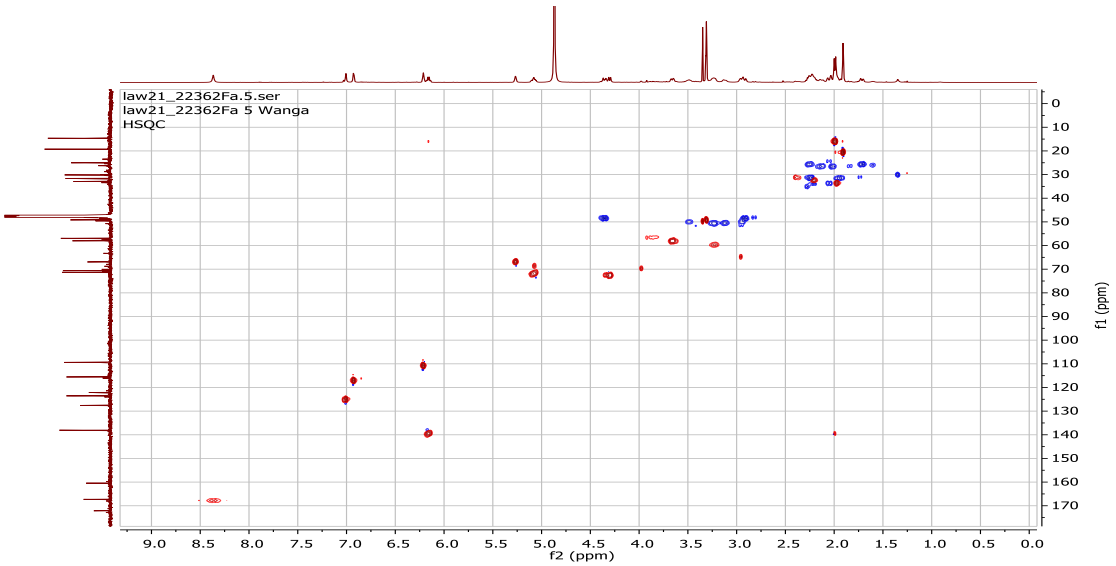

Appendix 24: ^{1}H, ^{13}C HMBC spectrum (500 MHz, CD_3OD) of compound **48**.

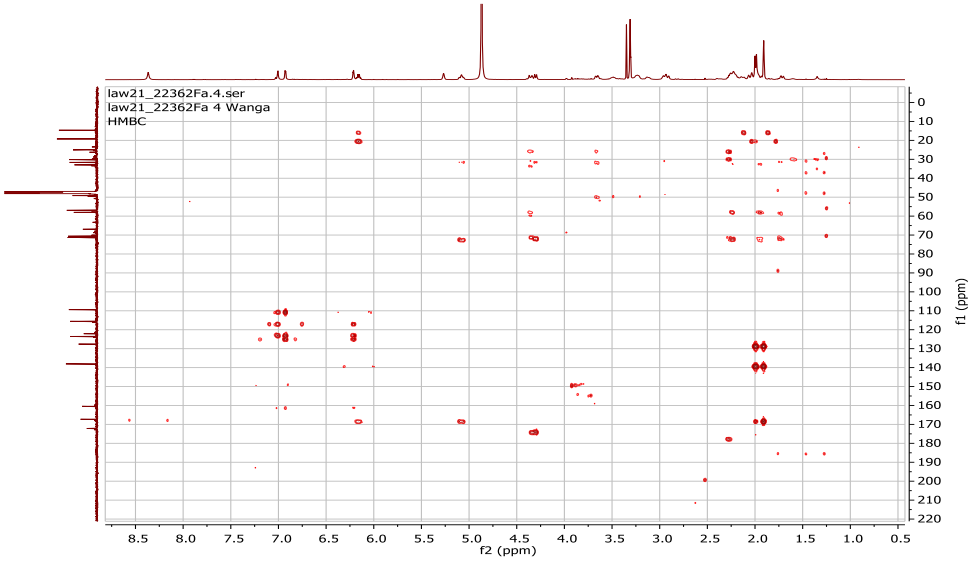

Appendix 25: ^{1}H- ^{1}H COSY spectrum (500 MHz, CD_3OD) of compound **48.**

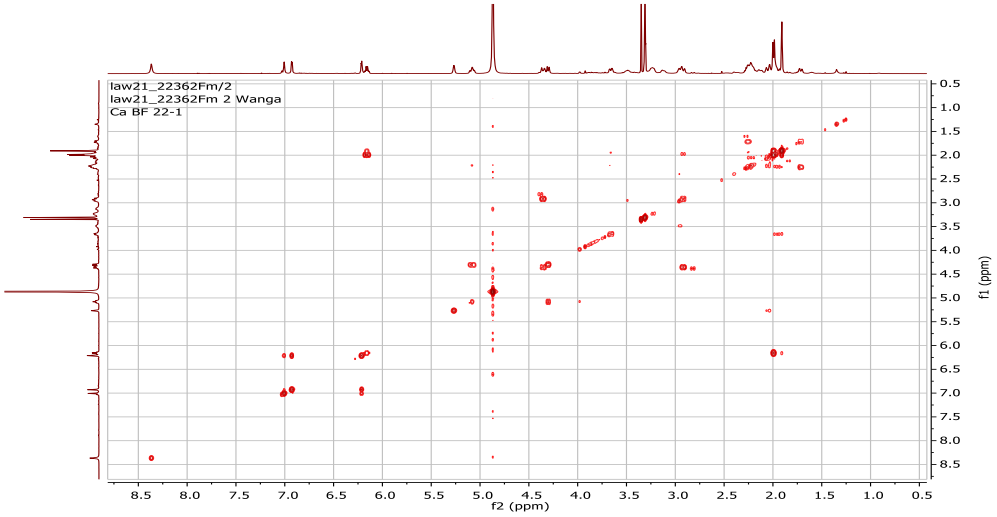

Appendix 26: ^{1}H- ^{1}H NOESY spectrum (500 MHz, CD_3OD) of compound **48**.

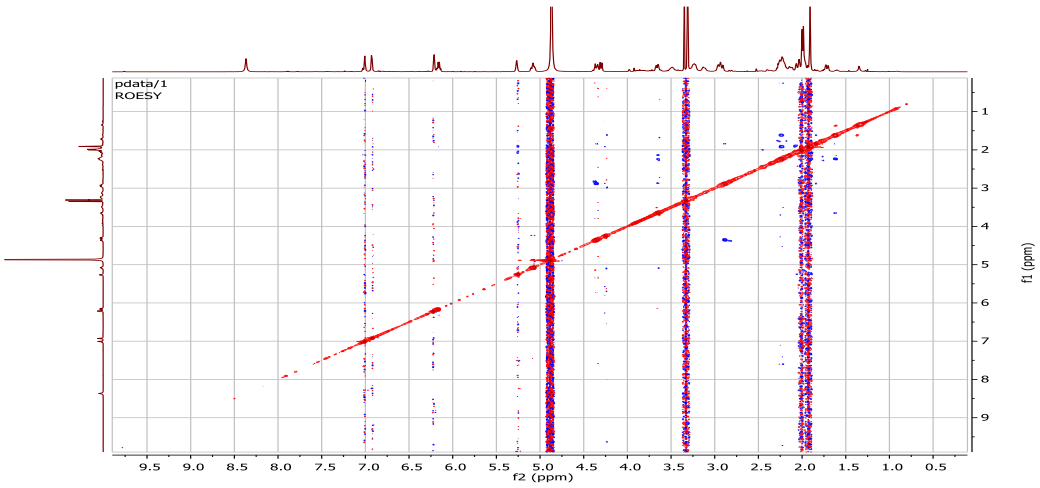

Appendix 27: UV/Vis spectrum of compound **48** in MeOH.

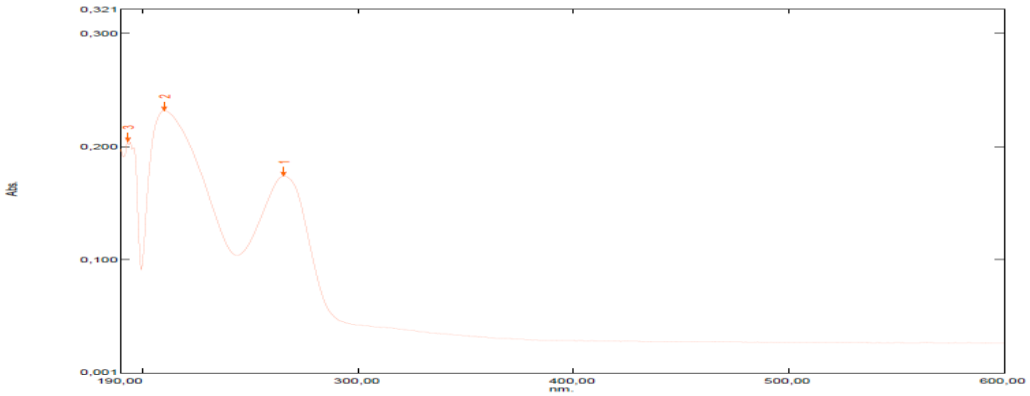

Appendix 28: HPLC-DAD chromatogram of compound **49**.

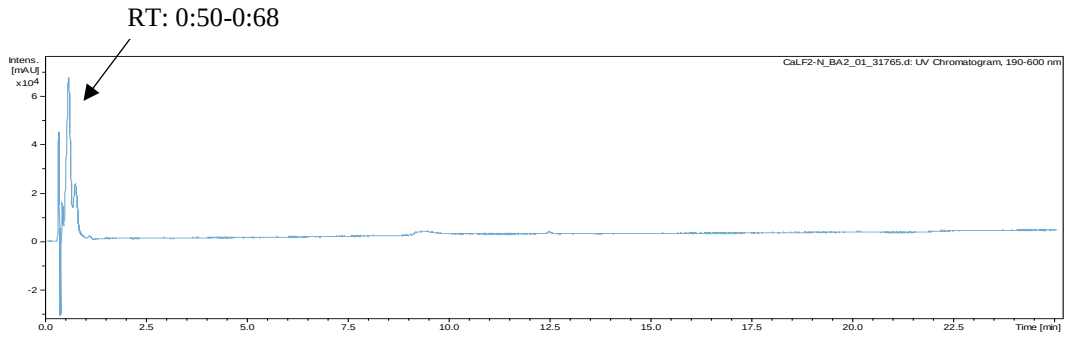

Appendix 29: HR-(+) ESIMS spectrum of compound **49**.

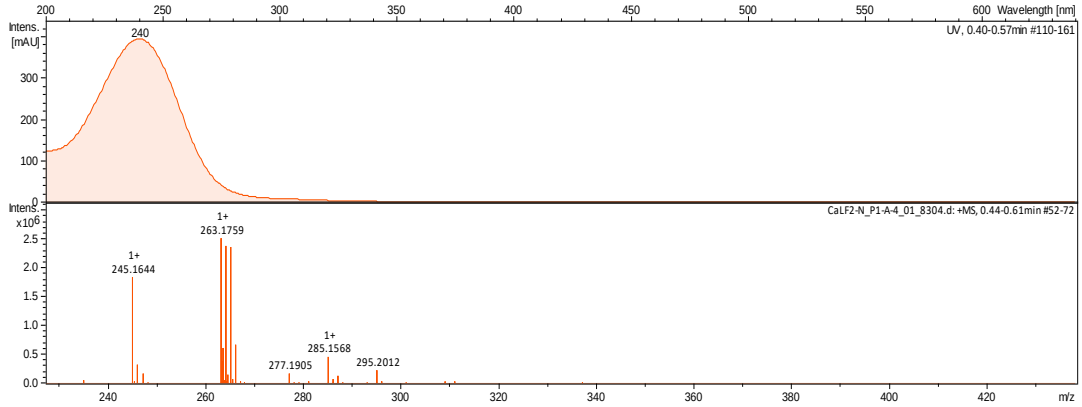

Appendix 30: ^{1}H NMR spectrum (500 MHz, CD_3OD) of compound **49**

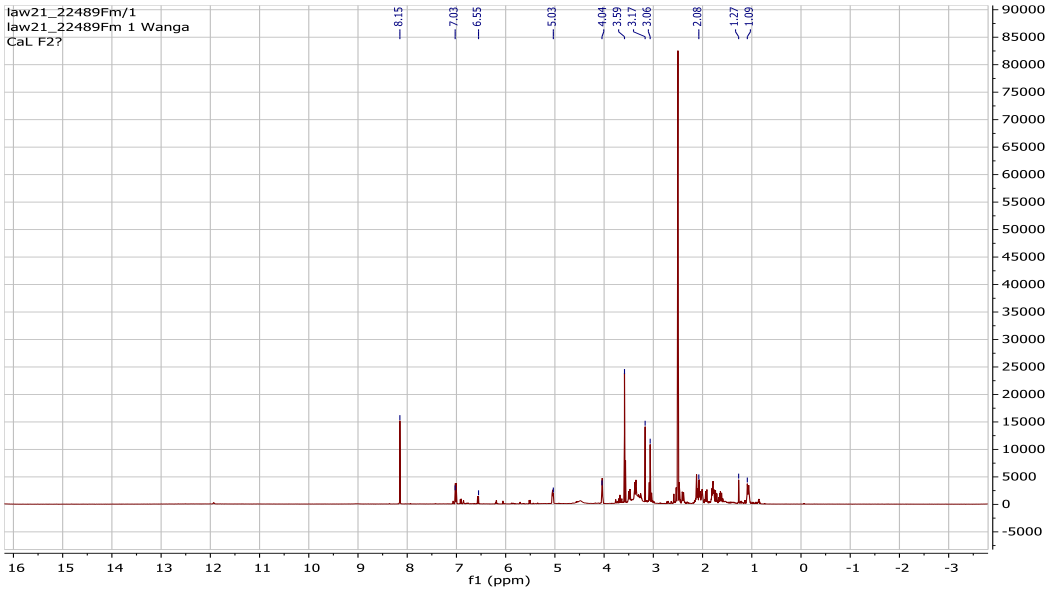

Appendix 31: ^{13}C NMR spectrum (500 MHz, CD_3OD) of compound **49**.

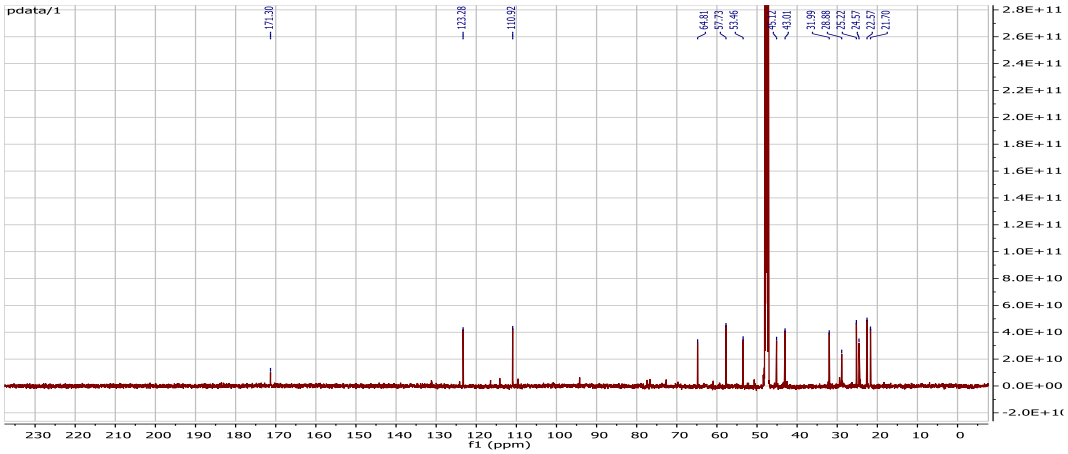

Appendix 32: ^{1}H, ^{13}C HSQC-DEPT spectrum (500 MHz, CD_3OD) of compound **49**.

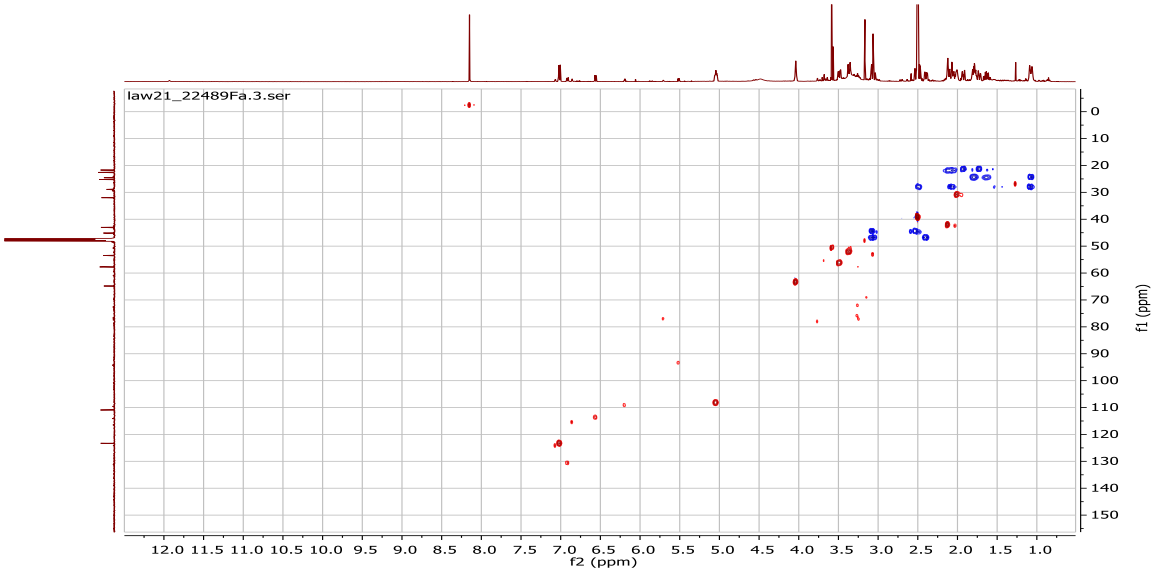

Appendix 33: ^{1}H, ^{13}C HMBC spectrum (500 MHz, CD_3OD) of compound **49.**

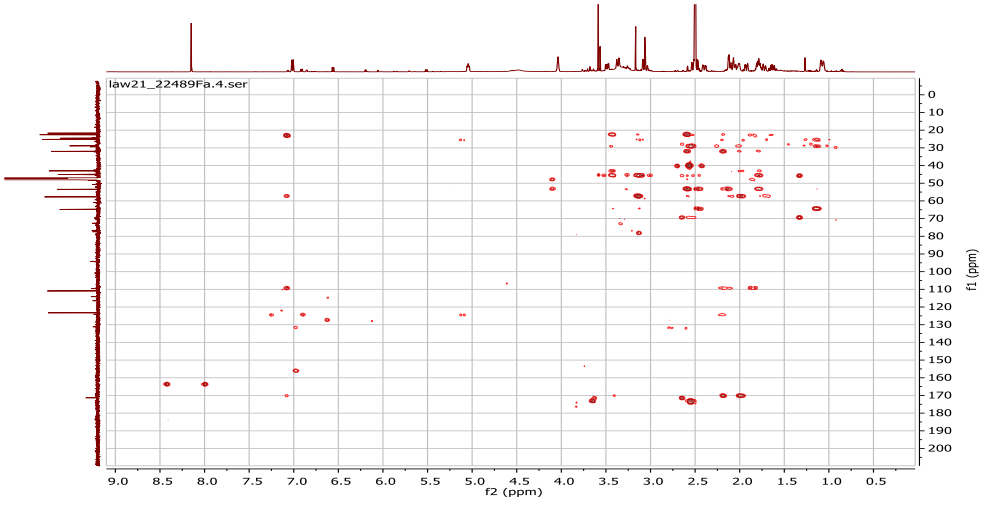

Appendix 34: ^{1}H-^{1}H COSY spectrum (500 MHz, CD_3OD) of compound **49.**

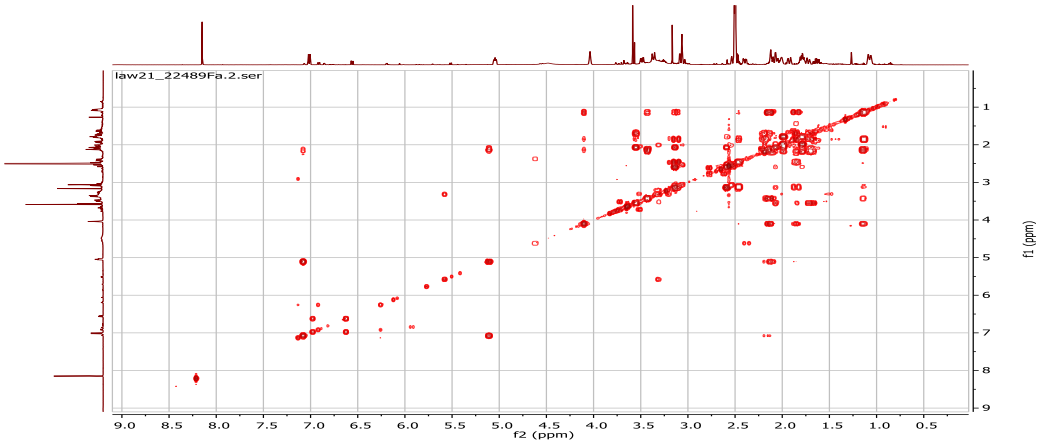

Appendix 35: ^{1}H- ^{1}H NOESY spectrum (500 MHz, CD_3OD) of compound **49**.

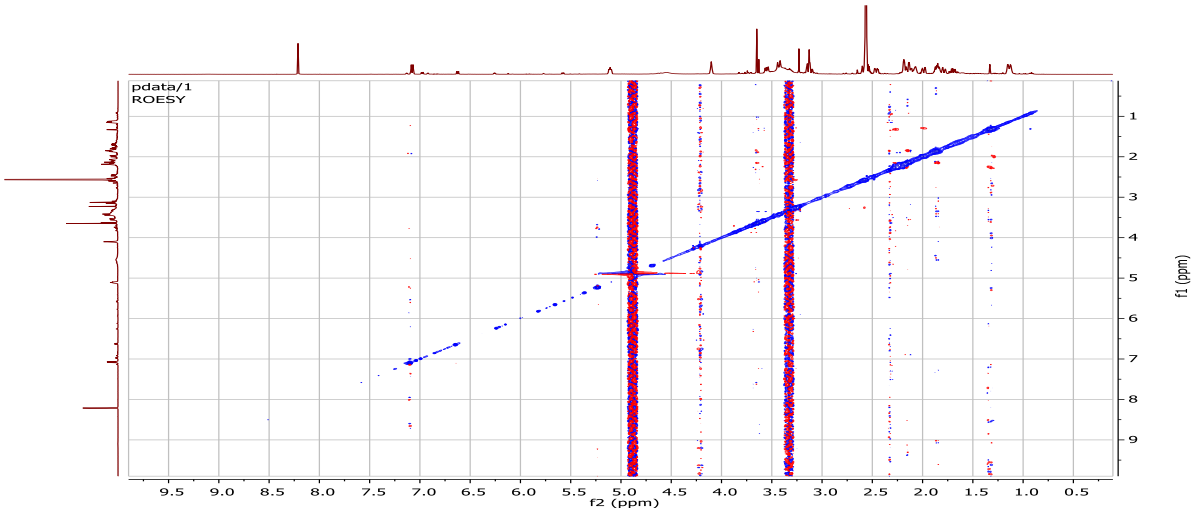

Appendix 36: UV/Vis spectrum of compound **49** in MeOH.

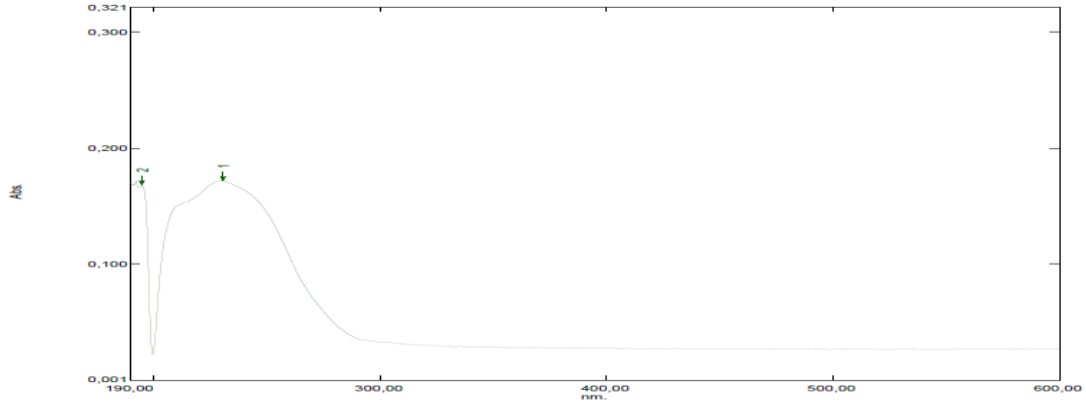

Appendix 37: HPLC-DAD chromatogram of compound **50**.

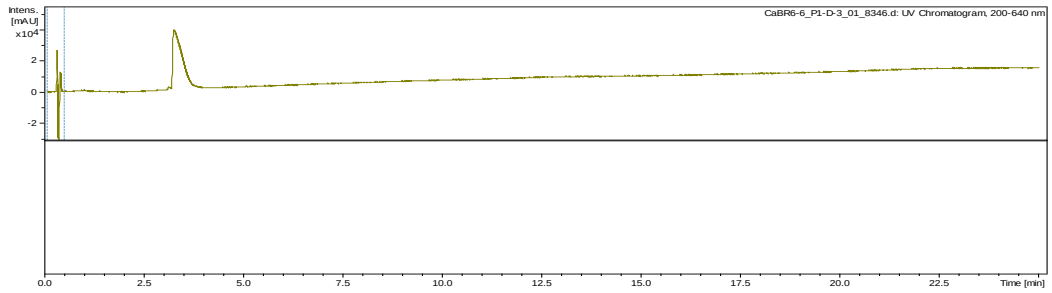

Appendix 38: HR-(+) ESIMS spectrum of compound **50**.

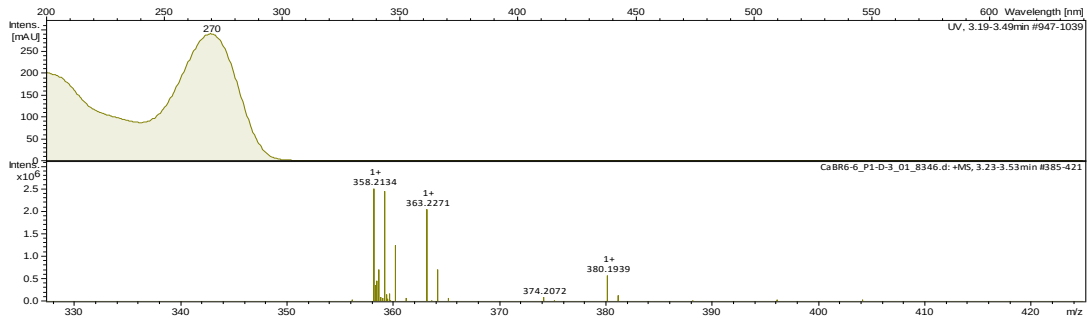

Appendix 39: ^{1}H NMR spectrum (500 MHz, CD_3OD) of compound **50**

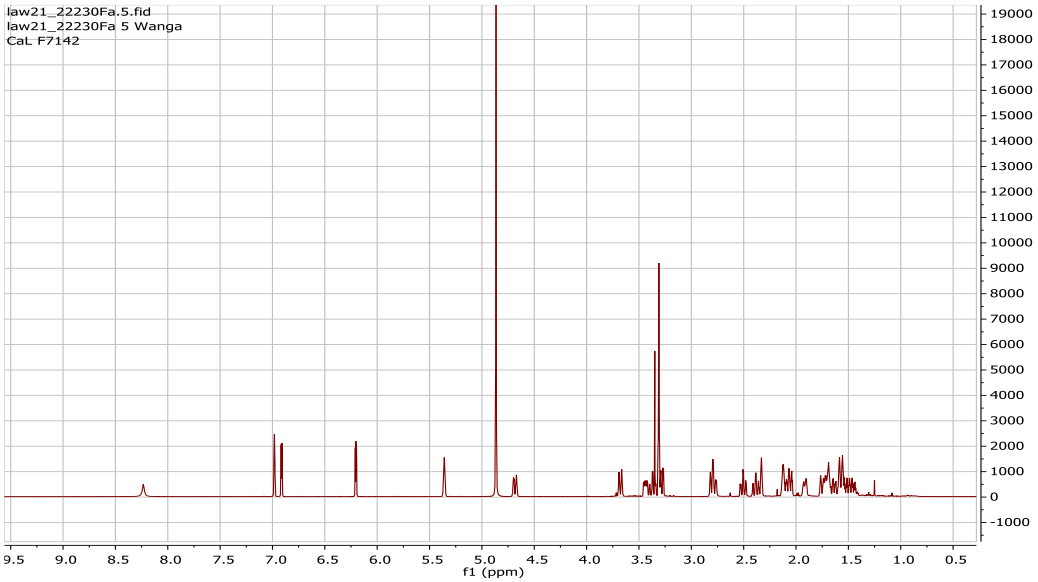

Appendix 40: ^{1}H, ^{13}C HSQC-DEPT spectrum (500 MHz, CD_3OD) of compound **50**.

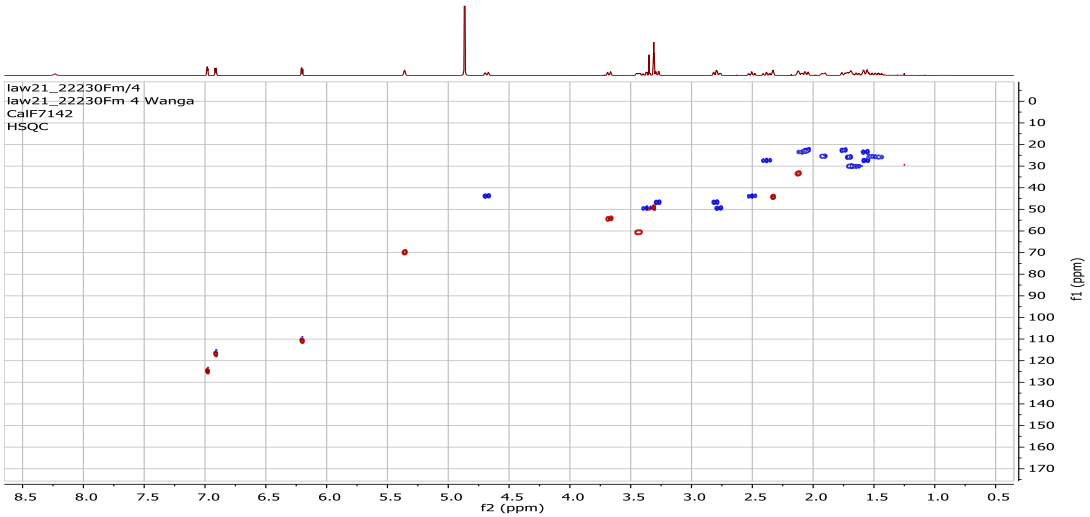

Appendix 41: ^{1}H, ^{13}C HMBC spectrum (500 MHz, CD_3OD) of compound **50.**

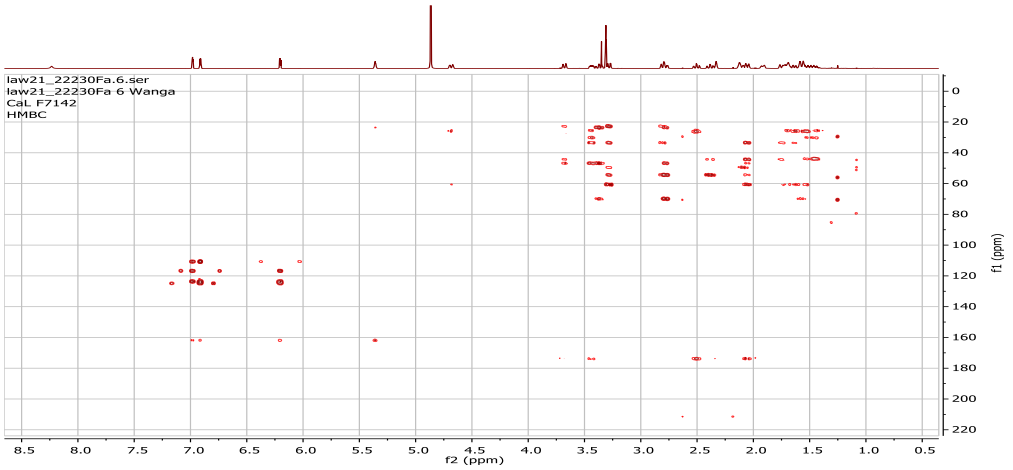

Appendix 42: ^{1}H-^{1}H COSY spectrum (500 MHz, CD_3OD) of compound **50.**

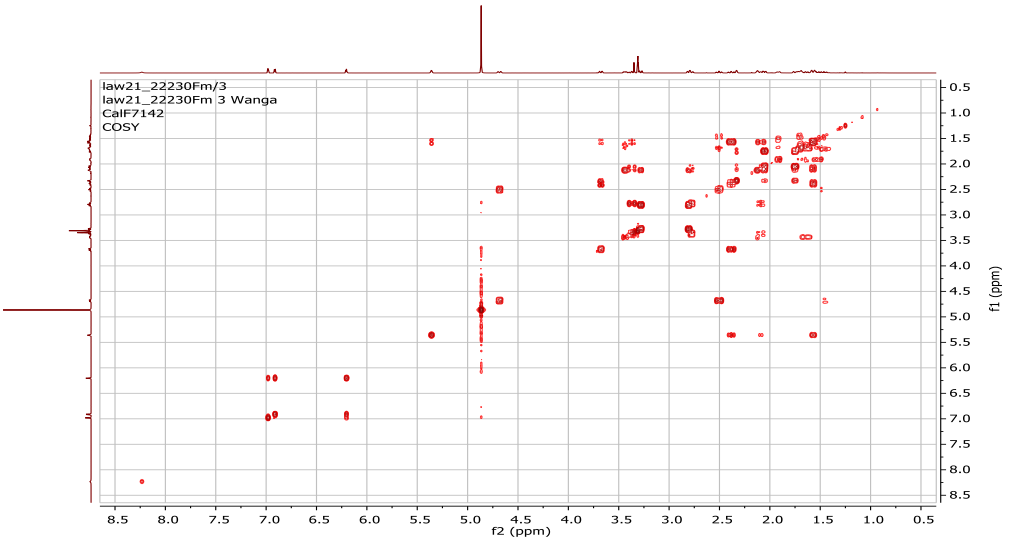

Appendix 43: UV/Vis spectrum of compound **50** in MeOH.

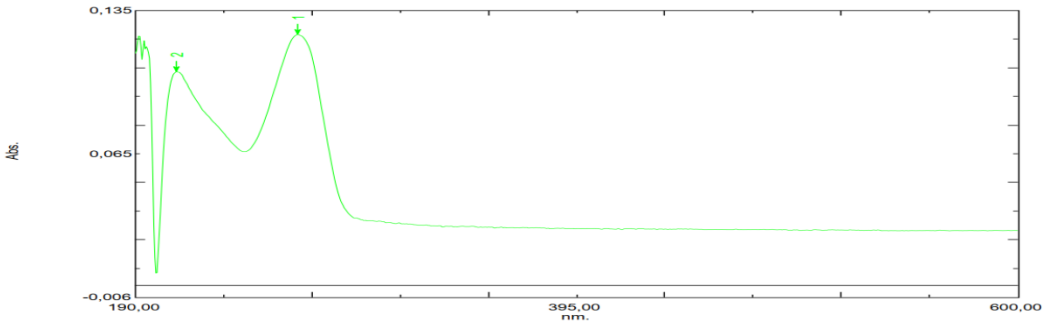

Appendix 44: HPLC-DAD chromatogram of compound **51**

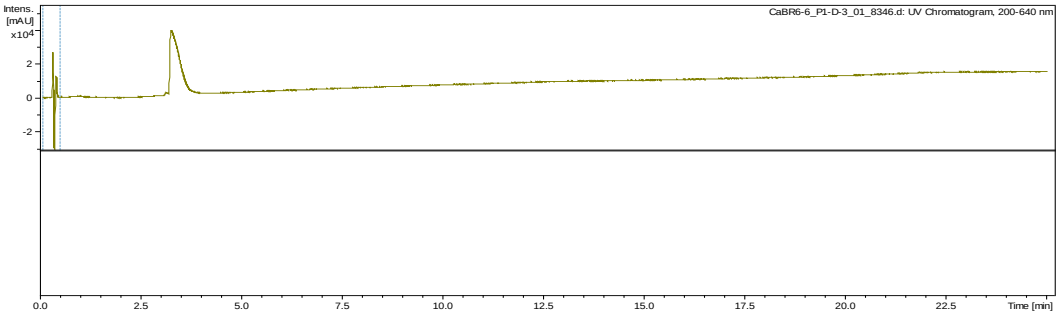

Appendix 45: HR-(+) ESIMS spectrum of compound **51**

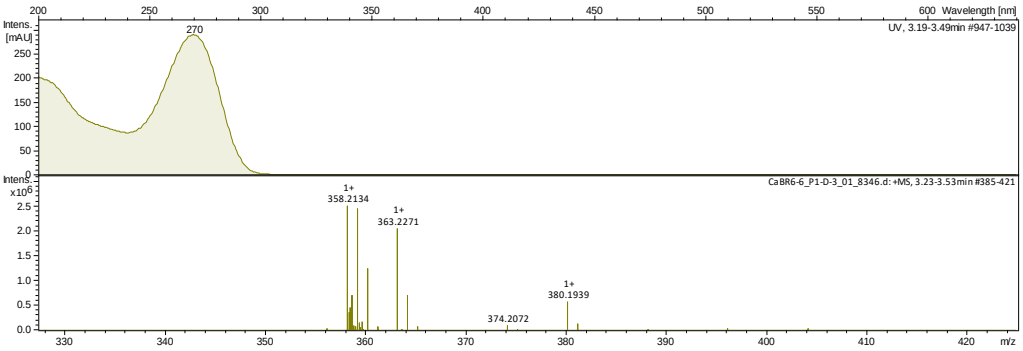

Appendix 46: ^{1}H NMR spectrum (500 MHz, MeOH) of compound **51**

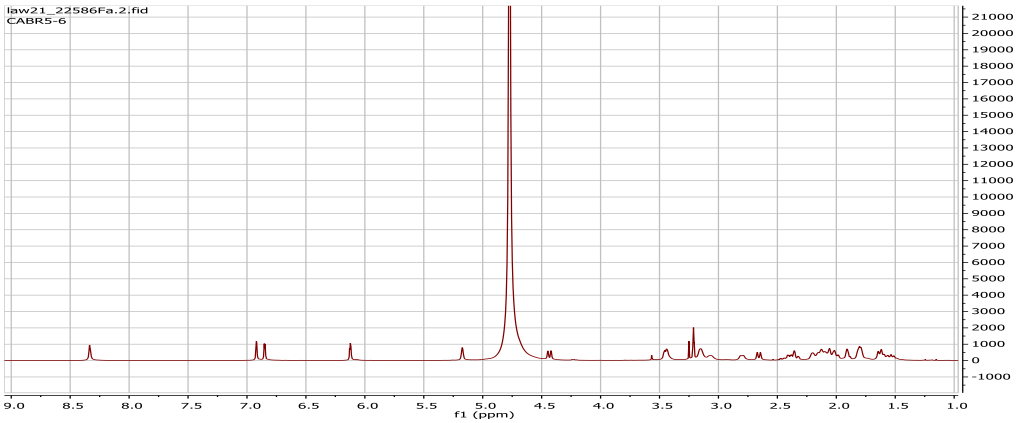

Appendix 47: ^{1}H, ^{13}C HSQC-DEPT spectrum (500 MHz, MeOH) of compound **51**

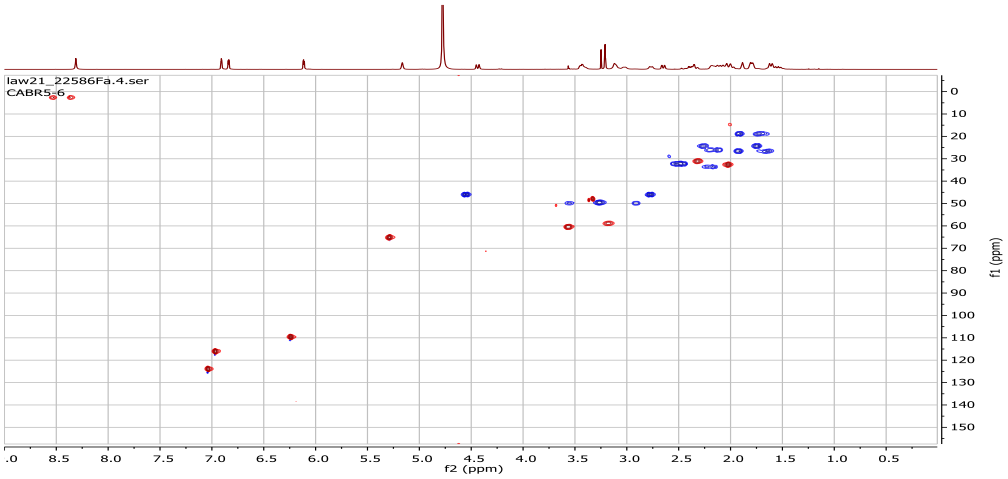

Appendix 48: ^{1}H, ^{13}C HMBC spectrum (500 MHz, MeOH) of compound **51**

Appendix 49: ^{1}H, ^{1}H COSY spectrum (500 MHz, MeOH) of compound **51**.

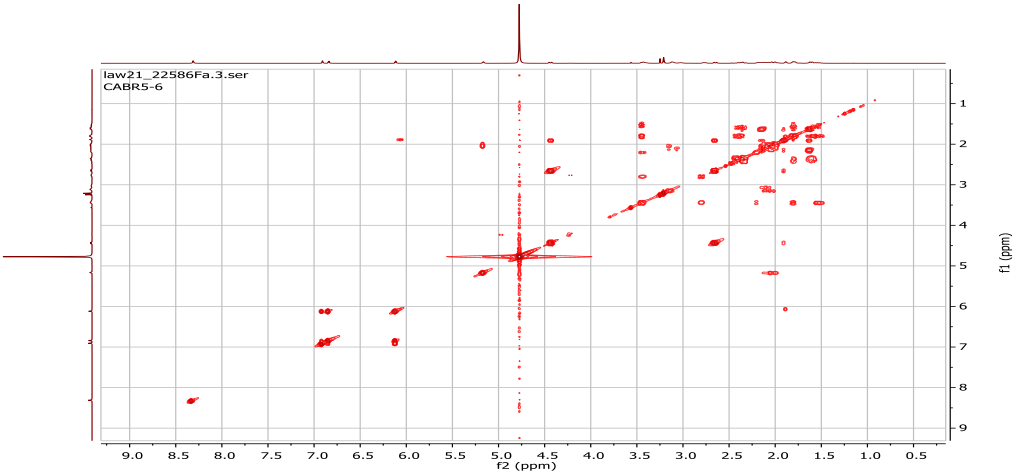

Appendix 50: UV/Vis spectrum of compound **51** in MeOH.

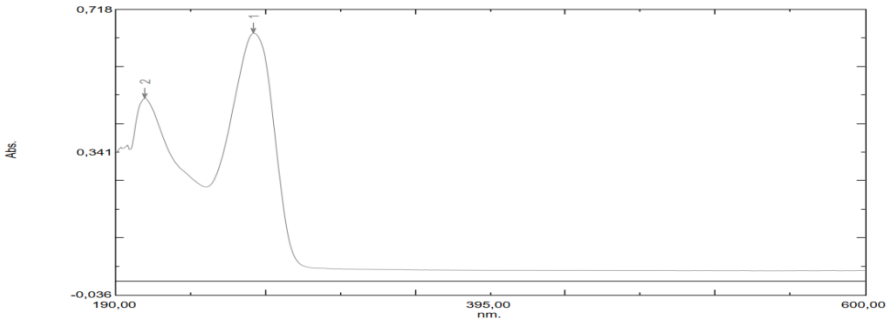

Appendix 51: HPLC-DAD chromatogram of compound **52**

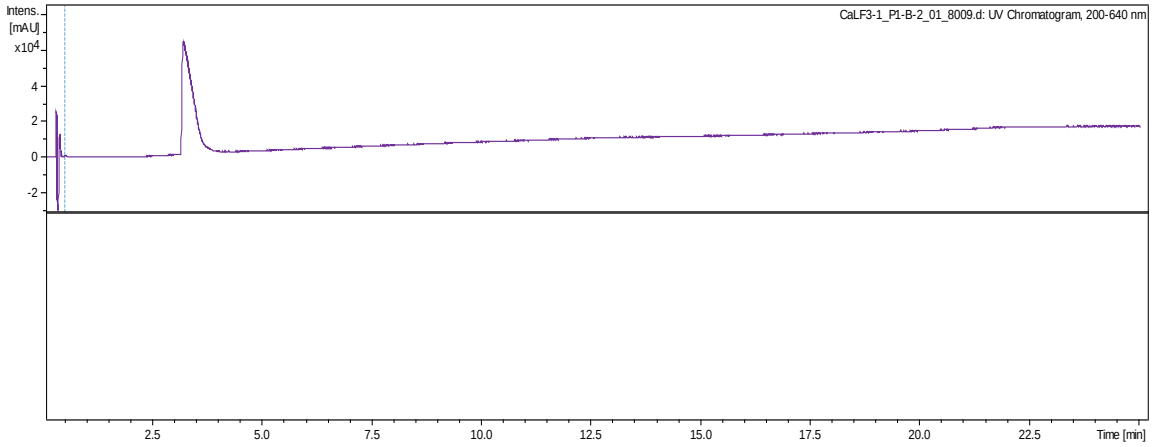

Appendix 52: HR-(+) ESIMS spectrum of compound **52**

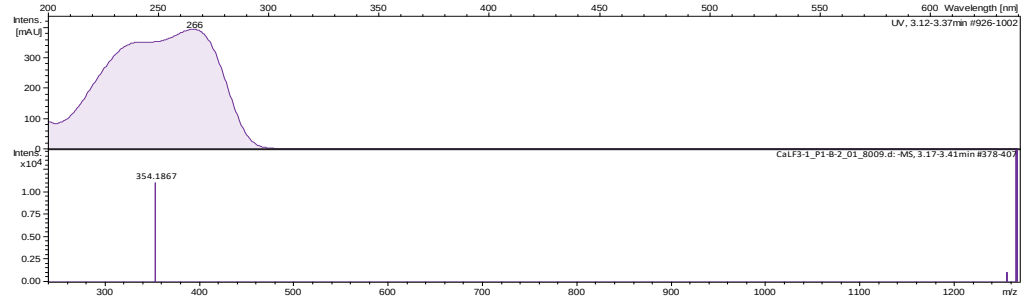

Appendix 53: 1H NMR spectrum (500 MHz, MeOH) of compound **52**

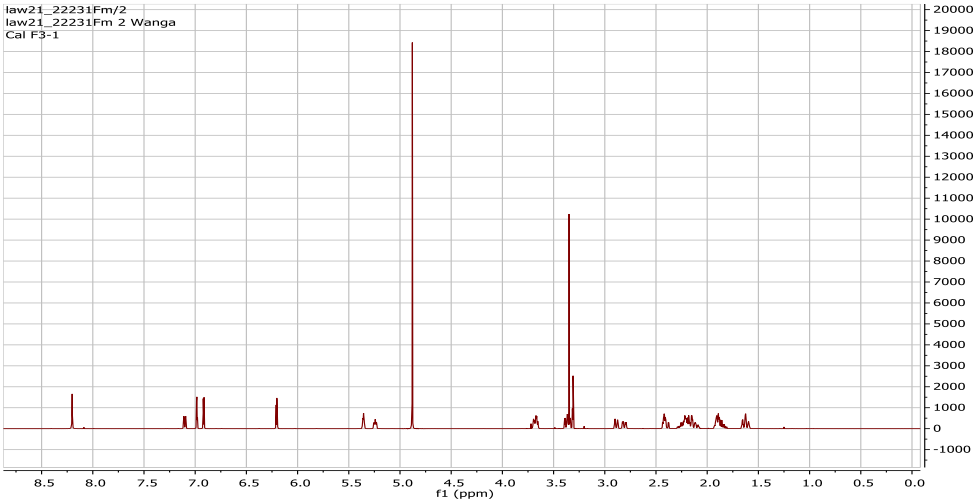

Appendix 54: ^{1}H, ^{13}C HSQC-DEPT spectrum (500 MHz, MeOH) of compound **52**.

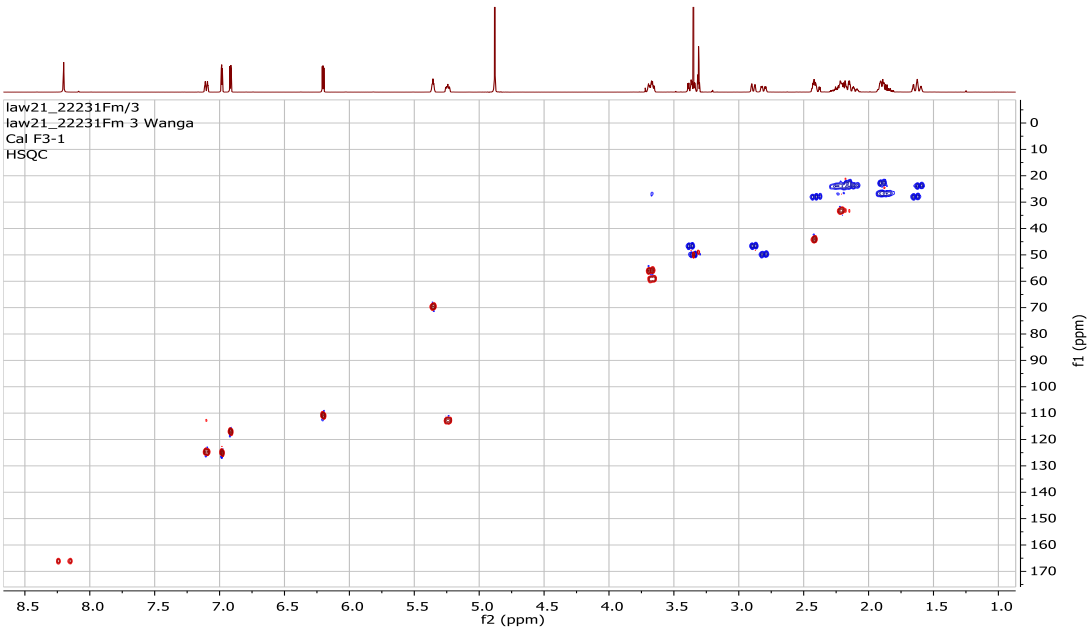

Appendix 55: ^{1}H, ^{13}C HMBC spectrum (500 MHz, MeOH) of compound **52**

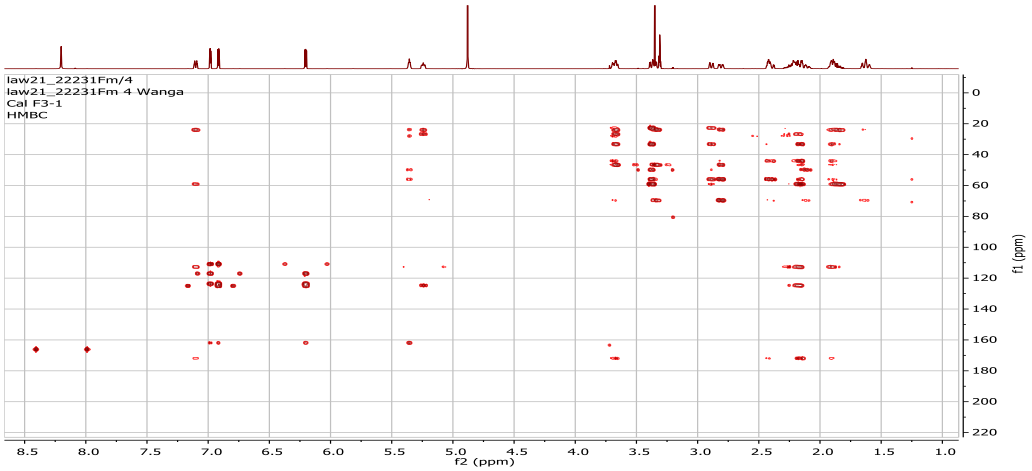

Appendix 56: ^{1}H, ^{1}H COSY spectrum (500 MHz, MeOH) of compound **52**.

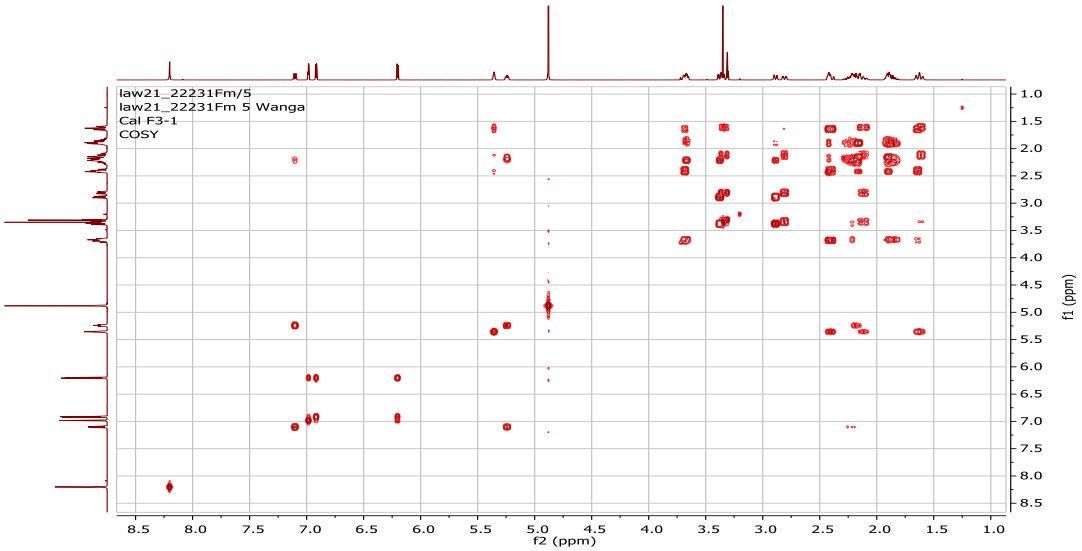

Appendix 57: HPLC-DAD chromatogram of compound **53**

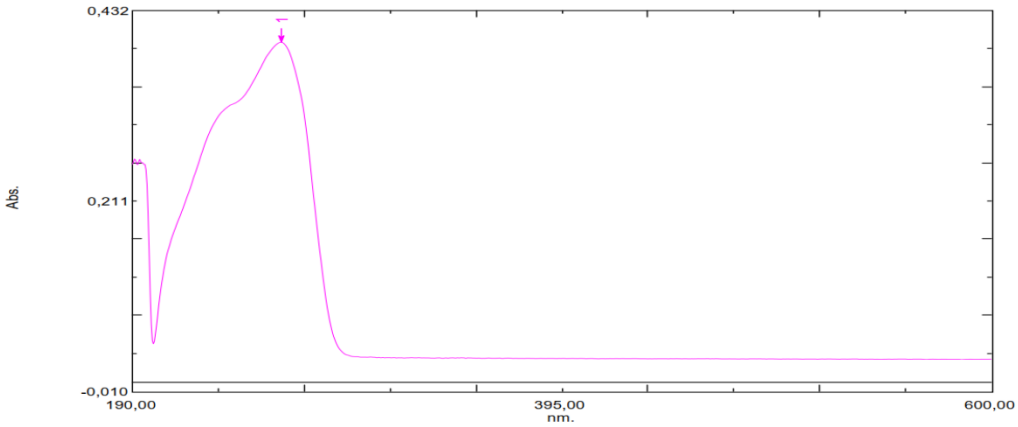

Appendix 58: ^{1}H NMR spectrum (500 MHz, MeOH) of compound **53**.

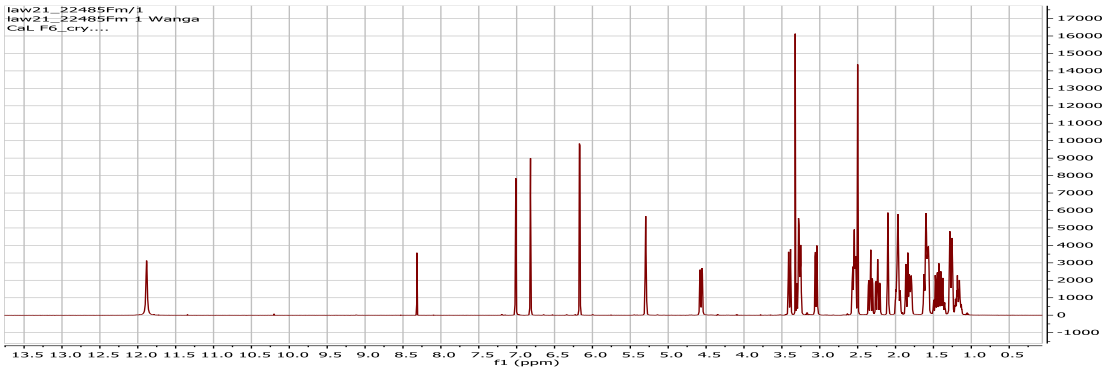

Appendix 59: ^{13}C NMR spectrum (500 MHz, MeOH) of compound **53.**

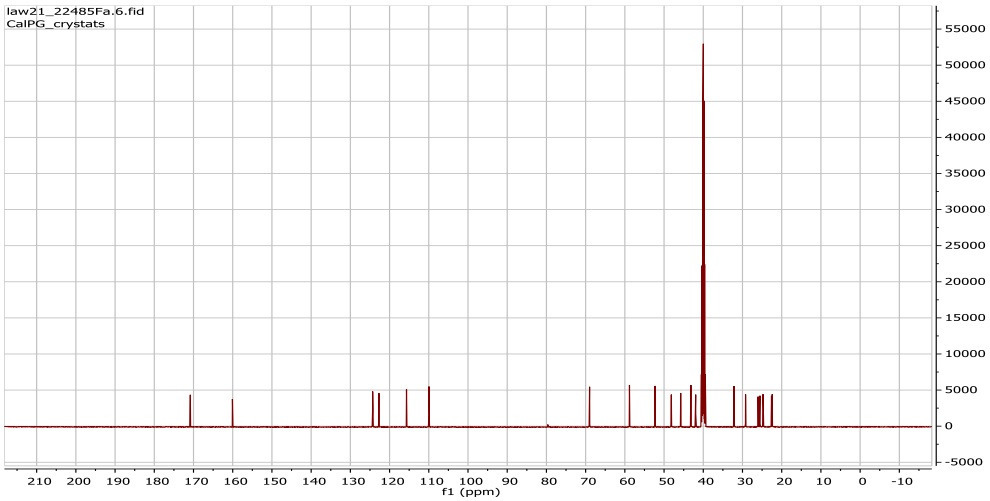

Appendix 60: ^{1}H, ^{13}C HSQC-DEPT spectrum (500 MHz, MeOH) of compound **53**.

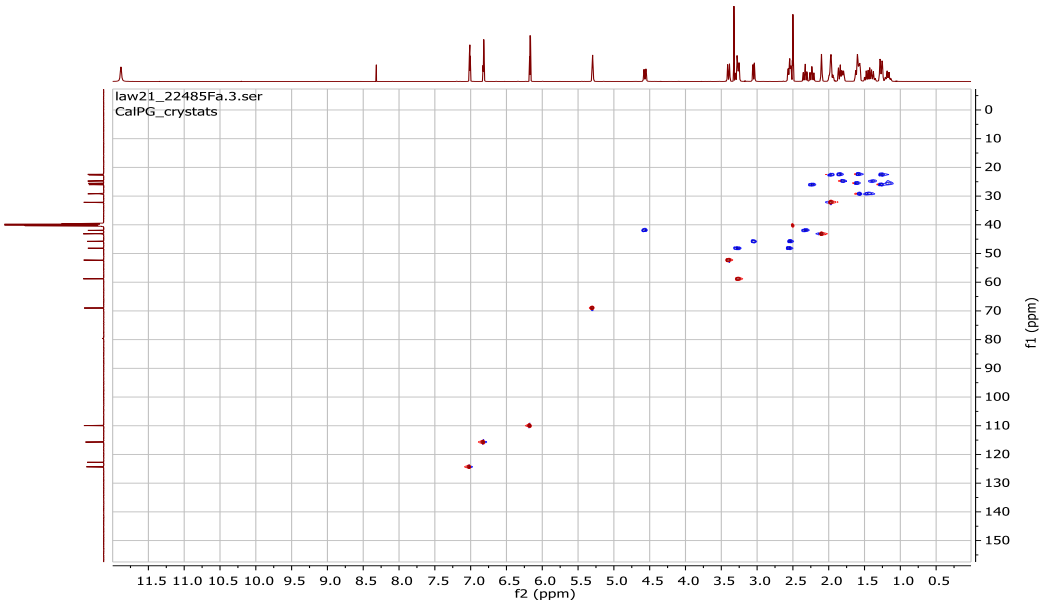

Appendix 61: ^{1}H, ^{13}C HMBC spectrum (500 MHz, MeOH) of compound **53**.

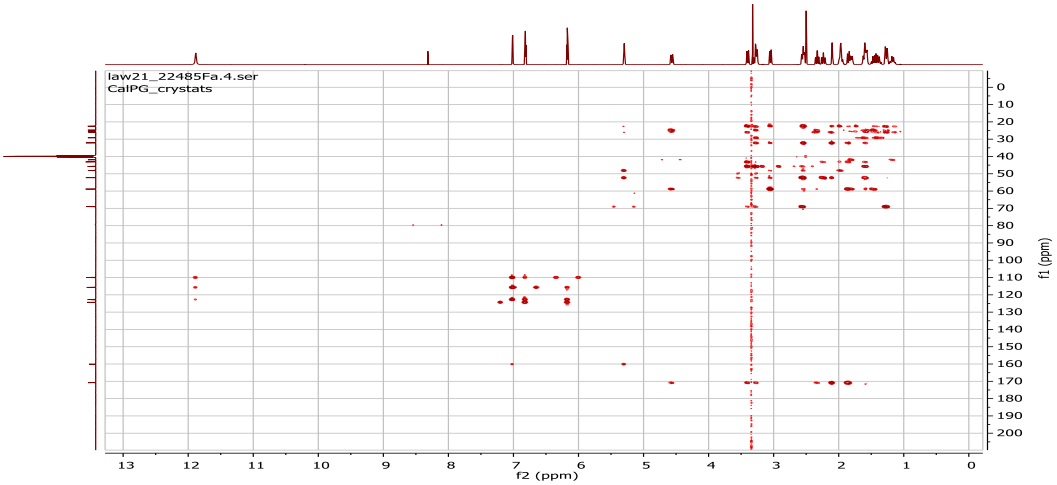

Appendix 62: ^{1}H, ^{1}H COSY spectrum (500 MHz, MeOH) of compound **53**.

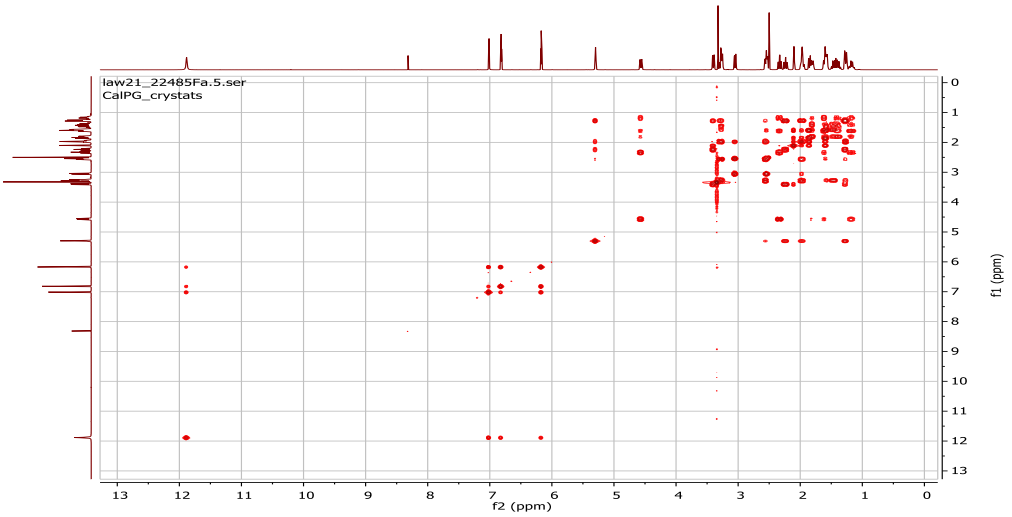

Appendix 63: UV/Vis spectrum of compound **53** in MeOH.

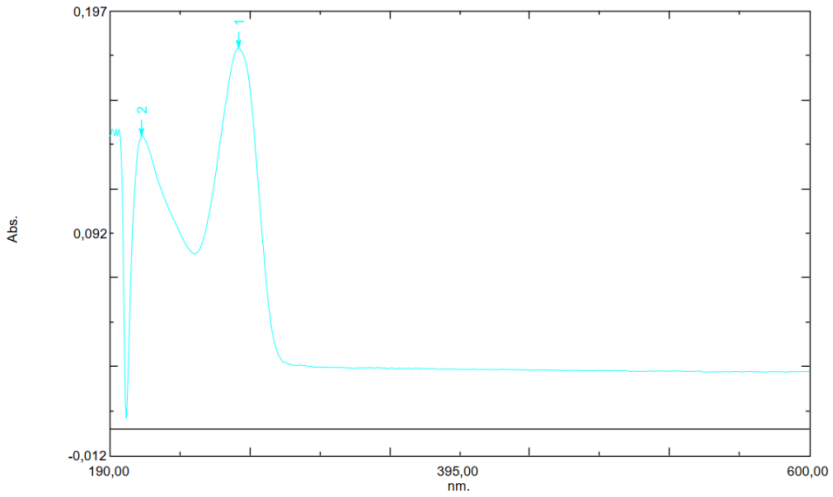

Appendix 64: HPLC-DAD chromatogram of compound **54**

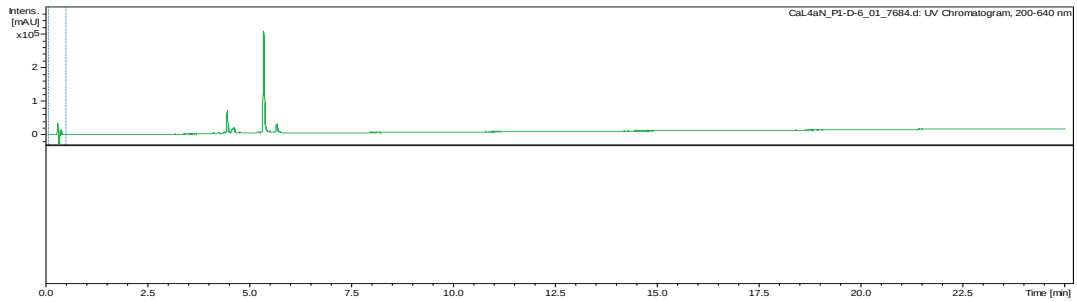

Appendix 65: HR-(+) ESIMS spectrum of compound **54**

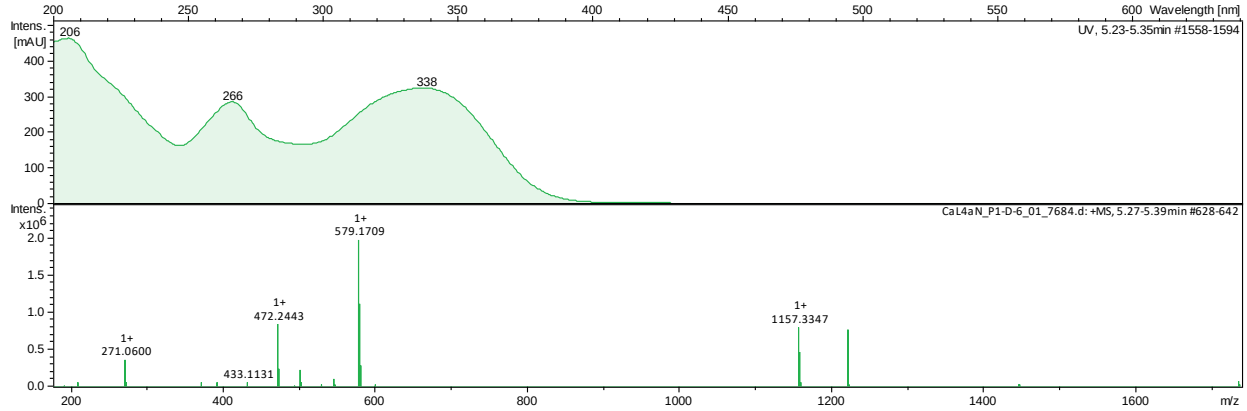

Appendix 66: ^{13}C NMR spectrum (700 MHz, CD_3OD) of compound **54**

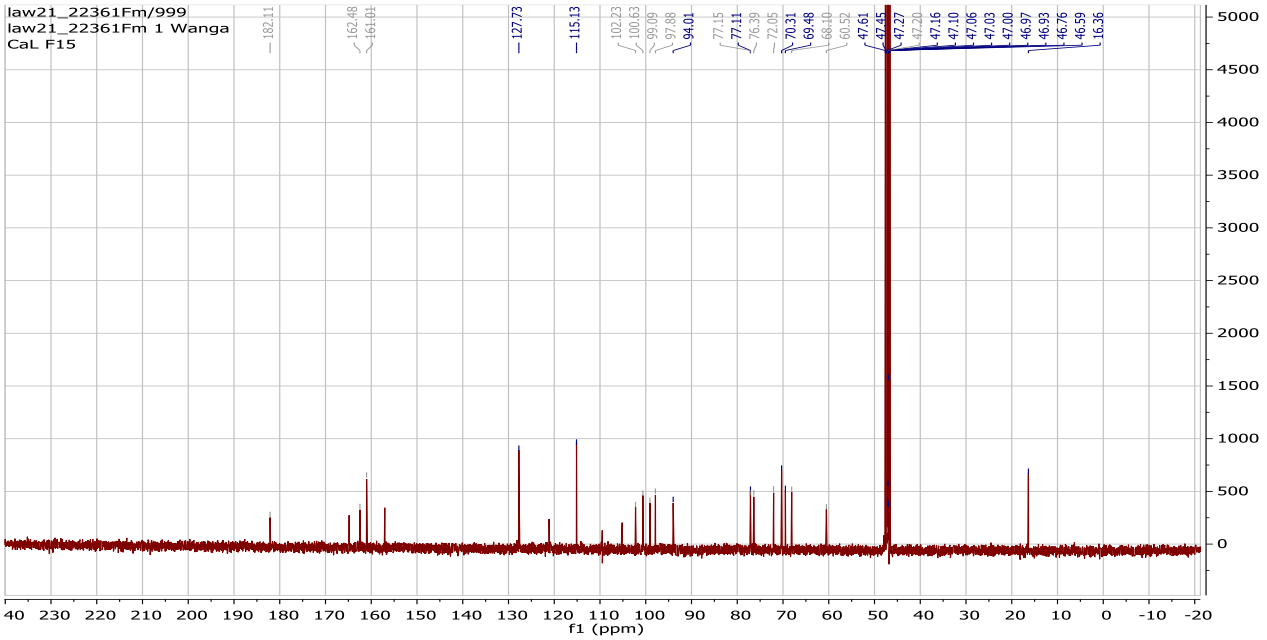

Appendix 67: ^{1}H NMR spectrum (700 MHz, CD_3OD) of compound **54**.

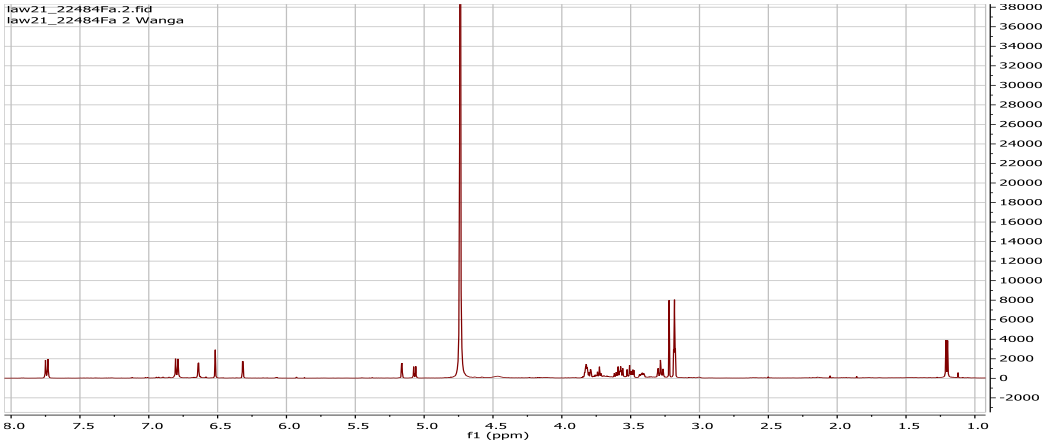

Appendix 68: ^{13}C HSQC-DEPT spectrum (500 MHz, CD_3OD) of compound **54**

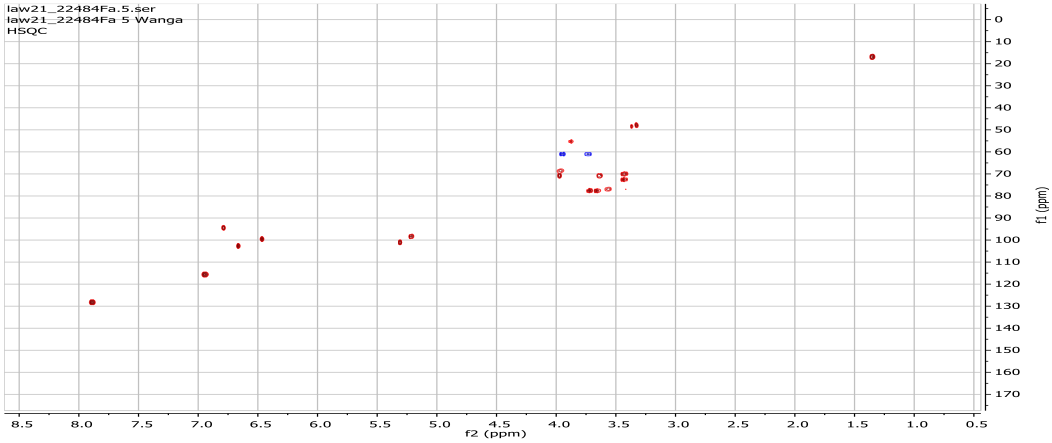

Appendix 69: ^{1}H, ^{13}C HMBC spectrum (500 MHz, MeOH) of compound **54**

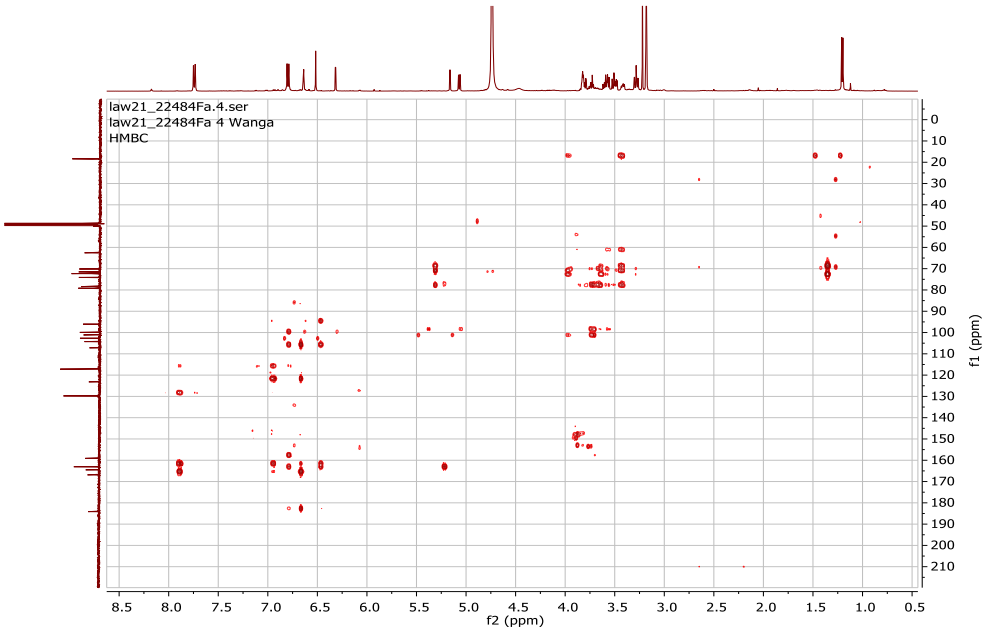

Appendix 70: ^{1}H, ^{1}H COSY spectrum (500 MHz, MeOH) of compound **54**

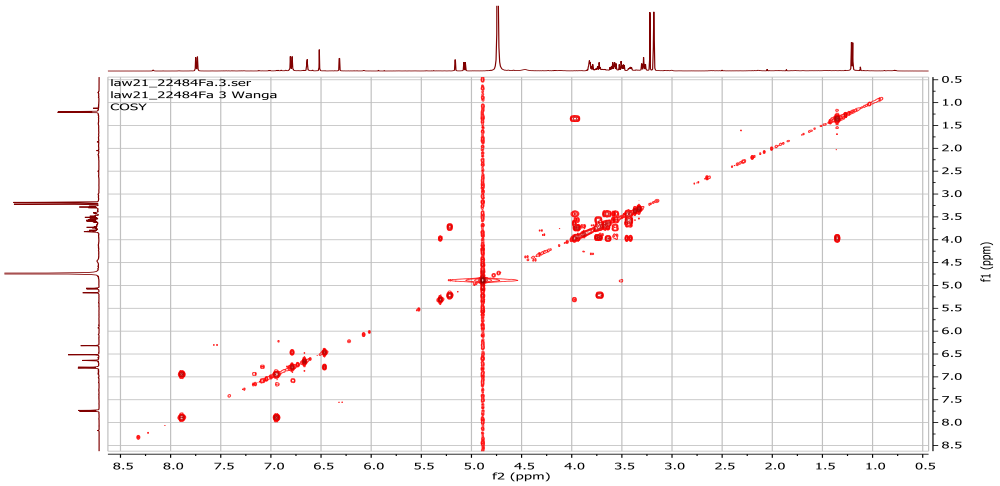

Appendix 71: UV/Vis spectrum of compound **54** in MeOH

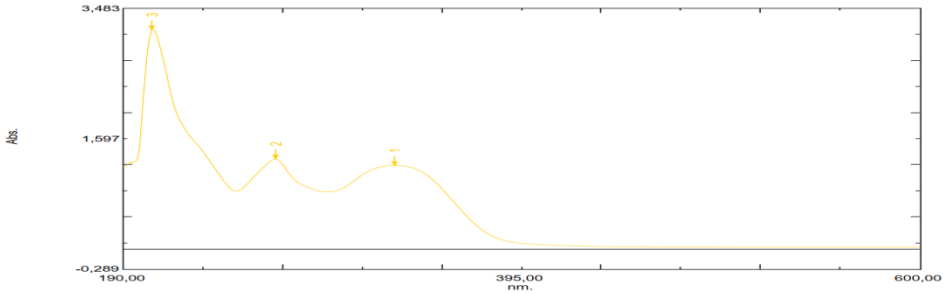

Appendix 72: HPLC-DAD chromatogram of compound **55.**

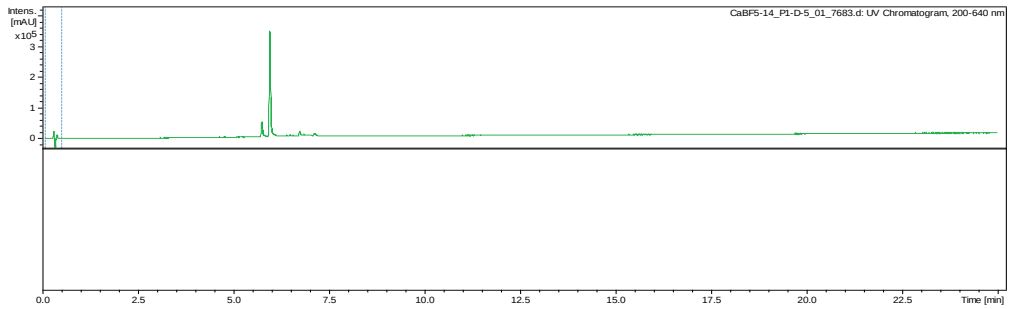

Appendix 73: HR-(+) ESIMS spectrum of compound **55**

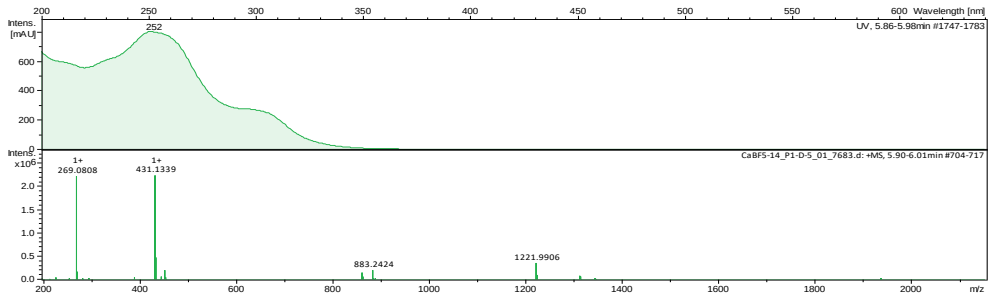

Appendix 74: ^{1}H NMR spectrum (500 MHz, MeOH) of compound **55**

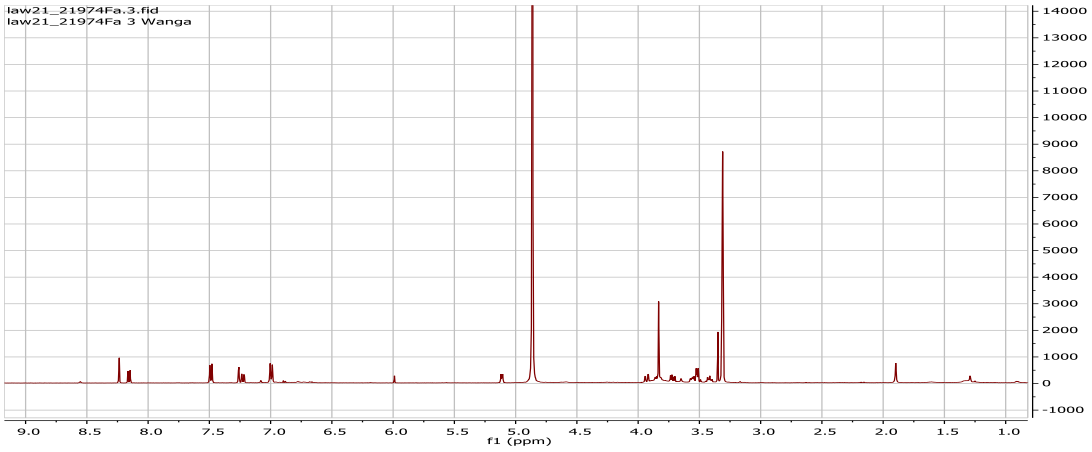

Appendix 75: ^{13}C HSQC-DEPT spectrum (500 MHz, CD_3OD) of compound **55**

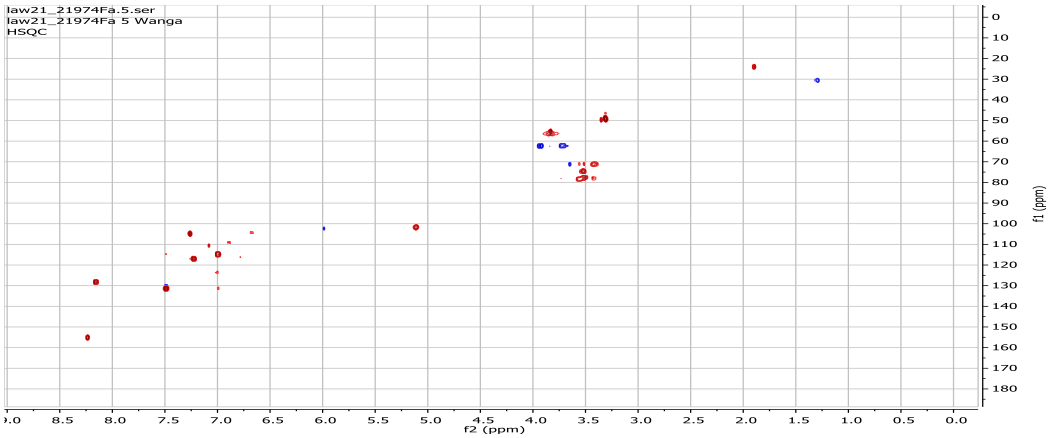

Appendix 76: ^{1}H, ^{13}C HMBC spectrum (500 MHz, MeOH) of compound **55**

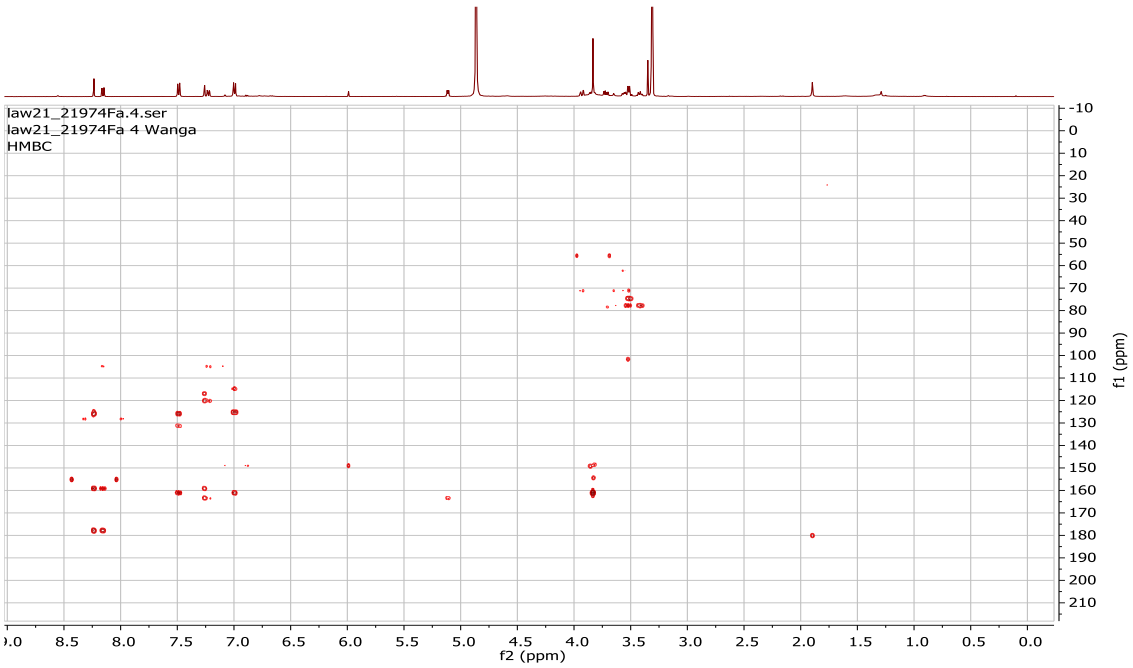

Appendix 77: ^{1}H, ^{1}H COSY spectrum (500 MHz, MeOH) of compound **55**

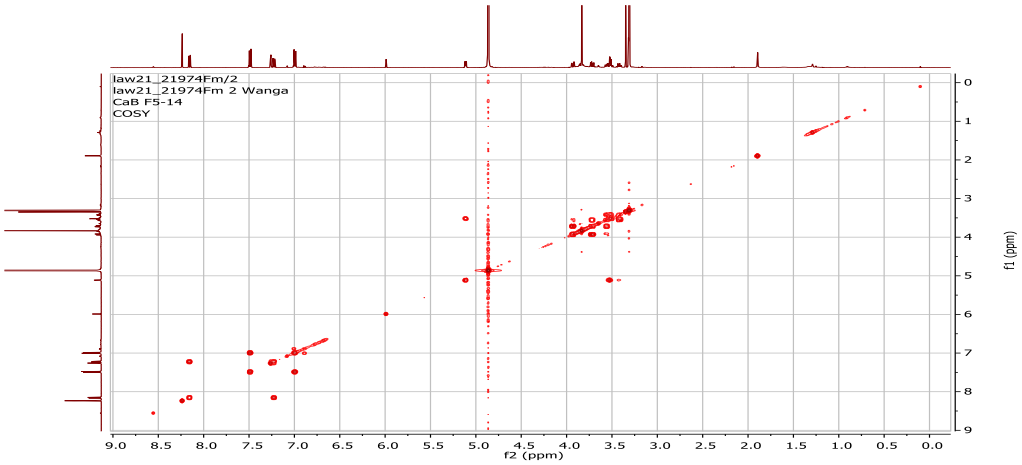

Appendix 78: UV/Vis spectrum of compound **55** in MeOH

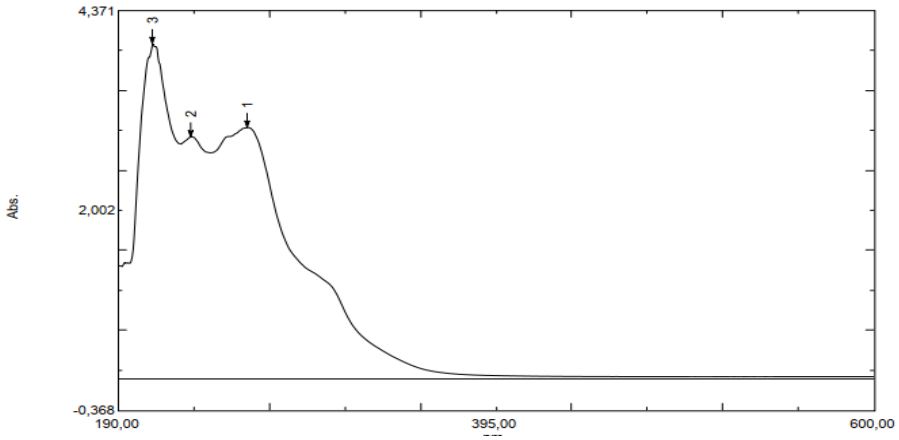

Appendix 79: HPLC-DAD chromatogram of compound **56**

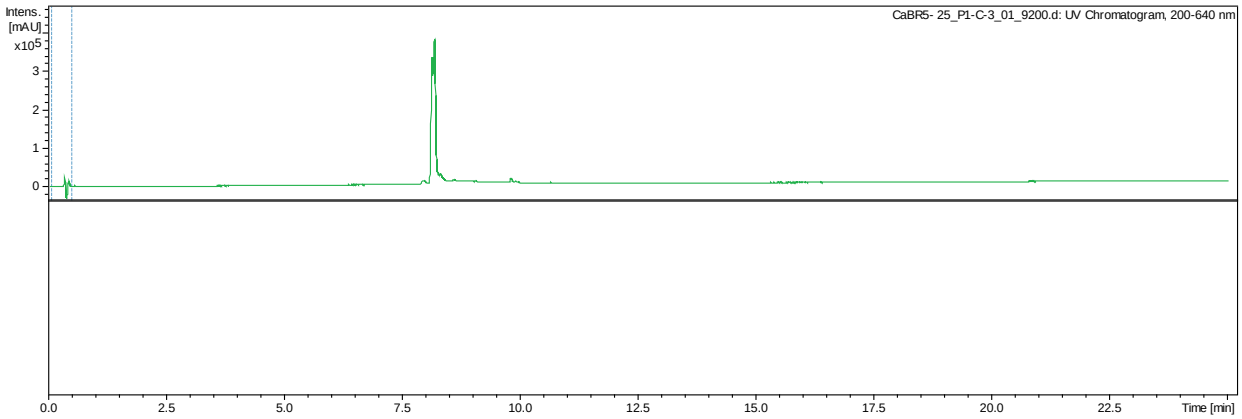

Appendix 80: HR-(+) ESIMS spectrum of compound **56**

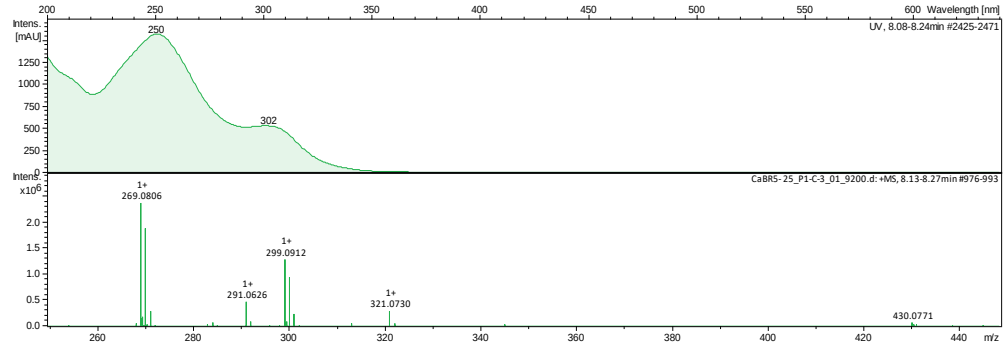

Appendix 81: ^{1}H NMR spectrum (700 MHz, CD_3OD) of compound **56**

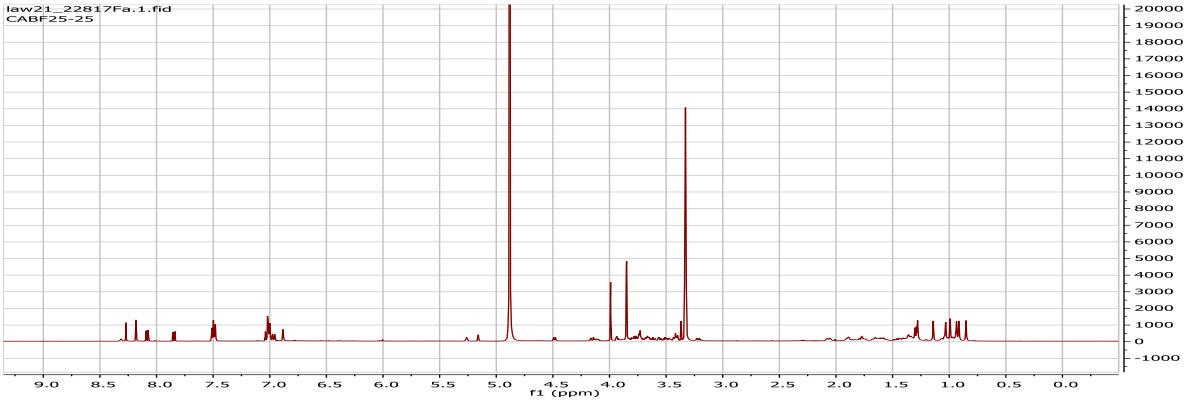

Appendix 82: ^{13}C HSQC-DEPT spectrum (500 MHz, CD_3OD) of compound **56**

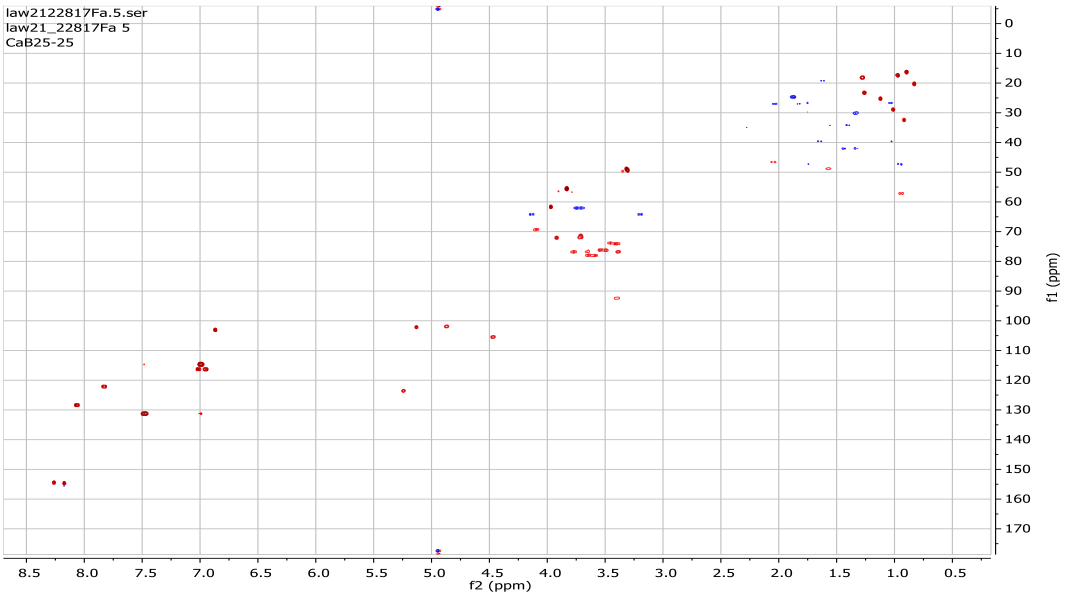

Appendix 83: ^{1}H, ^{13}C HMBC spectrum (500 MHz, MeOH) of compound **56**

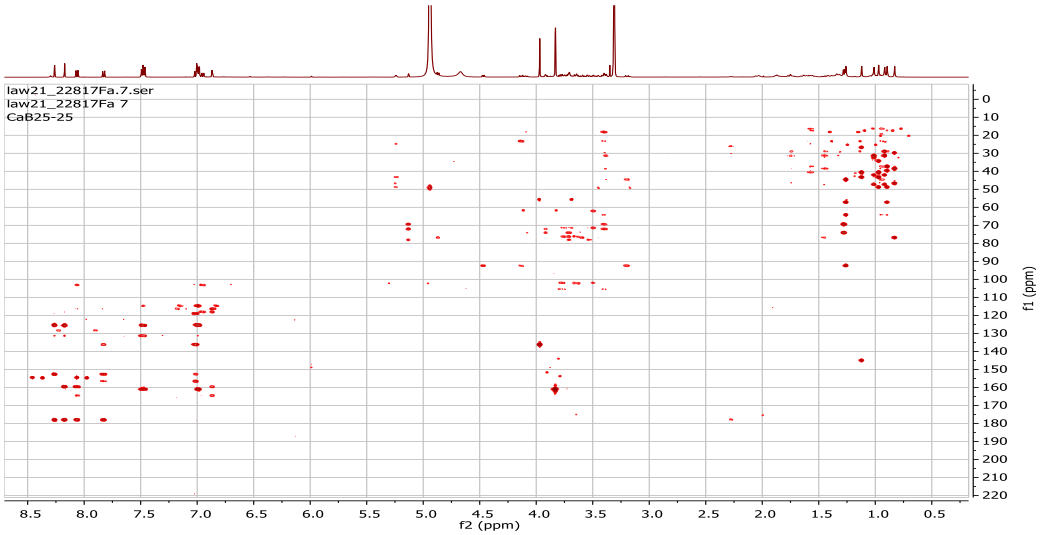

Appendix 84: ^{1}H, ^{1}H COSY spectrum (500 MHz, MeOH) of compound **56**.

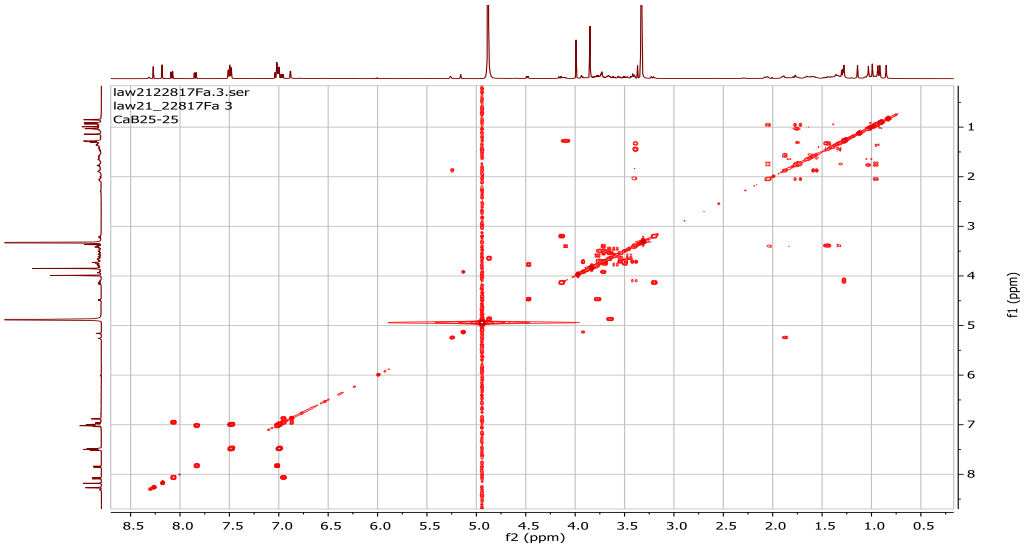

Appendix 85: UV/Vis spectrum of compound **56** in MeOH

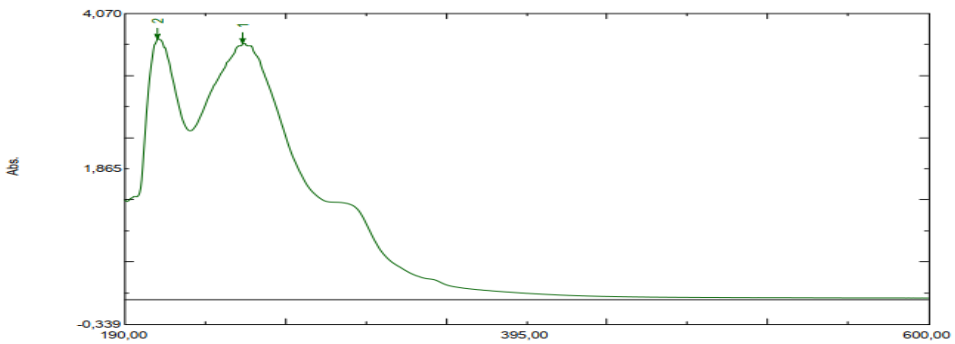

Appendix 86: HPLC-DAD chromatogram of compound **57**

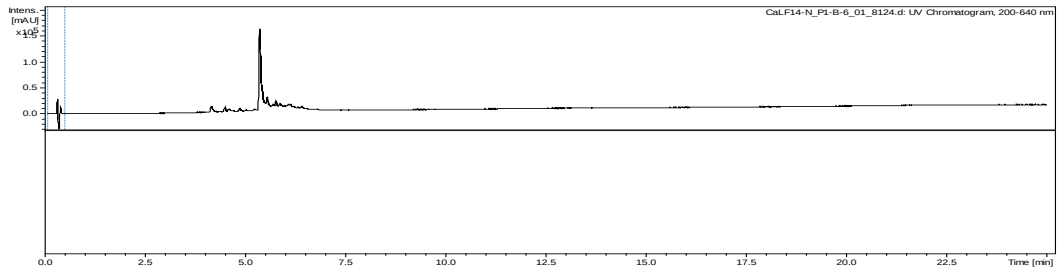

Appendix 87: HR-(+) ESIMS spectrum of compound **57**

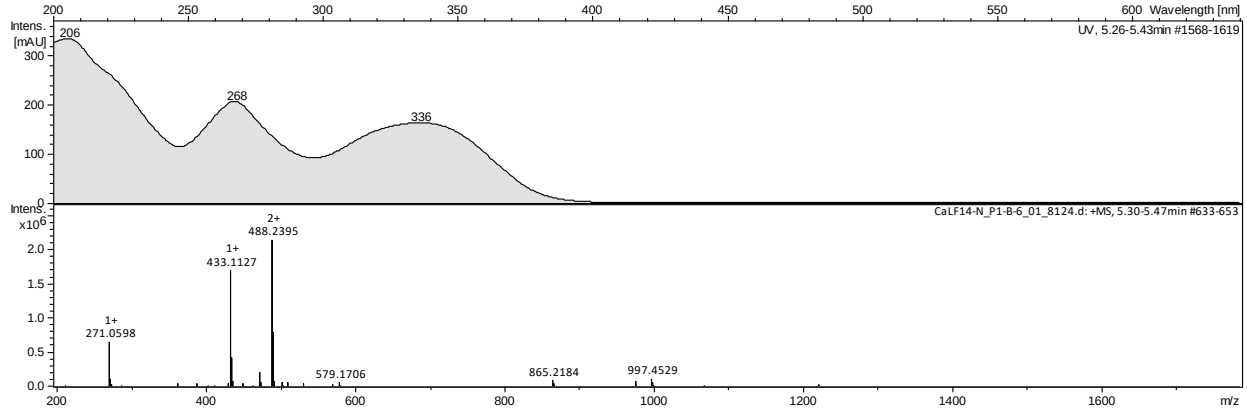

Appendix 88: ^{1}H NMR spectrum (700 MHz, CD_3OD) of compound **57**

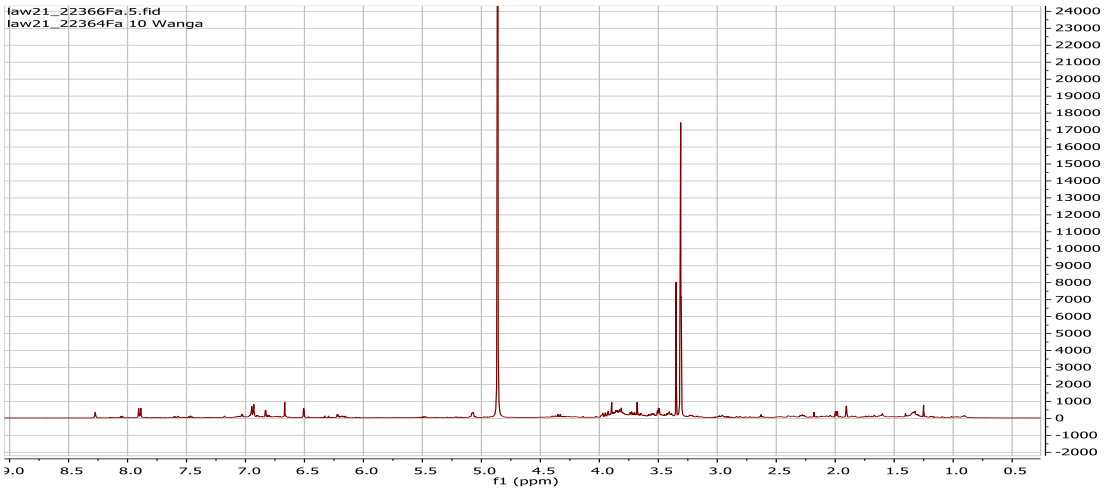

Appendix 89: ^{1}H, ^{13}C HSQC-DEPT spectrum (500 MHz, MeOH) of compound **57**

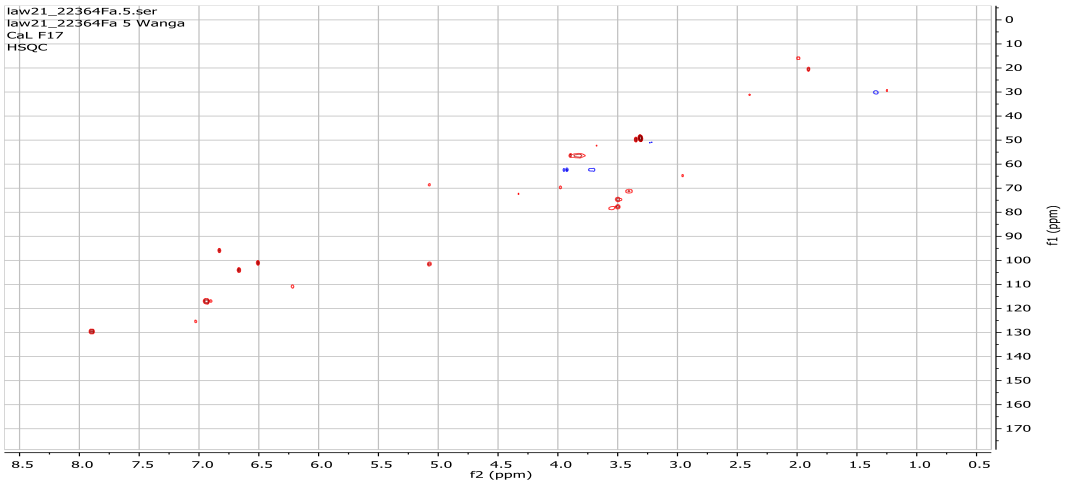

Appendix 90: ^{1}H, ^{13}C HMBC spectrum (500 MHz, MeOH) of compound **57**

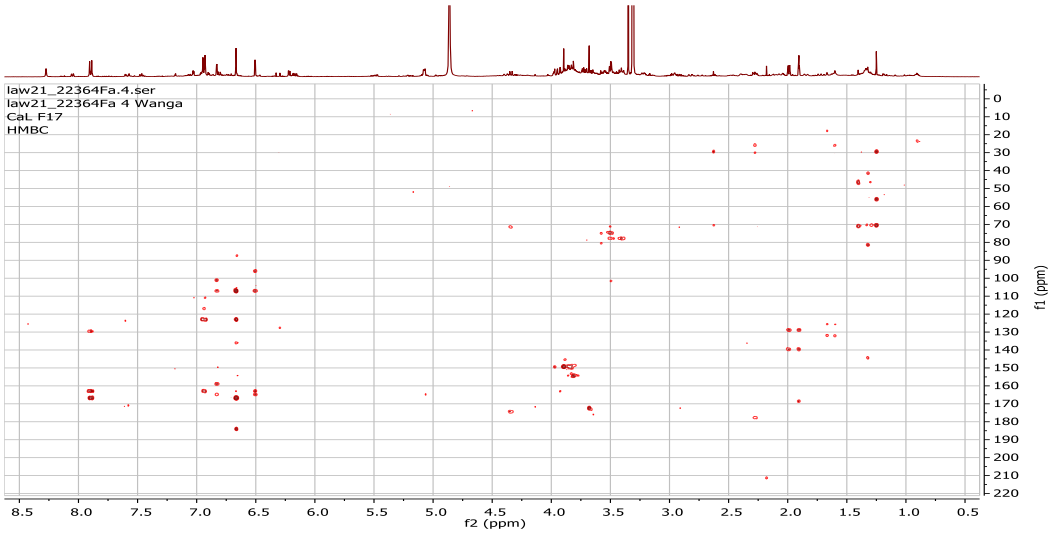

Appendix 91: ^{1}H, ^{1}H COSY spectrum (500 MHz, MeOH) of compound **57**

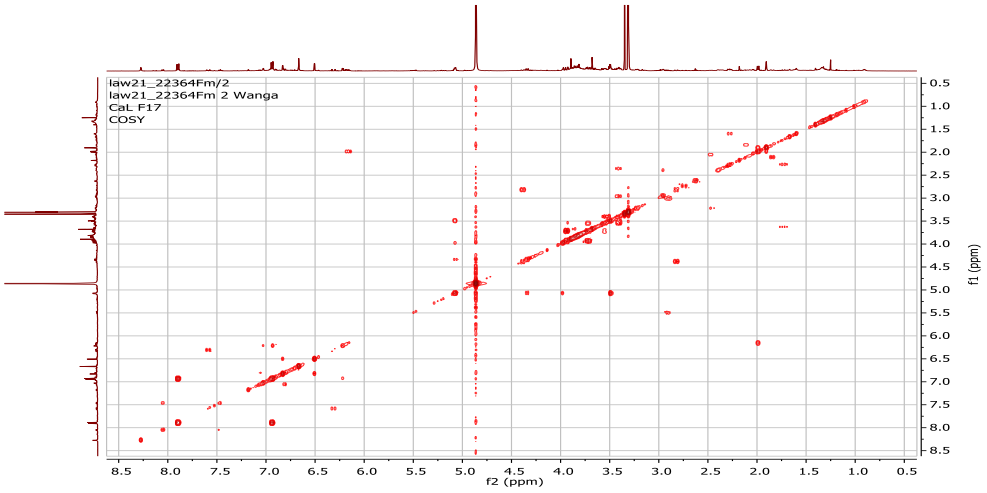

Appendix 92: UV/Vis spectrum of compound **57** in MeOH.

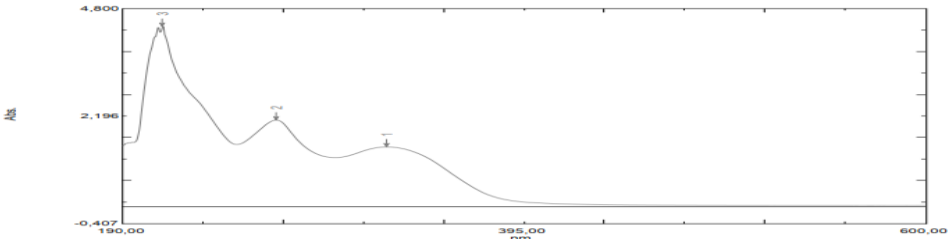

Appendix 93: HPLC-DAD chromatogram of compound **58**

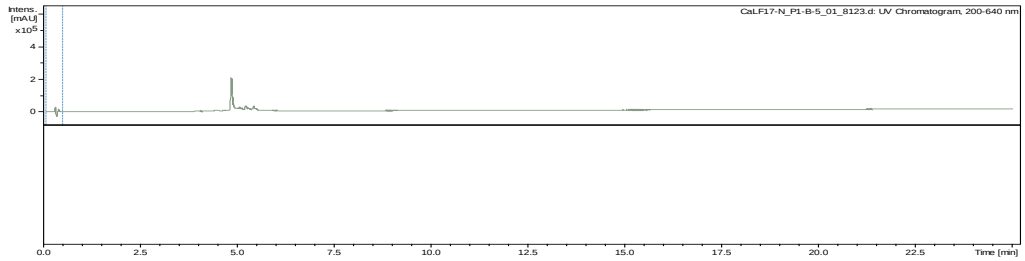

Appendix 94: HR-(+) ESIMS spectrum of compound **58**

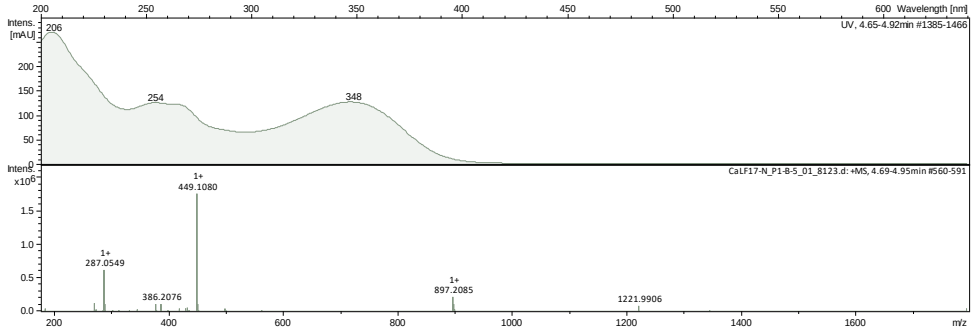

Appendix 95: ^{1}H NMR spectrum (700 MHz, CD_3OD) of compound **58**

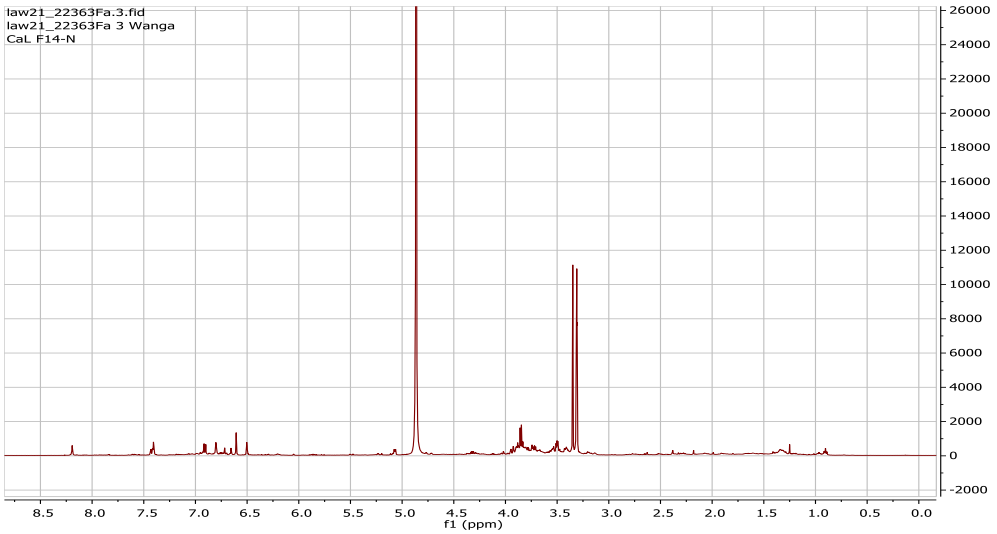

Appendix 96: ^{1}H, ^{13}C HSQC-DEPT spectrum (500 MHz, MeOH) of compound **58**

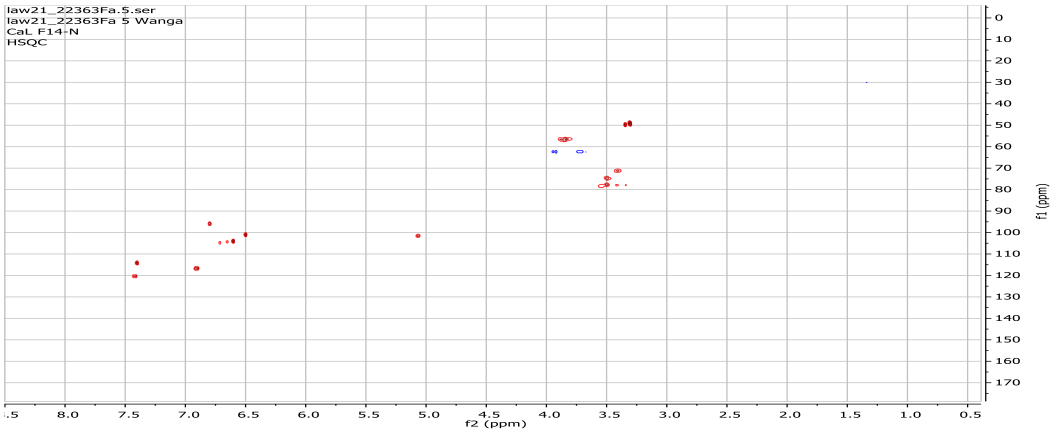

Appendix 97: ^{1}H, ^{13}C HMBC spectrum (500 MHz, MeOH) of compound **58**

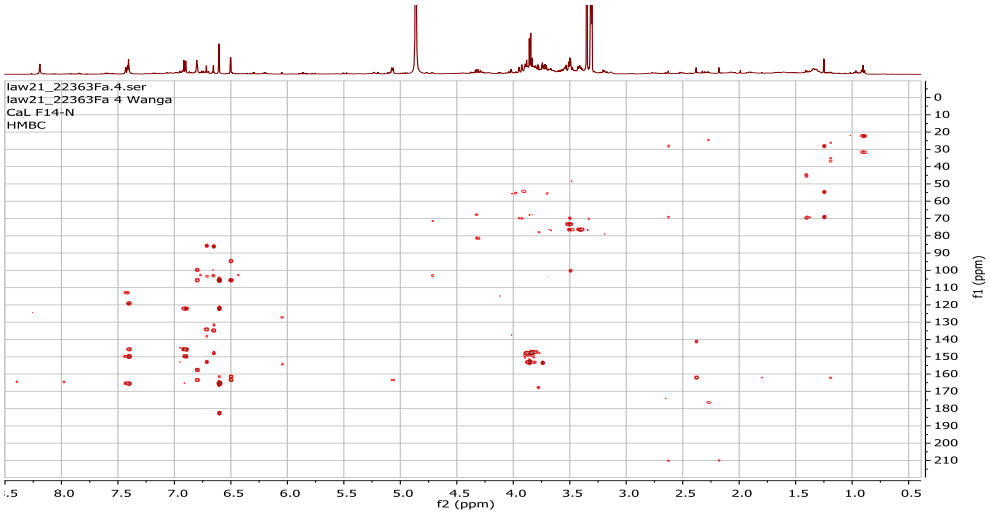

Appendix 98: ^{1}H, ^{1}H COSY spectrum (500 MHz, MeOH) of compound **58**

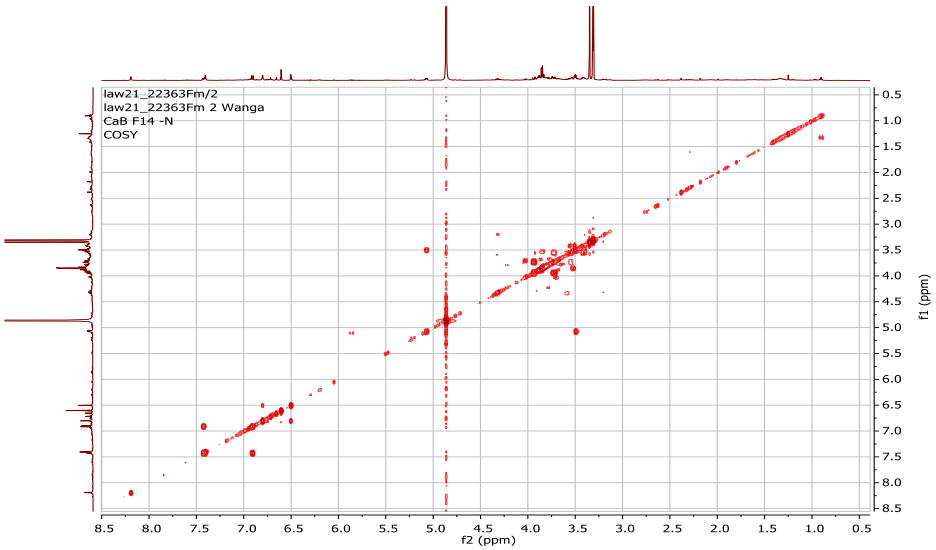

Appendix 99: UV/Vis spectrum of compound **58** in MeOH.

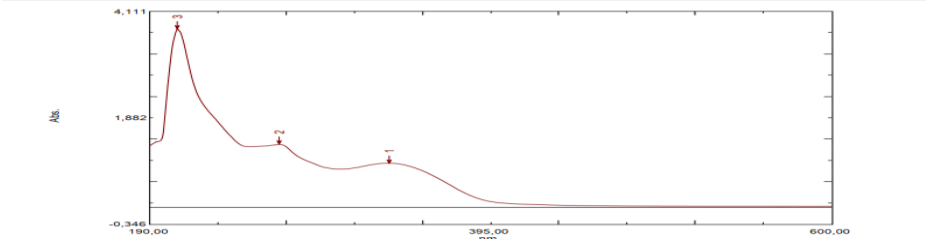

Appendix 100: HPLC-DAD chromatogram of compound **59**

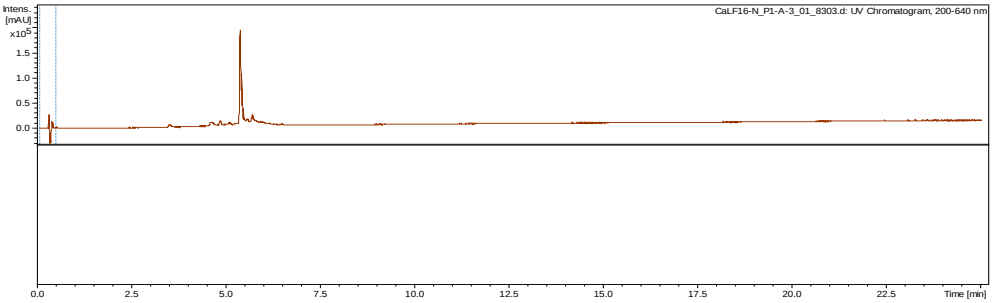

Appendix 101: HR-(+) ESIMS spectrum of compound **59**

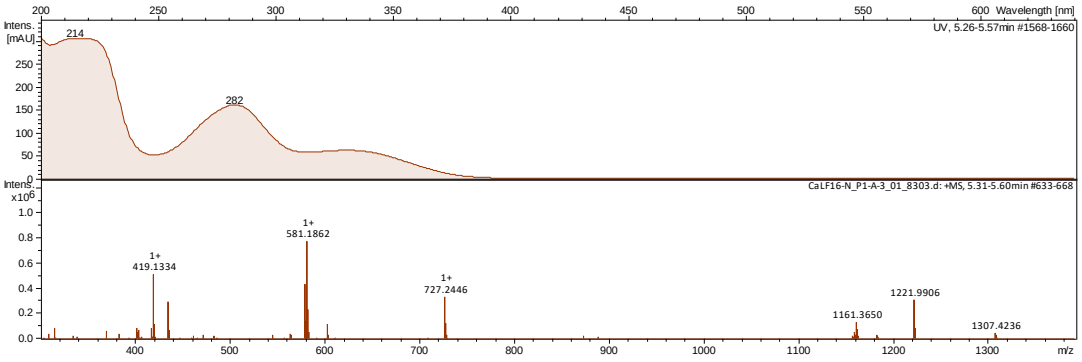

Appendix 102: ^{1}H NMR spectrum (700 MHz, CD_3OD) of compound **59**

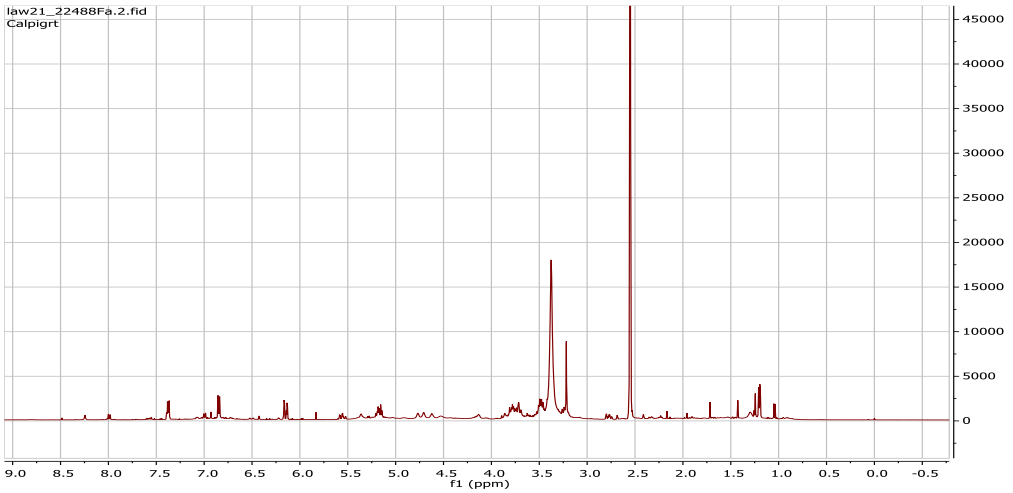

Appendix 103: ^{1}H, ^{13}C HSQC-DEPT spectrum (500 MHz, MeOH) of compound **59**

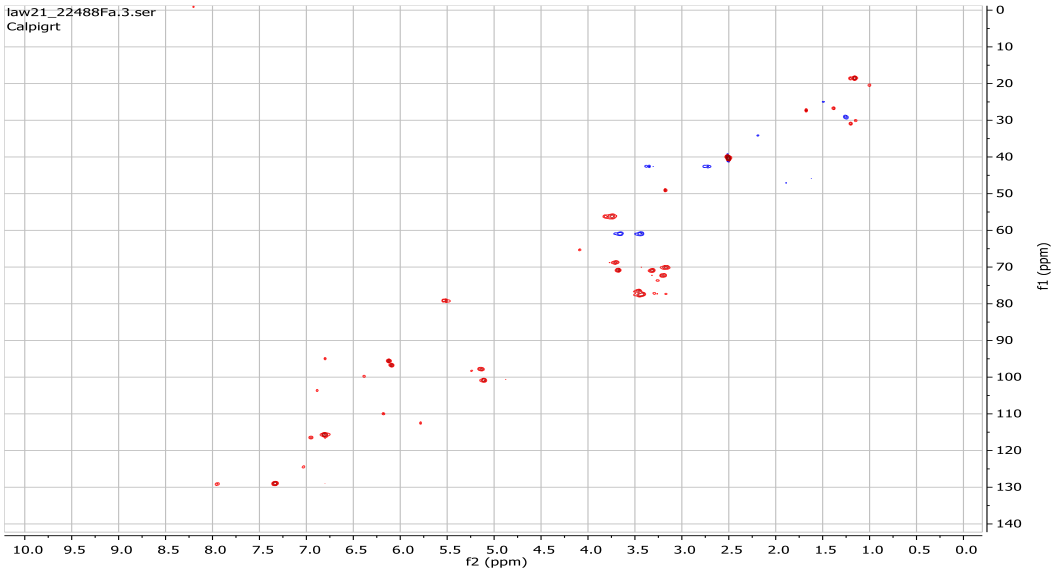

Appendix 104: ^{1}H, ^{13}C HMBC spectrum (500 MHz, MeOH) of compound **59**

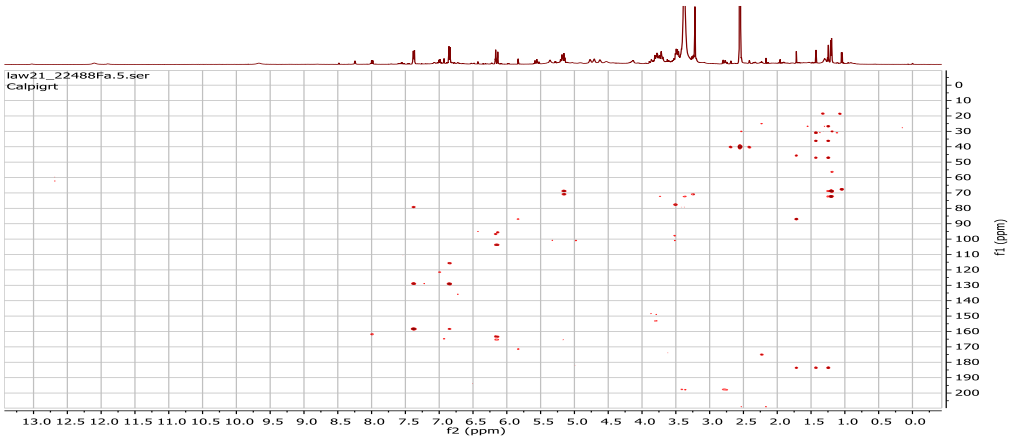

Appendix 105: ^{1}H, ^{1}H COSY spectrum (500 MHz, MeOH) of compound **59**.

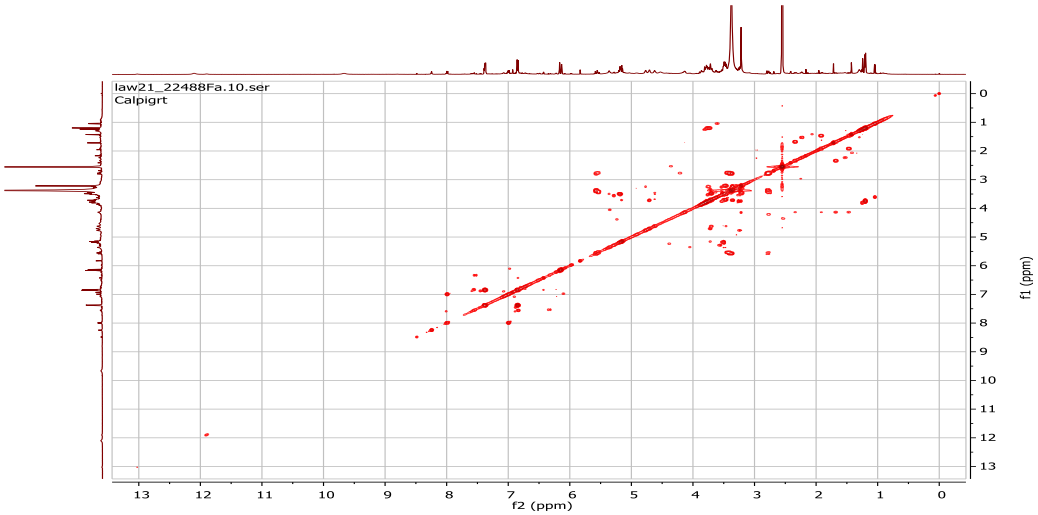

Appendix 106: UV/Vis spectrum of compound **59** in MeOH.

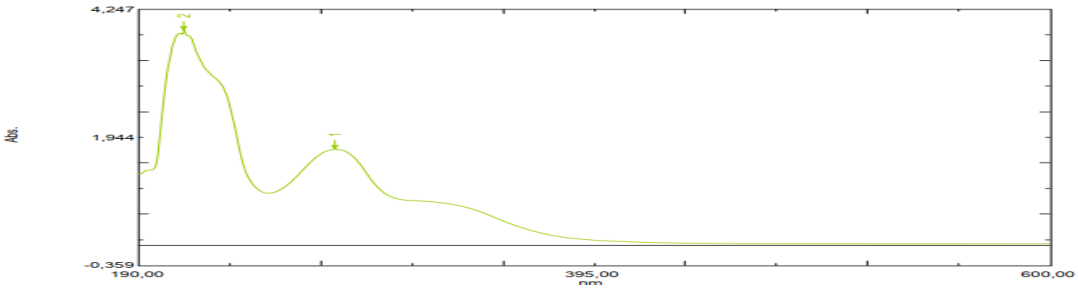

Appendix 107: HPLC-DAD chromatogram of compound **60**

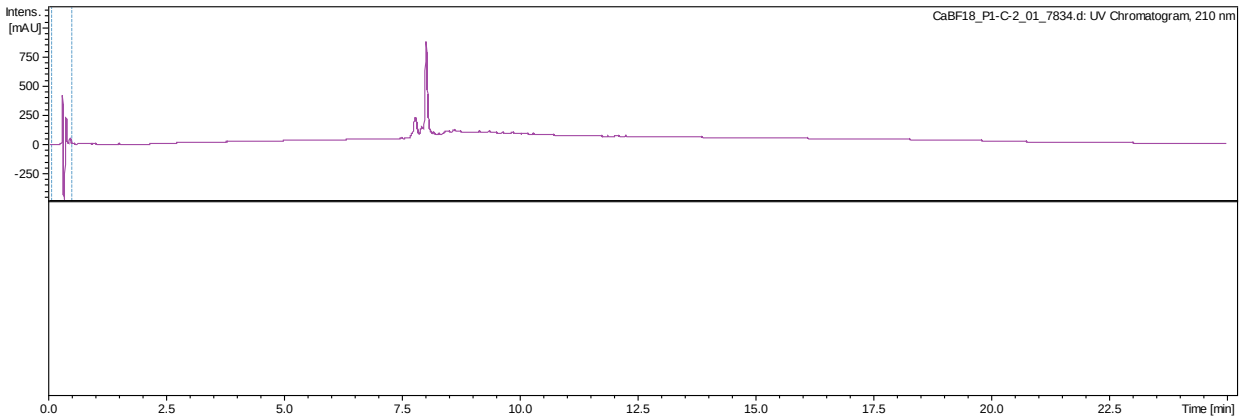

Appendix 108: HR-(+) ESIMS spectrum of compound **60**

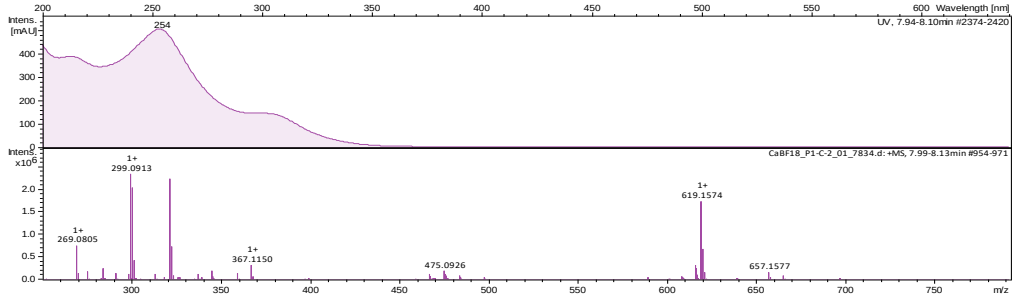

Appendix 109: ^{1}H NMR spectrum (700 MHz, CD_3OD) of compound **60**

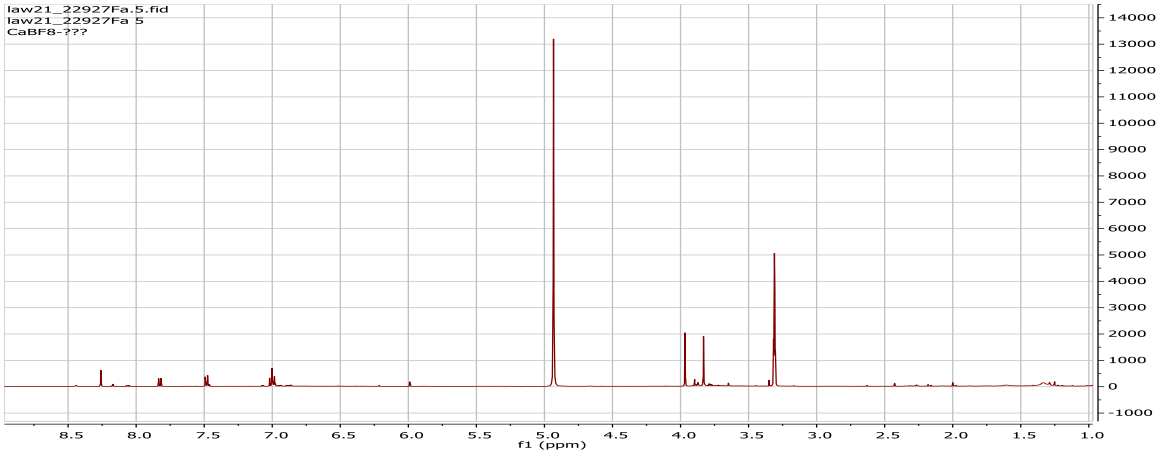

Appendix 110: ^{1}H, ^{13}C HSQC-DEPT spectrum (500 MHz, MeOH) of compound **60**

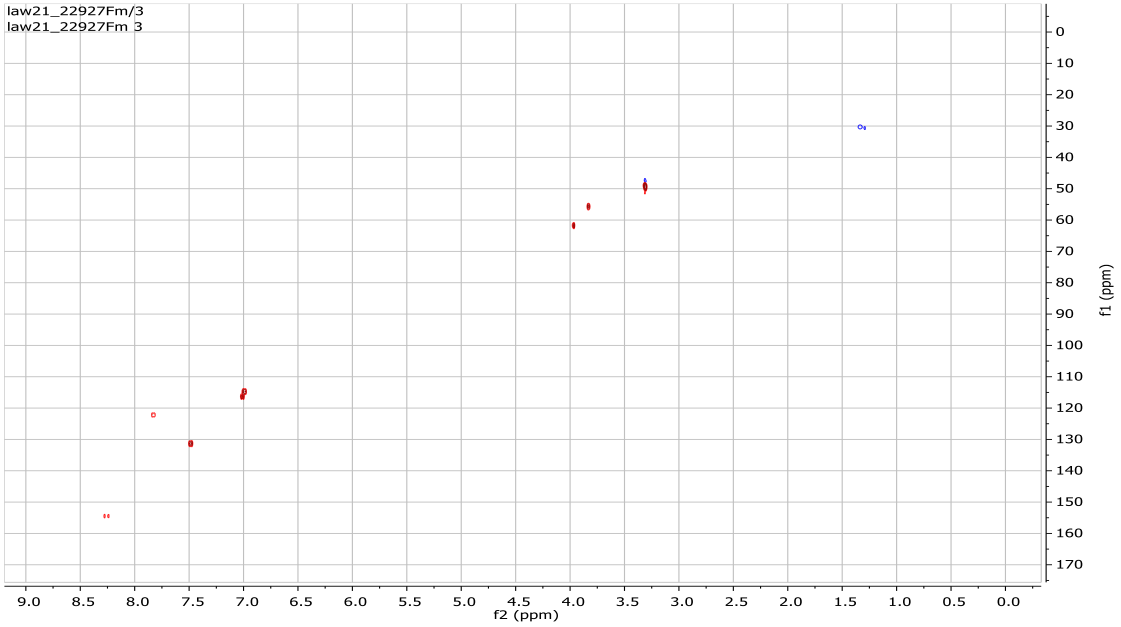

Appendix 111: ^{1}H, ^{13}C HMBC spectrum (500 MHz, MeOH) of compound **60**

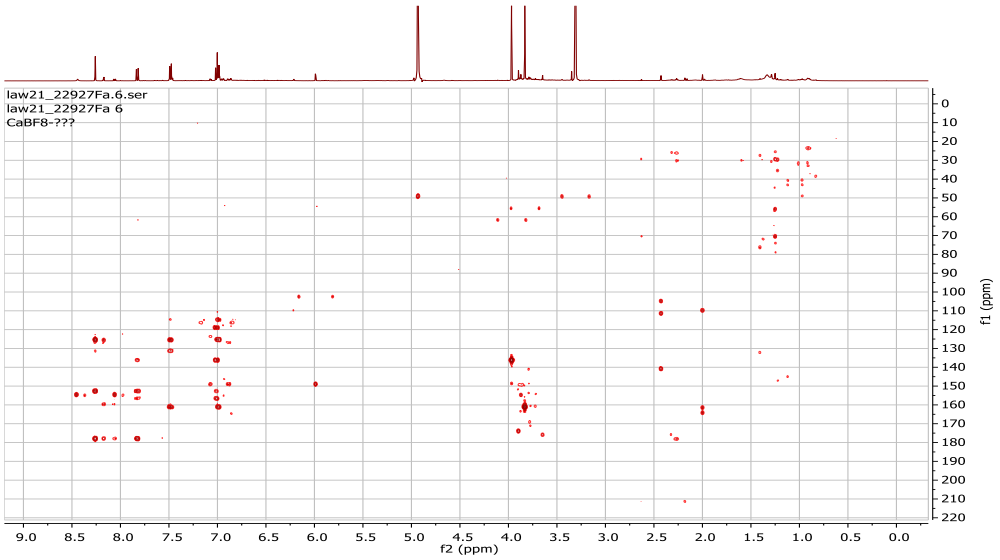

Appendix 112: ^{1}H, ^{1}H COSY spectrum (500 MHz, MeOH) of compound **60**

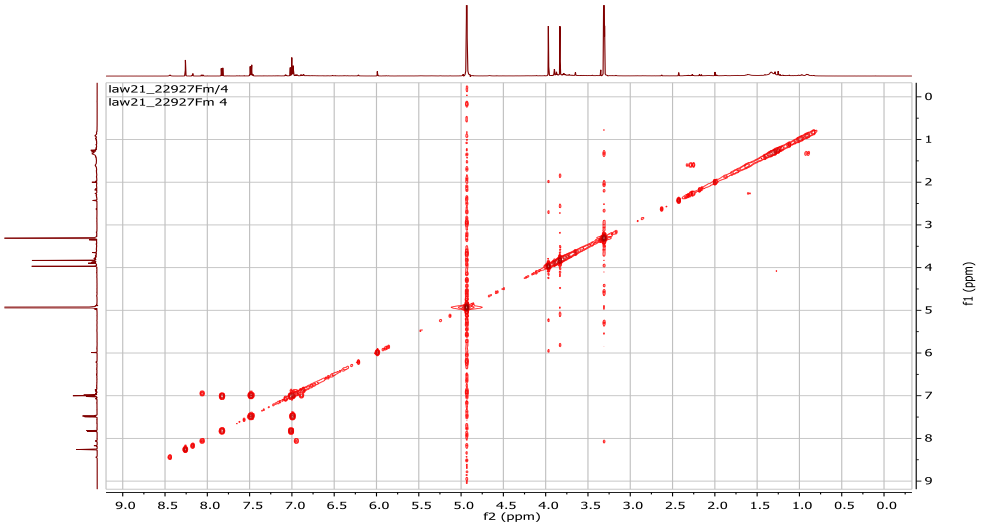

Appendix 113: UV/Vis spectrum of compound **60** in MeOH

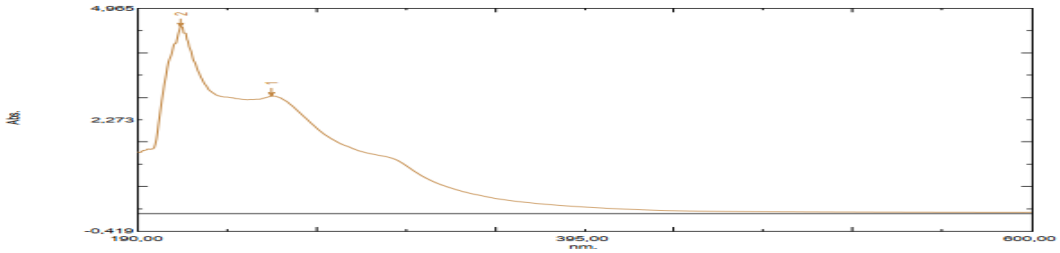

Appendix 114: HPLC-DAD chromatogram of compound **61**

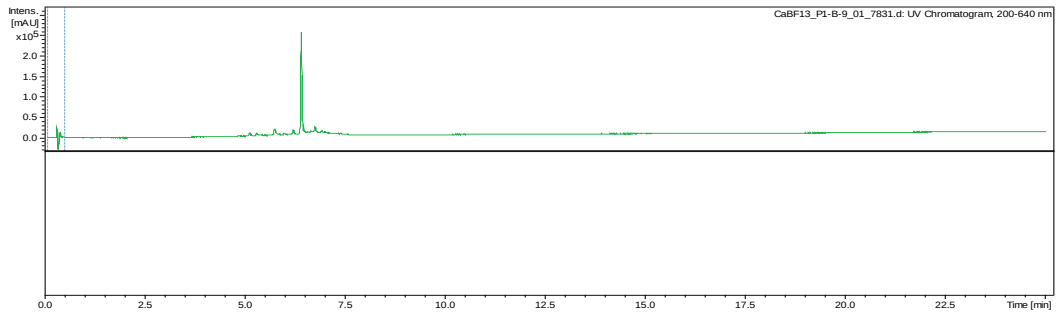

Appendix 115: HR-(+) ESIMS spectrum of compound **61**.

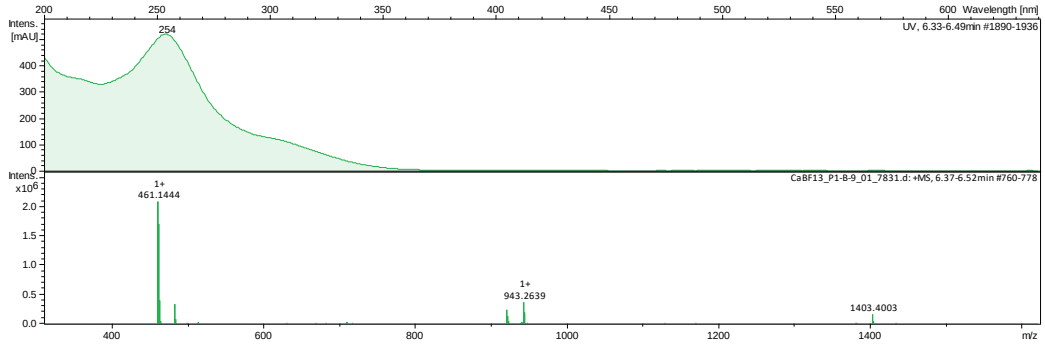

Appendix 116: ^{1}H NMR spectrum (700 MHz, CD_3OD) of compound **61**

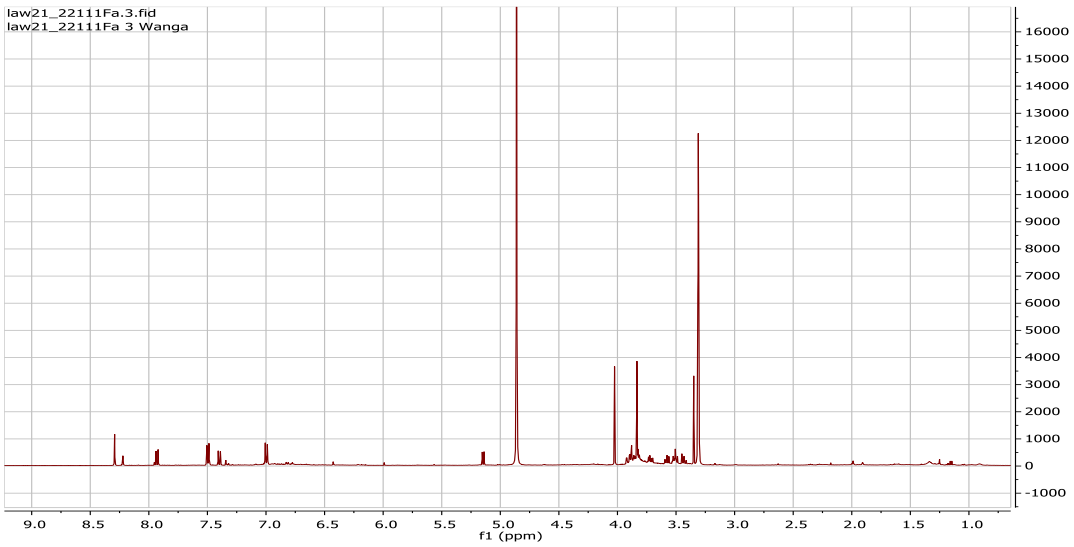

Appendix 117: ^{1}H, ^{13}C HSQC-DEPT spectrum (500 MHz, MeOH) of compound **61**

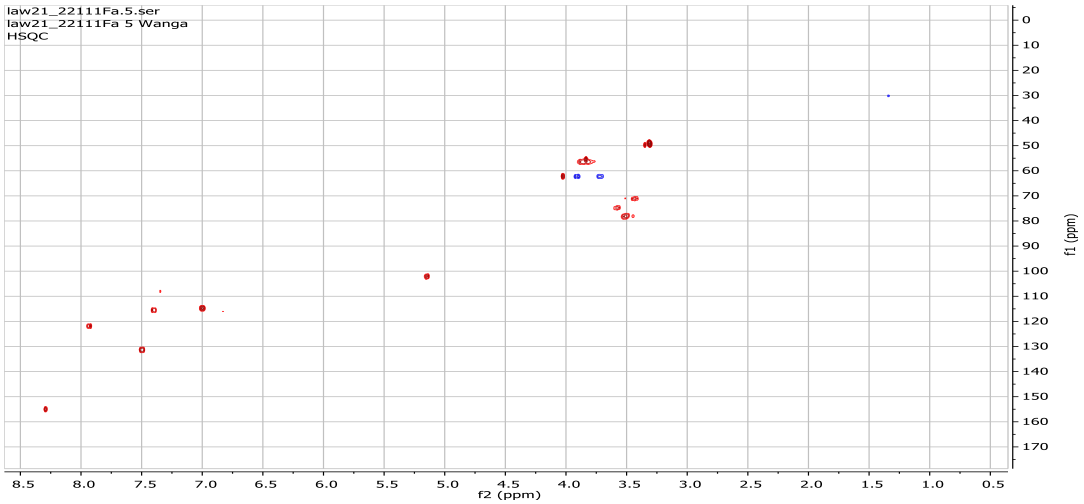

Appendix 118: ^{1}H, ^{13}C HMBC spectrum (500 MHz, MeOH) of compound **61**

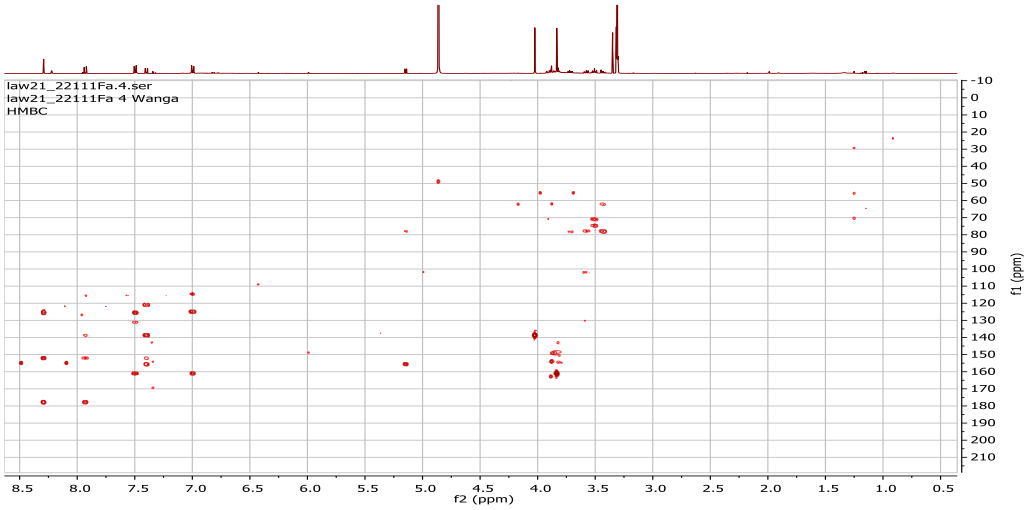

Appendix 119: ^{1}H, ^{1}H COSY spectrum (500 MHz, MeOH) of compound **61**

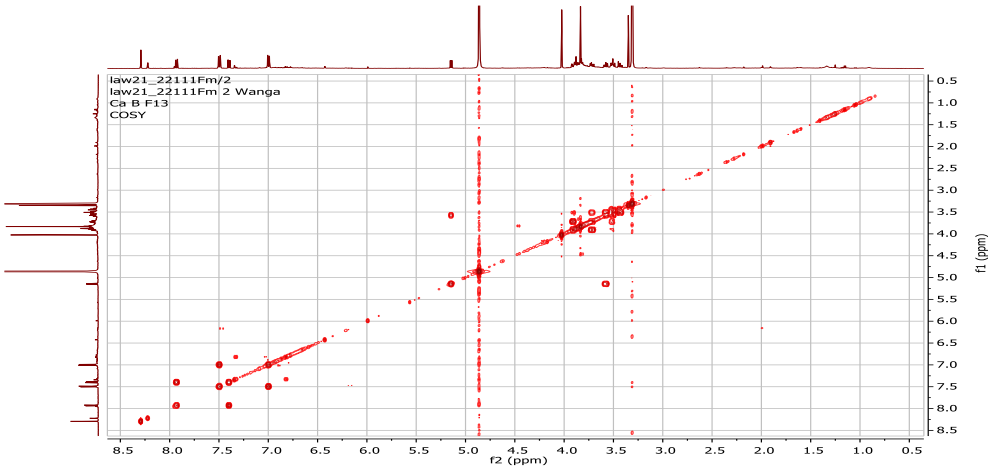

Appendix 120: UV/Vis spectrum of compound **61** in MeOH

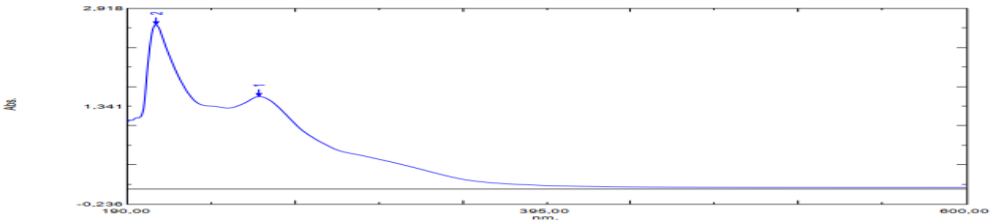

Appendix 121: HPLC-DAD chromatogram of compound **62**

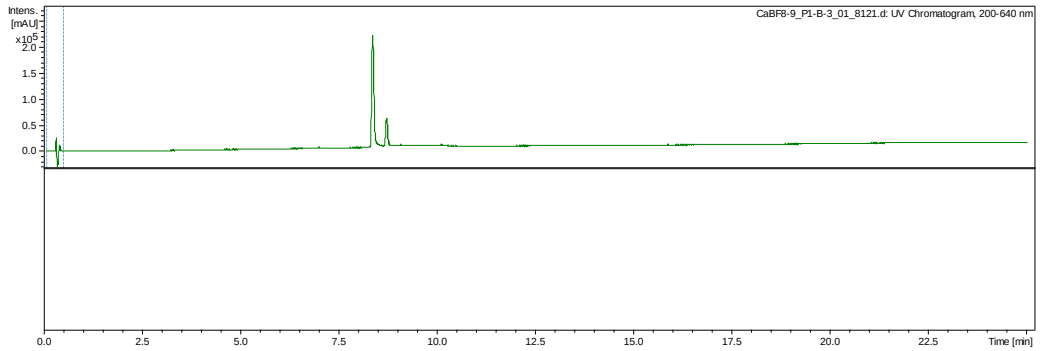

Appendix 122: HR-(+) ESIMS spectrum of compound **62**

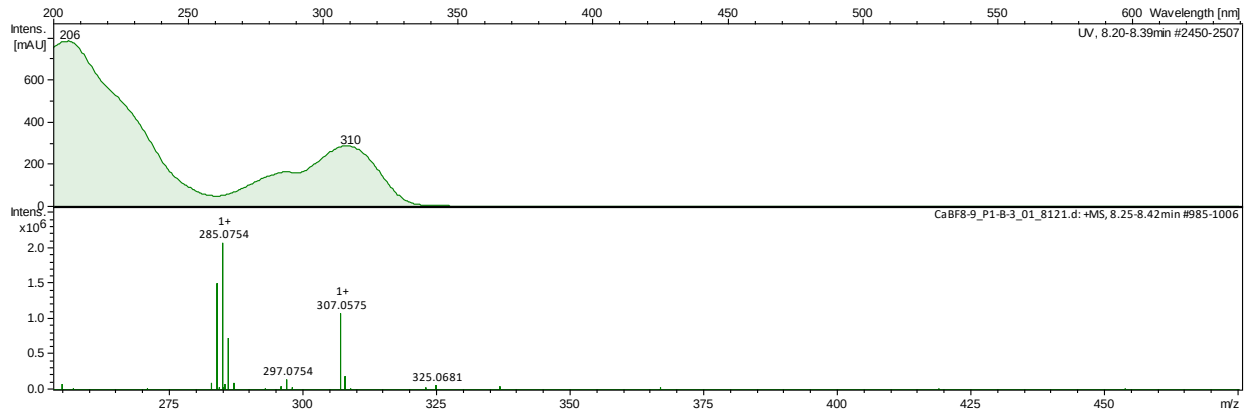

Appendix 123: ^{1}H NMR spectrum (700 MHz, CD_3OD) of compound **62**

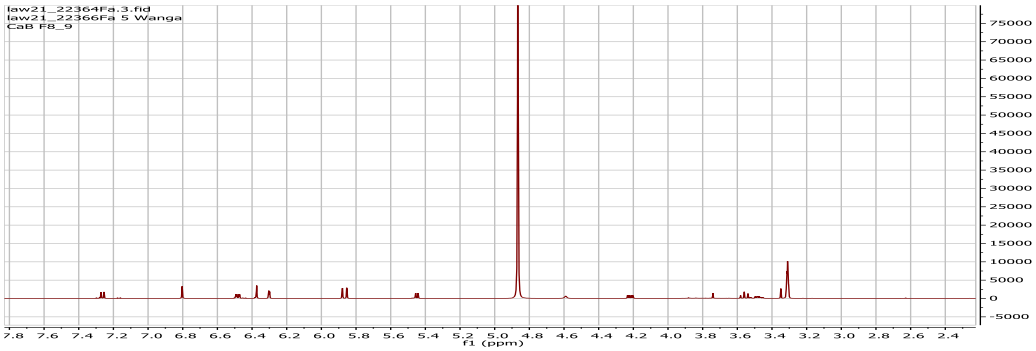

Appendix 124: ^{1}H, ^{13}C HSQC- DEPT spectrum (500 MHz, MeOH) of compound **62**

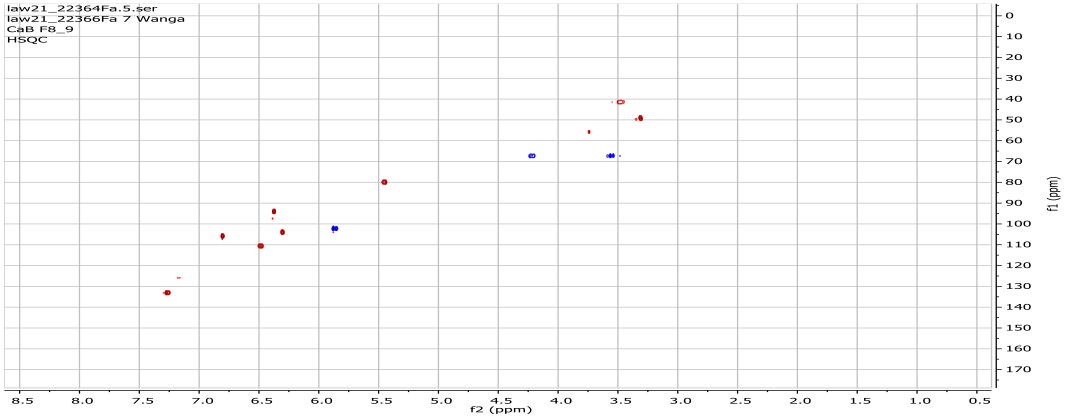

Appendix 125: ^{1}H, ^{13}C HMBC spectrum (500 MHz, MeOH) of compound **62**

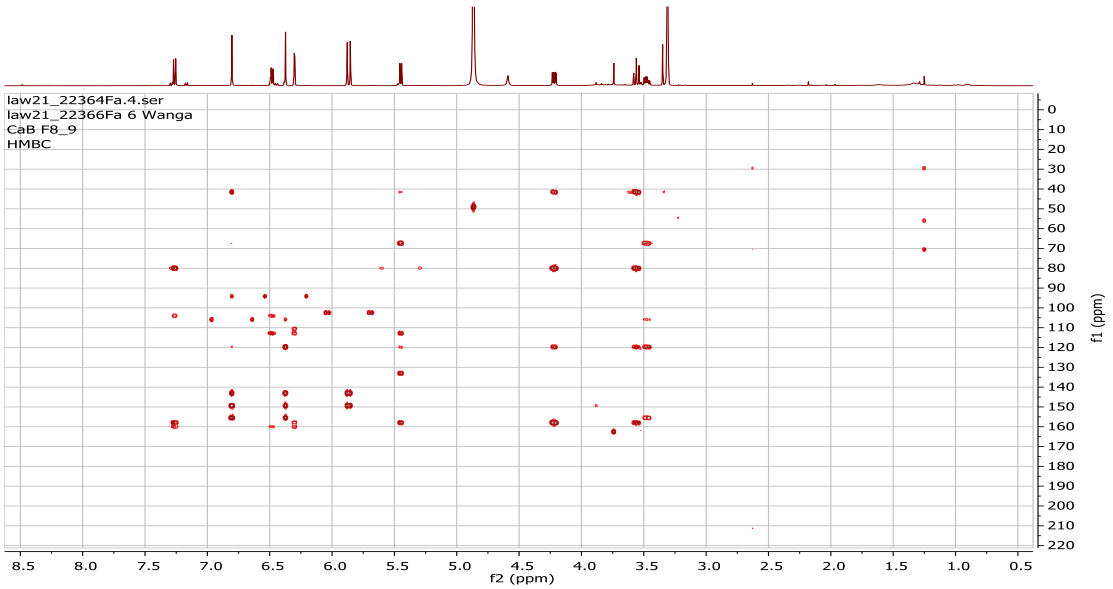

Appendix 126: ^{1}H, ^{1}H COSY spectrum (500 MHz, MeOH) of compound **62**

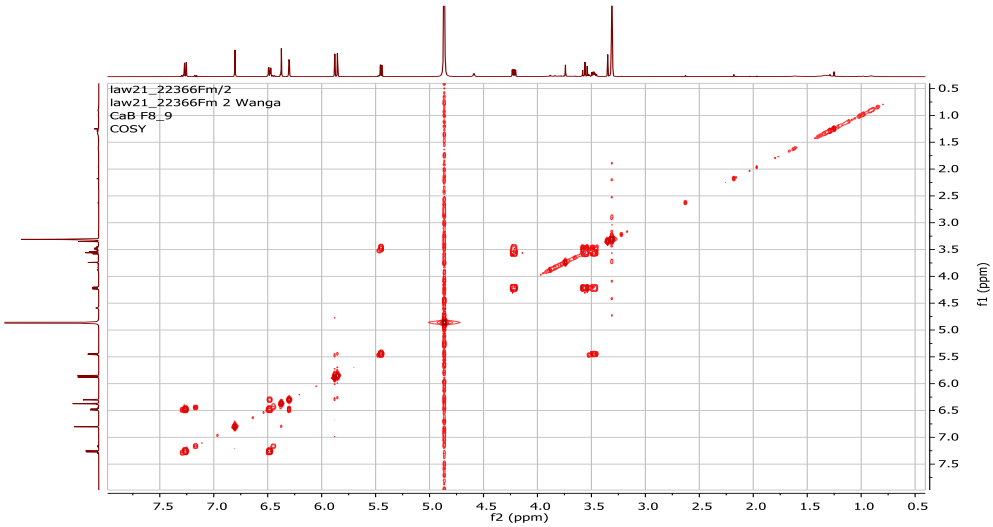

Appendix 127: UV/Vis spectrum of compound **62** in MeOH.

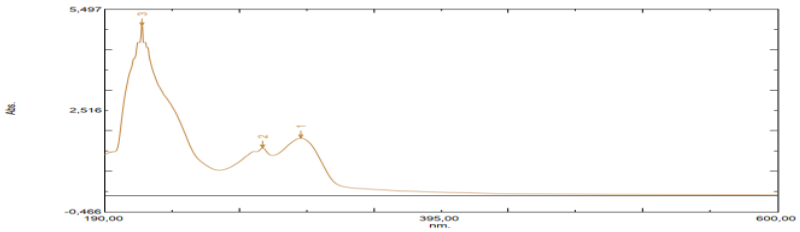

Appendix 128: HPLC-DAD chromatogram of compound **63**

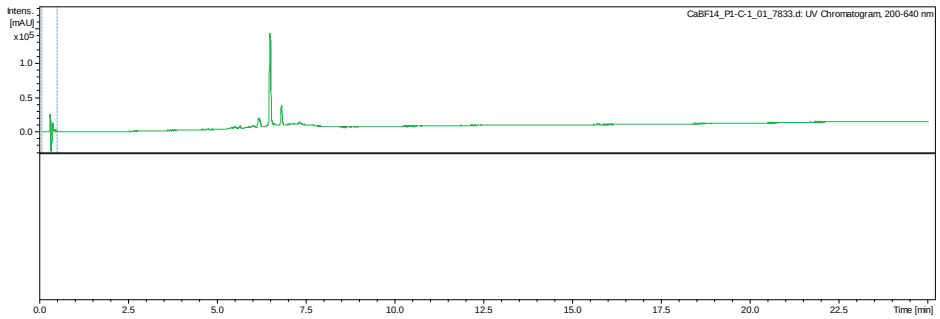

Appendix 129: HR-(+) ESIMS spectrum of compound **63**

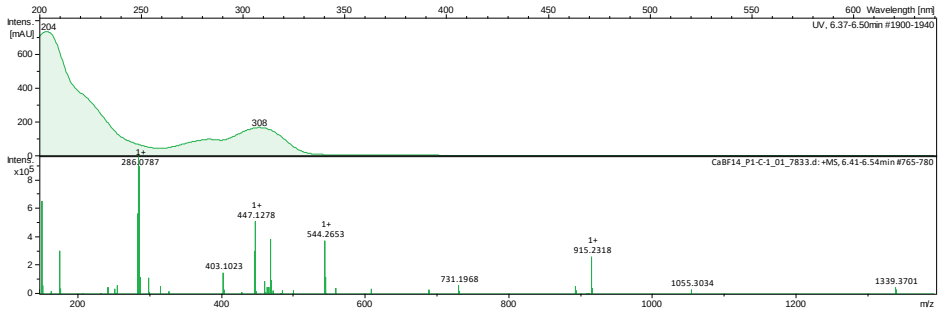

Appendix 130: ^{1}H NMR spectrum (700 MHz, CD_3OD) of compound **63**

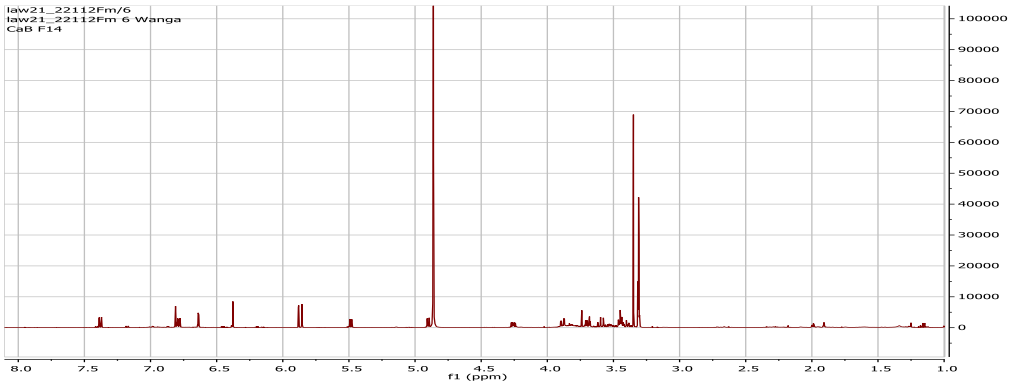

Appendix 131: ^{1}H, ^{13}C HSQC-DEPT spectrum (500 MHz, MeOH) of compound **63**

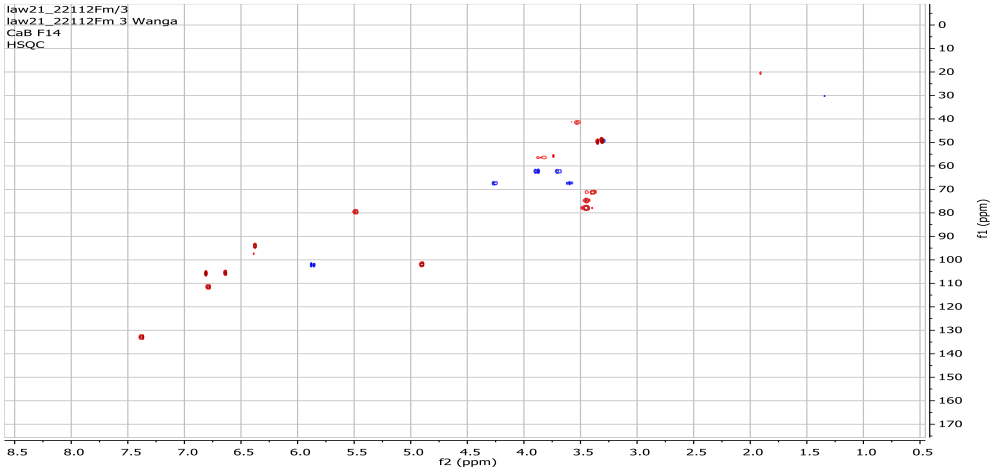

Appendix 132: ^{1}H, ^{13}C HMBC spectrum (500 MHz, MeOH) of compound **63**

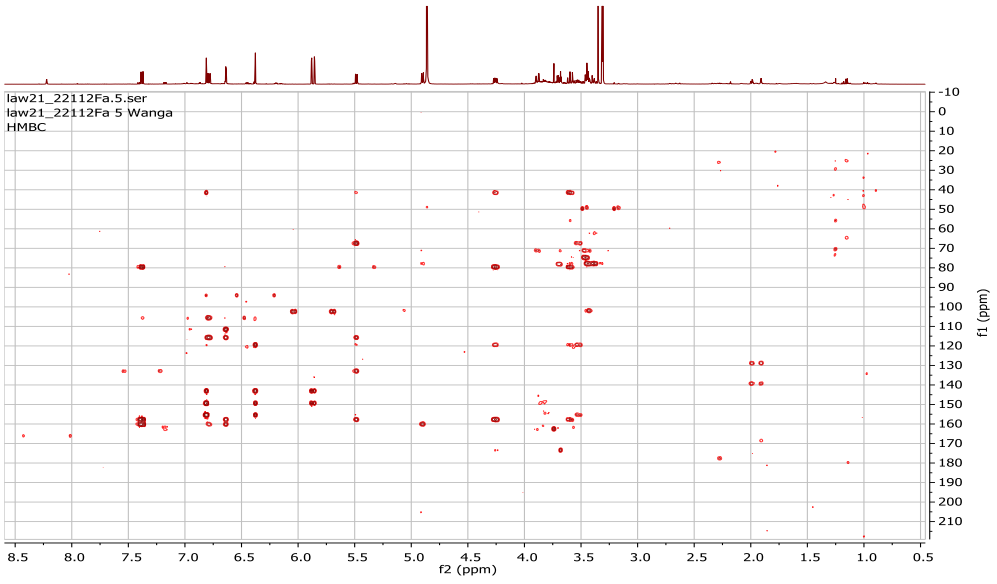

Appendix 133: ^{1}H, ^{1}H COSY spectrum (500 MHz, MeOH) of compound **63**

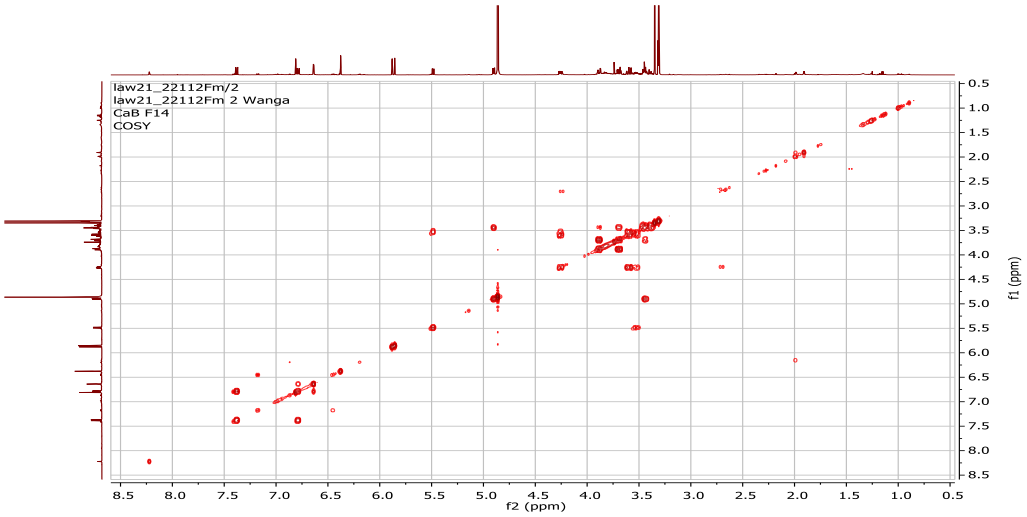

Appendix 134: UV/Vis spectrum of compound **63** in MeOH

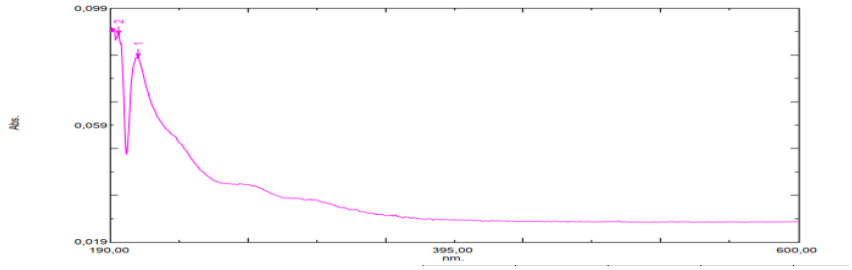

Appendix 135: HPLC-DAD chromatogram of compound **64**

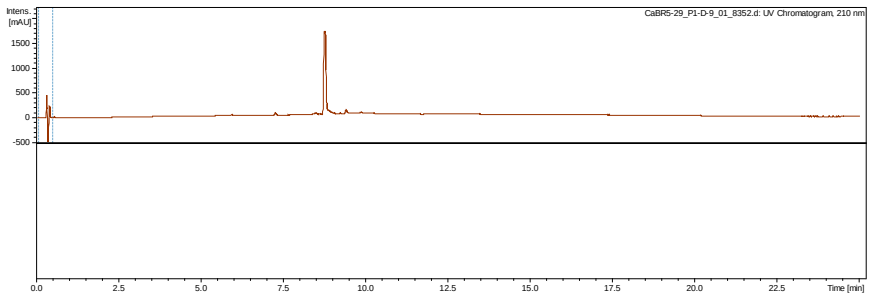

Appendix 136: HR-(+) ESIMS spectrum of compound **64**

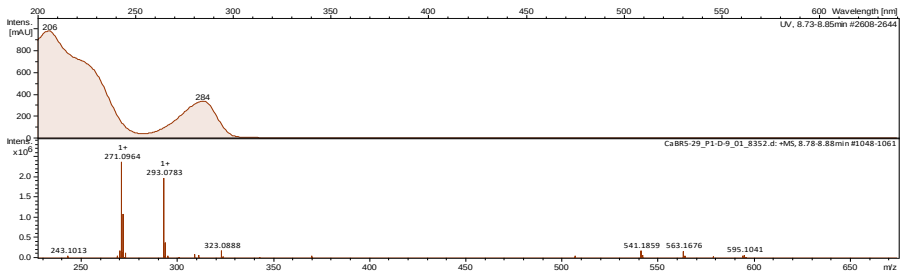

Appendix 137: ^{1}H NMR spectrum (700 MHz, CD_3OD) of compound **64**

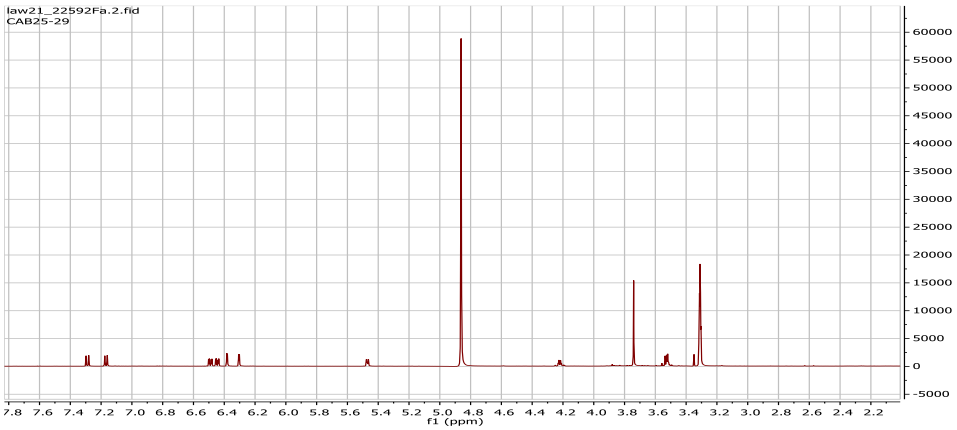

Appendix 138: ^{1}H, ^{13}C HSQC-DEPT spectrum (500 MHz, MeOH) of compound **64**

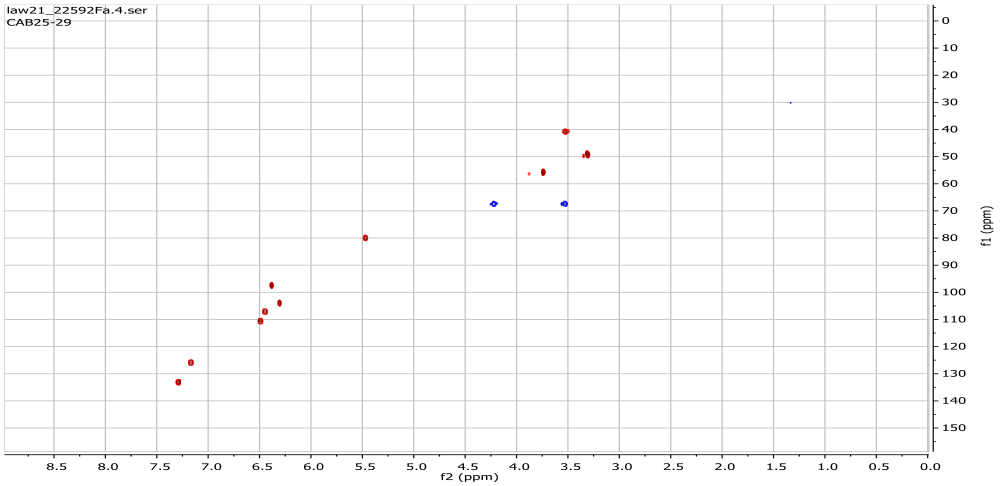

Appendix 139: ^{1}H, ^{13}C HMBC spectrum (500 MHz, MeOH) of compound **64**

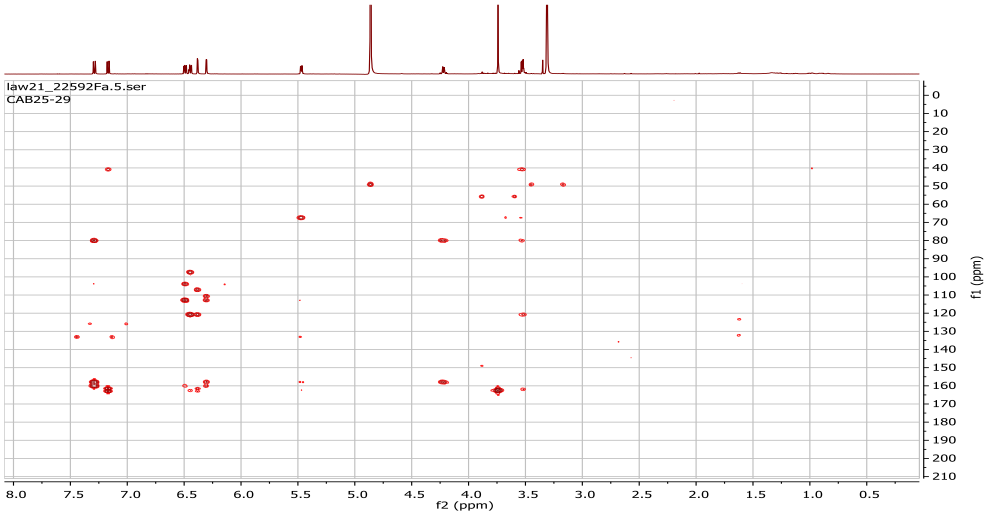

Appendix 140: ^{1}H, ^{1}H COSY spectrum (500 MHz, MeOH) of compound **64**

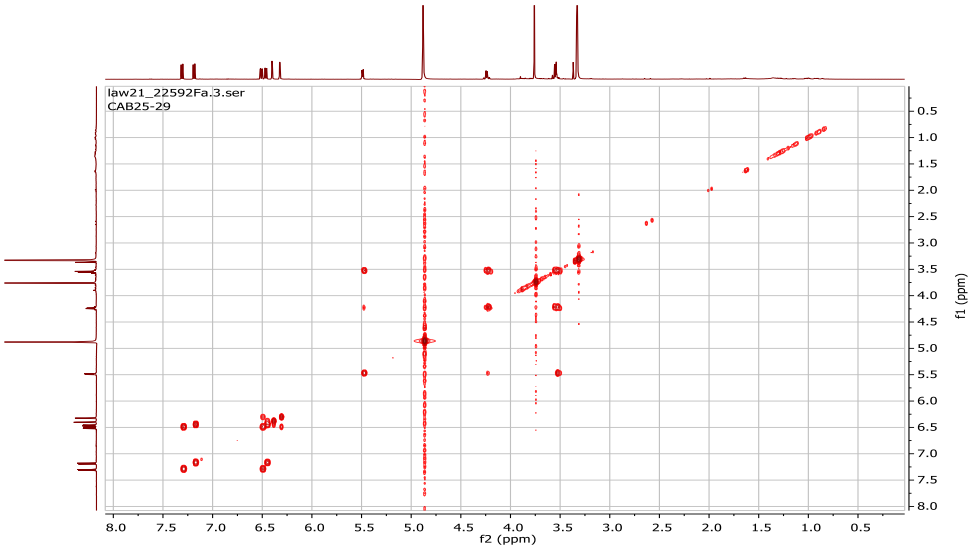

Appendix 141: UV/Vis spectrum of compound **64** in MeOH

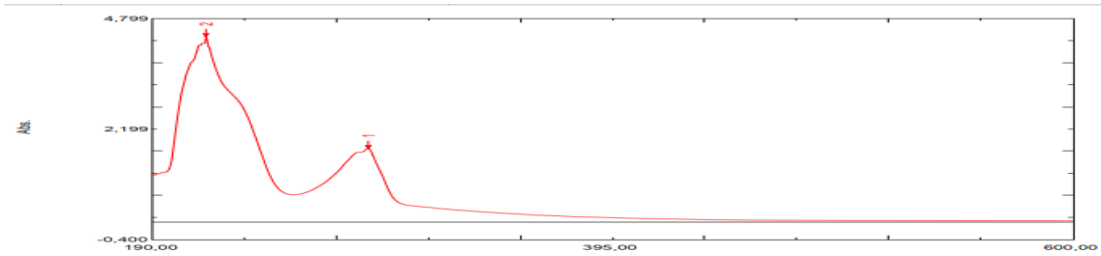

Appendix 142: HPLC-DAD chromatogram of compound **65**

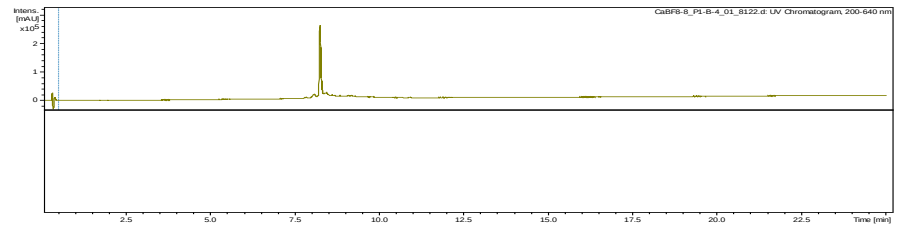

Appendix 143: HR-(+) ESIMS spectrum of compound **65**

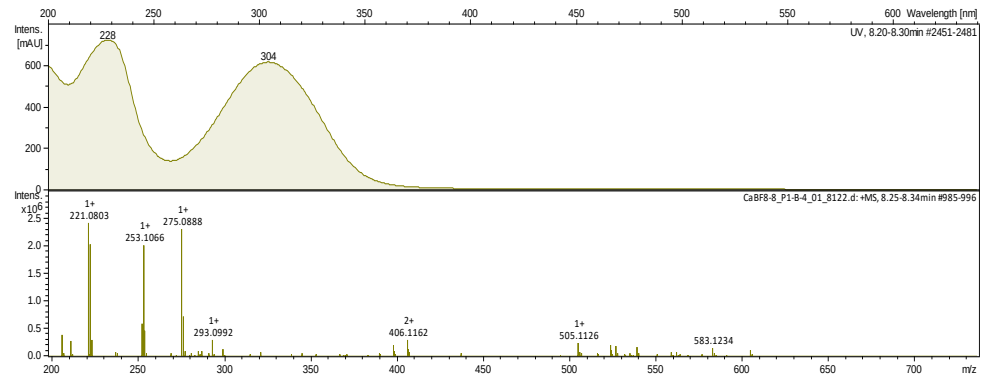

Appendix 144: ^{1}H NMR spectrum (700 MHz, CD_3OD) of compound **65**

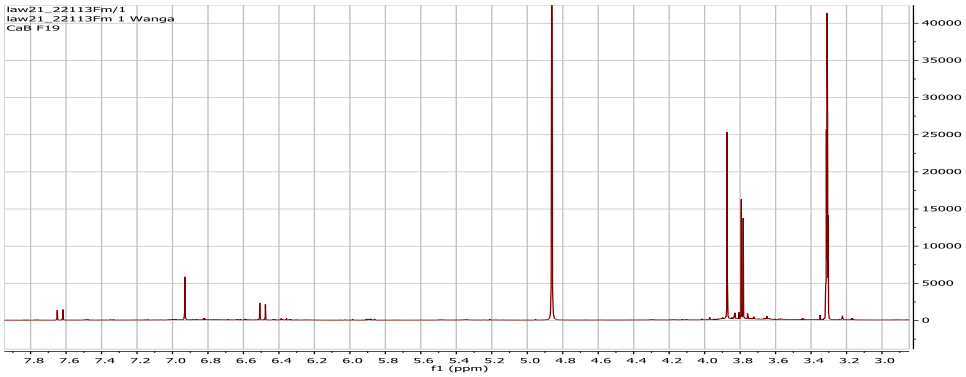

Appendix 145: ^{1}H, ^{13}C HSQC-DEPT spectrum (500 MHz, MeOH) of compound **65**

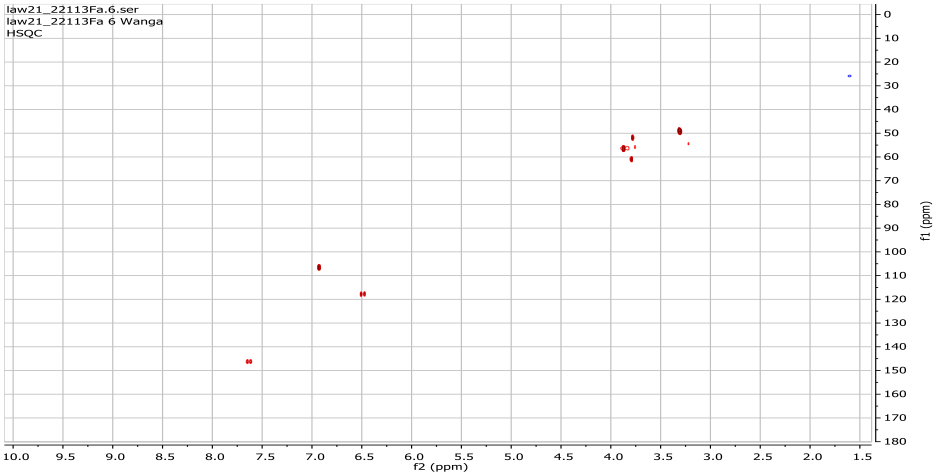

Appendix 146: ^{1}H, ^{13}C HMBC spectrum (500 MHz, MeOH) of compound **65**

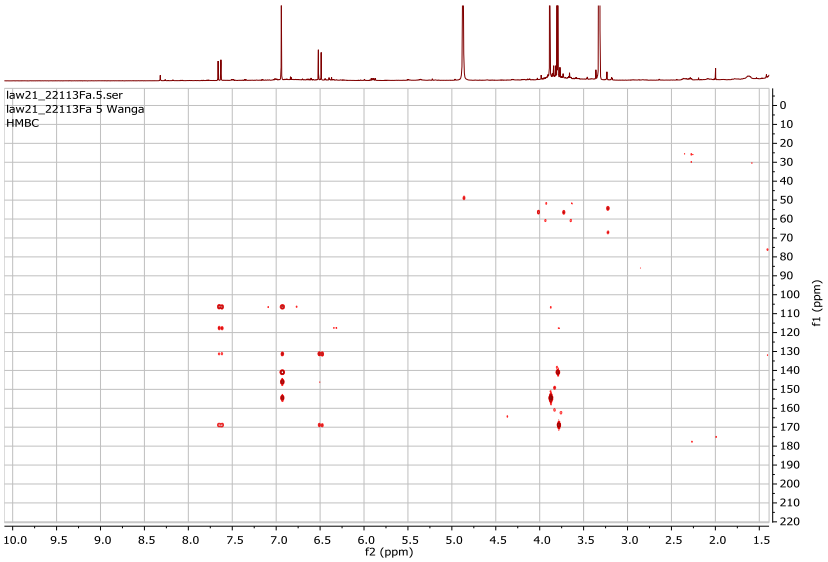

Appendix 147: ^{1}H, ^{1}H COSY spectrum (500 MHz, MeOH) of compound **65**

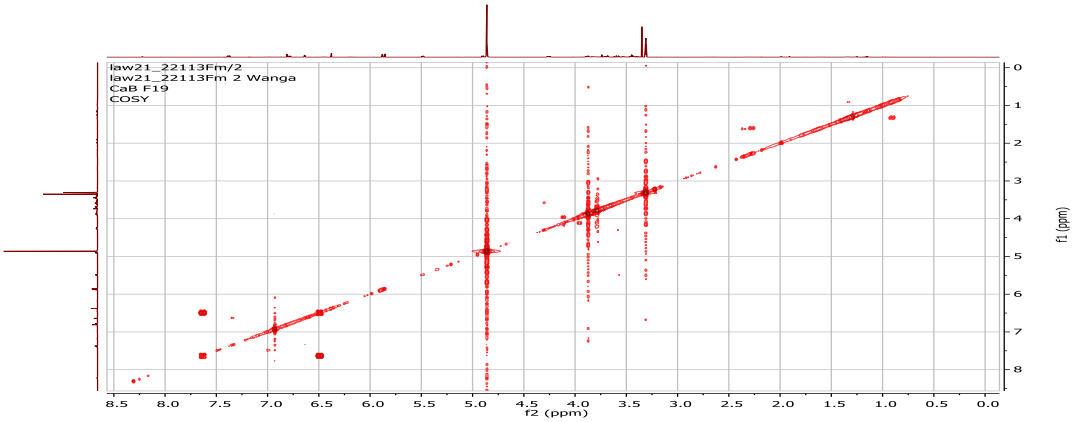

Appendix 148: UV/Vis spectrum of compound **65** in MeOH

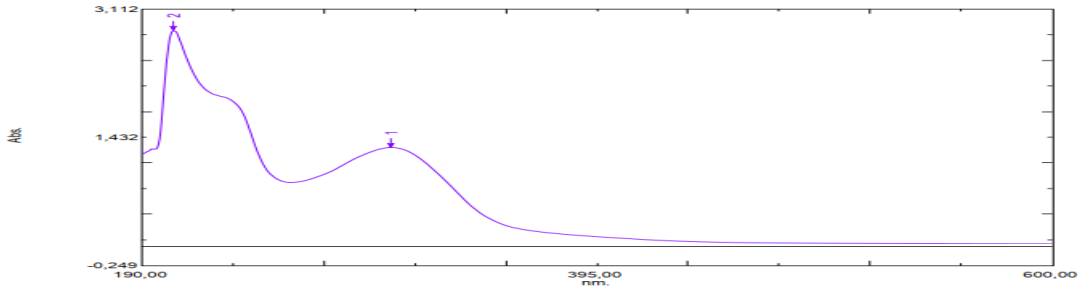

Appendix 149: HPLC-DAD chromatogram of compound **66**

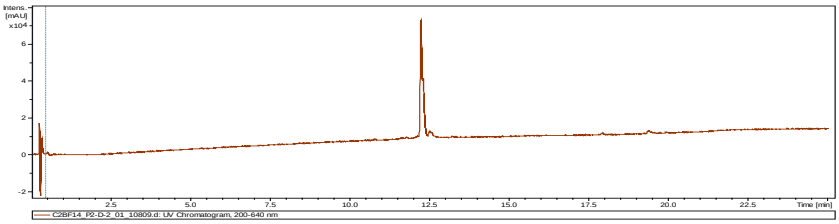

Appendix 150: HR-(+) ESIMS spectrum of compound **66**

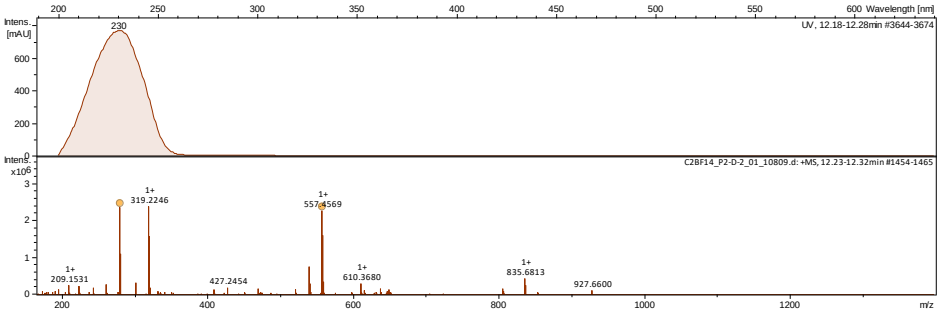

Appendix 151: 1H NMR spectrum (700 MHz, CD_3OD) of compound **66**

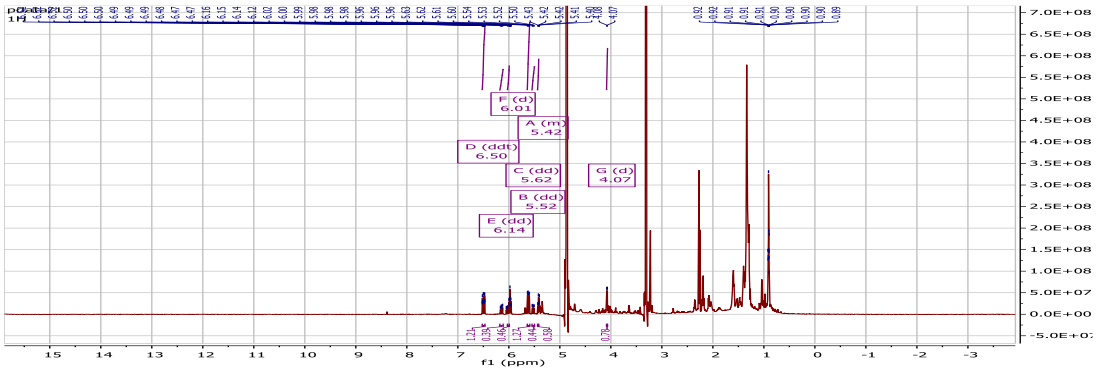

Appendix 152: ^{13}CNMR spectrum (700 MHz, CD_3OD) of compound **66**

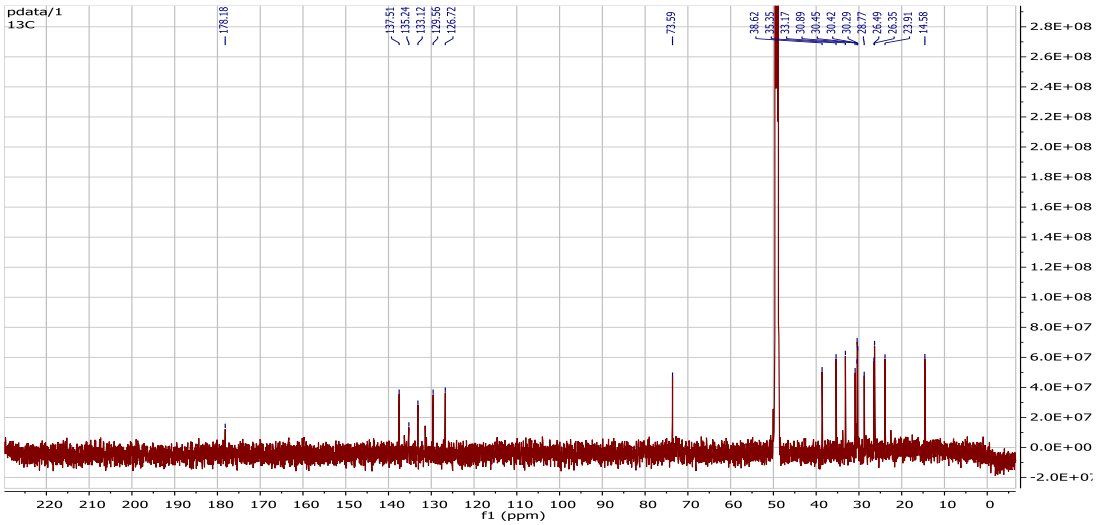

Appendix 153: ^{1}H, ^{13}C HSQC-DEPT spectrum (500 MHz, CD_3OD) of compound **66**

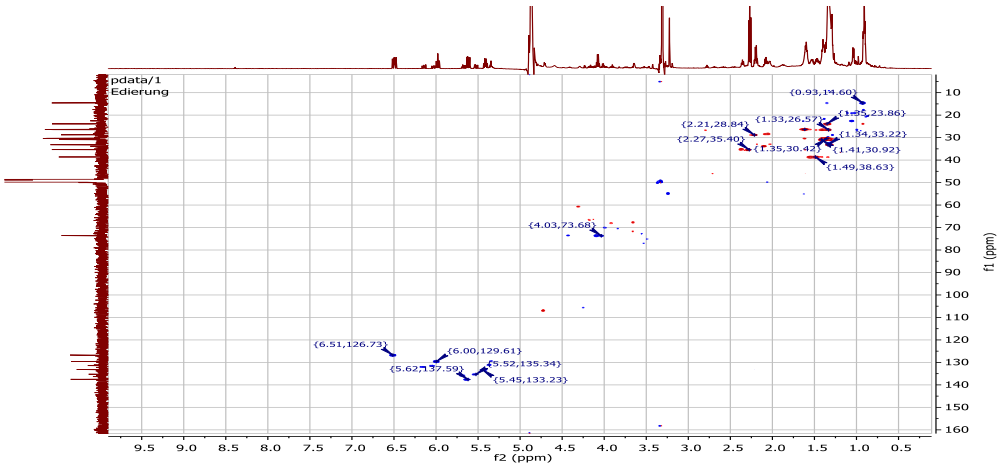

Appendix 154: ^{1}H, ^{13}C HMBC spectrum (500 MHz, CD3OD) of compound **66**

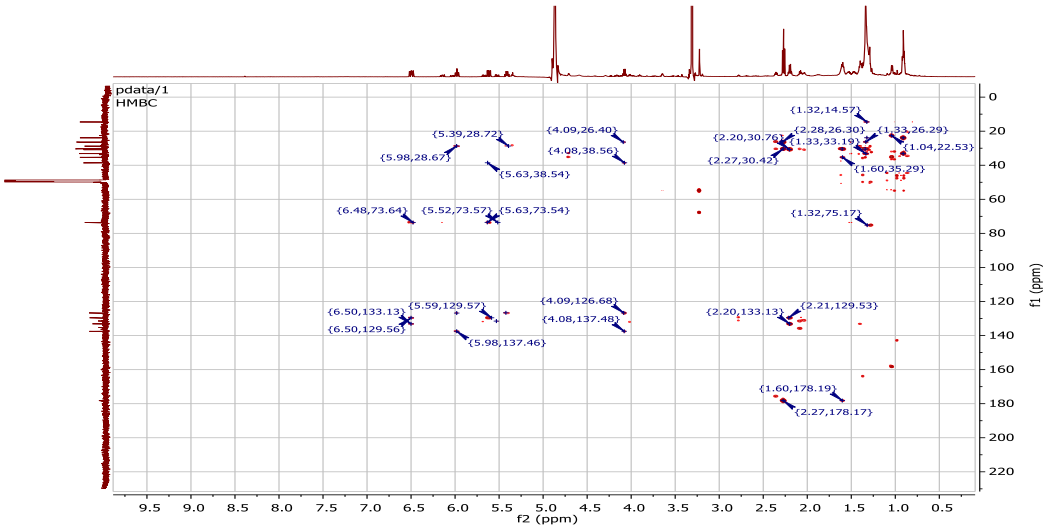

Appendix 155: ^{1}H- ^{1}H COSY spectrum (500 MHz, CD_3OD) of compound **66**

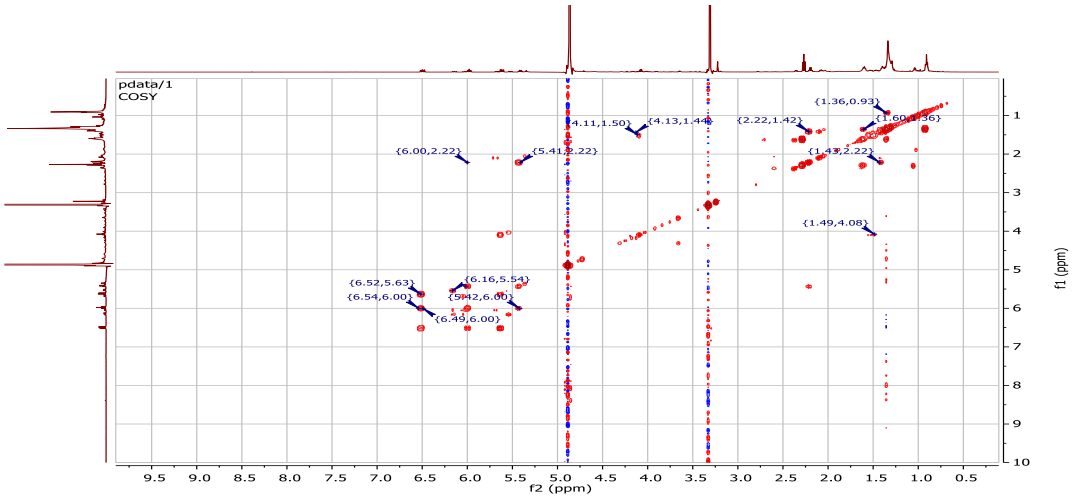

Appendix 156: ^{1}H, ^{1}H NOESY spectrum (500 MHz, CD3OD) of compound **66**

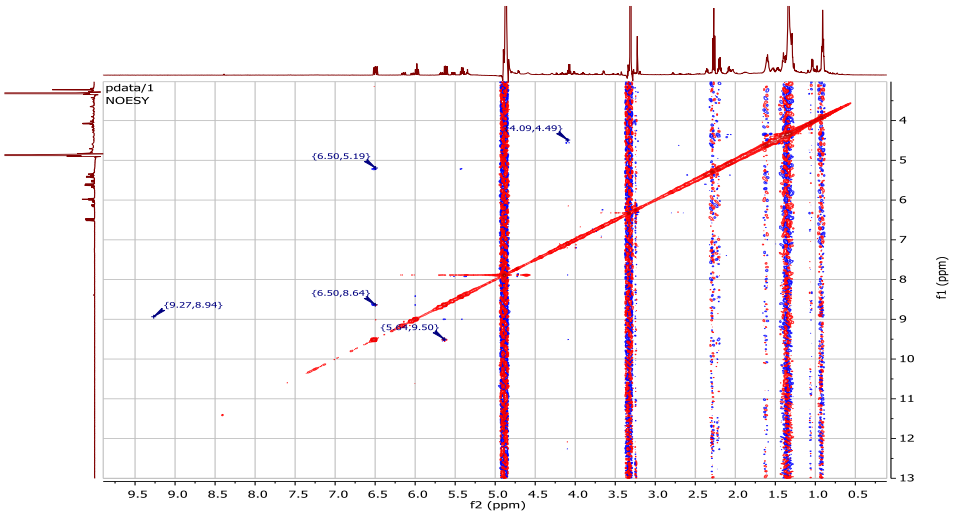

Appendix 157: HPLC-DAD chromatogram of compound **67**.

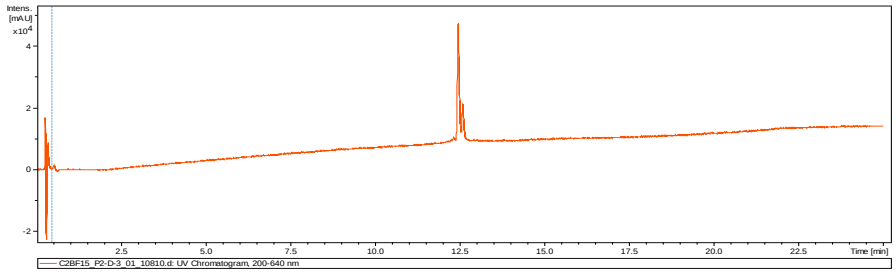

Appendix 158: HR-(+) ESIMS spectrum of compound **67**

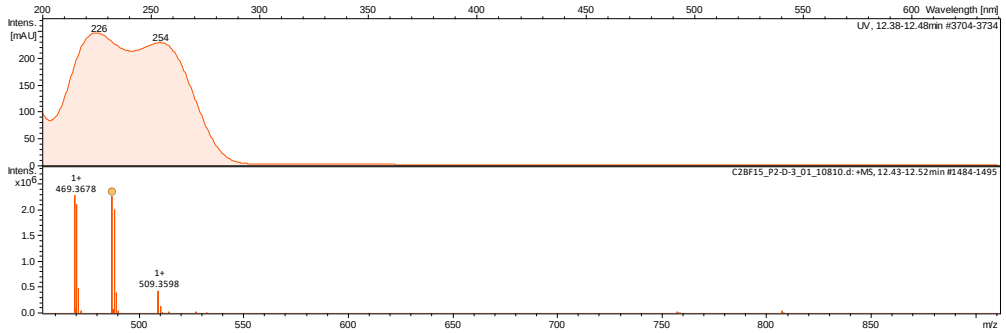

Appendix 159: ^{1}H NMR spectrum (700 MHz, CD3OD) of compound **67**

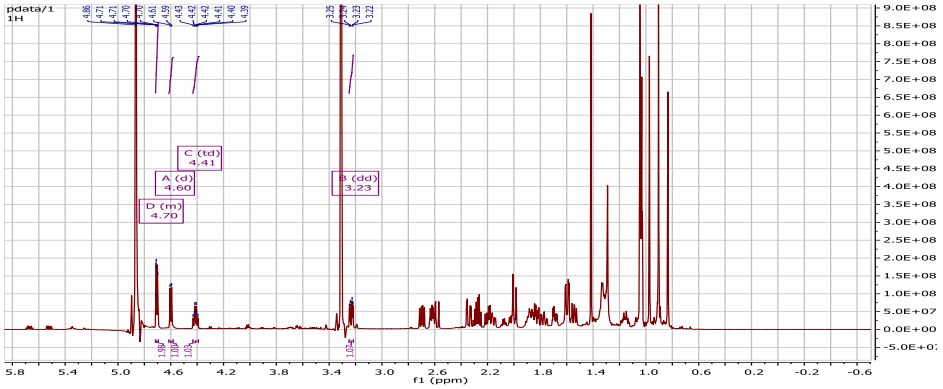

Appendix 160: ^{13}C NMR spectrum (700 MHz, CD3OD) of compound **67**.

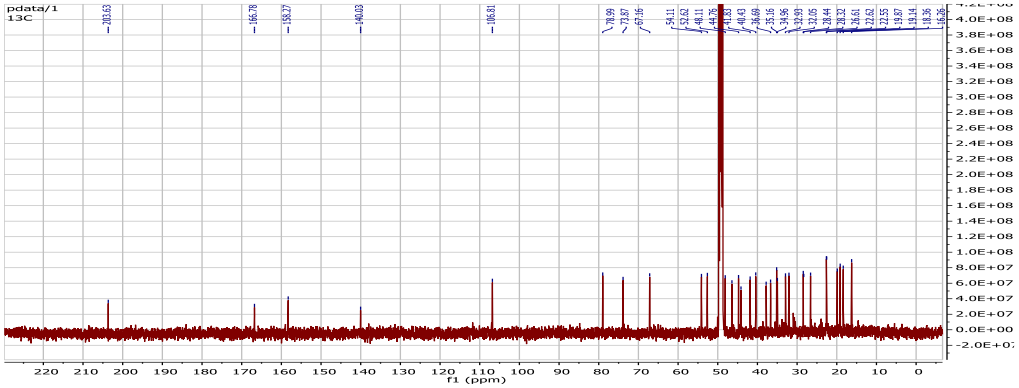

Appendix 161: ^{1}H, ^{13}C HSQC-DEPT spectrum (500 MHz, CD3OD) of compound **67**

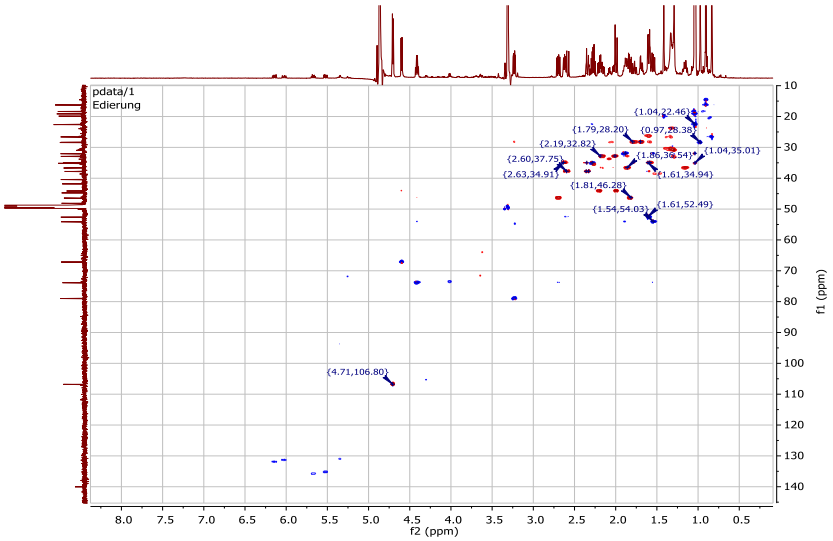

Appendix 162: ^{1}H, ^{13}C HMBC spectrum (500 MHz, CD3OD) of compound **67**

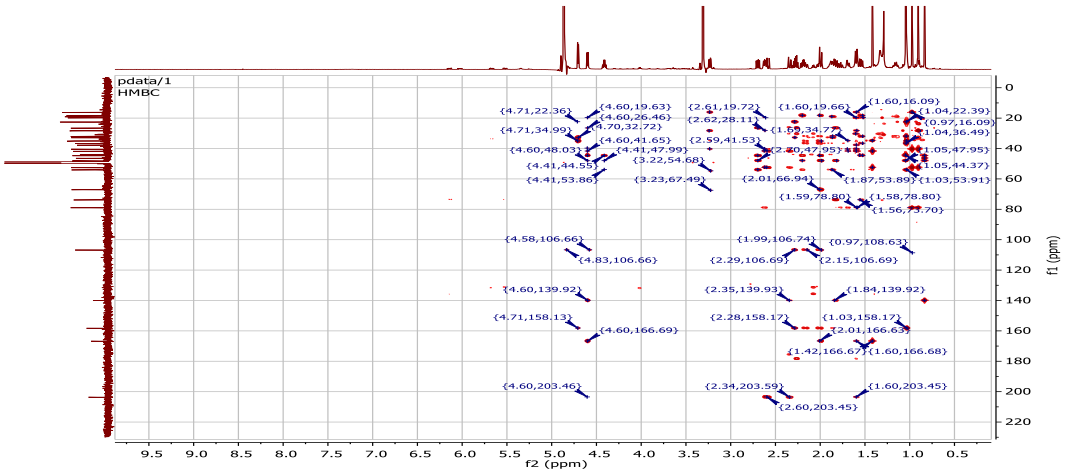

Appendix 163: ^{1}H- ^{1}H COSY spectrum (500 MHz, CD3OD) of compound **67**

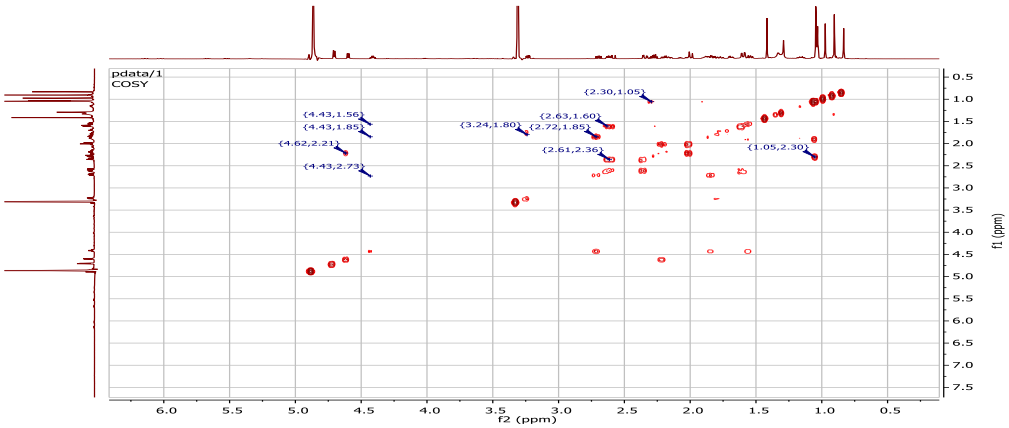

Appendix 164: ^{1}H, ^{1}H NOESY spectrum (500 MHz, CD3OD) of compound **67**

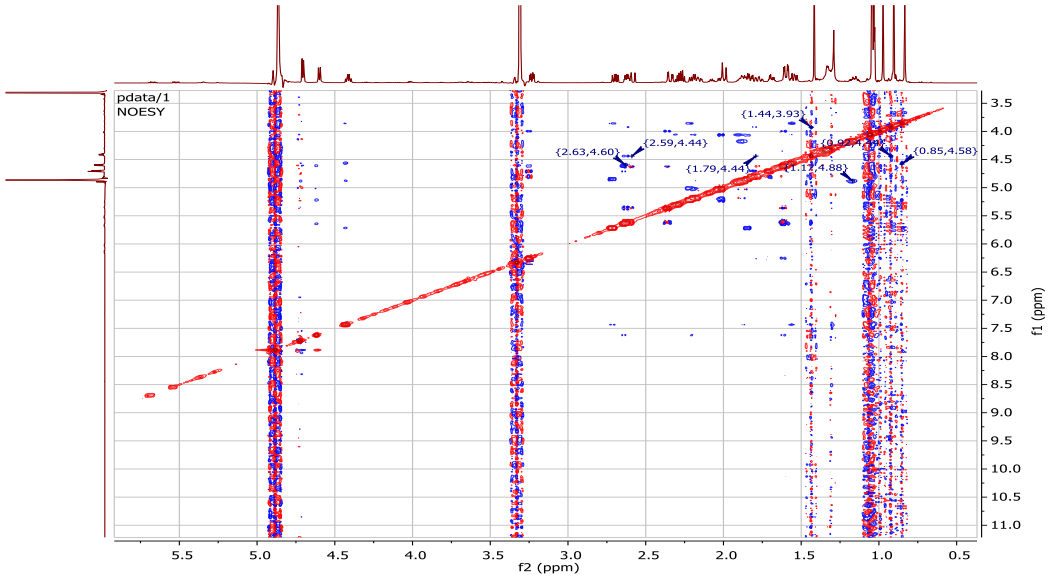

Appendix 165: The ITS, LSU/ Tef sequences and the identification of the isolated fungal endophytes

No	Endophytic Code	ITS Consensus Sequence	LSU Consensus Sequence/ Elongation Factor	NCBI data	Reference
1.	Cs2b-1a	>Consensus TAACAAGGGCTTCTTACATATTTAAA GTTTGAGAATGGATGAAGGCAATAT ATAGCCCCCGAGTCCCTAATCATTCG CTTTACCTCATAAAACTGAAGATCAA CACTGCTATCCKGAGGGAAACTTCG GCGGTWACCAGCTACTAGACAGTTC GATTAGTCTTTCGCCCCCCATGCTCA	>Consensus CCTTACCAAGCTCGGCGGCTGTACAGAT AGAAAGGTCAGCATGGATTTCTATGTGA TTTCTGACACATCGTGTTGGGAGCGGAC GATGAGGTTGATGGTAGGCGTATTGGTG GCGGGCAGTGGGTGATGCAACAGGGTTT TGGGCGTAAGAGATAAGCTCCCTGATAA GCGCACCCCGCACCCGCACTGAAAATGG	Diaporthe canthii culture-collection CBS:132533 translation elongation factor 1-alpha gene, partial cds 303/335(90%) 1/335(0%) KC843120.1	https://www.ingentaconnect.com/content/nhn/pimj/2014/00000032/00000001/art00005

		AATTTGACGATCGATTTGCACGTCAG AACCGCTGCGAGCCTCCACCAGAGT TTCCTCTGGCTTCACCCTATTCAAGC ATAGTTCACTGTCTTTCGGGTCCGTC CGTTAAAACTCTTACTCAAATCCTTC CGAGAACATCAGGATCGGTCGATGA TGCGCCGAAGCTCTCACCTGCGTTCA CTTTCATTACGCGTGCGGGTTTTACA CCCAAACGCTCGCTCTAATGGACGA CTCCTTGGTCCGTGTTTCAAGACGGG TCACTGATGACCATTACGCCAGCATC CTTGCGGAGCGCGGACCTCGGTCCC CACGGGGGTATCGTCCGCCAGGCTA TAACACACCCCGGAGGGTGCTACGT TCCTGACGGTCTTATCCCCCCACGAG AACCGATGCTGGCCTGTGCCGGGCG GAGTGCACAGGGGAGAACCCCTGAT GAGCCGCCCGGCCCAAGTCTGGTCA TAAGTGCTTCCCTTTCAACAATTTCA CGTACTATTTAACCCCCTTTTCAAGG TGCTTTTCATCTTTCGATCACTCTACT TGTGCGCTATCGGTCTCTGGCCGGTA TTTAGCTTTAGAAGAGATTTACCTCC CATTTAGAGCAGCATTCCCAAACTAC TCGACTCGTCGAAGGAGCTTCACAC AGGGCTTGGTGTCCGACCATACGGG GCTCTCACCCTCTGTGGCGTCCCGTT CCAGGRAACTCGGAAGGCACCGCGC CAGAAGCATCCTCTGCAAATTACAA CTCGGGCCGARGCCAGATTTCAAATT TGAGCTGTTGCCGCTTCCTCGCGTAC A	AAAATCCAGAGGGAGGGGTCAAAATGC GCCTCTCAGTGCGACGAAGCCGCGAGAG CAGCCGCACGCTGATGATTTGTGGCAAG ATGCGAGGGCAAGGCAAGTTGTTCTGTG AATGCGATGTTTACTAACCTTCCTTCTC	Diaporthe vangueriae culture CBS:137985 strain CPC 22703 28S ribosomal RNA gene, partial sequence 818/823(99%) 3/823(0%) KJ869194.1	https://www.ingentaconnect.com/content/nhn/pimj/2014/00000032/00000001/art00011
2.	Cs2b-2a	>Consensus TCGTAACAAGGTCTCCGTTGGTGAAC CAGCGGAGGGATCATTGCTGGAACG	>Consensus CAACTAAGTAACAAGGGCTTCTTACATA TTTAAAGTTTGAGAATGGATGAAGGCAA	Diaporthe velutina CGMCC 3.18286 ITS region; from TYPE material	https://link.springer.com/article/10.5598/i

		CGCCCCAGGCGCACCCAGAAACCCT TTGTGAACTTATACCTTACTGTTGCC TCGGCGCAGGCCGTCCCCTATGGGG TCCCTCTGGAGACAGAGGAGCAGCC GGCCGGCGGCCAAGTTAACTCTGTTT TTAAACTGAAACTCTGAGTACAAAA CATAAATGAATCAAAACTTTCAACA ACGGATCTCTTGGTTCTGGCATCGAT GAAGAACGCAGCGAAATGCGATAAG TAATGTGAATTGCAGAATTCAGTGA ATCATCGAATCTTTGAACGCACATTG CGCCCTCTGGTATTCCGGAGGGCATG CCTGTTCGAGCGTCATTTCAACCCTC AAGCCTGGCTTGGTGTTGGGGCACT GCCTGTAAAAGGGCAGGCCCTGAAA TATAGTGGCGAGCTCGCCAGGACTC CGAGCGTAGTAGTTAAACCCTCGCTT TGGAAGGCCTGGCGGTGCCCTGCCG TTAAACCCCAACTTCTGAAAATTTGA CCTCGGATCAGGTAGGAATACCCGC TGAACTTAAGCATATC	TATATAGCCCCCGAGTCCCTAATCATTCG CTTTACCTCATAAAACTGAAGATCAACA CTGCTATCCTGAGGGAAACTTCGGCGGK WACCAGCTACTAGACAGTTCGATTAGTC TTTCGCCCCCCATGCTCAAATTTGACGAT CGATTTGCACGTCAGAACCGCTGCGAGC CTCCACCAGAGTTTCCTCTGGCTTCACCC TATTCAAGCATAGTTCACTGTCTTTCGGG TCCGTCCGTTAAAACTCTTACTCAAATCC TTCCGAGAACATCAGGATCGGTCGATGA TGCGCCGAAGCTCTCACCTGCGTTCACTT TCATTACGCGTGCGGGTTTTACACCCAAA CGCTCGCTCTAATGGACGACTCCTTGGTC CGTGTTTCAAGACGGGTCACTGATGACC ATTACGCCAGCATCCTTGCGGAGCGCGG ACCTCGGTCCCCACGGGGGTATCGTCCG CCAGGCTATAACACACCCCGGAGGGTGC TACGTTCCTGACGGTCTTATCCCCCCACG AGAACCGATGCTGGCCTGTGCCGGGCGG AGTGCACAGGGGAGAACCCCTGATGAGC CGCCCGGCCCAAGTCTGGTCATAAGTGC TTCCCTTTCAACAATTTCACGTACTATTT AACCCCCTTTTCAAGGTGCTTTTCATCTT TCGATCACTCTACTTGTGCGCTATCGGTC TCTGGCCGGTATTTAGCTTTAGAAGAGAT TTACCTCCCATTTAGAGCAGCATTCCCAA ACTACTCGACTCGTCGAAGGAGCTTCAC ACAGGCTTGGTGTCCGACCATACGGGGC TCTCACCCTCTGTGGCGTCCCGTTCCAGG GAACTCGGAAGGCACCGCGCCAGAAGCA TCCTCTGCAAATTACAACTCGGGCCGAG GCCAGATTTCAAATTTGAGCTGTTGCCGC TTCA	568/573(99%) 0/573(0%) NR_152470.1 Diaporthe canthii CBS 132533 28S rRNA, partial sequence; from TYPE material 827/829(99%) 1/829(0%) NG_042677.1	mafungus.2017.08.01.11

3.	Cs2b-2b	>Consensus TAACAAGGTTTCCGTAGGTGAACCT GCGGAAGGATCATTATCCATAACCG GGTGTGGCTGCGGCCTCCGGGGGCA TGTCTCCCGGGTGGTAGAGGTAAAA CTCGCACGCACCACATGTCTGAATCC TTTTTTTACGAGCACCTTTCGTTCTCC TTCGGTGGGGTGACCTGCCGTTGGA ACCCATCAAAACCCTTTTTTGCATCT AGCATTACCTGTTCTGATACAAACAA TCGTTACAACTTTCAACAATGGATCT CTTGGCTCTGGCATCGATGAAGAAC GCAGCGAAATGCGATAAGTAGTGTG AATTGCAGAATTCAGTGAATCATCG AATCTTTGAACGCACATTGCGCCCCT TGGTATTCCATGGGGCATGCCTGTTC GAGCGTCATCTACACCCTCAAGCTCT GCTTGGTGTTGGGCGTCTGTCCCGCC TACGTGCGCGGACTCGCCCCAAATTC ATTGGCAGCGGTCCTTGCCTCCTCTC GCGCAGCACATTGCGCTTCTCGAGGT GCGCGGCCCGCGTCCACGAAGCAAC ATTACCGTCTTTGACCTCGGATCAGG TAGGGATACCCGCTGAACTTAAGCA TA	>Consensus AACAAGGACTTCTTACATATTTAAAGTTT GAGAATAGGTGAAGGTTGTTTCAACCCC CATGCCTCTWATCATTCGCTTTACCTCAT AAAACTGAAAACGTTAYTGCTATCCTGA GGGAAACTTCGGCAGGRACCAGCTACTA GATGGTTCGATTAGTCTTTCGCCCCTATG CCCAAATTTGACGATCGATTTGCACGTCA GAACCGCTGCGAGCCTCCACCAGAGTTT CCTCTGGCTTCACCCTATTCAAGCATAGT TCACCATCTTTCGGGTCCCAACAGCTATG CTCTTACTCAAATCCATCCGAAGACATCA GGATCGGTCGATGGTGCACCCAAAGGGT TCCCACCTCCGTTCACTTTCATTGCGCGC CCGGGCTTGACACCCAAACACTCGCATA GATGTTAGACTCCTTGGTCCGTGTTTCAA GACGGGCCGCTTACAGCCATTACGCCAG CATCCTAGCAGATGCGCGGACCTCAGTC CGGGCTGGTTGCATTGCGCCTCCCCTATA AGGTCACCCCGAAGGGAGATACGTGACA GAGGCCTTTATCCAACCGCCCAAACTGA TGCTGGCCTGCCCGCAGAAGAGTGCCCC AGGCCAAAGCCTAGGTGAGCAACTGCGG GCAAGTCTGGCTGCAAGCGCTTCCCTTTC AACAATTTCACGTGCTTTTTGACTCTCTT TCCAAAGTACTTTTCATCTTTCGATCACT CTACTTGTGCGCTATCGGTCTCTGGCCGG TATTTAGCTTTAGAAGAAATTTACCTCCC ATTTAGAGCTGCATTCCCAAACAACTCG ACTCGTCGAAGGAGCTTTACACGGCAAA GGCAGGCGCCCACGTACGGGATTCTCAC CCTCTGCGATGTCCTGTTCCAAGGAACTT AGACCGCCGCCAATGCCAAAGCATCCTC TGCAAATTACAACTCGGACCCCCAAAGA	Paracamarosporium hawaiiense strain Ct-BC55 internal transcribed spacer 1, partial sequence; 5.8S ribosomal RNA gene, complete sequence; and internal transcribed spacer 2, partial sequence 516/519(99%) 0/519(0%) MH305504.1 Paraconiothyrium sp. CBS 194.82 28S ribosomal RNA gene, partial sequence 856/857(99%) 0/857(0%) JX496165.1	https://peerj.com/articles/9342/ https://www.ingentaconnect.com/content/nhn/pimj/2014/00000032/00000001/art00003

			GAGCCAGATTTCAAATTTGAGCTGTTGCC GCTTCACTC		
4.	CsB-1a	>Consensus CTCCGTTGGTGAACCAGCGGAGGGA TCATTGCTGGAACGCGCCCCTGGCGC ACCCAGAAACCCTTTGTGAACTTATA CCTTACTGTTGCCTCGGCGCGGGCCG TCCCCTATGGGGTCCCTCTGGAGACA GAGGAGCAGCCGGCCGGTGGCCAAG TTAACTCTGTTTTTAAATTGAAACTC TGAGTAAAAAACATAAATGAATCAA AACTTTCAACAACGGATCTCTTGGTT CTGGCATCGATGAAGAACGCAGCGA AATGCGATAAGTAATGTGAATTGCA GAATTCAGTGAATCATCGAATCTTTG AACGCACATTGCGCCCTCTGGTATTC CGGAGGGCATGCCTGTTCGAGCGTC ATTTCAACCCTCAAGCCTGGCTTGGT GTTGGGGCACTGCTTTCTAACGGGA GCAGGCCCTGAAATATAGTGGCGAG CTCGCCAGGACTCCGAGCGCAGTAG TTAAACCCTCGCTCTGGAAGGCCTGG CGGTGCCCTGCCGTTAAACCCCCAAC TTCTGAAAATTTGACCTCGGATCAGG TAGGAATACCCGCTGAAACTTAAG	>Consensus AACAAGGGCTTCTTACATATTTAAAGTTT GAGAATGGATGAAGGCAATATATAGCCC CCGAGTCCCTAATCATTCGCTTTACCTCA TAAAACTGAAGATCAACACTGCTATCCK GAGGGAAACTTCGGCGGTWACCAGCTAC TAGACAGTTCGATTAGTCTTTCGCCCCCC ATGCTCAAATTTGACGATCGATTTGCACG TCAGAACCGCTGCGAGCCTCCACCAGAG TTTCCTCTGGCTTCACCCTATTCAAGCAT AGTTCACTGTCTTTCGGGTCCGTCCGTTA AAACTCTTACTCAAATCCTTCCGAGAAC ATCAGGATCGGTCGATGATGCGCCGAAG CTCTCACCTGCGTTCACTTTCATTACGCG TGCGGGTTTTACACCCAAACGCTCGCTCT AATGGACGACTCCTTGGTCCGTGTTTCAA GACGGGTCACTGATGACCATTACGCCAG CATCCTTGCGGAGCGCGGACCTCGGTCC CCACGGGGGTATCGTCCGCCAGGCTATA ACACACCCCGGAGGGTGCTACGTTCCTG ACGGTCTTATCCCCCCACGAGAACCGAT GCTGGCCTGTGCCGGGCGGAGTGCACAG GGGAGAACCCCTGATGAGCCGCCCGGCC CAAGTCTGGTCATAAGTGCTTCCCTTTCA ACAATTTCACGTACTATTTAACCCCCTTT TCAAGGTGCTTTTCATCTTTCGATCACTC TACTTGTGCGCTATCGGTCTCTGGCCGGT ATTTAGCTTTAGAAGAGATTTACCTCCCA TTTAGAGCAGCATTCCCAAACTACTCGA CTCGTCGAAGGAGCTTCACACAGGGCTT GGTGTCCGACCATACGGGGCTCTCACCC TCTGTGGCGTCCCGTTCCAGGRAACTCGG AAGGCACCGCGCCAGAAGCATCCTCTGC	Diaporthe foeniculina isolate SCF 006-685 small subunit ribosomal RNA gene, partial sequence; internal transcribed spacer 1, 5.8S ribosomal RNA gene, and internal transcribed spacer 2, complete sequence; and large subunit ribosomal RNA gene, partial sequence 553/562(98%) 3/562(0%) MW959695.1 Diaporthe vangueriae culture CBS:137985 strain CPC 22703 28S ribosomal RNA gene, partial sequence 817/823(99%) 4/823(0%) KJ869194.1	https://www.ingentaconnect.com/content/nhn/pimj/2014/00000032/00000001/art00011

			AAATTACAACTCGGGCCGARGCCAGATT TCAAATTTGAGCTGTTGCGCTTCCTCGCG TACAG		
5.	CsB-1b	>Consensus CGTAACAAGGTCTCCGTTGGTGAAC CAGCGGAGGGATCATTGCTGGAACG CGCCCCTGGCGCACCCAGAAACCCT TTGTGAACTTATACCTTACTGTTGCC TCGGCGCGGGCCGTCCCCTATGGGG TCCCTCTGGAGACAGAGGAGCAGCC GGCCGGTGGCCAAGTTAACTCTGTTT TTAAATTGAAACTCTGAGTAAAAAA CATAAATGAATCAAAACTTTCAACA ACGGATCTCTTGGTTCTGGCATCGAT GAAGAACGCAGCGAAATGCGATAAG TAATGTGAATTGCAGAATTCAGTGA ATCATCGAATCTTTGAACGCACATTG CGCCCTCTGGTATTCCGGAGGGCATG CCTGTTCGAGCGTCATTTCAACCCTC AAGCCTGGCTTGGTGTTGGGGCACT GCTTTCTAACGGGAGCAGGCCCTGA AATATAGTGGCGAGCTCGCCAGGAC TCCGAGCGCAGTAGTTAAACCCTCG CTCTGGAAGGCCTGGCGGTGCCCTG CCGTTAAACCCCCAACTTCTGAAAAT TTGACCTCGGATCAGGTAGGAATAC CCGCTGAACTTAAGC	>Consensus CGTTCAACTAAGTAACAAGGGCTTCTTA CATATTTWAAGTTTGAGAATGGATGAAG GCAATATAGCGCCCCCGAGTCCCTAATC ATTCGCTTTACCTCATAAAACTGAAGATC AACACTGCTATCCTGAGGGAAACTTCGG CGGTWACCAGCTACTAGACAGTTCGATT AGTCTTTCGCCCCCATGCTCAAATTTGAC GATCGATTTGCACGTCAGAACCGCTGCG AGCCTCCACCAGAGTTTCCTCTGGCTTCA CCCTATTCAAGCATAGTTCACTGTCTTTC GGGTCCGTCCGTTAAAACTCTTACTCAAA TCCTTCCGAGAACATCAGGATCGGTCGA TGATGCGCCGAAGCTCTCACCTGCGTTCA CTTTCATTACGCGTGCGGGTTTTACACCC AAACGCTCGCTCTAATGGACGACTCCTT GGTCCGTGTTTCAAGACGGGTCACTGAT GACCATTACGCCAGCATCCTTGCAGTGC GCGGACCTCGGTCCCCACGGGGGTATCG TCCGCCAGGCTATAACACACCCCGGAGG GTGCTACGTTCCTGACGGTCTTATCCCCC CGCGAGAACCGATGCTGGCCTGTGCCGG GCGGAGTGCACAGGGGAGAACCCCTGAT GAGCCGCCCGGCCCAAGTCTGGTCATAA GTGCTTCCCTTTCAACAATTTCACGTACT ATTTAACCCCCTTTTCAAGGTGCTTTTCA TCTTTCGATCACTCTACTTGTGCGCTATC GGTCTCTGGCCGGTATTTAGCTTTAGAAG AGATTTACCTCCCATTTAGAGCAGCATTC CCAAACTACTCGACTCGTCGAAGGAGCT TCACACAGGCTTGGTGTCCGACCATACG GGGCTCTCACCCTCTGTGGCGTCCCGTTC	Diaporthe foeniculina isolate SCF 006-683 small subunit ribosomal RNA gene, partial sequence; internal transcribed spacer 1, 5.8S ribosomal RNA gene, and internal transcribed spacer 2, complete sequence; and large subunit ribosomal RNA gene, partial sequence 560/568(99%) 2/568(0%) MW959694.1 Diaporthe foeniculina voucher MFLU:16-1132 large subunit ribosomal RNA gene, partial sequence 813/817(99%) 0/817(0%)	https://link.springer.com/article/10.1007/s10658-021-02342-4 https://link.springer.com/article/10.1007/s13225-020-00440-y

			CAGGGAACTCGGAAGGCACCGCGCCAGA AGCATCCTCTGCAAATTACAACTCGGGC CGAGGCCAGATTTCAAATTTGAGCTGTT GCCGCTTCACT		
6.	CsL-1a	>Consensus CTCCGTTGGTGAACCAGCGGAGGGA TCATTGCTGGAACGCGCCCCAGGCG CACCCAGAAACCCTTTGTGAACTTAT ACCTTACTGTTGCCTCGGCGCAGGCC GTCCCCTATGGGGTCCCTCTGGAGAC AGAGGAGCAGCCGGCCGGCGGCCAA GTTAACTCTGTTTTTAAACTGAAACT CTGAGTACAAAACATAAATGAATCA AAACTTTCAACAACGGATCTCTTGGT TCTGGCATCGATGAAGAACGCAGCG AAATGCGATAAGTAATGTGAATTGC AGAATTCAGTGAATCATCGAATCTTT GAACGCACATTGCGCCCTCTGGTATT CCGGAGGGCATGCCTGTTCGAGCGT CATTTCAACCCTCAAGCCTGGCTTGG TGTTGGGGCACTGCCTGTAAAAGGG CAGGCCCTGAAATATAGTGGCGAGC TCGCCAGGACTCCGAGCGTAGTAGT TAAACCCTCGCTTTGGAAGGCCTGGC GGTGCCCTGCCGTTAAACCCCAACTT CTGAAAATTTGACCTCGGATCAGGT AGGAATACCCGCTGAACTTAAGCA	>Consensus AACTAAGTAACAAGGGCTTCTTACATAT TTAAAGTTTGAGAATGGATGAAGGCAAT ATATAGCCCCCGAGTCCCTAATCATTCGC TTTACCTCATAAAACTGAAGATCAACAC TGCTATCCTGAGGGAAACTTCGGCGGTW ACCAGCTACTAGACAGTTCGATTAGTCTT TCGCCCCCATGCTCAAATTTGACGATCGA TTTGCACGTCAGAACCGCTGCGAGCCTC CACCAGAGTTTCCTCTGGCTTCACCCTAT TCAAGCATAGTTCACTGTCTTTCGGGTCC GTCCGTTAAAACTCTTACTCAAATCCTTC CGAGAACATCAGGATCGGTCGATGATGC GCCGAAGCTCTCACCTGCGTTCACTTTCA TTACGCGTGCGGGTTTTACACCCAAACG CTCGCTCTAATGGACGACTCCTTGGTCCG TGTTTCAAGACGGGTCACTGATGACCATT ACGCCAGCATCCTTGCGGAGCGCGGACC TCGGTCCCCACGGGGGTATCGTCCGCCA GGCTATAACACACCCCGGAGGGTGCTAC GTTCCTGACGGTCTTATCCCCCCACGAGA ACCGATGCTGGCCTGTGCCGGGCGGAGT GCACAGGGGAGAACCCCTGATGAGCCGC CCGGCCCAAGTCTGGTCATAAGTGCTTCC CTTTCAACAATTTCACGTACTATTTAACC CCCTTTTCAAGGTGCTTTTCATCTTTCGA TCACTCTACTTGTGCGCTATCGGTCTCTG GCCGGTATTTAGCTTTAGAAGAGATTTAC CTCCCATTTAGAGCAGCATTCCCAAACTA CTCGACTCGTCGAAGGAGCTTCACACAG GCTTGGTGTCCGACCATACGGGGCTCTC	Diaporthe velutina isolate RY-4 internal transcribed spacer 1, partial sequence; 5.8S ribosomal RNA gene and internal transcribed spacer 2, complete sequence; and large subunit ribosomal RNA gene, partial sequence 509/513(99%) 0/513(0%) MK429860.1 Diaporthe parapterocarpi culture CBS:137986 strain CPC 22729 28S ribosomal RNA gene, partial sequence 819/820(99%) 0/820(0%) KJ869195.1	https://link.springer.com/chapter/10.1007/978-981-16-2922-8_2 https://www.ingentaconnect.com/content/nhn/pimj/2014/00000032/00000001/art00011

			ACCCTCTGTGGCGTCCCGTTCCAGGRAAC TCGGAAGGCACCGCGCCAGAAGCATCCT CTGCAAATTACAACTCGGGCCGAGGCCA GATTTCAAATTTGAGCTGTTGCCGCTTCA CTCGCCG		
7.	CsL-2b	>Consensus GTTTCCGTAGGTGAACCTGCGGAAG GATCATTACCGAGTGAGGGCCCTCT GGGTCCAACCTCCCACCCGTGTTTAT TTTACCTTGTTGCTTCGGCGGGCCCG CCTTAACTGGCCGCCGGGGGGCTTA CGCCCCCGGGCCCGCGCCCGCCGAA GACACCCTCGAACTCTGTCTGAAGAT TGTAGTCTGAGTGAAAATATAAATT ATTTAAAACTTTCAACAACGGATCTC TTGGTTCCGGCATCGATGAAGAACG CAGCGAAATGCGATACGTAATGTGA ATTGCAAATTCAGTGAATCATCGAGT CTTTGAACGCACATTGCGCCCCCTGG TATTCCGGGGGGCATGCCTGTCCGA GCGTCATTTCTGCCCTCAAGCACGGC TKGTGTGTTGGGCCCCGTCCTCCGAT CCCGGGGGACGGGCCCGAAAGGCAG CGGCGGCACCGCGTCCGGTCCTCGA GCGTATGGGGCTTTGTCACCCGCTCT GTAGGCCCGGCCGGCGCTTGCCGAT CAACCCAAATTTTTATCCAGGTTGAC CTCGGATCAGGTAGGGATACCCGCT GAACTTAAGCA	>Consensus CGTTCAATTAAGCAACAAGGCTTCTTAC ATATTTAAAGTTTGAGAATAGGTTAAGG TTGTTTCAACCCCAAGGCCTCTAATCATT CGCTTTACCTCATAAAACTGAATTCGCGT TACTGCTATCCTGAGGGAAACTTCGGCA GGAACCAGCTACCAGATGGTTCGATTAG TCTTTCGCCCCTATACCCAAATTCGACGA TCGATTTGCACGTCAGAACCGCTACGAG CCTCCACCAGAGTTTCCTCTGGCTTCGCC CTATTCAGGCATAGTTCACCATCTTTCGG GTCCCAACAGCTACGCTCTTACTCAAATC CATCCGAAGACTTCAGGATCGGTCGATG GTGCACCCGTGAGGGTTCCCACCTCCGTT CGCTTTCACTTCGCGCACGGGTTTGACAC CCGAACACTCGCGTAGATGTTAGACTCC TTGGTCCGTGTTTCAAGACGGGTCGTTTA CGACCATTATGCCAGCGTCCGAGCCGAA GCGCGTTCCTCGGTCTAGGCAGGTCGCA TTGCACCCTCGGCTATAAGACGCCCCTA GGGGCGTTACCTTCCGAGGGCCTTTGAC CGACCGCCCAAACCGACGCTGGCCCGCC CGCGGGGAAGTACACCGGCACGAATGCC GGCTGAACCCCGCGAGCGAGTCTGGTCG CAAGCGCTTCCCTTTCAACAATTTCACGT GCTTTTTAACTCTCTTTTCAAAGTGCTTTT CATCTTTCGATCACTCTACTTGTGCGCTA TCGGTCTCCGGCCAATATTTAGCTTTAGA TGAAATTTACCACCCATTTAGAGCTGCAT TCCCAAACAACTCGACTCGTCGAAGGAG	Penicillium camemberti clone SF_592 small subunit ribosomal RNA gene, partial sequence; internal transcribed spacer 1, 5.8S ribosomal RNA gene, and internal transcribed spacer 2, complete sequence; and large subunit ribosomal RNA gene, partial sequence 570/571(99%) 0/571(0%) MT529868.1 Penicillium chrysogenum culture CBS:127368 strain CBS 127368 large subunit ribosomal RNA gene, partial sequence 860/860(100%) 0/860(0%) MH875985.1	Vu, D., Groenewald, M., De Vries, M., Gehrmann, T., Stielow, B., Eberhardt, U., ... & Verkley, G. J. M. (2018). Large-scale generation and analysis of filamentous fungal DNA barcodes boosts coverage for kingdom fungi and reveals thresholds for fungal species and higher taxon delimitation. Studies in mycology, 91(1), 23-36.

			CTTCACACGGGCGCGGACACCCCATCCC ATACGGGATTCTCACCCTCTATGACGTCC CGTTCCAGGGCACTTAGATGGGGACCGC TCCCGAAGCATCCTCTACAAATTACAAT GCGGACCCCGAAGGAGCCAGCTTTCAAA TTTGAGCTCTTGCCGCTTCACTCGCCG		
8.	CsL2b-1	>Consensus TGCTTAAGTTCAGCGGGTATCCCTAC CTGATCCGAGGTCAACCTGGATAAA AATTTGGGTTGATCGGCAAGCGCCG GCCGGGCCTACAGAGCGGGTGACAA AGCCCCATACGCTCGAGGACCGGAC GCGGTGCCGCCGCTGCCTTTCGGGCC CGTCCCCCGGGATCGGAGGACGGGG CCCAACACACMAGCCGTGCTTGAGG GCAGAAATGACGCTCGGACAGGCAT GCCCCCCGGAATACCAGGGGGCGCA ATGTGCGTTCAAAGACTCGATGATTC ACTGAATTTGCAATTCACATTACGTA TCGCATTTCGCTGCGTTCTTCATCGA TGCCGGAACCAAGAGATCCGTTGTT GAAAGTTTTAAATAATTTATATTTTC ACTCAGACTACAATCTTCAGACAGA GTTCGAGGGTGTCTTCGGCGGGCGC GGGCCCGGGGGCGTAAGCCCCCGG CGGCCAGTTAAGGCGGGCCCGCCGA AGCAACAAGGTAAAATAAACACGGG TGGGGAGGTTGGACCCAGAGGGCCC TCACTCGGTAATGATCCTTCCGCAGG TTCACCTACGGAAACCTTGTTACGA	>Consensus CCCACGTTCAATTAAGCAACAAGGGCTT CTTACATATTTAAAGTTTGAGAATAGGTT AAGGTTGTTTCAACCCCAAGGCCTCTAAT CATTCGCTTTACCTCATAAAACTGAATTC GCGTTACTGCTATCCTTGAGGGAAACTTC GGCAGGRACCAGCTACCAGATGGTTCGA TTAGTCTTTCGCCCCCTATACCCAAATTC GACGATCGATTTGCACGTCAGAACCGCT ACGAGCCTCCACCAGAGTTTCCTCTGGCT TCGCCCTATTCAGGCATAGTTCACCATCT TTCGGGTCCCAACAGCTACGCTCTTACTC AAATCCATCCGAAGACTTCAGGATCGGT CGATGGTGCACCCGTGAGGGTTCCCACC TCCGTTCGCTTTCACTTCGCGCACGGGTT TGACACCCGAACACTCGCGTAGATGTTA GACTCCTTGGTCCGTGTTTCAAGACGGGT CGTTTACGACCATTATGCCAGCGTCCGA GCCGAAGCGCGTTCCTCGGTCTAGGCAG GTCGCATTGCACCCTCGGCTATAAGACG CCCCTAGGGGCGTTACCTTCCGAGGGCC TTTGACCGACCGCCCAAACCGACGCTGG CCCGCCCGCGGGGAAGTACACCGGCACG AATGCCGGCTGAACCCCGCGAGCGAGTC TGGTCGCAAGCGCTTCCCTTTCAACAATT TCACGTGCTTTTTAACTCTCTTATTCRAA GTGCTTTTCRTCTTTCKATCACTCTACTTG TGCGCTATCGGTCTCCGGCCAATATTTAG CTTTAGATGAAATTTACCACCCATTTAKA	Penicillium rubens strain DTO269E3 small subunit ribosomal RNA gene, partial sequence; internal transcribed spacer 1, 5.8S ribosomal RNA gene, and internal transcribed spacer 2, complete sequence; and large subunit ribosomal RNA gene, partial sequence 580/582(99%) 1/582(0%) MN413181.1 Penicillium chrysogenum strain DAOM 215337 28S ribosomal RNA (LSU) gene, partial sequence 840/847(99%) 2/847(0%) JN938948.1	https://www.pnas.org/doi/abs/10.1073/pnas.1117018109

			GCTGCATTCYCAAACAACTCGACTCGTC GAAGGAGCTTCACACGGGCGCGGACACC CCATCCCATACGGGATTCTCACCCTCTAT GACGTCCCGTTCCAGGGCACTTAGATGG GGACCGCTCCCGAAGCATCCTCTACAAA TTACAATGCGGACCCCGAAGGAGCCAGC TTTCAAATTTGAGCTCTTGCCGCTTCACT CGCC		
9.	CsR-1	>Consensus TCGTAACAAGGTTTCCGTAGGTGAA CCTGCGGAAGGATCATTACCGAGTG CGGGCCCTCGCGGCCCAACCTTCCC MCCCTTGTCTCTATACACCTGTTGCT TTGGCGGGCCCACCGGGGCCACCTG GTCGCCGGGGGACGCACGTCTCCGG GCCCGCGCCCGCCGAAGCGCTCTGT GAACCCTGATGAAGATGGGCTGTCT GAGTACTGTGAAAATTGTCAAAACT TTCAACAATGGATCTCTTGGTTCCGG CATCGATGAAGAACGCAGCGAAATG CGATAAGTAATGTGAATTGCAGAAT TCCGTGAATCATCGAATCTTTGAACG CACATTGCGCCCCCTGGCATTCCGGG GGGCATGCCTGTCCGAGCGTCATTTC TGCCCTCAAGCACGGCTTGTGTGTTG GGGTGTGGTCCCCCCGGGGACCTGC CCGAAAGGCAGCGGCGACGTCCGTC TGGTCCTCGAGCGTATGGGGCTCTGT CACTCGCTCGGGAAGGACCTGCGGG GGGTTGGTCACCACCATGTTTTACCA CGGTTGACCTCGGATCAGGTAGGAG TTACCCGCTGAACTTAA	>Consensus CTTCTTACATATTTAAAGTTTGAGAATAG GTTAAGGTTGTTTCAACCCCAAGGCCCTC TAATCATTCGCTTTACCTCATAAAACTGA TGTCGTTACTGCTATCCTGAGGGAAACTT CGGCAGGRACCAGCTACCAGATGGTTCG ATTAGTCTTTCGCCCCTATACCCAAATT TGACGATCGATTTGCACGTCAGAACCGC TGCGAGCCTCCACCAAGAGTTTCCTCTGG CTTCGCCCTATTCAGGCATAGTTCACCAT CTTTCGGGTCCCAACAGCTATGCTTCTTA CTCAAATCCATCCGAAGACATCAGGATC GGTCGATGGTGCGCCCCGAGGGGCTCCC ACCTTCCGTTCGCTTTCACTGCGCGGACG GGTTTGACACCCGAACACTCGCATAGAT GTTAGACTCCTTGGTCCGTGTTTCAAGAC GGGCCGTTGACCACCATTACGCCAGCAT CCTCGCCGAAGCGCGGGCCTCGGTCCAG GCTGGCTGTATGGCACCCCGGGCTATAA GGCACCCCGAAGGGTGGCACATTCCCGG GGCCTTTCACCAGCCGCCCAAACCGATG CTGGCCCGCCCGGAGAGGAGTACACCGG CACACGTGCCGGCTGAACCCCCCCGGGC GAGTCTGGTGGACAACGCTTCCCTTTCAA CAATTTCACGTGCTGTTTAACTCTCTTTT CAAAGTGCTTTTCATCTTTCGATCACTCT ACTTGTGCGCTATCGGTCTCCGGCCAGTA	Talaromyces pinophilus strain 17F4103 small subunit ribosomal RNA gene, partial sequence; internal transcribed spacer 1, 5.8S ribosomal RNA gene, and internal transcribed spacer 2, complete sequence; and large subunit ribosomal RNA gene, partial sequence 571/575(99%) 3/575(0%) MT093464.1 Talaromyces pinophilus isolate Ashna.16 large subunit ribosomal RNA gene, partial sequence 805/811(99%) 5/811(0%) ON738239.1	https://link.springer.com/article/10.1007/s11418-020-01400-1

			TTTAGCTTTAGATGAAATTTACCACCCGC TTAGAGCTGCATTCCCAAACAACTCGAC TCGTCGAAGGAGCTTCACACGGGCGCGG CCGCCCATCCCAGAACGGGATTCTCACC CTCTATGACGGCCCGTTCCAGGSCACTTA GACGGGGACCGCACCCGAAGCATCCTCT GCAAATTACAACTCGGACCCCAAAGGGG CCAGATTTCAAATTTGAGCTCTKCCGC		
10.	CsR-1a	>Consensus CGTAACAAGGTTTCCGTAGGTGAAC CTGCGGAAGGATCATTAACGAGTTTT GAAACGGGTTGTTGCTGGCCTTCCGA GGCATGTGCACGCCCTGCTCATCCAC TCTACACCTGTGCACTTACTGTAGGT TGGCGTGGGTTTCTGACCTCCGGGTT GGAAGCATTCTGCCGGCCTATGTAC ACTACAAACTCTTAAAGTATCAGAA TGTAAACGCGTCTAACGCATCTTAAT ACAACTTTCAGCAACGGATCTCTTGG CTCTCGCATCGATGAAGAACGCAGC GAAATGCGATAAGTAATGTGAATTG CAGAATTCAGTGAATCATCGAATCTT TGAACGCACCTTGCGCTCCTTGGTAT TCCGAGGAGCATGCCTGTTTGAGTGT CATGAAATTCTCAACCCATAAATCCT TGTGATCTATGGGCTTGGATTTGGAG GCTTGCTGGCCCTAGTGGTCGGCTCC TCTTGAATGCATTAGCTTGATTCCGT GCGGATCGGCTCTCAGTGTGATAATT GTCTACGCTGTGACCGTGAAGCGTTT TGGCGAGCTTCTAACCGTCCATTAGG ACAATCTTTCAACATCTGACCTCAAA TCAGGTAGGACTACCCGCTGAACTT AA	>Consensus CGACGGCTCGTTCTTACATATTTAAAGTT TGAGAATAGGTTAAGGTTGTTTCAACCC CCAAGGCCCTCTAATCATTCGCTTTACCA CATAAATTCTGATATGAGTTTCTGCTATC CTGAGGGAAACTTCGGCAGGGAACCAGC TACTAGATGGTTCGATTAGTCTTTCGCCC CCTATACCCAAATTTGACGATCGATTTGC ACGTCAGAATCGCTACGAGCCTCCACCA GAGTTTCCTCTGGCTTCACCCTATTCAGG CATAGTTCACCATCTTTCGGGTCCCAACA TACATGCTCTACCGCGGATCCGTCAGAG AACTTCAGGTCCGGGCGTCGATGCCCTC CACGACAGAGGTCTCAACTTTCACTTTCA TTACGCGCTCGGGTTTTCCACCCAAACAC TCGCAGGCATGTTAGACTCCTTGGTCCGT GTTTCAAGACGGGTCGTTTAAAGCCATT ATGCCAGCATCCTAAGCACGAATGTGGG CGAACCCCAGCCATAAGGCGTGCTGCGT TCCTCGATCCCAACCGCTGTATGCGACTG AAGGCTATAACACACCCGAAGGTGCCAC ATTCCTCCAGCCCTTTTCCAGCGGTCAAA ATCGATGCTGGCCCGTCAACCGGAAAGT GCACCAAGCCGAAGCAAGGCTGAGTTCC GGACGACGCGACTGACTTCAAGCGTTTC CCTTTCAGCAATTTCACGTACTGTTTAAC TCTCTTTCCAAAGTGCTTTTCATCTTTCCC	Trametes hirsuta strain DMC716 18S ribosomal RNA gene, partial sequence; internal transcribed spacer 1, 5.8S ribosomal RNA gene, and internal transcribed spacer 2, complete sequence; and 28S ribosomal RNA gene, partial sequence 619/620(99%) 0/620(0%) KC589147.1 Trametes hirsuta isolate SJY-4 large subunit ribosomal RNA gene, partial sequence 969/975(99%) 4/975(0%) ON139208.1	

			TCACGGTACTTGTTCGCTATCGGTCTCTC GCCAATATTTAGCTTTAGAAGGAATTCA CCTCCCATTTTGCGCTGCATTCCCAAACA ACGCGACTCTTTGAGAGCGCATCACAAA GCATTGGTAGTCCGTGTCAAAGACGGGA TTCTCACCCTCTATGACGCTCTGTTCCAA GAGACTTGTACACGGTCCAACGCGGAAG ACGCTTCTCCAGACTACAACTCGGACGG CCAAAGACCGCCAGAWTTTAAATTTGAG CTTTTCCCGCTTCACTCGC		
11.	CsR1aN	>Consensus TCGTAACAAGGTTTCCGTAGGTGAA CCTGCGGAAGGATCATTACCGAGTG TAGGGTTCCTAGCGAGCCCAACCTCC CCACCCGTGTTTACTGTACCTTAGTT GCTTCGGCGGGCCCGCCATTCATGGC CGCCGGGGGCTCTCAGCCCCGGGCC CGCGCCCGCCGGAGACACCACGAAC TCTGTCTGATCTAGTGAAGTCTGAGT TGATTGTATCGCAATCAGTTAAAACT TTCAACAATGGATCTCTTGGTTCCGG CATCGATGAAGAACGCAGCGAAATG CGATAACTAGTGTGAATTGCAGAAT TCCGTGAATCATCGAGTCTTTGAACG CACATTGCGCCCCCTGGTATTCCGGG GGGCATGCCTGTCCGAGCGTCATTGC TGCCCATCAAGCACGGCTTGTGTGTT GGGTCGTCGTCCCCTCTCCGGGGGG GACGGGCCCCAAAGGCAGCGGCGGC ACCGCGTCCGATCCTCGAGCGTATG GGGCTTTGTCACCCGCTCTGTAGGCC CGGCCGGCGCTTGCCGAACGCAAAT CAATCTTTTCCAGGTTGACCTCGGAT CAGGTAGGGATACCCGCTGAACTTA A	>Consensus GGGCTTCTTACATATTTAAAGTTTGAGAA TAGGTTAAGGTTGTTTCAACCCCAATGCC TCTAATCATTCGCTTTACCTCATAAAACT GAATTCGCGTTACTGCTATCCTGAGGGA AACTTCGGCAGGAACCAGCTACTAGATG GTTCGATTAGTCTTTCGCCCCTATACCCA AATTTGACGATCGATTTGCACGTCAGAA CCGCTGCGAGCCTCCACCAGAGTTTCCTC TGGCTTCGCCCTATTCAGGCATAGTTCAC CATCTTTCGGGTCCCCACATTTACGCTCT TACTCAAATCCATCCGAAGACATCAGGA TCGGTCGATGGTGCGCCCCACGAGGGGG CTCCCACCTCCGTTCGCTTTCACTGCGCG TACGGGTTTGACACCCGAACACTCGCGT AGATGTTAGACTCCTTGGTCCGTGTTTCA AGACGGGTCGTTTACGACCATTATGCCA GCGTCCGTGCCGAAGCGCGTTCCTCGGT CCAGGCTGGCCGCATTGCACTCCCGGCT ATAAGGTGCCCCGGAGGGCACTACATTC CGGGAGCCTTTGACCGGCCGCCCAAACC GACGCTGGCCCGCCCCCAGGGAAGTACA CCGGCACGAATGCCGGCTGAACCCTGGA GGCGAGTCTGGTCGCAAGCGCTTCCCTTT CAACAATTTCACGTGCTTTTTAACTCTCT	Aspergillus flavus clone SF_652 small subunit ribosomal RNA gene, partial sequence; internal transcribed spacer 1, 5.8S ribosomal RNA gene, and internal transcribed spacer 2, complete sequence; and large subunit ribosomal RNA gene, partial sequence 587/588(99%) 1/588(0%) MT529928.1 Aspergillus flavus strain KSRCT-BT-MS5 small subunit ribosomal RNA gene, partial sequence; internal transcribed spacer 1, 5.8S ribosomal RNA gene, and internal transcribed spacer 2, complete sequence; and large subunit ribosomal RNA gene, partial sequence 969/972(99%)	https://link.springer.com/article/10.1007/s11101-016-9473-1

			TTTCAAAGTGCTTTTCATCTTTCGATCAC TCTACTTGTGCGCTATCGGTCTCCGGCCA GTATTTAGCTTTAGATGAAATTTACCACC CATTTAGAGCTGCATTCCCAAACAACTC GACTCGTCGAAGGAGCTTCACACGGGCG CGGACACCCCATCCCAGACGGGATTCTC ACCCTCTCTGACGGCCCGTTCCAGGGCA CTTAGACGGGGGCCGCACCCGAAGCATC CTCTGCAAATTACAATGCGGACCCCGAA GGAGCCGCTTTCAAATTTGAGCTCTTGCG CTT	2/972(0%) MT509808.1	
12.	CsR1C-1	>Consensus CGTAACAAGGTTTCCGTAGGTGAAC CTGCGGAAGGATCATTACCGAGTGA GGGCCCTCTGGGTCCAACCTCCCACC CGTGTTTATTTTACCTTGTTGCTTCGG CGGGCCCGCCTTAACTGGCCGCCGG GGGGCTTACGCCCCCGGGCCCGCGC CCGCCGAAGACACCCTCGAACTCTG TCTGAAGATTGTAGTCTGAGTGAAA ATATAAATTATTTAAAACTTTCAACA ACGGATCTCTTGGTTCCGGCATCGAT GAAGAACGCAGCGAAATGCGATACG TAATGTGAATTGCAAATTCAGTGAAT CATCGAGTCTTTGAACGCACATTGCG CCCCCTGGTATTCCGGGGGGCATGCC TGTCCGAGCGTCATTTCTGCCCTCAA GCACGGCTTGTGTGTTGGGCCCCGTC CTCCGATCCCGGGGGACGGGCCCGA AAGGCAGCGGCGGCACCGCGTCCGG TCCTCGAGCGTATGGGGCTTTGTCAC CCGCTCTGTAGGCCCGGCCGGCGCTT GCCGATCAACCCAAATTTTTATCCAG GTTGACCTCGGATCAGGTAGGGATA CCCGCTGAACTTAAGCAT	>Consensus CGTTCAATTAAGCAACAAGGGCTTCTTA CATATTTAAAGTTTGAGAATAGGTTAAG GTTGTTTCAACCCCAAGGCCTCTAATCAT TCGCTTTACCTCATAAAACTGAATTCGCG TTACTGCTATCCTGAGGGAAACTTCGGC AGGAACCAGCTACCAGATGGTTCGATTA GTCTTTCGCCCCTATACCCAAATTCGACG ATCGATTTGCACGTCAGAACCGCTACGA GCCTCCACCAGAGTTTCCTCTGGCTTCGC CCTATTCAGGCATAGTTCACCATCTTTCG GGTCCCAACAGCTACGCTCTTACTCAAAT CCATCCGAAGACTTCAGGATCGGTCGAT GGTGCACCCGTGAGGGTTCCCACCTCCG TTCGCTTTCACTTCGCGCACGGGTTTGAC ACCCGAACACTCGCGTAGATGTTAGACT CCTTGGTCCGTGTTTCAAGACGGGTCGTT TACGACCATTATGCCAGCGTCCGAGCCG AAGCGCGTTCCTCGGTCTAGGCAGGTCG CATTGCACCCTCGGCTATAAGACGCCCCT AGGGGCGTTACCTTCCGAGGGCCTTTGA CCGACCGCCCAAACCGACGCTGGCCCGC CCGCGGGGAAGTACACCGGCACGAATGC CGGCTGAACCCCGCGAGCGAGTCTGGTC	Penicillium rubens strain DTO269E3 small subunit ribosomal RNA gene, partial sequence; internal transcribed spacer 1, 5.8S ribosomal RNA gene, and internal transcribed spacer 2, complete sequence; and large subunit ribosomal RNA gene, partial sequence 581/581(100%) 0/581(0%) MN413181.1 Penicillium rubens CBS 129667 28S rRNA gene, partial sequence; from TYPE material 826/833(99%) 2/833(0%) NG_070009.1	https://www.nature.com/articles/s41598-019-49966-5 Vu, D., Groenewald, M., De Vries, M., Gehrmann, T., Stielow, B., Eberhardt, U., ... & Verkley, G. J. M. (2018). Large-scale generation and analysis of filamentous fungal DNA barcodes boosts coverage for

			GCAAGCGCTTCCCTTTCAACAATTTCACG TGCTTTTTAACTCTCTTTTCAAAGTGCTTT TCATCTTTCGATCACTCTACTTGTGCGCT ATCGGTCTCCGGCCAATATTTAGCTTTAG ATGAAATTTACCACCCATTTAGAGCTGC ATTCYCARACAACTCGACTCGTCGAAGG AGCTTCACACGGGCGCGGACACCCCATC CCATACGGGATTCTCACCCTCTATGACGT CCCGTTCCAGGGCACTTAGATGGGGACC GCTCCCGAAGCATCCTCTACAAATTACA ATGCGGACYCCGAAGGAGCCAGCTTTCA AATTTGGAGCTCTTGCCGCTTCACTCGCC		kingdom fungi and reveals thresholds for fungal species and higher taxon delimitation. Studies in mycology, 91(1), 23-36.
13.	CsR1C-2	>Consensus AGTCGTAACAAGGTTTCCGTAGGTG AACCTGCGGAAGGATCATTAACGAG TTTTGAAACGGGTTGTTGCTGGCCTT CCGAGGCATGTGCACGCCCTGCTCAT CCACTCTACACCTGTGCACTTACTGT AGGTTGGCGTGGGTTTCTGACCTCCG GGTTGGAAGCATTCTGCCGGCCTATG TACACTACAAACTCTTAAAGTATCAG AATGTAAACGCGTCTAACGCATCTTA ATACAACTTTCAGCAACGGATCTCTT GGCTCTCGCATCGATGAAGAACGCA GCGAAATGCGATAAGTAATGTGAAT TGCAGAATTCAGTGAATCATCGAAT CTTTGAACGCACCTTGCGCTCCTTGG TATTCCGAGGAGCATGCCTGTTTGAG TGTCATGAAATTCTCAACCCATAAAT CCTTGTGATCTATGGGCTTGGATTTG GAGGCTTGCTGGCCCTAGTGGTCGG CTCCTCTTGAATGCATTAGCTTGATT CCGTGCGGATCGGCTCTCAGTGTGAT AATTGTCTACGCTGTGACCGTGAAGC	>Consensus TATTTAAAGTTTGAGAATAGGTTAAGGTT GTTTCAACCCCCAAGGCCCTCTAATCATT CGCTTTACCACATAAATTCTGATATGAGT TTCTGCTATCCTGAGGGAAACTTCGGCA GGGAACCAGCTACTAGATGGTTCGATTA GTCTTTCGCCCCCTATACCCAAATTTGAC GATCGATTTGCACGTCAGAATCGCTACG AGCCTCCACCAGAGTTTCCTCTGGCTTCA CCCTATTCAGGCATAGTTCACCATCTTTC GGGTCCCAACATACATGCTCTACCGCGG ATCCGTCAGAGAACTTCAGGTCCGGGCG TCGATGCCCTCCACGACAGAGGTCTCAA CTTTCACTTTCATTACGCGCTCGGGTTTT CCACCCAAACACTCGCAGGCATGTTAGA CTCCTTGGTCCGTGTTTCAAGACGGGTCG TTTAAAGCCATTATGCCAGCATCCTAAGC ACGAATGTGGGCGAACCCCAGCCATAAG GCGTGCTGCGTTCCTCGATCCCAACCGCT GTATGCGACTGAAGGCTATAACACACCC GAAGGTGCCACATTCCTCCAGCCCTTTTC CAGCGGTCAAAATCGATGCTGGCCCGTC	Trametes hirsuta strain DMC716 18S ribosomal RNA gene, partial sequence; internal transcribed spacer 1, 5.8S ribosomal RNA gene, and internal transcribed spacer 2, complete sequence; and 28S ribosomal RNA gene, partial sequence 626/627(99%) 0/627(0%) KC589147.1 Trametes hirsuta strain DMC341 28S ribosomal RNA gene, partial sequence 874/876(99%) 1/876(0%) KC589166.1	https://onlinelibrary.wiley.com/doi/abs/10.1002/tax.606003?casa_token=z3mJPp0sGuIAAAAA:wm4Y-ttM4803CPql-abtqSorwqw5rgHhgeJbKCQ36JACWLjFLYyobimPETuw2LFNkhv2vSS382RnrTdk

		GTTTTGGCGAGCTTCTAACCGTCCAT TAGGACAATCTTTCAACATCTGACCT CAAATCAGGTAGGACTACCCGCTGA ACTTAAGCAT	AACCGGAAAGTGCACCAAGCCGAAGCA AGGCTGAGTTCCGGACGACGCGACTGAC TTCAAGCGTTTCCCTTTCAGCAATTTCAC GTACTGTTTAACTCTCTTTCCAAAGTGCT TTTCATCTTTCCCTCACGGTACTTGTTCG CTATCGGTCTCTCGCCAATATTTAGCTTT AGAAGGAATTCACCTCCCATTTTGCGCTG CATTCCCAAACAACGCGACTCTTTGAGA GCGCATCACAAAGCATTGGTAGTCCGTG TCAAAGACGGGATTCTCACCCTCTATGA CGCTCTGTTCCAAGAGACTTGTACACGGT CCAACGCGGAAGACGCTTCTCCAGACTA CAACTCGGACGGCCAAAGACCGCCRGAT TTTAAATTTGAGCTTTTCCCGCTT		
14.	CsR1e	>Consensus TAACAAGGTTTCCGTAGGTGAACCT GCGGAAGGATCATTAACGAGTTTTG AAACGGGTTGTTGCTGGCCTTCCGAG GCATGTGCACGCCCTGCTCATCCACT CTACACCTGTGCACTTACTGTAGGTT GGCGTGGGTTTCTGACCTCCGGGTTG GAAGCATTCTGCCGGCCTATGTACAC TACAAACTCTTAAAGTATCAGAATGT AAACGCGTCTAACGCATCTTAATAC AACTTTCAGCAACGGATCTCTTGGCT CTCGCATCGATGAAGAACGCAGCGA AATGCGATAAGTAATGTGAATTGCA GAATTCAGTGAATCATCGAATCTTTG AACGCACCTTGCGCTCCTTGGTATTC CGAGGAGCATGCCTGTTTGAGTGTC ATGAAATTCTCAACCCATAAATCCTT GTGATCTATGGGCTTGGATTTGGAGG CTTGCTGGCCCTAGTGGTCGGCTCCT CTTGAATGCATTAGCTTGATTCCGTG CGGATCGGCTCTCAGTGTGATAATTG	>Consensus TCTTCCCTATTTAAAGTTTGAGAATAGGT TAAGGTTGTTTCAACCCCMAGGCCTCTW ATCATTCGCTTTACCACATAAATCTGATA TGAGTTTCTGCTATCCTGAGGGAAACTTC GGCMGGAACCAGYTACWARATGGTTCG ATTAGTCTTTCGCCCCTATACCCAAATTT GACGATCGATTTGCACGTCAGAATCGCT ACGAGCCTCCACCAGAGTTTCCTCTGGCT TCACCCTATTCAGGCATAGTTCACCATCT TTCGGGTCCCAACATACATGCTCTACCGC GGATCCGTCAGAGAACTTCAGGTCCGGG CGTCGATGCCCTCCACGACAGAGGTCTC AACTTTCACTTTCATTACGCGCTCGGGTT TTCCACCCAAACACTCGCAGGCATGTTA GACTCCTTGGTCCGTGTTTCAAGACGGGT CGTTTAAAGCCATTATGCCAGCATCCTAA GCACGAATGTGGGCGAACCCCAGCCATA AGGCGTGCTGCGTTCCTCGATCCCAACC GCTGTATGCGACTGAAGGCTATAACACA CCCGAAGGTGCCACATTCCTCCAGCCCTT	Trametes hirsuta strain DMC716 18S ribosomal RNA gene, partial sequence; internal transcribed spacer 1, 5.8S ribosomal RNA gene, and internal transcribed spacer 2, complete sequence; and 28S ribosomal RNA gene, partial sequence 617/618(99%) 0/618(0%) KC589147.1 Trametes hirsuta strain DMC341 28S ribosomal RNA gene, partial sequence 890/896(99%) 3/896(0%) KC589166.1	https://onlinelibrary.wiley.com/doi/abs/10.1002/tax.606003?casa_token=PxFtkwfxhuIAAAAA:rXdWwaFd_NdhEtXFTdrf_IMmzTDel-fSqrvpFOkEQ_qT9IqL-tAu90f2P2-4-1AFYP_AtIxrQuF8RIAx

		TCTACGCTGTGACCGTGAAGCGTTTT GGCGAGCTTCTAACCGTCCATTAGG ACAATCTTTCAACATCTGACCTCAAA TCAGGTAGGACTACCCGCTGAACTT AA	TTCCAGCGGTCAAAATCGATGCTGGCCC GTCAACCGGAAAGTGCACCAAGCCGAAG CAAGGCTGAGTTCCGGACGACGCGACTG ACTTCAAGCGTTTCCCTTTCAGCAATTTC ACGTACTGTTTAACTCTCTTTCCAAAGTG CTTTTCATCTTTCCCTCACGGTACTTGTTC GCTATCGGTCTCTCGCCAATATTTAGCTT TAGAAGGAATTCACCTCCCATTTTGCGCT GCATTCCCAAACAACGCGACTCTTTGAG AGCGCATCACAAAGCATTGGTAGTCCGT GTCAAAGACGGGATTCTCACCCTCTATG ACGCTCTGTTCCAAGAGACTTGTACACG GTCCAACGCGGAAGACGCTTCTCCAGAC TACAACTCGGACGGCCAAAGACCGCCAG ATTTCTAAATTTGAGCTTTCCCGCTTCCT CGCAGTTACTAGGGGA		
15.	CsR1e-1	>Consensus TAACAAGGTTTCCGTAGGTGAACCT GCGGAAGGATCATTAACGAGTTTTG AAACGGGTTGTTGCTGGCCTTCCGAG GCATGTGCACGCCCTGCTCATCCACT CTACACCTGTGCACTTACTGTAGGTT GGCGTGGGTTTCTGACCTCCGGGTTG GAAGCATTCTGCCGGCCTATGTACAC TACAAACTCTTAAAGTATCAGAATGT AAACGCGTCTAACGCATCTTAATAC AACTTTCAGCAACGGATCTCTTGGCT CTCGCATCGATGAAGAACGCAGCGA AATGCGATAAGTAATGTGAATTGCA GAATTCAGTGAATCATCGAATCTTTG AACGCACCTTGCGCTCCTTGGTATTC CGAGGAGCATGCCTGTTTGAGTGTC ATGAAATTCTCAACCCATAAATCCTT GTGATCTATGGGCTTGGATTTGGAGG CTTGCTGGCCCTAGTGGTCGGCTCCT	>Consensus TTCTTACAGTCATTTAAAGTTTGAGAATA GGTTAAGGTTGTTTCAACCCCAAGGCCTC TAATCATTCGCTTTACCACATAAATCTGA TATGAGTTTCTGCTATCCTGAGGGAAACT TCGGCAGGAACCAGCTACTARATGGTTC GATTAGTCTTTCGCCCCTATACCCAAATT TGACGATCGATTTGCACGTCAGAATCGC TACGAGCCTCCACCAGAGTTTCCTCTGGC TTCACCCTATTCAGGCATAGTTCACCATC TTTCGGGTCCCAACATACATGCTCTACCG CGGATCCGTCAGAGAACTTCAGGTCCGG GCGTCGATGCCCTCCACGACAGAGGTCT CAACTTTCACTTTCATTACGCGCTCGGGT TTTCCACCCAAACACTCGCAGGCATGTTA GACTCCTTGGTCCGTGTTTCAAGACGGGT CGTTTAAAGCCATTATGCCAGCATCCTAA GCACGAATGTGGGCGAACCCCAGCCATA AGGCGTGCTGCGTTCCTCGATCCCAACC	Trametes hirsuta strain DMC716 18S ribosomal RNA gene, partial sequence; internal transcribed spacer 1, 5.8S ribosomal RNA gene, and internal transcribed spacer 2, complete sequence; and 28S ribosomal RNA gene, partial sequence 620/621(99%) 0/621(0%) KC589147.1 Trametes hirsuta culture CBS:320.29 strain CBS 320.29 large subunit ribosomal RNA gene, partial sequence 854/856(99%)	https://onlinelibrary.wiley.com/doi/abs/10.1002/tax.606003?casa_token=gi8eWL7X4ooAAAAA:zsjjr5-sDrEnUtvRLASVJZm4lISMh8N8HEWhJKs55r6ZVxfB3AfNK_p6wLDo8z_dfKzuRLVY4dCiGF1q Vu, D., Groenewald,

		CTTGAATGCATTAGCTTGATTCCGTG CGGATCGGCTCTCAGTGTGATAATTG TCTACGCTGTGACCGTGAAGCGTTTT GGCGAGCTTCTAACCGTCCATTAGG ACAATCTTTCAACATCTGACCTCAAA TCAGGTAGGACTACCCGCTGAACTT AAGCA	GCTGTATGCGACTGAAGGCTATAACACA CCCGAAGGTGCCACATTCCTCCAGCCCTT TTCCAGCGGTCAAAATCGATGCTGGCCC GTCAACCGGAAAGTGCACCAAGCCGAAG CAAGGCTGAGTTCCGGACGACGCGACTG ACTTCAAGCGTTTCCCTTTCAGCAATTTC ACGTACTGTTTAACTCTCTTTCCAAAGTG CTTTTCATCTTTCCCTCACGGTACTTGTTC GCTATCGGTCTCTCGCCAATATTTAGCTT TAGAAGGAATTCACCTCCCATTTTGCGCT GCATTCCCAAACAACGCGACTCTTTGAG AGCGCATCACAAAGCATTGGTAGTCCGT GTCAAAGACGGGATTCTCACCCTCTATG ACGCTCTGTTCCAAGAGACTTGTACACG GTCCAACGCGGAAGACGCTTCTCCAGAC TACAACTCGGACGGCCAAAGACCGCCAG	0/856(0%) MH866536.1	M., De Vries, M., Gehrmann, T., Stielow, B., Eberhardt, U., ... & Verkley, G. J. M. (2018). Large-scale generation and analysis of filamentous fungal DNA barcodes boosts coverage for kingdom fungi and reveals thresholds for fungal species and higher taxon delimitation. *Studies in mycology*, *91*(1), 23-36.
16.	CsR-2	>Consensus CGTAACAAGGTCTCCGTTGGTGAAC CAGCGGAGGGATCATTGCTGGAACG CGCCCCTGGCGCACCCAGAAACCCT TTGTGAACTTATACCTTACTGTTGCC TCGGCGCGGGCCGTCCCCTATGGGG	>Consensus TGCCCACGTTCAACTAAGTAACAAGGGC TTCTTACATATTTAAAGTTTGAGAATGGA TGAAGGCAATATAGCGCCCCCGAGTCCC TAATCATTCGCTTTACCTCATAAAACTGA AGATCAACACTGCTATCCTGAGGGAAAC	Diaporthe foeniculina isolate SCF 006-683 small subunit ribosomal RNA gene, partial sequence; internal transcribed spacer 1, 5.8S ribosomal RNA gene, and internal	https://link.springer.com/article/10.1007/s13225-020-00440-y

		TCCCTCTGGAGACAGAGGAGCAGCC GGCCGGTGGCCAAGTTAACTCTGTTT TTAAATTGAAACTCTGAGTAAAAAA CATAAATGAATCAAAACTTTCAACA ACGGATCTCTTGGTTCTGGCATCGAT GAAGAACGCAGCGAAATGCGATAAG TAATGTGAATTGCAGAATTCAGTGA ATCATCGAATCTTTGAACGCACATTG CGCCCTCTGGTATTCCGGAGGGCATG CCTGTTCGAGCGTCATTTCAACCCTC AAGCCTGGCTTGGTGTTGGGGCACT GCTTTCTAACGGGAGCAGGCCCTGA AATATAGTGGCGAGCTCGCCAGGAC TCCGAGCGCAGTAGTTAAACCCTCG CTCTGGAAGGCCTGGCGGTGCCCTG CCGTTAAACCCCCAACTTCTGAAAAT TTGACCTCGGATCAGGTAGGAATAC CCGCTGAACTTAAGC	TTCGGCGGTWACCAGCTACTAGACAGTT CGATTAGTCTTTCGCCCCCATGCTCAAAT TTGACGATCGATTTGCACGTCAGAACCG CTGCGAGCCTCCACCAGAGTTTCCTCTGG CTTCACCCTATTCAAGCATAGTTCACTGT CTTTCGGGTCCGTCCGTTAAAACTCTTAC TCAAATCCTTCCGAGAACATCAGGATCG GTCGATGATGCGCCGAAGCTCTCACCTG CGTTCACTTTCATTACGCGTGCGGGTTTT ACACCCAAACGCTCGCTCTAATGGACGA CTCCTTGGTCCGTGTTTCAAGACGGGTCA CTGATGACCATTACGCCAGCATCCTTGCA GTGCGCGGACCTCGGTCCCCACGGGGGT ATCGTCCGCCAGGCTATAACACACCCCG GAGGGTGCTACGTTCCTGACGGTCTTATC CCCCCGCGAGAACCGATGCTGGCCTGTG CCGGGCGGAGTGCACAGGGGAGAACCCC TGATGAGCCGCCCGGCCCAAGTCTGGTC ATAAGTGCTTCCCTTTCAACAATTTCACG TACTATTTAACCCCCTTTTCAAGGTGCTT TTCATCTTTCGATCACTCTACTTGTGCGC TATCGGTCTCTGGCCGGTATTTAGCTTTA GAAGAGATTTACCTCCCATTTAGAGCAG CATTCCCAAACTACTCGACTCGTCGAAG GAGCTTCACACAGGCTTGGTGTCCGACC ATACGGGGCTCTCACCCTCTGTGGCGTCC CGTTCCAGGRAACTCGGAAGGCACCGCG CCAGAAGCATCCTCTGCAAATTACAACT CGGGCCGAGGCCAGATTTCAAATTTGAG CTGTTGCGCTT	transcribed spacer 2, complete sequence; and large subunit ribosomal RNA gene, partial sequence 560/568(99%) 2/568(0%) MW959694.1 Diaporthe foeniculina voucher MFLU:16-1132 large subunit ribosomal RNA gene, partial sequence 807/813(99%) 1/813(0%) MT183467.1	
17.	CsR2b	>Consensus GTAACAAGGTCTCCGTTGGTGAACC AGCGGAGGGATCATTGCTGGAACGC GCCCCTGGCGCACCCAGAAACCCTTT GTGAACTTATACCTTACTGTTGCCTC	>Consensus AACAAGGGCTTCTTACATATTTAAGTTTG AGAATGGATGAAGGCAATATAGCGCCCC CGAGTCCCTAATCATTCGCTTTACCTCAT AAAACTGAAGATCAACACTGCTATCCTG	Diaporthe foeniculina isolate SCF 006-683 small subunit ribosomal RNA gene, partial sequence; internal transcribed spacer 1, 5.8S ribosomal	https://link.springer.com/article/10.1007/s10658-021-02342-4

		GGCGCGGGCCGTCCCCTATGGGGTC CCTCTGGAGACAGAGGAGCAGCCGG CCGGTGGCCAAGTTAACTCTGTTTTT AAATTGAAACTCTGAGTAAAAAACA TAAATGAATCAAAACTTTCAACAAC GGATCTCTTGGTTCTGGCATCGATGA AGAACGCAGCGAAATGCGATAAGTA ATGTGAATTGCAGAATTCAGTGAAT CATCGAATCTTTGAACGCACATTGCG CCCTCTGGTATTCCGGAGGGCATGCC TGTTCGAGCGTCATTTCAACCCTCAA GCCTGGCTTGGTGTTGGGGCACTGCT TTCTAACGGGAGCAGGCCCTGAAAT ATAGTGGCGAGCTCGCCAGGACTCC GAGCGCAGTAGTTAAACCCTCGCTCT GGAAGGCCTGGCGGTGCCCTGCCGT TAAACCCCCAACTTCTGAAAATTTGA CCTCGGATCAGGTAGGAATACCCGC TGAACTTAAGCAT	AGGGAAACTTCGGCGGTAACCAGCTACT AGACAGTTCGATTAGTCTTTCGCCCCCAT GCTCAAATTTGACGATCGATTTGCACGTC AGAACCGCTGCGAGCCTCCACCAGAGTT TCCTCTGGCTTCACCCTATTCAAGCATAG TTCACTGTCTTTCGGGTCCGTCCGTTAAA ACTCTTACTCAAATCCTTCCGAGAACATC AGGATCGGTCGATGATGCGCCGAAGCTC TCACCTGCGTTCACTTTCATTACGCGTGC GGGTTTTACACCCAAACGCTCGCTCTAAT GGACGACTCCTTGGTCCGTGTTTCAAGAC GGGTCACTGATGACCATTACGCCAGCAT CCTTGCAGTGCGCGGACCTCGGTCCCCA CGGGGGTATCGTCCGCCAGGCTATAACA CACCCCGGAGGGTGCTACGTTCCTGACG GTCTTATCCCCCCGCGAGAACCGATGCT GGCCTGTGCCGGGCGGAGTGCACAGGGG AGAACCCCTGATGAGCCGCCCGGCCCAA GTCTGGTCATAAGTGCTTCCCTTTCAACA ATTTCACGTACTATTTAACCCCCTTTTCA AGGTGCTTTTCATCTTTCGATCACTCTAC TTGTGCGCTATCGGTCTCTGGCCGGTATT TAGCTTTAGAAGAGATTTACCTCCCATTT AGAGCAGCATTCCCAAACTACTCGACTC GTCGAAGGAGCTTCACACAGGGCTTGGT GTCCGACCATACGGGGCTCTCACCCTCTG TGGCGTCCCGTTCCAGGRAACTCGGAAG GCACCGCGCCAGAAGCATCCTCTGCAAA TTACAACTCGGGCCGAGGCCAGATTTCA AATTTGAGCTGTTGCCGCTTCACTC	RNA gene, and internal transcribed spacer 2, complete sequence; and large subunit ribosomal RNA gene, partial sequence 560/568(99%) 2/568(0%) MW959694.1 Diaporthe ravennica isolate IT_22732 28S ribosomal RNA gene, partial sequence 838/842(99%) 1/842(0%) KU900308.1	https://link.springer.com/article/10.1007/s13225-016-0371-z
18.	CsR-2C	>Consensus TCGTAACAAGGTTTCCGTAGGTGAA CCTGCGGAAGGATCATTACCGAGTG AGGGTTCCTCGCGAGCCCAACCTCCC ACCCGTGTTTATTACTACCTTGTTGC	>Consensus GTTCAACTAAGCAACAAGGGCTTCTTAC ATATTTAAAGTTTGAGAATAGGTTAAGG TTGTTTCAACCCCAATGCCCTCTAATCAT TCGCTTTACCTCATAAAACTGAATTCGCG	Aspergillus hancockii strain AsM 4.2.4 internal transcribed spacer 1, partial sequence; 5.8S ribosomal RNA gene and internal	https://sfamjournals.onlinelibrary.wiley.com/doi/full/10.1111/1462-

		TTCGGCGGGCCCGCCGCAAGGCCGC CGGGGGGCTTCATTGCCCCCGGGCC CGCGCCCGCCGGAGACACTTGAACA CTGTTTGATACCATGCAGTCTGAGTT GATTGTCTTGCAATCAGTTAAAACTT TCAACAATGGATCTCTTGGTTCCGGC ATCGATGAAGAACGCAGCGAAATGC GATAACTAATGTGAATTGCAGAATT CCGTGAATCATCGAGTCTTTGAACGC ACATTGCGCCCCCTGGTATTCCGGGG GGCATGCCTGTCCGAGCGTCATTGCT GCCCATCAAGCACGGCTTGTGTGTTG GGTCCCGTCCCCCTTCCCGGGGGGAC GGACCCGAAAGGCAGCGGCGGCACC GCGTCCGGTCCTCGAGCGTATGGGG CTTTGTCACCCGCTCTGTAGGCCCGG CCGGCGCTGGCCGACTTCTCAACCAT TTTTCTTCAGGTTGACCTCGGATCAG GTAGGGATACCCGCTGAACTTAAGC AT	TTACTGCTATCCTTGAGGGAAACTTCGGC AGGRACCAGCTACTAGATGGTTCGATTA GTCTTTCGCCCCCTATACCCAAATTCGAC GATCGATTTGCACGTCAGAACCGCTGCG AGCCTCCACCAGGAGTTTCCTCTGGCTTC ACCCTTATTCAGGCATAGTTCACCATCTT TCGGGTCCCCACATTTACGCTCTTACTCA AATCCATCCGAAGACATCAGGATCGGTC GATGGTGCGCCCCGCAAGGGGGCTCCCA CCTCCGTTCGCTTTCACTGCGCGTACGGG TTTGACACCCGAACACTCGCGTAGATGTT AGACTCCTTGGTCCGTGTTTCAAGACGG GTCGTTTGCGACCATTATGCCAGCGTCCG TGCCGAAGCGCGTTCCTCGGTCCAGGCT GGCCGCATTGCACTCCCGGCTATAAGGT ACCCCGGAGGGTACTACATTCCGGGAGC CTTTGACCGGCCGCCCAAACCGACGCTG GCCCGCCCCCGGGGAAGTACACCGGCAC GAATGCCGGCTGAACCCCGAGGGCGAGT CTGGTCGCAAGCGCTTCCCTTTCAACAAT TTCACGTGCTTTTTAACTCTCTTTTCAAA GTGCTTTTCATCTTTCGATCACTCTACTT GTGCGCTATCGGTCTCCGGCCAGTATTTA GCTTTAGATGAAATTTACCACCCATTTAG AGCTGCATTCCCAAACAACTCGACTCGT CGAAGGAGCTTCACACGGACACGGACAC CCCATYCCAGACGGGATTCTCACCCTCTC CGACGGCCCGTTCCAGGGCACTTAGACA GGGGCCGTATCCGAAGCATCCTCTGCAA ATTACAATGCGGACCCCGAAGGAGCCAG CTTTCAAATTTGAGCTCTTGCCGCTTCAC TCGC	transcribed spacer 2, complete sequence; and large subunit ribosomal RNA gene, partial sequence 551/551(100%) 0/551(0%) MT279259.1 Aspergillus leporis culture CBS:129235 strain CBS 129235 large subunit ribosomal RNA gene, partial sequence 838/844(99%) 4/844(0%) MH876695.1	2920.15395?casa_token=7aNesZfFs7EAAAAA%3ASTQVkPpfk5lYPIwwfEreVwpPfnAeVlW7Nw2-_6qr3VkfjwAC4dukc2DZwNu4ca1tYE0_fU-Z8P5h0CD8 Vu, D., Groenewald, M., De Vries, M., Gehrmann, T., Stielow, B., Eberhardt, U., ... & Verkley, G. J. M. (2018). Large-scale generation and analysis of filamentous fungal DNA barcodes boosts coverage for kingdom fungi and

					reveals thresholds for fungal species and higher taxon delimitation. *Studies in mycology*, *91*(1), 23-36.
19.	CsR3a	>Consensus ACTGAGTGAGGGCCCCTCGGGGTCC AACCTCCCACCCGTGTTTAACGAACC GTGTTGCTTCGGCGGGCCCGCCTCAC GGCCGCCGGGGGGCATCCGCCCCCG GGCCCGCGCCCGCCGAAGCCCCCTG TGAACGCTGTCTGAAGTATGCAGTCT GAGACAATTATTCAATTAATTAAAA CTTTCAACAACGGATCTCTTGGTTCC GGCATCGATGAAGAACGCAGCGAAA TGCGATAACTAATGTGAATTGCAGA ATTCAGTGAATCATCGAGTCTTTGAA CGCACATTGCGCCCTCTGGTATTCCG GAGGGCATGCCTGTCCGAGCGTCAT TGCTGCCCTCCAGCCCGGCTGGTGTG TTGGGCCCCGCCCCCCTTCCCGGGGG GGCGGGCCCGAAAGGCAGCGGCGGC ACCGCGTCCGGTCCTCGAGCGTATG GGGCTTTGTCACCCGCTCTTGCAGGC CCGGCCGGCGCCAGCCGACCCCCTC AATCTATTTTTTCAGGTTGACCTCGG ATCAGGTAGGGATACCCGCTGAACT TAAGCATATCAGTAAGACGAGA	>Consensus GCCCACGTTCAATTAAGCAACAAGGGCT TCTTACATATTTAAAGTTTGAGAATAGGT TAAGGTTGTTTCAACCCCAAGGCCYYTA ATCATTCGCTTTACCTCATAAAACTGAAT TCGCGTTACTGCTATCCTGAGGGAAACTT CGGCAGGRACCAGCTACTAGATGGTTCG ATTAGTCTTTCGCCCCTAWACCCAAATTT GACGATCGATTTGCACGTCAGAACCGCT GCGAGCCTCCACCAGAGTTTCCTCTGGCT TCGCCCTATTCAGGCATAGTTCACCATCT TTCGGGTCCCAACAGCTACGCTCTTACTC AAATCCATCCGAAGACATCAGGATCGGT CGATGGTGCACCCCGAGGGGTTCCCACC TCCGTTCGCTTTCACTGCGCGCACGGGTT TGACACCCGAACACTCGCGTAGATGTTA GACTCCTTGGTCCGTGTTTCAAGACGGGT CGCTTACGACCATTATGCCAGCGTCCGA GCCGAAGCGCGTTCCTCGGTCCGGGCAG GCCGCATGGCACCCCTGGCTATAAGACG CCCCGAGAGGCGTTACATTCCAGGGGCC TTTGACCGGCCGCCCAAACCGACGCTGG CCCGCCCGCGGGGAAGTACACCGGCCCG AAGGCCGGCTGAACCCCGCGAGCGAGTC TGATCGCAAGCGCTTCCCTTTCAACAATT	Penicillium manginii CBS 253.31 ITS region; from TYPE material 538/538(100%) 0/538(0%) NR_111489.1 Penicillium manginii culture CBS:126232 strain CBS 126232 large subunit ribosomal RNA gene, partial sequence 837/839(99%) 0/839(0%) MH875443.1	https://academic.oup.com/database/article/doi/10.1093/database/bau061/2634542 Vu, D., Groenewald, M., De Vries, M., Gehrmann, T., Stielow, B., Eberhardt, U., ... & Verkley, G. J. M. (2018). Large-scale generation and analysis of filamentous fungal DNA

			TCACGTGCTGTTTAACTCTCTTTTCAAAG TGCTTTTCATCTTTCGATCACTCTACTTGT GCGCTATCGGTCTCCGGCCAATATTTAGC TTTAGATGAAATTTACCACCCAATTAGA GCTGCATTCCCAAACAACTCGACTCGTC GAAGGAGCTTCACACGGGCGCGGGCACC CCATCCCATACGGGATTCTCACCCTCTAT GACGGCCCGTTCCAGGGCACTTAGATGG GGACCGCTCCCGAAGCATCCTCTGCAAA TTACAATGCGGACCCCGAAGGGGCCAGC TTTCARATTTGAGCTCTTACCGCTTCACT CGCCGTTACTA		barcodes boosts coverage for kingdom fungi and reveals thresholds for fungal species and higher taxon delimitation. *Studies in mycology*, *91*(1), 23-36.

REPUBLIC OF KENYA

NATIONAL COMMISSION FOR SCIENCE,TECHNOLOGY & INNOVATION

Ref No: **103825**

Date of Issue: **14/July/2023**

RESEARCH LICENSE

This is to Certify that Miss.. Lucy Aketch Wanga of Egerton University, has been licensed to conduct research as per the provision of the Science, Technology and Innovation Act, 2013 (Rev.2014) in Nakuru, Transnzoia on the topic: EVALUATION OF ANTIMICROBIAL ACTIVITY OF Calpurnia aurea (L'HERIT) SECONDARY METABOLITESAND ASSOCIATED FUNGAL ENDOPHYTES AGAINST SELECTED SKIN PATHOGENS for the period ending : 14/July/2024.

License No: **NACOSTI/P/23/26933**

103825

Applicant Identification Number

Director General
NATIONAL COMMISSION FOR SCIENCE,TECHNOLOGY & INNOVATION

Verification QR Code

NOTE: This is a computer generated License. To verify the authenticity of this document, Scan the QR Code using QR scanner application.

See overleaf for conditions

Fitoterapia 171 (2023) 105698

Contents lists available at ScienceDirect

Fitoterapia

journal homepage: www.elsevier.com/locate/fitote

Antidermatophytic quinolizidine alkaloids from *Calpurnia aurea* subsp. *aurea* (Aiton) Benth

Lucy Aketch Wanga [a,b,c,d], Abwao Stephen Indieka [b], Josphat Clement Matasyoh [a,*]

[a] Department of Chemistry, Faculty of Sciences, Egerton University, P.O. Box 536, Egerton 20115, Kenya
[b] Department of Biochemistry and Molecular Biology, Faculty of Sciences, Egerton University, P.O. Box 536, Egerton 20115, Kenya
[c] Department of Microbial Drugs, Helmholtz Centre for Infection Research, Braunschweig 38124, Germany
[d] Institute of Microbiology of the Czech Academy of Sciences, VIDENSKA 1083, PRAHA 4, 142 00, Czech Republic

ARTICLE INFO

Keywords:
Calpurnia aurea subps *aurea*
Fabaceae
Antidermatophytic activity
Quinolizidine alkaloids
Dermatophytes

ABSTRACT

From the leaves and stem bark of the Kenyan medicinal plant *Calpurnia aurea* subsp. *aurea*, four previously undescribed quinolizidine alkaloids namely, 2β-methoxy-13α-*O*-(2′-pyrrolylcarbonyl) virgiline, 2α-methoxy-13β-*O*-(2′-pyrrolylcarbonyl) virgiline, 3α-*O*-angelate-2β-hydroxy-13α-*O*-(2′-pyrrolylcarbonyl) virgiline, 2,3-dehydro-virgiline were isolated together with four known ones. Structural elucidation of the compounds was based on 1D and 2D NMR spectroscopy and mass spectrometry. Their relative configurations were determined by NOESY correlations and literature. The quinolizidine alkaloids were tested against *Trichophyton rubrum*, *Trichophyton interdigitale*, *Trichophyton benhamiae*, *Microsporum canis* and *Nannizzia gypsea*, common causative agents of most of the tinea infections in human. All the isolated quinolizidine alkaloids exhibited antidermatophytic activity with MIC ranging from 37.5 μg/ml to 300 μg/ml.

1. Introduction

Dermatophytic infections is a worldwide problem with low and middle income countries experiencing the highest number of incidences. These infections affect approximately 20–25% of the world's population [1] and thus pose a serious threat to public health. Tinea infections, caused by fungal pathogens belonging to genera *Microsporum*, *Trichophyton* and *Epidermophyton* spp., have been reported to cause serious physical and psychological effects to patients [2,3]. Several antifungal drugs have been introduced [4] however problems associated with prolonged treatment duration, drug toxicity and interaction, development of resistance and high cost of these drugs are of great concern [5]. Thus intensive research on alternative novel compounds for development of effective, safe and less costly antifungal drugs is inevitable.

Calpurnia aurea subsp. *aurea* (Ait) Benth. (*Fabaceae*) (syn. *Calpurnia subdecandra* (L'Hérit.) is a medicinal plant widely distributed in Africa, from South Africa to North tropical countries such as Ethiopia and healing activities [12]. From previous studies, a number of quinolizidine alkaloids with insecticidal activity have also been isolated from *C. aurea* subsp. *aurea* [13,14] hence this class of secondary metabolites are regarded as chemotaxonomic markers of the *Fabaceae* family [15]. Despite being used traditionally for the treatment of wounds and ringworms, there has been no scientific report of their antidematophytic activity.

As part of the ongoing research on the Kenyan medicinal plants, phytochemical investigations of extracts from the leaves and stem bark of *C. aurea* subsp. *aurea* collected from Mt. Elgon forest in Kenya, led to the isolation of four undescribed quinolizidine alkaloids derivatives and four others previously reported. These alkaloids exhibited a wide range of antidermatophytic activities against *Trichophyton rubrum*, *Trichophyton interdigitale*, *Trichophyton benhamiae*, *Microsporum canis* and *Nannizzia gypsea*. To the best of our knowledge, this is the first report on the antidermatophytic bioactivity of quinolizidine alkaloids.

The Microbe 8 (2025) 100421

Contents lists available at ScienceDirect

The Microbe

journal homepage: www.sciencedirect.com/journal/the-microbe

Phenolic compounds from *Calpurnia aurea* subsp. aurea (Aiton) Benth and their antimicrobial, antidermatophytic, antiproliferative and cytotoxic activities

Lucy Aketch Wanga [a,b,c,d], Abwao Stephen Indieka [b], Josphat Clement Matasyoh [a,*]

[a] Department of Chemistry, Faculty of Sciences, Egerton University, P.O. Box 536, Egerton 20115, Kenya
[b] Department of Biochemistry and Molecular Biology, Faculty of Sciences, Egerton University, P.O. Box 536, Egerton 20115, Kenya
[c] Department of Microbial Drugs, Helmholtz Centre for Infection Research, Braunschweig 38124, Germany
[d] Institute of Microbiology of the Czech Academy of Sciences, Videnska 1083, Praha 4, 142 00, Czech Republic

ARTICLE INFO

Keywords:
Phenolic compounds
Calpurnia aurea subsp. *aurea*
Fabaceae
Antimicrobial
Antidermatophytic
Antiproliferative
Cytotoxic

ABSTRACT

Plants serve as an alternative and/or augmentation to modern medicine. *Calpurnia aurea* subsp. *aurea* is an important plant historically used for wound healing and the treatment of various bacterial and fungal illnesses. The methanol extracts obtained from the leaves and stem bark were purified using chromatographic methods. Twelve (12) phenolic compounds were isolated: rhoifolin (1), apigenin 7-*O*-glucoside (2), luteolin-7-*O*-glucoside (3), naringin (4), ononin (5), formononetin (6), 8-*O*-methylretusin (7), 8-*O*-methylretusin-7-*O*-*β*-D-glucopyranoside (8), maackiainn (9), trifolirhizin (10), medicarpin (11), and methyl (*E*)-3,4,5-trimethoxycinnamate (12). Compounds 1, 5, 7, 9, and 11 exhibited antifungal activity against *Mucor hiemalis* and *Schizosaccharomyces pombe*, with a minimum inhibitory concentration of 66.6 μg/mL. Conversely, compound 12 exhibited antibacterial activity against *Bacillus subtilis* (DSM 10), with a minimum inhibitory concentration (MIC) of 16.6 μg/mL. Compounds 1, 7, 9, 11, and 12 exhibited cytotoxic and antiproliferative properties, with IC_{50} values between 15 μg/mL and 24 μg/mL against the KB3.1 and L929 cell lines. The compounds exhibited significant antidermatophytic action against *Trichophyton rubrum*, *Trichophyton interdigitale*, *Trichophyton benhamiae*, *Microsporum canis*, and *Nannizzia gypsea*, with minimum inhibitory concentration (MIC) values ranging from 6.6 μg/mL to 300 μg/mL. This paper provides the initial reports on compounds 1, 3, 4, 5, 6, 8, 9, 10, 11, and 12 obtained from *C. aurea* subsp. *aurea*. Moreover, the results of this study provide a scientific foundation for the conventional use of this plant in treating numerous illnesses, therefore facilitating the production of more effective medications.

1. Introduction

Calpurnia aurea subsp. *aurea* (Aiton) Benth, referred to as wild laburnum, is a perennial shrub or diminutive tree within the *Fabaceae* family. This pharmacologically significant plant is distinguished by its vibrant yellow flowers organized in drooping racemes, pinnately complex leaves comprising 5–13 leaflets, and smooth, grayish-brown bark. Conversely, the stem bark has a coarse texture and a dark hue (Trytsman et al., 2023). The species demonstrates considerable morphological variety across its distribution, with certain specimens reaching heights of up to 7 m under optimal conditions. Botanically, it is characterized by its papilionaceous blooms and leguminous pods carrying 4–8 seeds, which are distributed via explosive dehiscence. The species exhibits extensive geographical distribution in sub-Saharan Africa, naturally ranging from Ethiopia and Somalia in the northeast, to East Africa, to South Africa (Trytsman et al., 2023). In Kenya, it is most prevalent in the highlands at elevations of 1500–3000 m above sea level, where it is a component of the natural flora in woodland and forest margin habitats (Trytsman et al., 2023). The plant has significant ecological adaptability, flourishing in many environments such as grasslands, riverbanks, and disturbed regions, hence enhancing its extensive traditional utilization across varied African groups (Maiyo et al., 2023).

In African ethnomedicine, diverse parts of *Calpurnia aurea* have been used for generations to address a range of diseases. Traditional healers use leaf decoctions to treat skin infections, facilitate wound healing, and address gastrointestinal illnesses, and root extracts are used for parasite

* Corresponding author.
E-mail address: jmatasyoh@egerton.ac.ke (J.C. Matasyoh).

https://doi.org/10.1016/j.microb.2025.100421
Received 3 March 2025; Received in revised form 28 May 2025; Accepted 11 June 2025
Available online 14 June 2025